GROUNDWATER POTENTIAL AND WELL YIELD DISCREPANCIES: HYDROGEOLOGICAL CONTROLS, DRILLING CHALLENGES, AND AQUIFER PARAMETER–RESISTIVITY RELATIONSHIPS IN UPPER BILATE RIVER BASIN, MAIN ETHIOPIAN RIFT VALLEY, SOUTHERN ETHIOPIA

MSc. THESIS

BY

Fisseha Teka Hailu

ID No CNSC/PS201/09

Advisor: Tesfamichael Gereyohannes (PhD)

Co-advisor: Fithanegest W/Mariam (PhD)

MEKELLE UNIVERSITY

SCHOOL OF EARTH SCIENCES

DEPARTMENT OF GEOLOGY

POST GRADUATE (M.Sc.) DEGREE PROGRAM IN HYDROGEOLOGY

AUGEST, 2025

MEKELLE, ETHIOPIA

MEKELLE UNIVERSITY
SCHOOL OF EARTH SCIENCES
DEPARTMENT OF GEOLOGY

GROUNDWATER POTENTIAL AND WELL YIELD DISCREPANCIES: HYDROGEOLOGICAL CONTROLS, DRILLING CHALLENGES, AND AQUIFER PARAMETER–RESISTIVITY RELATIONSHIPS IN UPPER BILATE RIVER BASIN, MAIN ETHIOPIAN RIFT VALLEY, SOUTHERN ETHIOPIA.

BY

FISSEHA TEKA HAILU

MSc THESIS

Submitted to The School of Earth Sciences Department of Geology, Mekelle University in Partial Fulfilment of the Requirements for The Degree of Master of Science in Hydrogeology

MEKELLE, ETHIOPIA

DECLARATION

I, the one who signed, declare that this Master of Science thesis entitled "Groundwater Potential and Well Yield Discrepancies: Hydrogeological Controls, Drilling Challenges, and Aquifer Parameter–Resistivity Relationships" in Upper Bilate River Basin, Main Ethiopian Rift Valley, Southern Ethiopia″ is my unique work and has not been presented for a Master's degree in any other University, and all sources of material used for this thesis have been properly acknowledged.

Fisseha Teka

16/10/2025
Date

MEKELLE UNIVERSITY

SCHOOL OF EARTH SCIENCES

ADVISOR'S THESIS APPROVAL SHEET

This is to certify that the thesis proposal entitled "Groundwater Potential and Well Yield Discrepancies: Hydrogeological Controls, Drilling Challenges, and Aquifer Parameter–Resistivity Relationships" has been developed by Fisseha Teka Hailu under our supervision. All the comments and corrections given by the advisors were incorporated into the proposal. Therefore, I confirm that the student has fulfilled the proposal writing requirements and can submit the thesis proposal to the department.

Name	Signature	Date
Fisseha Teka (Candidate)	 Signature	16/10/2025 Date
Tesfamichael Gebreyohanes (PhD) (Main Advisor)	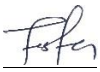 Signature	20/10/2025 Date
Fithanegest W/Mariam (PhD) (Co Adviser)	Signature	Date
Fithanegest W/Mariam (PhD) (Department Head)	Signature	Date

MEKELLE UNIVERSITY

SCHOOL OF EARTH SCIENCES

EXAMINERS COMMITTEE THESIS APPROVAL SHEET

We, the undersigned, members of the board of examiners of the final open defence have read and evaluated his thesis entitled "**Groundwater Potential and Well Yield Discrepancies: Hydrogeological Controls, Drilling Challenges, and Aquifer Parameter–Resistivity Relationships**", and examined the candidate's oral presentation. This is, therefore, to certify that, the thesis has been accepted in partial fulfilment of the Master of Science degree in Hydrogeology.

Approved by:

Hindeya Gebru (PhD) (Name of External Examiner)	 Signature	16/10/2025 Date
Ermiyas Hagos (PhD) (Name of Internal Examiner)	 Signature	16/10/2025 Date
Tesfamichael Gebreyohanes (PhD) (Name of Advisor)	 Signature	20/10/2025 Date
Fithanegest W/Mariam (PhD) (Name of Department head)	---------- Signature	---------- Date

TABLE OF CONTENTS

LIST OF FIGURES

LIST OF TABLES

LIST OF ABBREVIATIONS AND ACRONYMS

ρ	electrical resistivity of saturated thickness
AHP	Analytical Hierarchy Process
ANOVA	One-Way Analysis of Variance
UBRB	Bilate River Basin
Bh	Borehole
Cw	Wellbore Storage Coefficient
CSA	Federal Republic of Ethiopia Central Statistical Agency
DEM	Digital Elevation Model
DZP	Dar Zarrouk parameters
EARV	East African Rift Valley
ERVLB	Ethiopian Rift Valley Lake Basin
ETo	Reference Evapotranspiration
FAO	Food and Agricultural Organization
GIS	Geographical Information System
GSE	Geological Survey of Ethiopia
GWPZ	Groundwater Potential Zone
h	Thickness of the aquifer
JICA	Japan International Corporation Agency
K	Hydraulic conductivity
LULC	Land Use Land Cover
MER	Main Ethiopian Rift
MOWE	Ministry of Water Resource and Energy
NMSA	National Metrological Service Agency
Q	Well Discharge
Q_{suf}	Surface runoff
R	Recharge amount
RMS	Root Mean Square
Sc	Longitudinal conductance
SDCSE	South Design Construction Enterprise
SNNPRS	South Nation Nationalities Peoples Regional State
SWWCE	South Water Works Construction Enterprise
T	Transmissivity
Tr	Transverse Resistance
UBRB	Upper Bilate River Basin
VES	Vertical Electrical Sounding
WMO	World Meteorological Organization

ACKNOWLEDGMENTS

I gratefully acknowledge Almighty God and the Blessed Virgin Mary for their guidance and blessings throughout this work.

I extend my sincere appreciation to my principal supervisor, Dr. Tesfamichael Gereyohannes, for his invaluable guidance, encouragement, and critical insights, and to my co-supervisor, Dr. Fithanegest W/Mariam, for constructive feedback and technical assistance. Their expertise in hydrogeology and commitment to scientific rigor were instrumental in the successful completion of this research.

I am thankful to the South Design and Construction Supervision Enterprise (SDCSE) for financial support, and to the South Water Works Construction Enterprise and the Meteorological Agency – Hawassa Branch for providing essential data, field access, and logistical assistance. I also acknowledge the contributions of the technical and field teams, my instructors, and the Earth Science Department staff at Mekelle University for their academic and administrative support.

I express my gratitude to the local administrators and communities of the Central and Southern Ethiopia Regional State for their cooperation, hospitality, and valuable local knowledge during fieldwork.

Special thanks go to my father, Ato Teka Hailu, and my brother, Dr. Betelay Teka, for their encouragement, and steadfast support. Above all, I am deeply indebted to my wife, W/ro Abrehat Gebremeskel, and my children, Adonay Fisseha and Yeabsira Fisseha, whose love, patience, and understanding were my greatest source of strength.

This work is dedicated to Almighty God. Any remaining errors are solely my responsibility.

ABSTRACT

Discrepancies in well yields within the Upper Bilate River Basin (UBRB) of the Ethiopian Rift Valley Lake Basin highlight the intricate hydrogeology of its volcanic aquifers and Quaternary deposits. This study examines the influence of drilling-challenges such as partial penetration, well loss coefficient, wellbore storage on yield variations, which may surpass the effects of natural hydrogeological variability. By integrating data from meteorological, hydrological, remote sensing, vertical electrical sounding, and pumping tests with historical well records, key aquifer parameters like transmissivity and hydraulic conductivity are quantified, while empirical relationships between aquifer productivity and resistivity are established. This study's water balance analysis for the Upper Bilate River Basin reveals a semi-humid system with a 254.6 mm annual surplus. A significant wet-season surplus facilitates groundwater recharge, estimated at 58.9 mm/year (6% of rainfall), indicating moderate infiltration and strong surface water-groundwater interaction

A hydrogeological framework and groundwater potential zone map, generated through weighted overlay analysis of ten thematic layers, categorized the basin into excellent (1.39%), very good (17.9%), good (79.17%), and low (1.54%) potential zones. Most wells align with high-potential zones, confirming predictive accuracy: 74% of Wells are in very good zones and 26% in good zones, with none in low-potential areas. Transmissivity (T) in the study area varies from 0.05 to 841.10 m^2/day, indicating a heterogeneous aquifer system. Moderate to moderately high transmissivity zones (59.77–89.93 m^2/day) dominate, covering nearly 60% of the area, mainly in the central and northern parts, suggesting good aquifer productivity. Geophysical investigations identify Layer 6 (highly weathered and fractured pyroclastic rocks) as the most promising aquifer, followed by Layers 5 and 4, while upper shallow layers function as aquitards. A strong correlation between transmissivity and transverse resistance ($r = 0.83$, $p = 1.32\times10^{-13}$) supports the integration of geophysical and pumping test data for aquifer assessment.

Well yield discrepancies in the UBRB are influenced more by drilling challenges than by aquifer natural heterogeneity. An analysis of 220 Wells indicates a partial penetration ratio (L/b) of 0.13 to 0.96, with a mean of 0.56, suggesting moderately penetrating wells. Wellbore storage shows that 49% of wells have high storage ($Cw \geq 0.9$), while 27% have low storage ($Cw < 0.1$), reflecting variable aquifer connectivity. In a study of 25 wells, loss coefficients (C) range from 4.0×10^{-7} to 5.0×10^{-5} day^2/m^5, with 72% classified as severely clogged and none being properly developed. Well efficiency varies between 11.2% to 100% (mean 70.3%), with 18% rated Poor, 22% Fair, 30% Good, and 30% Excellent. This highlights the need for better well design, development, and maintenance practices. The correlation between transmissivity and well efficiency demonstrates that aquifer transmissivity primarily governs well performance, with high-transmissivity zones hosting the most efficient wells. In contrast, low efficiency in moderately transmissive areas mainly stems from technical issues—such as improper well design, partial penetration, or excessive wellbore storage—rather than aquifer limitations. Enhancing well construction and maintenance practices is therefore crucial to fully realize groundwater potential in these zones.

Keywords: Groundwater Potential, Aquifer characteristics, Well Yield challenge, Thematic analysis, Empirical relationship, Upper Bilate River Basin, Ethiopia

1 INTRODUCTION

1.1 Background

Water is the most imperative natural resource, essential for all life. Often seen as a gift from GOD, it sustains plants and animals, provides energy, aids transportation, and serves many other important purposes. Water supply provision and agricultural production based on groundwater is the major one of numerous social, economic, and environmental factors that determine food security.

Research on problems of groundwater resources investigation, well yield challenges, groundwater flow dynamics modelling, water balances, aquifer characterization, recharge estimation and groundwater development etc., are extremely significant to understand and advance the knowledge and skills of groundwater resources for sustainable utilization and management. Integration of Remote Sensing(RS) data and Geographical Information System(GIS) is a breakthrough in the field of groundwater research as this techniques is found efficient to reduce the time ,labour, and cost thereby enables quick decision-making for sustainable water resources management(Magesh et al., 2012). Hydrogeological investigation to delineation of groundwater Potential zones by integrating tools of RS, GIS and Fuzzy Analytical Hierarchy Process (FAHP) to achieve multi-attribute decision making choice among various thematic layers which affect the groundwater resources such as geology, geomorphology, lineament density, slope, soil, rainfall, drainage density, land use / land cover, normalized difference vegetation index and elevation(Singh et al., 2020). Interpreting the subsurface geophysical investigations particularly Vertical Electrical Sounding (VES) coupled with geological and hydrogeological studies, revealed several characteristics of groundwater; demarcation of groundwater Potential for proper utilization and management(Elango, 2015;Israil et al., 2006). A number of empirical correlations have been achieved between the hydraulic properties measured through geoelectrical methods(VES and water well data for determination of hydraulic parameters of groundwater (Khalilidermani et al., 2021;Shang et al., 2021 ; Hasan et al., 2020 and Soupios et al., 2007).

The main task in solving hydrogeological problems is to obtain consistent solutions of the aquifers' properties. Hydrogeology solves problems of geological and tectonic natural phenomena regarding the different properties of water in subsurface environments using

principles of hydrology. In general, groundwater resources are abundant in the underground geological formations. However, when needed, the spatial and temporal distribution is usually unavailable in efficient quantities and may not be of acceptable quality. Groundwater consists of water that comes in the form of precipitation percolating through the soil and moves downward until it reaches saturated rock formation of varying thickness and at different depths below the earth's surface (Kebede, 2013). The Upper Bilate River basin often experiences large discrepancies in water production capacity from Wells, which is a topic for contemplation. Furthermore, climate change is a global threat. Although Ethiopia's contribution to global climate change is insignificant, recent studies show that the country is the most vulnerable to unforeseen climate changes and has the lowest resilience. As Zegeye,(2018) notes, these circumstances are intensified by hasty population growth, and heavy dependency on agriculture and natural resources for livelihood. Ethiopia has 12 major and 12 minor lakes, mainly in the Rift Valley and volcanic areas, covering about 7,300 km² and containing around 70 billion cubic meters of water(Berhanu et al., 2014). The country's 12 river basins produce an annual runoff of roughly 124.4 billion cubic meters, with 97% (120.7 billion cubic meters) flowing to neighboring countries, leaving only 3% (3.7 billion cubic water) within Ethiopia. This hydrological significance has led to Ethiopia being called the "Water Tower of Africa (Makombe et al., 2011). Numerous works have been carried out on Ethiopia's status of water resources. Deformation features and geomorphology of igneous rocks and related volcanic sediments are the key hydrogeological frameworks that regulate the flow and existence of groundwater. However, faults determine the majority of groundwater movement in the rift and slope areas (Ayenew et al., 2008).

The study conducted by JICA, Kokusai Kogyo Co.(2012) is the most famous work in the ERVLB, focuses on the assessment of groundwater resources and attempts to characterize the productivity of aquifers using drilling data and with few test wells. Although the study provided limited data, these do not constitute a requirement for the use of specific methods to analyse pumping tests. Apart from the Addis Ababa region, there are no observation wells for monitoring wells in Ethiopia, so traditional pumping test analyses cannot be easily carried out. Ethiopia is one of the countries that is lagging in this area. The predictable groundwater resource of an anisotropic and heterogeneous geological formation is typically limited by inadequate knowledge about it. Efficient use of groundwater requires the creation of an appropriate well design based on high-quality well data(Moss & Company., 1990).

Groundwater is the primary source of water supply in the Upper Bilate River Basin (UBRB), located within the Main Ethiopian Rift (MER). The observed well-yield disparities, combined with limited understanding of aquifer heterogeneity, necessitate a systematic investigation of both natural and human-induced factors affecting groundwater productivity. This study addresses these gaps by characterizing hydrogeological and topographic controls, integrating geophysical data through vertical electrical sounding (VES) surveys, evaluating well-yield challenges, and developing empirical relationships between aquifer parameters and resistivity. The findings will support predictive identification of productive zones, optimization of well design, and sustainable groundwater management in the UBRB.

The well data has been provided by the South Nationalities Peoples Regional State (SNNPRS) offices, specifically by the Water Mine and Energy Development Bureau, South Water Works Construction Enterprise (SWWCE), and South Design Construction Enterprise (SDCSE) of SNNPRS. Kruseman & Ridder, (2000) claim that determining consistent solutions of the aquifer parameters of the rock strata wherein groundwater flows is the first step in solving the groundwater challenges. Pumping tests are considered to be the best and most effient strategies for a one of the most effective ways to attain such values (Kruseman & Ridder, 2000). Using CSA, (2007), by 2032 the basin is expected to have a projected population of 6,896,443, with 1,206,671 in cities and 5,689,773 in rural areas. Due to population growth, it is critical to address the use and management of groundwater at an early stage. This research contributes to advancing the quantification of groundwater resources and their development through efficient well construction. The results will have significant implications for future groundwater resource management.

1.2 Problem statement

Groundwater is the primary source of water supply in the Upper Bilate River Basin (UBRB), located within the Main Ethiopian Rift. Until 2016, well yields across the basin were relatively consistent, even in areas with similar hydrogeological settings, and drilling challenges were not considered significant. More recently, however, a striking disparity has emerged: newly drilled wells record yields of 20–60 L/s, while nearby wells under comparable conditions produce only 8–10 L/s. This unexplained variation signals a fundamental shift in groundwater productivity and highlights a critical knowledge gap.

The basin's aquifer system is highly heterogeneous, shaped by complex volcanic lithologies and Quaternary deposits. While natural hydrogeological variability plays a role, emerging evidence suggests that drilling challenges—such as partial penetration, poor well design, wellbore storage, and well-losses—may now exert greater influence on yield differences than previously assumed. These uncertainties pose serious challenges to groundwater exploration and management, particularly as water demand in the basin continues to rise. Despite its importance, no integrated study has examined groundwater productivity in the UBRB by linking hydrogeological conditions with well performance and geophysical parameters. This lack of comprehensive understanding limits the capacity of water managers and planners to predict productive zones, improve well design, and ensure sustainable utilization of the resource.

This study addresses these gaps by investigating the hydrogeological and drilling-related controls on well productivity in the UBRB. It integrates meteorological, hydrological, remote sensing, and geoelectrical data (VES) with pumping test results and historical well records to quantify key aquifer parameters such as transmissivity and storativity. Furthermore, it seeks to establish empirical relationships between aquifer productivity and resistivity. The findings will contribute to a novel framework for identifying productive groundwater zones and guiding sustainable groundwater development in the UBRB and the broader Main Ethiopian Rift.

1.3 Objectives

1.3.1 General objective

To investigate the hydrogeological controls and well-yield challenges affecting groundwater productivity in the Upper Bilate River Basin (UBRB), and to develop an integrated framework linking aquifer characteristics, geophysical parameters, and well performance for sustainable groundwater management.

1.3.2 Specific objectives

1. To evaluate the influence of hydrogeological controls on groundwater potential and delineate the hydrogeological framework of UBRB.
2. To evaluate key aquifer parameters (transmissivity, thickness) and hydrostratigraphic sequences of the basin.
3. To estimate subsurface electrical resistivity and delineate aquifer layers using vertical electrical sounding (VES) surveys.
4. To develop empirical relationships between aquifer hydraulic parameters and geoelectrical resistivity variables.
5. To assess well yield challenges (partial penetration, wellbore storage effects, well losses, and well conditions) that result in well yield discrepancies.

1.4 Scope of the study

This research focus on two critical areas: (1) the hydrogeological investigation of groundwater resources using an integrated approach, and (2) the evaluation of water well-yielding capacity, along with the identification and mapping of associated well yield challenges, such as partial penetration and wellbore storage, and poorly designed well zones. The study relies on a combination of primary and secondary data sources, including well-completion reports, geo-electrical surveys (particularly vertical electrical sounding, or VES), meteorological station data, river flow data, and remote sensing (RS) data. Key datasets to be utilized include a Digital Elevation Model (DEM) with a 12.5-meter resolution, Land Use and Land Cover (LULC) data at a 10-meter resolution, soil maps with 1km-by-1km resolution, slope maps, lineament density, drainage density, and the Topographic Wetness Index (SLOPE). Additionally, the researcher's firsthand experience with drilling challenges provided valuable insights to

complement the analytical findings. Each map in this study was generated at an identical scale of 1:530,000 in order to ensure consistency and comparability across thematic levels.

1.5 Significance of the Study

This study holds significant benefits in both scientific and practical contexts. From a scientific perspective, it contributes to the limited body of hydrogeological research specific to the Upper Bilate River Basin (UBRB), an area where groundwater yields can vary significantly among wells with similar conditions, and the influence of drilling challenges on these yield discrepancies is often overlooked. By integrating Well lithological & pumping test data with vertical electrical sounding (VES) surveys, the study provides a comprehensive approach to evaluating well yield challenges and aquifer characteristics.

Practically, the findings can guide government agencies, water resource planners, and development organizations in making informed decisions related to groundwater development and management. The insights gained from this research can support more accurate well siting, improved yield estimation, and sustainable use of groundwater resources — all of which are critical for rural water supply, agriculture, and climate resilience in the UBRB.

Moreover, the methodology and results of this investigation offer a foundation for future studies in similar geological and hydrogeological settings. The integration of geophysical and Well data serves as a replicable model that can be applied to other regions facing comparable groundwater challenges.

2 LITERATURE REVIEW

2.1 Groundwater importance and threats

Groundwater constitutes a critical natural resource that is fundamental to the maintenance of ecosystems, agriculture, industry, and human consumption. It is located beneath the Earth's surface within the pore spaces of soil and the fractures of rock formations, creating aquifers that provide water to wells and springs. The following sections outline the importance of groundwater, supported by references from scientific and environmental research studies. Groundwater is unevenly distributed globally, with availability depending on geological formations, climate, and human extraction rates. However, unsustainable use and environmental changes pose significant threats to this vital resource. Groundwater is stored in aquifers—permeable rock or sediment layers that hold and transmit water. The largest aquifers include: the Ogallala Aquifer (USA): Which supports agriculture in the Great Plains but is rapidly depleting. Nubian Sandstone Aquifer (Africa): One of the world's largest fossil aquifers, but non-renewable (United Nations, 2022). Ganges-Brahmaputra Basin (South Asia): Highly exploited for irrigation, leading to severe depletion (World Bank, 2019). Guarani Aquifer (South America): One of the largest renewable reserves, shared by Brazil, Argentina, Paraguay, and Uruguay (Hirata & Foster, 2020).

Groundwater is a critical resource in semi-arid environments, particularly in regions like sub-Saharan Africa, where surface water is often scarce and unreliable. In these areas, groundwater serves as a vital source of water for drinking, agriculture, and industrial activities, supporting livelihoods and economic development. Groundwater, stored in aquifers, provides a more reliable and resilient water source compared to surface water, which is highly susceptible to seasonal variations and climate change. The economic significance of groundwater are: Agricultural productivity, Drinking Water Supply, Industrial and Urban Use, and Climate Resilience: Groundwater provides a buffer against climate variability and change, ensuring water availability during periods of drought. Poverty alleviation: Access to groundwater reduces the time and effort required to fetch water, particularly for women and children, freeing up time for education and income-generating activities. Groundwater development projects, such as Well drilling, create employment opportunities and stimulate local economies.

Groundwater is the most important source of potable water in the globe comprising 20 percent of freshwater resources worldwide and 0.61% of all water(Kumar et al., 2021). Beneath the Earth's surface lies vast groundwater resources, totalling 30 times the volume of accessible surface water. However, most of these reserves are too deep to access cost-effectively and are at risk of overexploitation. More than 80% of the groundwater beyond a kilometer deep is considered "fossil water," over 12,000 years old. Utilizing this ancient water source is likely to deplete the aquifer.(Richter & D. Ho, 2022). Groundwater is essential for almost 40% of irrigated crop production and provides drinking water for over two billion people, as well as supporting nearly half of all freshwater ecosystems.

A decline in the water table caused by groundwater pumping can have a direct impact on surface water sources that are linked to the aquifer (Liu et al., 2020). This can harmfully impact the overall flow and diminish the physical condition of river ecosystems in rivers where base flow contributes a substantial percentage of the streamflow(Vainu & Terasmaa, 2016). Effective groundwater management requires reliable basic data about the utilization and replenishment of the groundwater, and this will be achieved by capitalizing on data collection, monitoring, and expert evaluation for a solid management plan.

2.2 Groundwater exploration method

The Analytical Hierarchy Process (AHP) is a structured decision-making methodology developed by Thomas L. Saaty in the 1970s, particularly useful in hydrogeological investigations for identifying groundwater Potential zones or evaluating water resource management strategies. It integrates multiple criteria and expert judgments to rank and prioritize alternatives based on their relative importance. The key steps of AHP in Hydrogeological Investigations: *Hierarchy Construction*: AHP organizes decision-making hierarchically, with the overall goal at the top (e.g., selecting a groundwater Potential zone), followed by criteria, sub-criteria, and alternatives. *Pairwise Comparisons*: AHP uses pairwise comparisons to evaluate the importance of criteria and alternatives on a scale from 1 to 9. For example, lineaments could be rated as "moderately more important" (3) than soil. *Consistency Check*: AHP ensures logical consistency by calculating a consistency ratio (CR). A CR above 0.1 indicates that revisions may be necessary. *Weight Calculation*: Pairwise comparison results provide weights for criteria and alternatives, reflecting their importance. *Synthesis of Priorities*:

The weights are aggregated to rank alternatives, with the highest weight representing the best choice.

Guduru & Jilo (2022) recognized Potential groundwater zones using a combined method that integrates RS, AHP, and GIS. Several variables were considered for groundwater recharge, including soil, slope, lithology, precipitation, drainage, lineament, and topographic moisture index (SLOPE)(Guduru & Jilo, 2022). Water table monitoring, Wells, electrical resistivity, and remote sensing data can be incorporated into GIS evaluation to determine groundwater partitioning. The resulting delineation of the groundwater Potential zones agrees with the currently available deep well yield data(Israil et al., 2006). It is significant but also challenging to study the physical relationship between surface and groundwater and its implications for resource control. Due to their different spatial and temporal behavior, sub-surface and surface water have been studied distinctly for a long ago. For effective water supply and management, their flow processes should be viewed as a single, integrated resource(B. Li et al., 2015), (Abbott & Refsgaard, 1996).

2.3 Water balance

The concept of water balance, water balance approaches, and water balance methods are interconnected components that together provide a comprehensive framework for understanding and managing water resources. The water balance concept is the foundational principle that water inputs, outputs, and changes in storage within a system must balance over a given period. Water balance refers to the equilibrium between the inputs, outputs, and storage changes of water within a defined system over a specific period. It is a fundamental concept in hydrology, environmental science, and water resource management. The water balance equation is typically expressed as: $P-ET-R-G=\Delta S$. Where: - P: Precipitation (input), ET: Evapotranspiration (output), R: Runoff (output), G: Groundwater flow (input/output), ΔS: Change in water storage. The equation ensures that the total water entering a system (e.g., a watershed, lake, or aquifer) is balanced by the water leaving the system and any changes in storage.

Water balance approaches refer to the conceptual frameworks or strategies used to analyze and model the water balance of a system. These approaches define how the system is

conceptualized, including its scale, spatial variability, and the level of detail in representing hydrological processes.

Key characteristics of Water Balance Approaches: - It focuses on how the system is structured and analyzed (e.g., lumped vs. distributed). It helps to provide a framework for understanding water inputs, outputs, and storage changes. For instance: -

- Lumped Approach: Treats the entire system as a single unit.
- Distributed Approach: Divides the system into smaller spatial units (e.g., grid cells or sub-basins).
- Process-Based Approach: Focuses on modeling individual hydrological processes (e.g., infiltration, evaporation).
- Empirical Approach: Relies on observed data and statistical relationships.
- Complexity: Varies from simple (lumped) to complex (distributed or process-based).
- Data Requirements: Depends on the approach (e.g., distributed approaches require more spatial data).

On the other hand, Water Balance Methods refer to the specific techniques or equations used to quantify the components of the water balance. These methods are applied within the framework of the chosen approach to calculate water inputs, outputs, and storage changes. Key characteristics of Water Balance Methods: The method focuses on quantifying specific water balance components (e.g., precipitation, evapotranspiration, runoff, storage changes), aiming to provide numerical estimates of water balance components. The data requirements depend on the method (e.g., Penman-Monteith requires detailed weather data). The complexity varies from simple equations (e.g., classical water balance) to advanced techniques (e.g., numerical modeling). For example:

- Classical Water Balance Equation: $P=ET+R+\Delta S$.
- Thornthwaite Method: Estimates evapotranspiration using temperature data.
- Penman-Monteith Method: Estimates evapotranspiration using meteorological data.
- Remote Sensing Methods: Uses satellite data to estimate water balance components.
- Isotopic Methods: Uses stable isotopes to trace water movement.

Szwed (2015) postulated that $P = H + E + \Delta R$, where P represents precipitation, H represents runoff, E represents evaporation, and ΔR represents storage change, can be used to express the

water balance formula. The equation P = H + E is the water balance formula, assuming storage remains constant (for a reasonably long period). The runoff is therefore calculated from the difference between precipitation and evaporation(Szwed, 2015). According to Dingman, (2015) the water balance equation for river catchment is given as: $P + GW_{in} - (Q + ET + GW_{out}) = \Delta S$. where P is precipitation, GW_{in} is groundwater inflow, Q is stream outflow, GW_{out} is groundwater outflow, and ΔS is the change in all forms of storage over the time period. Unless there are obvious reasons for thinking otherwise (e.g., melting of glaciers, construction of large reservoirs, large-scale water transfers in or out, extensive pumping and export of ground water), it is commonly assumed that water storage is not significantly increasing or decreasing over time, so that $\Delta S \approx 0$. And, because watersheds are topographically defined and groundwater flow is driven by gravity, we can often also assume that ground water and watershed divides coincide so that GW_{in} is negligible. With these assumptions, we can write: $Q + GW_{out} = P - ET$. The sum of streamflow and ground-water outflow is called runoff (R_O), i.e., $R_O = Q + GW_{out}$. However,(Nata et al., 2010) In their study, applied the water balance equation: P – ET – Q – I = 0, taking into account factors such as evapotranspiration (ET), infiltration (I), precipitation (P), and river runoff (Q). It is important to note that errors may occur in the measurement and calculation of water balance elements due to the limitations of the methods used. For a time series of 5-10 years, the change in storage(ΔS) can be disregarded.(Seiler & Gat, 2007). According to Gidafie et al.,(2019), and Melo et al.(2015),

Baseflow is the flow component in a river in which the reaction to rainfall occurs slowly and is usually associated with groundwater discharge (Eckhardt, 2008) Its determination is essential for the comprehension of the water budget and the relation between groundwater and surface water in a watershed(Borges et al., 2017). The hydrograph separation approach was used to calculate the amount of baseflow. Maintaining flow in streams and rivers depends largely on groundwater runoff, i.e., groundwater discharge into streams. The graphical separation method evaluates the baseflow amount(Poernomo et al., 2020).

2.4 Aquifer parameters and Dar–Zarrouk parameters

Groundwater investigation relies on understanding of several key aquifer parameters that influence the availability, and movement of groundwater. And, these parameters are essential for evaluating groundwater potential, designing effective well placement, and ensuring sustainable groundwater management. The most significant parameters include: Hydraulic

conductivity (K) which is the ability of an aquifer to transmit water. It is influenced by the porosity and permeability of the aquifer material. High hydraulic conductivity indicates that water can move more freely through the aquifer, making it more productive for groundwater extraction. Transmissivity (T) is the rate at which water flows through a unit width of the aquifer under a unit hydraulic gradient. It is the product of hydraulic conductivity and the saturated thickness of the aquifer. High transmissivity values indicate a greater capacity for groundwater flow, and a good potential for groundwater extraction. The storage coefficient (S) (or storativity) in confined aquifer represents the volume of water released from or taken into storage per unit surface area of the aquifer per unit change in hydraulic head. It is critical for understanding how much water an aquifer can store and release. Aquifer Thickness impacts aquifer's capacity to store and transmit water. Accurate measurements of aquifer thickness are important for resource estimation and well design.

However, proper groundwater investigation requires quality well data and ensures the determination of its amount, distribution, sustainable utilization, and management in the future. Groundwater exploitation that exceeds the recharge amount initiates undesirable impacts, such as mining of groundwater, and causes unsustainable aquifers. A lower value of aquifer transmissivity results in a higher drawdown at a pumping well. This relationship is inversely proportional (linear) for confined aquifers: decreasing the transmissivity (T) by a factor would increase the drawdown approximately by the same factor (Kresic, 2007). Transmissivity (T) and Hydraulic Conductivity (K) evaluations can contribute to aquifer vulnerability status since aquifers in areas/zones with higher T and K rates are, in general, more vulnerable to contamination, as they enable contaminant migration into the saturated zone.

Bhuiyan (2020) examines the benefits of using well productivity rather than yield, normalized yield or specific capacity for the estimation and confirmation of groundwater Potential (GWP), and recommends the use of these parameters. Furthermore, he concludes that productivity is a more meaningful variable for GWP because it compares the groundwater resources of different aquifers based on water yield rate and viability of groundwater resources(Bhuiyan, 2020). Graham et al. (2009) provided statistical summaries of aquifer productivity statistics, such as transmissivity (T), specific capacity (Sc), and Well yield, and showed the productivity of an aquifer. When transmissivity or specific capacity is unavailable, Well yield data can be a useful

indicator of aquifer productivity. However, he stresses that more reliable data is needed, especially for aquifers with very low or poor production(Graham et al., 2009).

Hydrogeological investigation can be done in different ways. For potential groundwater exploitation and sustainable groundwater management, precise hydraulic parameter values are essential preliminary data. In situ wells are important because realistic aquifer values are required to create simulation models for various management scenario assessments. Laboratory testing has disadvantages for obtaining reliable values of aquifer parameters; however, the well method provides more comprehensive information about hydraulic parameters of the well, aquifer, and aquifer boundaries all at once. The well is a vital method to determine the aquifer parameters such as hydraulic conductivity (K), transmissivity (T), and specific yield (Sy).(Hossain Khan et al., 2022),(Valigi et al., 2021), and (LANG., 1961). Akinfemiwa Akanbi (2023) emphasizes that to maintain long-term productivity, a proper understanding of the occurrence, transport, and recharge mechanisms of groundwater is required in hard rock areas. The development of groundwater recharge processes and the hydraulic characterization of water-bearing zones are crucial for long-term groundwater yield. The study uses single-well pumping and recovery testing to evaluate groundwater recharge and aquifer production.(Akinfemiwa Akanbi, 2023).

2.5 Application of geoelectrical investigation

Ullah et al.(2020) used pumping test data and a geophysical technique to define an aquifer system and accurately estimate aquifer parameters. If well data is not available, these parameters can be derived for areas with the same hydrogeological framework. To this end, pump test data and interpreted aquifer parameters are used to support an empirical relationship(Ullah et al., 2020). This was also studied by(Hasan et al., 2020), pump tests are a necessary procedure for measuring crucial parameters in wells. However, they provide little spatial information and are costly and time-consuming. A more economical and effective method for assessing aquifer parameters is to use an integrated approach that combines geophysical methods with pumping tests(Hasan et al., 2020). A Vertical Electrical Sounding (VES) geophysical survey is an essential tool in groundwater exploration and assessment. It is part of the Electrical Resistivity Method, which investigates subsurface geologic formations by measuring the resistance of earth materials to the flow of electric current. Vertical Electrical

Sounding (VES) is a dependable, effective, and widely adopted technique in groundwater evaluation. It plays a crucial role in locating and characterizing aquifers, estimating water table depth, understanding subsurface geology, and planning sustainable groundwater development. This method increases the success rate of Well drilling and supports integrated water resource management, especially in water-scarce or geologically complex areas(Osuagwu, 2024).

2.6 Pumping Test and Dar Zarrouk Parameters (DZP)

Initial pumping test data were used to determine the hydraulic conductivity (K) and transmissivity (T) of existing production wells. Empirical relationships were then established between Kw and aquifer resistivity (ρa) and between Tw and transverse resistance (Tr). This enabled the estimation of hydraulic conductivity (K) and transmissivity (T) for VES stations without pumping tests.(Hasan et al., 2020). Using the two important relations obtained from the integration of Darcy's law for horizontal fluid flow and Ohm's law of current flow in a medium, studies conducted by (Hasan et al., 2020),(Ullah et al., 2020), and (Chandra et al., 2009) demonstrated a convincing connection between geoelectrical and aquifer characteristics.

Pumping tests are essential in hydrogeology to determine the hydraulic properties of aquifers, such as transmissivity, storativity, and hydraulic conductivity. There are several types of pumping tests, each with its own advantages, limitations, and applications. Below is a comparison of the main types of pumping tests:

Constant-Rate Test: Water is pumped from a well at a constant rate, and the drawdown (decline in water level) is measured over time in the pumping well and observation wells. Most commonly used for determining aquifer properties for confined, unconfined, and leaky aquifers. And simple to conduct and interpret, and provides reliable estimates of transmissivity and storativity. However, constant rate test limitations require a steady pumping rate, which may be difficult to maintain, and a long duration may be needed to reach equilibrium (steady-state conditions).

Step-Drawdown Test: The pumping rate is increased in steps, and the drawdown is measured at each step. This test evaluates well performance and aquifer characteristics. This test type is used to assess well efficiency and well loss, and helps identify the optimal pumping rate for a well. Its principal advantages are to provide information on well performance (e.g., well loss and aquifer loss), and require shorter duration compared to constant-rate tests. The drawbacks

for this type of test are that it does not provide detailed aquifer properties like storativity and requires careful control of pumping rates.

Recovery Test: After pumping stops, the recovery of water levels in the pumping well or observation wells is measured over time. Its applications are to estimate aquifer properties after a pumping test and can be conducted after a constant-rate or step-drawdown test.

The advantages of a recovery test stem from its simplicity: (1) a recovery test follows naturally from a pumping test, because it only requires the recording of heads after pumping has ceased; (2) it can be used even when pumping rates are difficult to control; (3) it is fairly inexpensive and no equipment or additional observation wells are required apart from a water-level measuring device; (4) provides reliable estimates of transmissivity, and (5) results are usually not sensitive to well losses. However, they require prior pumping to induce a drawdown and less effective for estimating storativity. The analysis of a recovery test follows the Theis solution to pumping a fully penetrating well of zero radius in an infinite, homogeneous aquifer. In recovery tests, heads are usually observed at the pumping well, so that r is the well radius. Interpretation of recovery tests using the simple Theis recovery method can provide valuable information about representative parameters in heterogeneous aquifers, even though the method was developed for homogeneous media (Willmann et al., 2007 , and Sindalovskiy, 2017).

Table 1. Comparison of pumping tests

No	Test Type	Duration	Complexity	Cost	Primary Use
1	Constant Rate Test	Long	Low	Moderator	Aquifer property estimation
2	Step-Drawdown Test	Short to Moderator	Moderator	Moderator	Well performance evaluation
3	Recovery Test	Short	Low	Low	Transmissivity estimation

The numerous variables that affect an aquifer's Potential yield are carefully outlined by Ali et al. (2022). These variables include recharge and depletion characteristics, long-term variations in the static groundwater level, hydrogeologic features, and the groundwater basin's safe yield. To effectively manage and investigate groundwater resources, the article emphasizes the necessity of lithological data and quantitative hydrogeological studies. It also details various methods for calculating the aquifer characteristics and underlines the magnitude of the most prevalent and reliable technique(Ali et al., 2022).

An empirical correlation equation will be developed using electrical resistivity and aquifer parameters to estimate hydraulic conductivity (K) and transmissivity (T) across the UBRB. Based on Darcy's law and Ohm's law, two key parameters—longitudinal unit conductance (Sc) and transverse unit resistance (Tr)—are derived. Sc is the layer thickness divided by resistivity, while Tr is the product of thickness and resistivity. And these parameters known as Dar Zarrouk Parameters (DZP), introduced by Maillet (1947), these form the basis for the correlation. DZP are calculated from interpreted aquifer resistivities and thicknesses(Khalilidermani et al., 2021),(Hasan et al., 2020), and (Soupios et al., 2007).

2.7 Well-yield Challenges and Well efficiency

Step-drawdown test evaluation is a common step in the investigation of well-yield challenges for particular basins to measure well efficiency. This test can clarify the relationship between a well's drawdown and discharge. Inadequate prior well development and unrealistic step-drawdown test protocols can have a major impact on the consistency of transmissivity values computed(Alam, 2007).

Numerous studies such as Ha et al.(2019), Zech et al.(2015), Avci et al.(2010), and Clark(1977) carefully analysed and evaluated step drawdown test data to establish an optimal testing program and comprehensive test analysis. The step drawdown test is a useful method for determining aquifer permeability and the wellhead losses component of the drawdown of a well. They can also be applied to estimate the storage coefficients of aquifers. When a pumped well sinks, well loss and aquifer loss are the two main causes. Well, losses are caused by resistance to turbulent flows near the well and through the screen, whereas aquifer losses are triggered by the struggle to laminal flows inside the aquifer(Clark, 1977). In certain circumstances, partially penetrating wells must be used for pumping, as fully penetrating wells are impractical due to the thickness of certain aquifers. However, the induction of vertical flow components near the well as a result of partial penetration invalidates the assumption that the well draws water only on horizontal flow (Boonstra, 1992).

Step-drawdown test method analysis is a commonly used technique for evaluating well performance. It provides insightful information about the hydraulic head losses caused by pumping in production wells. This is critical for decisions such as choosing a permanent

pumping system and routinely reassessing the effectiveness of wells (Karami & Younger, 2016). The effectiveness of a production well in extracting water from an aquifer is largely influenced by its design. Well loss can result from factors like disturbances during drilling, improper development (e.g., leaving drilling fluid or mud cake in the well), or poorly designed gravel packs and screens. Evaluating well loss is essential to determine performance. Over time, all wells will experience decreased efficiency, or well aging, indicated by an increase in well loss. The three-step pumping test is essential for quantifying well loss and should be conducted after well completion and periodically during operation to assess performance and determine the need for rehabilitation. Drawdown behavior is influenced by factors like aquifer type, well effects (well losses and wellbore storage and partial penetration), and boundary conditions (barrier or recharge boundaries). To identify an aquifer system, its drawdown behavior is compared to theoretical models, with the closest match used for calculating hydraulic parameters (Kruseman and de Ridder, 1990).

Drilling water wells without sufficiently considering the site-specific hydrogeological conditions can result in significant well-yield challenges, including partial penetration, inadequate well design, and poor development. It is essential to understand that these drilling challenges negatively impact well productivity and efficiency, and this effect needs to be thoroughly examined. For example, partial penetration happens in an aquifer with thickness b when a well has a screen or open interval of length L. If the dimensionless screen length L/b is less than 1, the well is considered partially penetrating(Driscoll, 2007). The well efficiency factor, which is typically expressed as a percentage, and defined as $\{[BQ/(BQ + CQ^2)]*100\}$(Alam, 2007).

2.8 Previous studies

Yehualaw et al.(2023) conducted magnetic and VES methods for mapping the aquifer system and groundwater resources of Central Ethiopian Rift in detail. The VES used to determine the possible groundwater depth and its spatial occurrence in the region. And, the magnetic investigations used to map the interface between lithological units and geological structures(Yehualaw et al., 2023). The results of the study revealed subsurface weak zones and vertical stratum of the subsurface geoelectric layers, both have significant impacts on groundwater movement and accumulation systems. The feasible water bearing formation in the

area was found to be 45-92 meters below the surface. However, the work did not address whether the results can be compared to currently available reliable drilling data, given the complex geomorphological features of the study area. Water industry experts are discussing this topic.

For the precipitation-runoff analysis, Genjebo et al.(2023) also used the Hydrologic Engineering Centre Hydrologic Modelling System (HEC-HMS) to estimate surface water resources of the upper Bilate watershed and select the optimal apportionment for different needs. The study calculated annual environmental demand is 75.32 MCM or 15% of the average yearly overall surface water of the watershed (502 MC M). The study showed 99.8 % of the water supply need can be met from the watershed for considered scenario, and only 0.2 percent of water needs are not yet met(Genjebo et al., 2023).

Bitsiet & Dessie (2018) measured groundwater recharge in the upper Bilate catchment using WetSpass, a physically based distributed recharge model. While the average annual recharge was nineteen percent, direct runoff was responsible for nineteen percent of the rainfall in the catchment(Bitsiet & Dessie, 2018). In addition, JICA, Kokusai Kogyo Co.(2012) conducted an important study to assess groundwater sources in the Rift Valley Lake Basin (RVLB). Due to the lack of data, the work is unable to fully utilize advanced pumping analysis methods to determine the aquifer properties(JICA, Kokusai Kogyo Co., 2012).

Tesfaye Tessema (2010) utilized an integrated GIS and RS to describe groundwater resources in Bilate River Basin. He produced a groundwater potential zone map with the distribution of Wells and springs having a maximum discharge of 6.25 lit./sec. considered as a high groundwater potential zone, which does not support the existence of the recently developed deep wells that yield 60 lit./sec. in the same groundwater probable zone. Indeed, the researcher included the limitation stating that "The precise Potential yield of the wells could not be ascertained from the point discharge data. This could be because of inadequate pumping test analysis and the use of an under capacity pump"(Tesfaye Tessema, 2010). On the other hand, Sintayehu Legesse (2009), studied the upper Bilate River Catchment. The study's objectives were to evaluate the Upper Bilate catchment's hydrogeological system and characterize the aquifer, with an emphasis on groundwater Potential study, recharge characteristics, and

surface-subsurface water interaction. Pumping test analysis show that hydraulic conductivity of upper Bilate River Catchment ranges 0.17 - 8.8 m/day. However, the study was limited by insufficient well data, as although wells had yields of up to 50 lit./sec. were reported, but the maximum well yield of the study area was only 10 lit./sec (Sintayehu Legesse, 2009).

According to Abebe, (1999), drilling problems and their underlying causes are inherently complex and often identified through speculation, as they occur deep beneath the surface. The most prevalent drilling challenges include: Loss of circulation, - Hole collapse (cave-in), - Bridging in wells, - Crookedness or deflection of wells, - Pollution and corrosion, - Mud cake formation, - Stacked tools. Additionally, other factors that may contribute to problems during well completion encompass: - Poor well design, - Careless casing and screen lowering, - Bridging during gravel packing, - Inadequate well development, - Negligence during pump installation, - Insufficient grouting and sealing of the well, - Poorly organized pumping tests, - Suboptimal well spacing.
(Abebe, 1999). And finally, remarked that the primary causes of drilling and completion problems can be categorized as follows: 1. Poor technical performance, 2. Unfavourable geological conditions, and 3. Technological defects (Abebe, 1999).

The main focus of all previous works has been on evaluating groundwater probable zones over the combination of GIS and RS data, as well as recharge estimation using WetSpass, These assessments have been validated with the available well data, ignoring issues that affect the effectiveness of well yield discrepancies located within the same hydrogeological frameworks. Ethiopia's major groundwater resources are located in fractured volcanoes covered with thick Quaternary graben sediments and fluvial gravels, as well as weathered, structurally deformed volcanoes in highland paleosols. The faulty and relatively permeable unconsolidated deposits in the rift and intermountain valley fill are responsible for the most promising aquifers. Ethiopia has complex aquifer systems consisting of Quaternary sediments and volcanic terrain. The location of plateaus, mountain ridges, and rift valleys influences the spatial distribution of groundwater.

Hailu (2015) effectively identified feasible sites for groundwater investigation in the northern Raya Valley of Ethiopia by combining RS and GIS. This required a thorough analysis of

thematic layers based on geology, geomorphology, lineament, drainage, slope, rainfall, and land use/cover. A multi-criterion ranking system based on GIS and Saaty's AHP used to precisely calculate rank and weights of thematic maps. However, it is vital to remember that this procedure of recognising the ideal locations for well drilling requires in-depth hydrogeological and geophysical studies within the established zones(Hailu, 2015). The topography, structural relationships, compositional diversity, and varying degrees of weathering of the Rift Valley and the UBRB further complicate this hydrogeologic framework(Ayenew et al., 2008)

3 DESCRIPTIONS OF STUDY AREA

3.1 Location and accessibility

The Upper Bilate Sub-Basin is located in the Main Ethiopian Rift Valley, mainly within Central Ethiopia and partly in South Ethiopia and Oromia Regional States. It spans coordinates 365008–423751E and 761063–896847N, covering an area of 3,357.9 km² with a 669.35 km perimeter.

3.2 Topography

The Bilate River basin's average annual rainfall varies significantly due to topography which is shaped by geological structures. The rift-controlled drainage system reflects these features. Extension styles in the UBRB align with stages of rift evolution. The absence of axial volcanism and boundary faulting suggests the southern MER is in an early rifting stage. Conversely, the northern MER is on the verge of breakup, as evidenced by concentrated tectonic-magmatic deformation at the rift axis and dormant rift margins(Molin & Corti, 2015). In highland areas, the streams follow a route synchronous with the underlying geological structure, while in flat areas, they assume the shape of intricate drainage patterns resembling dendritic type(Figure 2)(Haji et al., 2018). The study area lies within the Rift Valley Lakes Basin (RVLB), where rift-related tectonic faulting has exposed pre-rift (Oligocene–Miocene) volcanic rocks along the escarpments, shaping the region’s physiography. The Upper Bilate Basin is mainly located between the Damota and Silte-Guraghe escarpments, on the southern edge of the Main Ethiopian Rift (MER), near its boundary with the central MER, stretching from Arikit town in the north to Lake Abaya's northern shore in the south.

3.3 Drainage

The complex interactions between geomorphological processes and volcano-tectonic activity shape the river basin's drainage patterns. The primary processes that shape the terrain are erosion and deposition, which are impacted by the dynamic interactions between tectonic and volcanic activity. The study area characterized by primarily dendritic, with minor local influences of radial drainage in elevated parts, this indicates erosion over homogeneous lithology with localized structure of volcanic topographic control.

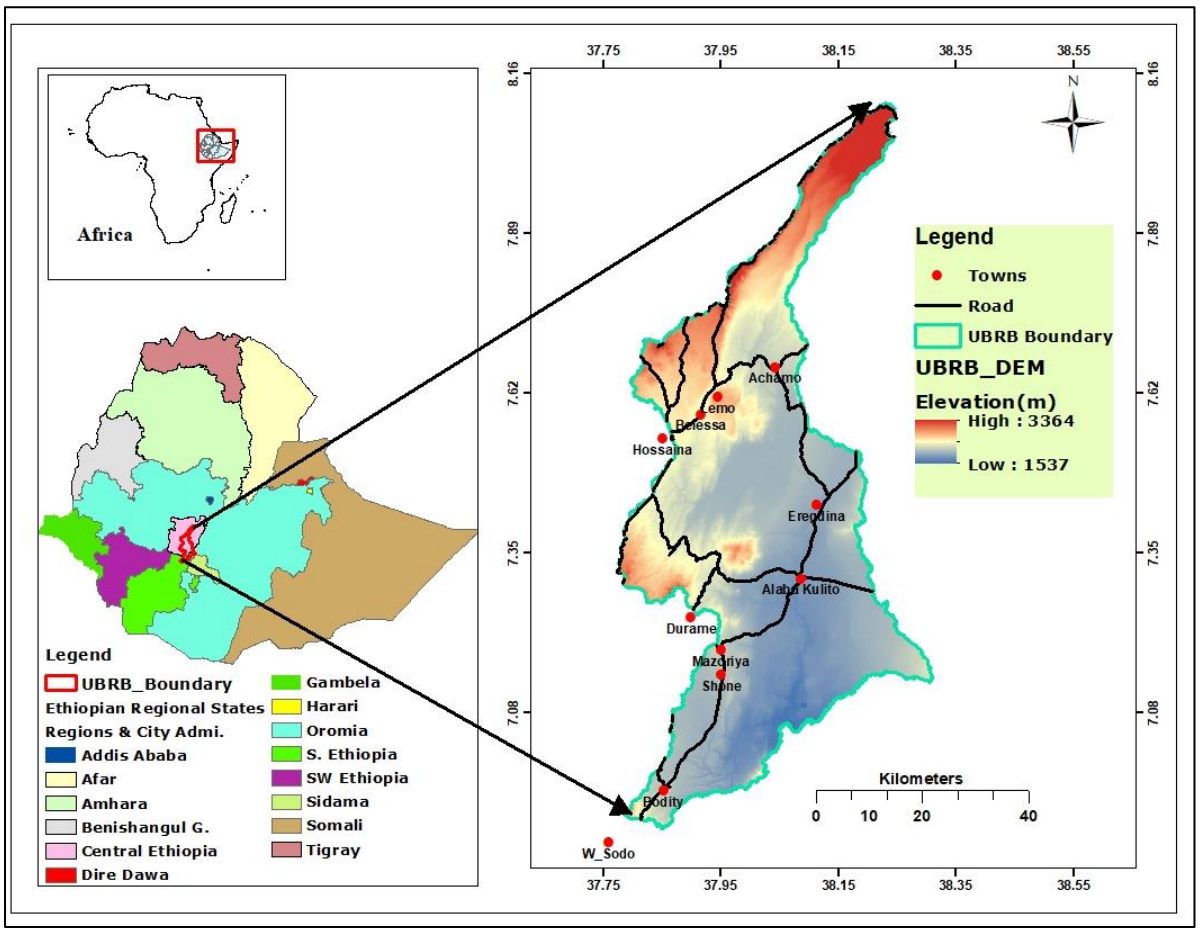

Figure 1. Location map of Upper Bilate River Basin

3.4 Climate

The climate varies from semi-arid on the rift floor to humid on the western escarpment, and highlands. Key topographic features include the rift floor, escarpments, and highlands, with elevations ranging from 1,600 to 3,300 meters above sea level. Rainfall in the basin varies in amount and intensity due to the tropical bimodal distributed precipitation pattern, which ranges from semi-humid to arid. Rainfall is the main factor in the water budget and the natural source of recharge. Variations in recharge rate are primarily caused by weather conditions. To take advantage of the water balance, the idea of potential evapotranspiration must first be understood(Thornthwaite & Mather, 1955). Measuring and computing rainfall is crucial because it is the primary cause of moisture on the lithosphere. The reliability of this process largely rests on its accuracy. Rainfall also significantly impacts surface water flow, recharge characteristics, infiltration, and groundwater Potential(Magesh et al., 2012). The distribution

and the volume of rainfall have a substantial influence on the basin's recharge(Rehman et al., 2024). The source of surface and groundwater in UBRB is rainfall

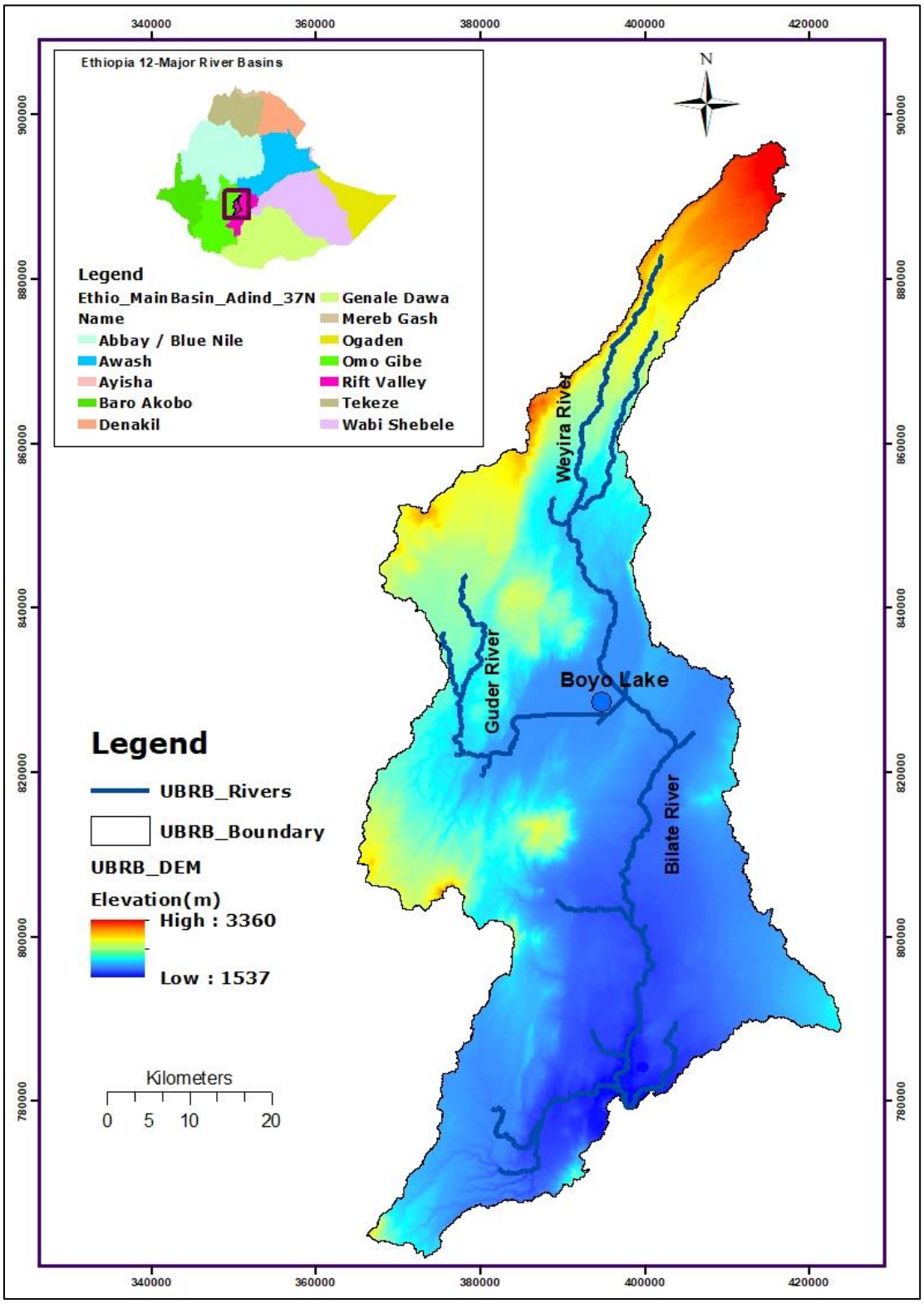

Figure 2. The drainage pattern of the Upper Bilate River Basin

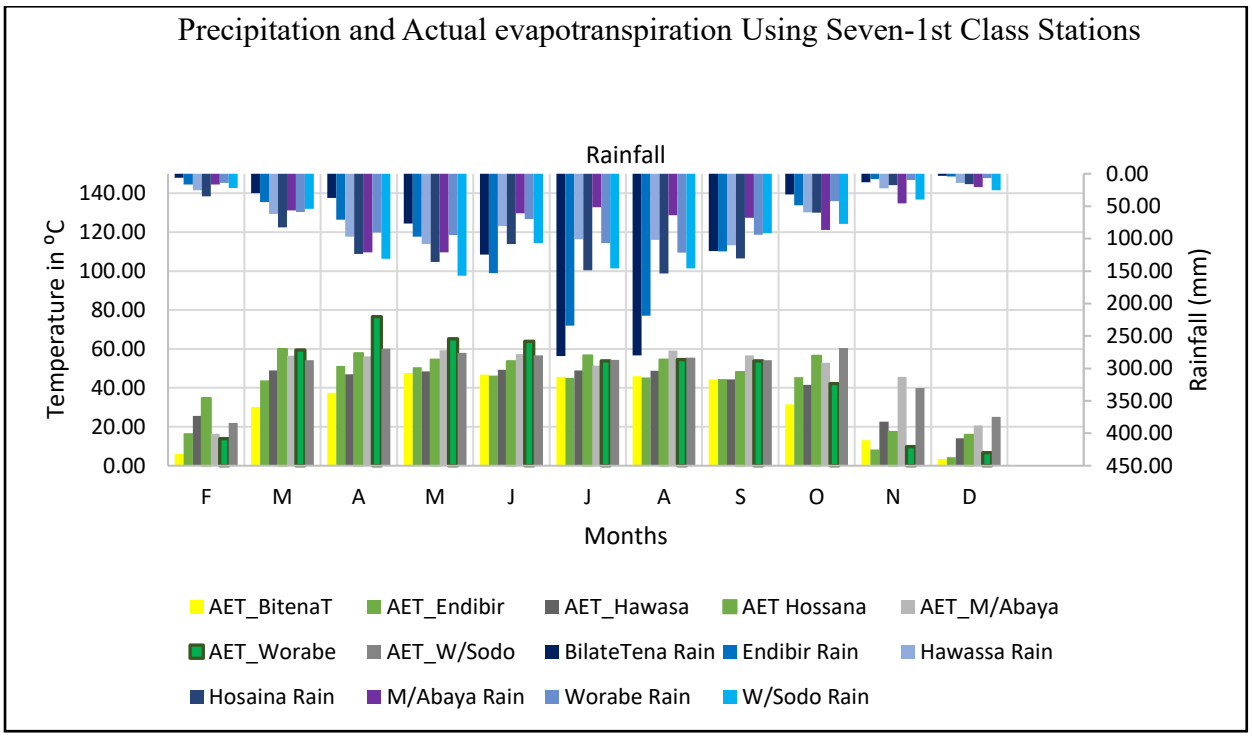

Figure 3. Graph of mean monthly Rainfall & Actual evapotranspiration.

3.4.1 Geomorphological features

Geomorphological analysis is essential in hydrogeological investigations for identifying groundwater potential and recharge areas. Landform characteristics influence soil properties and erosion processes, affecting groundwater recharge primarily through rainfall infiltration and soil permeability. Shallow profiles and clay-rich formations often lead to high surface runoff, limiting recharge, while gently sloping landscapes promote better groundwater replenishment (Meijerink et al., 2007). In the Upper Bilate River Basin (UBRB), the groundwater behavior of the region is influenced by its diverse landforms, including mountains, escarpments, pediments, the rift floor, bajadas, maars, and the swampy lowland near Boyo Lake. Boyo Lake, which is fed by the Guder River and drained by the Fofo River, contributes to the Bilate River system, along with the Weyra and Konkoye rivers. The Boyo River system acts as both a discharge area for upstream regions, where surface-water accumulation promotes groundwater emergence, and a recharge area downstream, where river and lake infiltration supports aquifer replenishment. Surrounding landforms impact soil deposition and runoff, regulating groundwater recharge and discharge patterns.

- **Western escarpment and mountains:** This landform features complex canyons, mountain ridges with intermittent streams, steep escarpments, and gently sloping areas, some covered in volcanic ash. Road and river cuttings reveal pyroclastic volcanic rocks. The dendritic drainage pattern indicates a relatively uniform underlying geology.
- **Pediment**: - The gently sloping surface is an erosional feature that emerges uphill from a bajada as the mountain fronts withdraw. These features are generally underlain by solid rock.
- **Bajada**: -Individual alluvial fans merge to form a gently sloping bajada—a depositional landform common in areas like the Woyira Dijdo kebeles, potentially serving as a groundwater source due to thick sediments. Maars are broad, shallow volcanic craters formed by explosive magma–groundwater interaction and often become shallow lakes.
- **Swampy lowland: -** Bilate river located in Humbo Woreda in the Wolaita Zone and have distinctive topography. These rivers flow into Abaya Lake and have a very shallow water table, suggesting a region where groundwater is leaking.

Figure 4. Budameda maar around Shone Town.

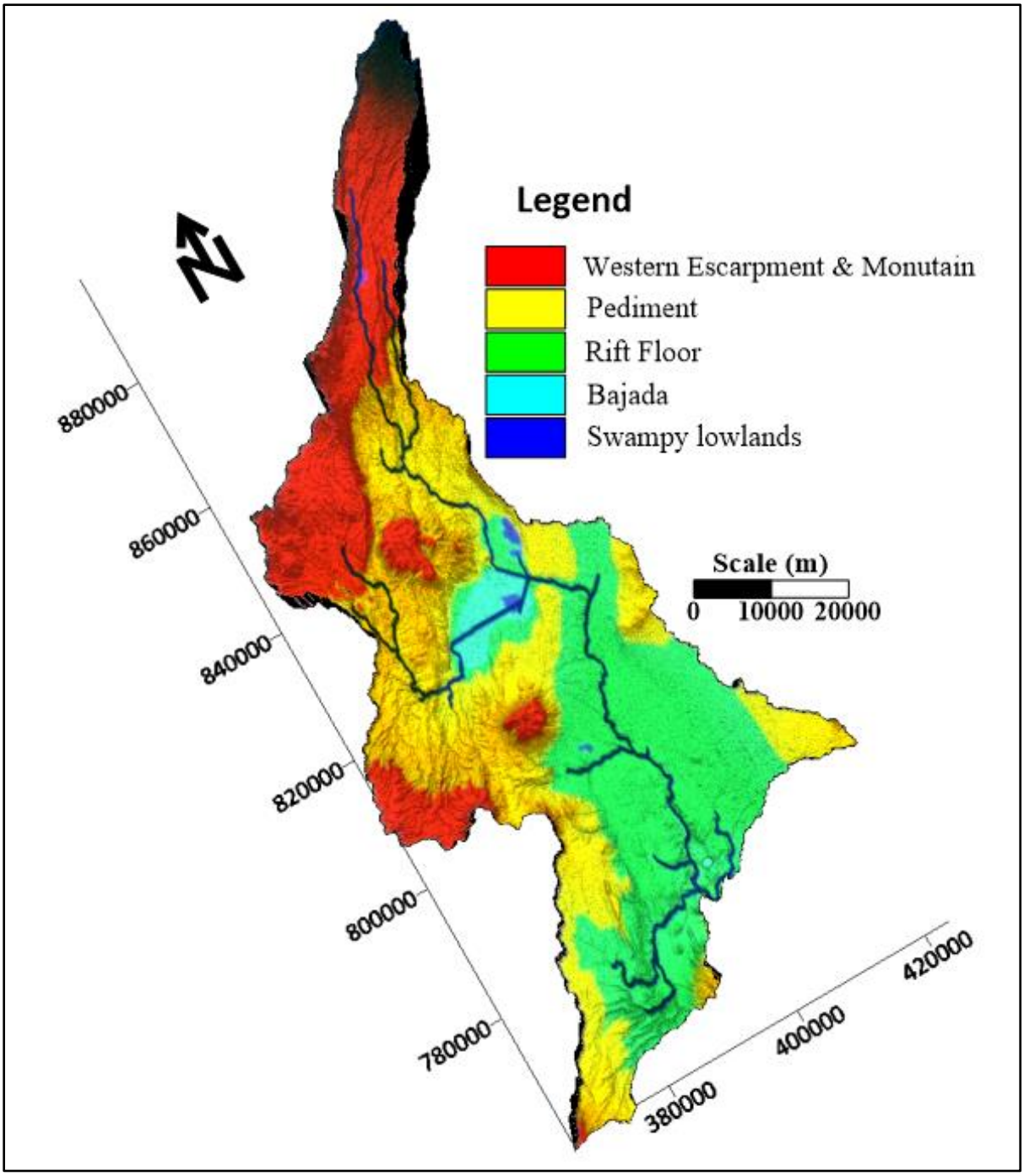

Figure 5. Geomorphological features of UBRB.

3.5 Regional geology

The regional geological units are described based on existing maps and reports of the geological map of Dilla Map Sheet NB37-6;2012, Hosaina Map Sheet NB37-2;2012, and Akaki-Beseka Map Sheet NC37-14;2009,] with 1:250,000 scale and field mapping from 2012. The study area includes Tertiary, Pre-Rift, Late Tertiary, and Quaternary Volcanic Rocks (Wonji Group), along with Quaternary Sediments.

Tertiary Volcanic Rocks (Nazret Group, undifferentiated – Upper Miocene to Pliocene) are widespread in the northwest and northeast. Outcrops appear along the Galena, Wabe, Bale, Dame, and Kulu rivers near Mt. Damote. The unit includes ignimbrites, rhyolites, basalts, and tuffs, with fresh ignimbrites ranging from light gray to brown due to weathering.

Pre-Rift Volcanic Rocks: - Alaji group (OMV) consists of basalt, trachy-basalt, trachyte and rhyolite. It is exposed on all sides of the Gibe gorge in the northwest part of the Hosaina Map Sheet NB37-2;2012. The dominating rock type is highly fractured aphanitic basalt and is found underlying the rhyolite. The base of the basalt is obscured by Holocene deposits of the Gibe River. The trachyte is found mostly on the western side of the Gibe River section. It is highly weathered, fractured and cut by frequent basaltic dykes.

Late Tertiary Volcanic Rocks: -This units contain Nazret group: (N1-2n), and (N1-2ar) consists of stratified silicic rocks—ignimbrites, unwelded tuffs, ash-flows, rhyolites, and trachytes (N1-2n)—widely covering the eastern rift escarpments near Munesa. On the rift floor, they are unconformably overlain by younger Dino Formation volcanics. Over 400 m of Nazret pyroclastics were encountered in a geothermal well at Aluto (Abebe, 1984; EIGS-ELC, 1985, and others). Silicic pyroclastic rocks mainly consist of ignimbrites, with minor trachyte lavas, trachytic tuffs, basalt, alkali trachyte flows, and sediments—exposed up to 500 m on the escarpments—and likely part of the Nazret Formation. Bofa Basalts (Nbb) overlay the Nazret group, the Bofa basalt is of fissural flood basalts which was named after its type locality at Bofa village outside the study area. It is considered to represent the upper part of the stratoid basaltic succession of the Afar Group younger than 4.5 Ma (Kazmin et.al., 1980 as cited in *Hosaena mapsheet*, 2012). Nazret Group and Dino Formation undifferentiated (NQs): The silicic rocks of the Dino Formation are not only confined to the rift floor but are extensively developed in escarpments and on the adjacent plateau where they could not be separated from the silicics of the Nazret Group, they were mapped as Nazret Group and Dino Formation undifferentiated (NQs).

Quaternary Volcanic Rocks / Wonji Group: -The latest volcanism in the Ethiopian Rift is related to the axial extensional zone, referred as the Wonji Fault Belt (Mohr, 1967 a, b, and Meyer et al. (1975) as cited in (*Hosaena mapsheet*, 2012) introduced the Wonji series for the volcanic rocks of the rift younger than 1.6 Ma that are related to the Wonji fault belt. The Pleistocene volcanism, however, is not confined to the Wonji Fault Belt only, but that it also occurred in other parts of the rift (Kazmin and Seife, 1978). On this account Kazmin and Seife M, (1978) changed Wonji series to Wonji group. The Wonji Group includes the entire rift volcanic formed after the last major event of rift faulting, following the accumulation of the Bofa basalts (Nbb) described before. Three main complexes are identified within the group (Kazmin and Seife M, 1978; Kazmin et. al., 1980) as cited in(*Hosaena mapsheet*, 2012). These are (1) stratoid silicic volcanics of the rift floor and shoulders, named as Dino Formation, (2) pantelleritic products of central volcanoes, and (3) fissural basaltic eruptions (basalts of the rift floor).

Quaternary Sediments: - This units represented by Volcano-Sedimentary Rocks (Qvs) and Lacustrine sediments (Ql). *Volcano-Sedimentary Rocks (Qvs):-* Lacustrine sediments intercalated with volcanics mainly ashes and tuffs, which in places are extensively developed and the sequence is shown as volcano-sedimentary (Kazmin et al., 1980 as cited in (*Hosaena mapsheet*, 2012). It is exposed at East of Shone town covering large area. *Lacustrine sediments (Ql)*:- are intercalated with Pliocene to Pleistocene ignimbrites and primarily consist of volcanic materials like pumice, ash, obsidian, rhyolite, and basaltic fragments. *Alluvial deposits (Qa):* - include gravels, sands, and silts forming alluvial fans at river entries into Lake Abaya.

Notably, the Bilate River's large delta is on Lake Boyo's northern edge, with a significant alluvial plain to the north of Arba Minch. Local geological map of UBRB (Figure 6) is prepared adapting from Geological Map of Dilla Map Sheet NB37-6;2012, Hosaina Map Sheet NB37-2;2012 and Akaki-Beseka Map Sheet NC37-14;2009,] with 1:250,000 scale.

3.6 Local geology

Based on Hosaena mapsheet, (2012) the geology of the study area and around the basin is divided into three major groups of rock units: - 1-Pyroclastic rocks (Ignimbrite and Tuff with minor obsidian), 2- Central Volcanic Complex (Rhyolite and Trachyte), 3- Fluvial Sediment (Unconsolidated). 4- Volcanic and Volcano-Sedimentary Formation.

Pyroclastic Rocks (Ignimbrite and Tuff with minor Pitchstones/Obsidian) units are widespread surficial in the UBRB of ash with white tuff mainly. In addition, in sub-sirface, outcropped in road, river exposure, and well lithological logging these units are the dominant lithological units Figure 6.

Central Volcanic Complex (Rhyolite and Trachyte) formation is scattered in elevated area of the study area showing a complex mixture of ignimbrite, tuff, and ash. In the central part of the study area and around Duguna-Fango Area, and Mout Damota. This formation is dominated by rhyolite and trachyte with minor pyroclastic fall deposit (ash) and unwelded tuff. These relatively weathered, fractured rhyolite and trachyte, tuff have a domed and high rugged topography. These rocks form a large section of the surface water divides of the Study area. They cover the minor part of the study area. Areas occupied especially by fractured and weathered ignimbrite and tuffs form flat to gently sloping topography favorable for recharge.
Volcanic and Volcano-Sedimentary Formation is volcanic and volcano-sedimentary rocks are associated with the main rifting events. The most important geologic units are alluvial and rare lacustrine sediments with interbedded pyroclastic and rare basalt with flow.

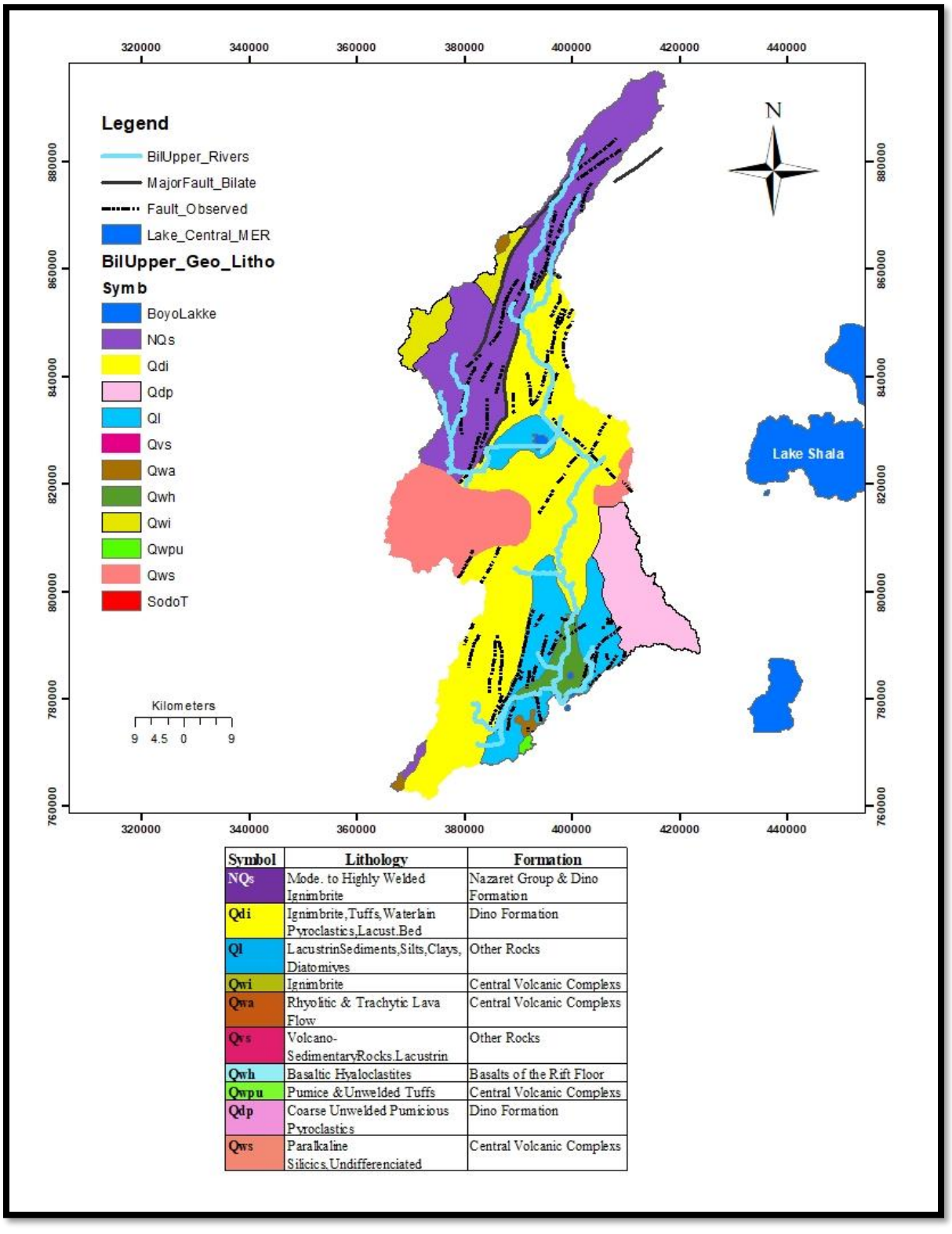

Symbol	Lithology	Formation
NQs	Mode. to Highly Welded Ignimbrite	Nazaret Group & Dino Formation
Qdi	Ignimbrite,Tuffs,Waterlain Pyroclastics,Lacust.Bed	Dino Formation
Ql	LacustrinSediments,Silts,Clays, Diatomives	Other Rocks
Qwi	Ignimbrite	Central Volcanic Complexs
Qwa	Rhyolitic & Trachytic Lava Flow	Central Volcanic Complexs
Qvs	Volcano-SedimentaryRocks.Lacustrin	Other Rocks
Qwh	Basaltic Hyaloclastites	Basalts of the Rift Floor
Qwpu	Pumice &Unwelded Tuffs	Central Volcanic Complexs
Qdp	Coarse Unwelded Pumicious Pyroclastics	Dino Formation
Qws	Paralkaline Silicics,Undifferenciated	Central Volcanic Complexs

Figure 6. Geological map of the Upper Bilate River Basin area

Source: Geological Map of Dilla Map Sheet NB37-6;2012, Hosaina Map Sheet NB37-2;2012 and Akaki-Beseka Map Sheet NC37-14;2009,] with 1:250,000 scale.

3.6.1 Determining subsurface lithology from well logs

The local lithology of the study area was mapped using data from lithological well logs (Figure 8 and Figure 9).and and descriptions of rock exposures found along roads, riverbanks, and in quarries(**Error! Reference source not found.**) .The lithological units that dominantly define t he UBRB are pyroclastic rocks (Ignimbrites, Pumice, Tuffs, Ash, flows), and volcanic rocks (Basalt, Trachy Basalt, Tachyte, Rhyolite, and Obsidian) constitute a considerable portion of the target area.in addition to these, there are also volcanic sedimentary deposits (alluvial and rare lacustrine sediments with interbedded pyroclastic and rare basalt with flow) at different corners of the study area.

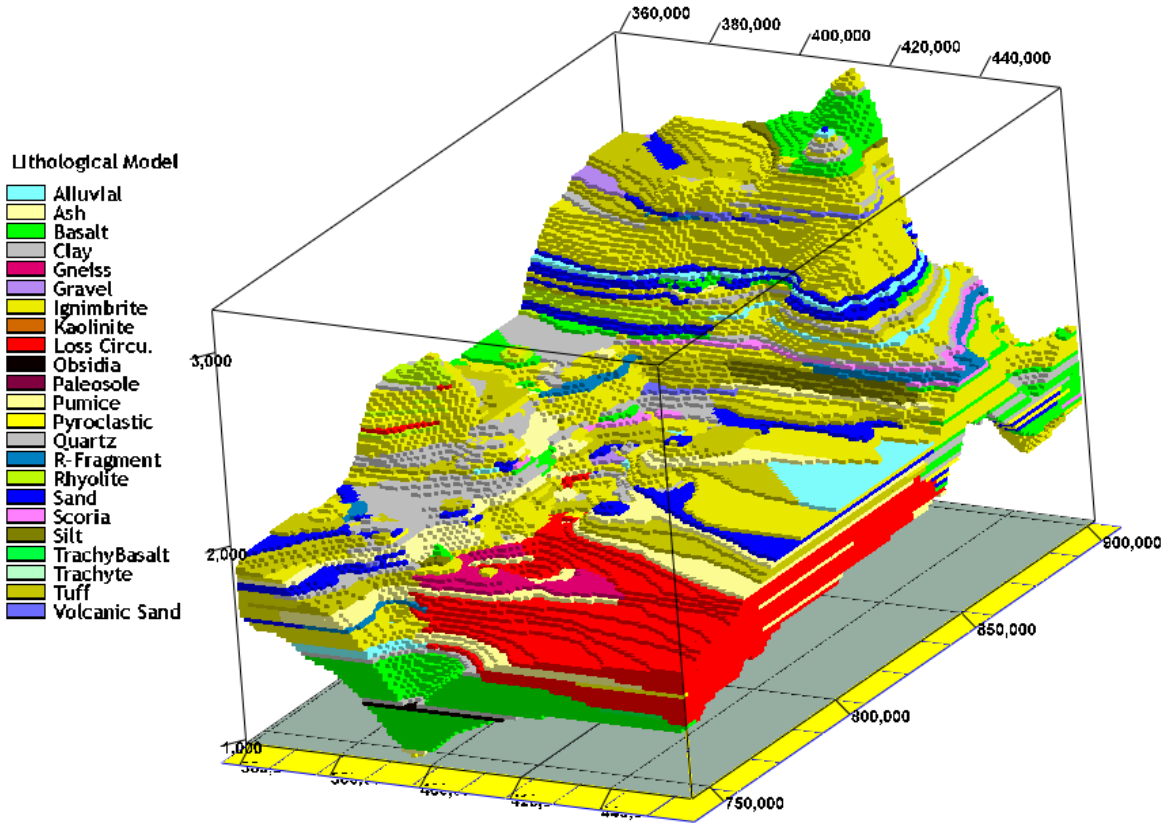

Figure 7. 3D Lithological units Model of in and around UBRB

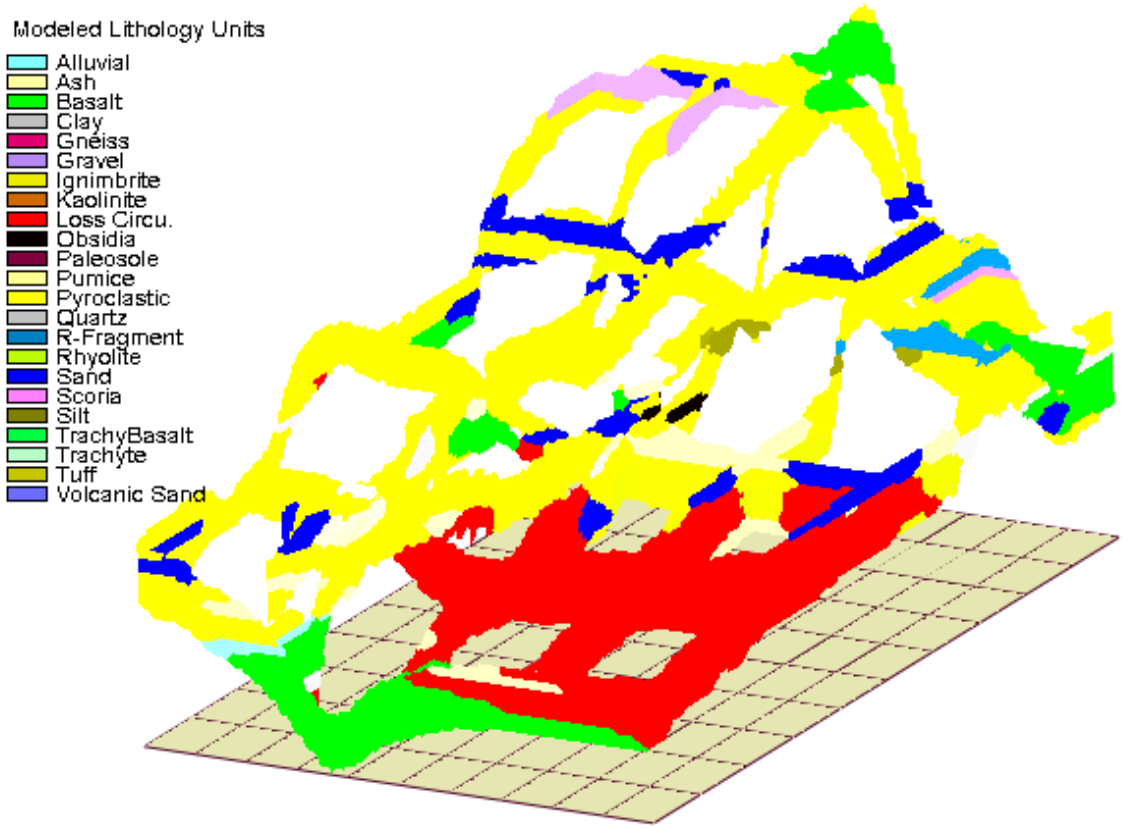

Figure 8. 3D Lithological units Model -Fence diagram for UBRB

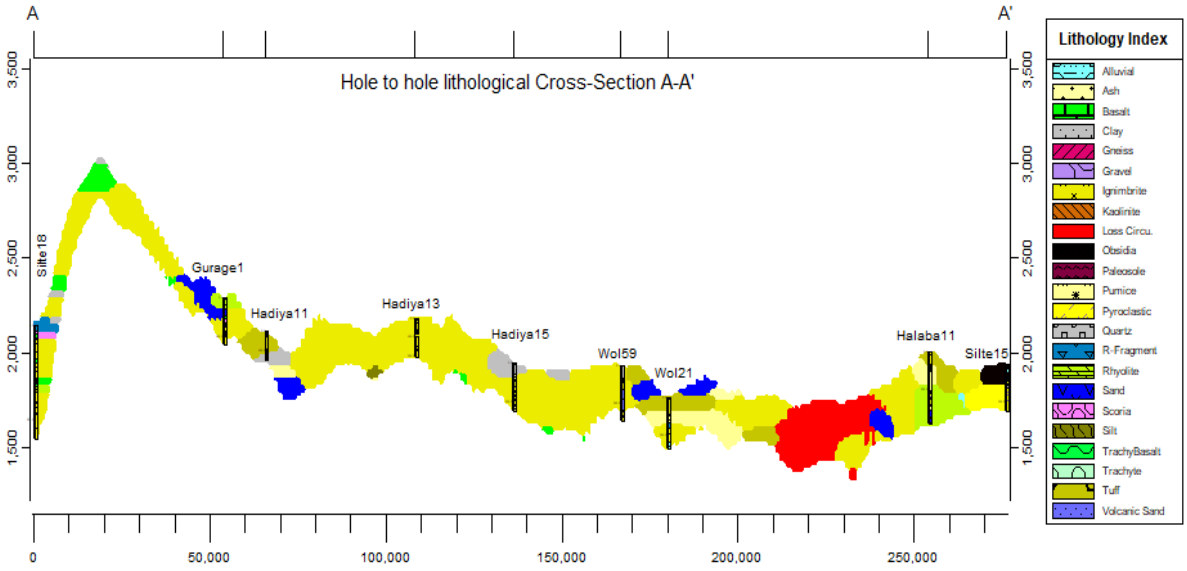

Figure 9.Lithological Cross-Section of UBRB fot A-A′

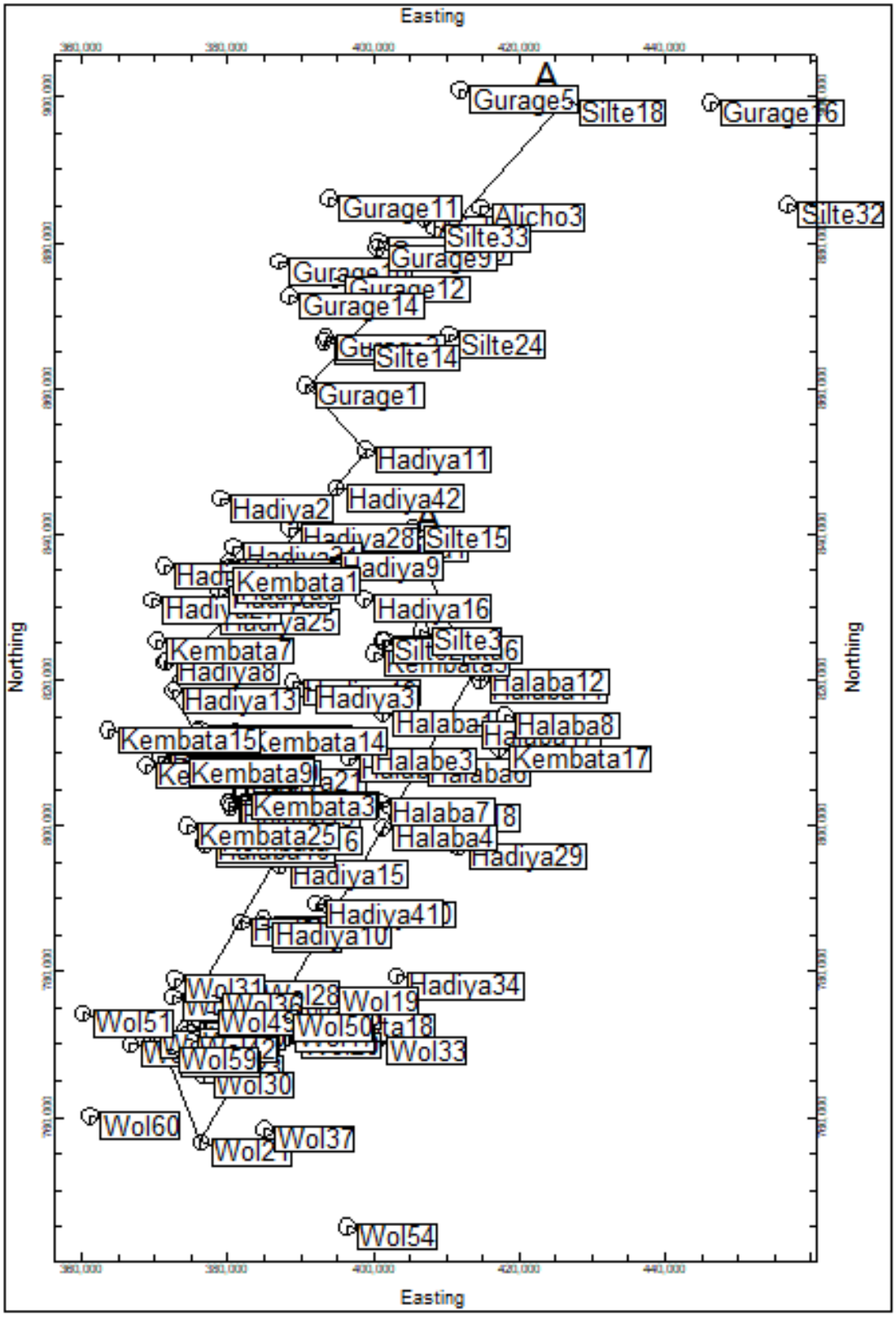

Figure 10. Section traverse map for lithological section

Figure 11. Pitchstone rocks are overlain by dino formation (B&C), obsidian is overlain by tuff (A). and ash of the dino formation (D), ignimbrite (E).

3.7 Geological structures of UBRB

The Main Ethiopian Rift constitutes an area characterized by active extensional tectonics with an E–W oriented direction of extension. Two main fault systems have been identified in the MER: an N30E–N40E trending fault system which characterizes the rift margins, and an N–S to N20E trending fault system, the Wonji fault belt (WFB), which shows several sigmoidal, overlapping, right stepping en-echelon fault zones obliquely cutting the rift floor. The margins of the MER are characterized by a few widely spaced faults with very large vertical displacements to the rift floor. The eastern margin is well developed and is defined by a more or less continuous system of boundary faults, whereas the western border is marked by a few major faults of the Mt. Gurage area. The MER attains a width of about 100 km in the central sector, between Fonko and Lake Langano, but narrows southward in the Lake Abaya region, where it is bifurcated by the N–S striking Amaro horst. In the study area boundary faults are developed in Late Miocene-Pliocene and characterized by quaternary deformation (Corti et al., 2013). Large-scale normal block faulting has disrupted the volcanic rocks. The rift valley is distinctly separated from adjacent plateaux by a Series of step faults usually trending parallel and sub-parallel to the rift axis. There are at least four sets of faults; NNE-SSW, N-S, NNW-SSE trending, and arcuate faults associated with volcanic vent structures (Tenalem Ayenew, 1998).

Figure 12. Young geological structures(fractures) of the study area.

4 METHODOLOGY

Hydrogeological features were analysed to identify the geomorphological controls that influence occurrence of groundwater potential in UBRB. This assessment provided insights into surface-subsurface interactions and assisted in identifying potential groundwater zones. Hydrostratigraphic sequences were employed to categorize subsurface layers as aquifers or aquitards. Groundwater potential was evaluated by examining aquifer properties such as thickness, transmissivity, and hydraulic conductivity. A Vertical Electrical Sounding (VES) study was performed to measure the electrical resistivity of subterranean formations. The resistivity measurements were used to distinguish lithological units and define aquifer layers. Empirical correlations were developed between aquifer parameters and resistivity data to enhance the accuracy of aquifer parameters prediction. Additionally, the challenges associated with water well drilling were investigated to identify factors that impact well efficiency and well-yield. Particular attention was given to challenges such as partial penetration, poor well design, well-losses, and etc. that lead to yield discrepancies.

The methodology was conducted in three phases: desk study, field study, and data analysis. The desk study involved reviewing literature, geological maps, hydrological reports, and previous studies. Additionally, analyse climate and river flow data, well and pumping test data, VES data, and remote sensing data, which include DEM, LULC, Soil, Drainage, Lineament, Slope, and Normalized Difference Vegetation Index (NDVI) of the study area. From well data, two important pieces of information can be obtained: - One, is related to the lithology, position, and thickness of the aquifer as described from the lithological logging collected at predetermined intervals of sample collection during the drilling progress. Another information is: that pumping test data has three types, constant rate drawdown, recovery and step-drawdown test. The field investigations included mapping rock types, structures, and stratigraphy, vertical electrical sounding (VES) to measures subsurface resistivity to identify water-bearing zones, and measuring static water level of existing Wells. And assess abandoned or less productive Wells. The collected data were analysed using Rockwork 17, Surfer-16, ArcGIS 10.5, and IPI2Win, spreadsheets to delineate aquifers, aquitards, recharge zones, and groundwater flow patterns, integrating information from both the desk and field studies for a comprehensive assessment.

4.1 Methods

The SWWCE, SDCSE, and SNNPR Water, Mine, and Energy Development Bureau have an excess of data available, including about 300 sets of well and pumping test data. Furthermore, SDCSE provides 190 VES measurements that are available. **Error! Reference source not f ound.** shows a map of these well locations and the VES. Moreover, eight VES data measurements at chosen well locations used for primary data calibration.

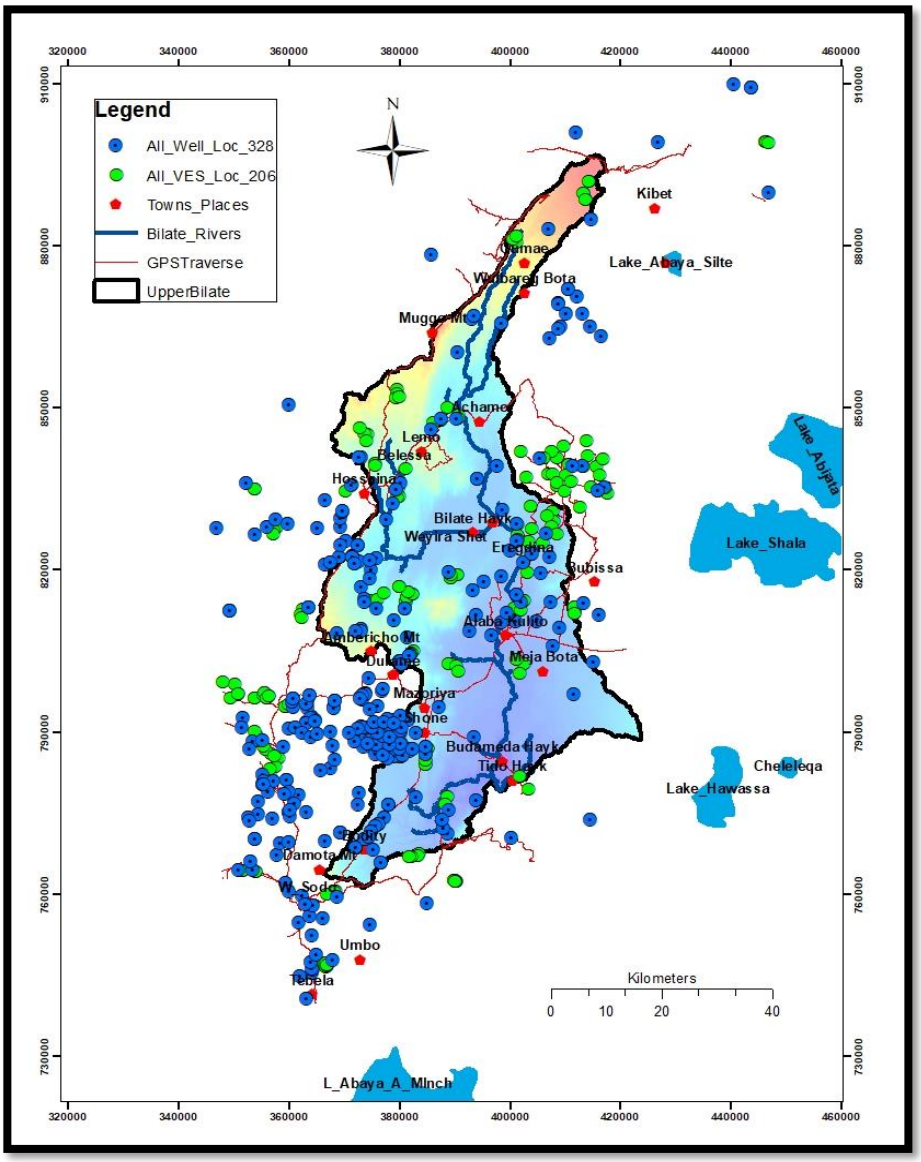

Figure 13. Location of wells and VES data in UBRB

High-resolution, transparent, accurate, comparable, and up-to-date land use land cover (LULC) maps are critical for decision-makers in developing countries and across sectors. These maps are essential for understanding important topics such as resource management planning, surface

water, and land use planning. In particular, Sentinel-2's 10 m land cover time series for the period 2017–2021 provides insightful information about land use dynamics worldwide(Karra et al., 2021)

Table 2. Data type and sources

Data types	**Sources**
Digital elevation model (DEM)	https://search.asf.alaska.edu/#/?dataset=ALOS
Land Use Land Cover(LULC)	https://www.arcgis.com/apps/instant/media
Soil data	FAO/IIASA/ISRIC/ISS-CAS/JRC,2012
Topo sheet 1:50,000 scale	Ethiopian mapping agency (EMA)
Meteorological data	Ethiopian Meteorological Institute (EMI) or Ministry of Water and Energy (MoWE)
Well Data	SWWCE, SDCSE, SNNPRS Water and Energy Bureau, and Field measurements
Geo-electrical (VES) data	SDCSE and Field Survey

Area Rainfall Estimation

The Thiessen Polygon Method is used to estimate areal rainfall by assigning weights to rain gauges based on the area of their surrounding polygons. Each polygon represents the region closest to its corresponding gauge, and the areal rainfall is calculated as the weighted average of all gauge measurements. This method effectively accounts for spatial variability while remaining simple and efficient for irregular gauge networks. The area rainfall map of the UBRB was created using 12-station grid data from the National Meteorology Institute for the years 1983 to 2019. Of the twelve stations, six are inside the UBRB, and the other six are in the surrounding region.

Estimation of Reference Evapotranspiration (ETo)

Reference evapotranspiration (ETo) is the maximum amount of water that can evaporate and transpire from land surfaces given sufficient soil moisture and rainfall. Estimating PET is challenging, as it represents the reverse of rainfall and plays a crucial role in the water cycle (Abbott & Refsgaard, 1996) , (Z. Li et al., 2009). (Ivezic et al., 2017). The widely accepted FAO-Penman-Monteith (FAO-PM) method, endorsed by the FAO and WMO, is based on physiological and aerodynamic principles. It reliably estimates PET across various climates, considering factors like altitude, latitude, temperature, wind speed, humidity, and solar radiation. Moreover, (Zotarelli et al., 2018) and (Allen et al., 1998) defined the standardized reference evapotranspiration equation, utilizing an albedo of 0.23.

$$\mathbf{ETo} = \frac{0.408\Delta(R_n - G) + \gamma\frac{900}{T_a+373}u_2(e_s - e_a)}{\Delta + \gamma(1+0.34u_2)}$$ ----------Eq- 1

Where: -

- $\mathrm{ETo} = \text{Reference Evapotranspiration}(\mathrm{mmday^{-1}})$
- $R_n = \text{Net radiation at the crop surface}(\mathrm{MJm^{-2}day^{-1}})$
- $G = \text{Soil heatfluxdensity}(\mathrm{MJm^{-2}day^{-1}})$
- T = Mean daily air temperature at 2m height (℃)
- $u_2 = \text{Windspeed at 2m height}\ (\mathrm{ms^{-1}})$
- $e_s = \text{Saturation vapour pressure}(\mathrm{kPa})$
- $e_a = \text{Actual vapour pressure}(\mathrm{kPa})$
- $e_s - e_a = \text{Saturation vapour pressure deficit}(\mathrm{kPa})$
- $\Delta = \text{Slope vapour pressure curve}(\mathrm{kPa℃^{-1}})$
- $\gamma = \text{Psychrometric constant}(\mathrm{kPa℃^{-1}})$

Estimating Areal Rainfall and Reference Evapotranspiration

The Thiessen Polygon Method is suitable for estimating areal rainfall, as rainfall is spatially variable and requires assigning representative zones of influence to each station. In contrast, reference evapotranspiration (ETo) is derived from meteorological parameters that vary more gradually over space; therefore, it is calculated using standard equations such as FAO Penman–Monteith, while its spatial distribution is better represented through interpolation (IDW, Kriging) or remote sensing rather than Thiessen polygons.

In ArcMap 10.5, after creating Thiessen polygons around rainfall stations, you can calculate their areas by adding a new numeric field to the attribute table, such as "Area_km2." To measure the area of each polygon, use the Calculate Geometry tool, which will utilize the dataset's projected coordinate system. The area values, which can be expressed in user-defined units such as square meters or square kilometers, reflect the spatial influence of each rainfall station. These values are then used as weights for estimating areal rainfall using the Thiessen method.

Actual Evapotranspiration

The measurement of water consumption or evaporation into the atmosphere caused by environmental factors in a specific geographic location is called actual evapotranspiration (AET) . A trustworthy, accurate, and practical method for evaluating regional water withdrawals for

irrigation and related consumptive purposes is to use the AET estimate. This is particularly true in dry farmland regions where rainfall, soil moisture, or groundwater are insufficient to ensure adequate natural water supplies(Savoca et al., 2013). That is, the actual amount of evapotranspiration that occurs: if $P < PET, then, AET = P - \Delta ST, and\ if\ P > PET\ then\ AET = PET$.

Turc Method

The mean annual actual evapotranspiration of the study area is estimated using the Turc empirical formula(Gudulas et al., 2013).Turc method is generally more applicable. It provides a broader estimate of evapotranspiration losses, which is crucial when calculating the residual water available for recharge

$$AET = \frac{P}{\sqrt{0.9 + \frac{P^2}{L^2}}}$$ ----------Eq- 2

Where: - AET =is mean annual actual evapotranspiration, (mm), P = is mean annual rainfall, T = is mean annual temperature, L = is a thermal indicator, defined by the following equation: $L=300+25T+ 0.005* T^3$.

Crop Coefficient (Kc) Approach

Designed for estimating actual evapotranspiration (AET) in agricultural settings. Highly accurate when ET_0 is known and crop-specific Kc values are available. Requires detailed crop data and assumes uniform land use, which may not reflect natural recharge conditions. AET is estimated by scaling reference evapotranspiration (ET_0, from FAO Penman–Monteith or similar) with a crop coefficient (Kc) linked to land use/land cover. Equation: $AET=Kc\times ETo$ (Allen et al., 1998)

Table 3. Crop Coefficient (Kc) for different LULC classes

LULC Class	Kc_ Representative
Built Area	0.15
Bare ground	0.2
Crops Rangeland	0.95
Trees	0.95
Water bodies	1.05

Hydrological and Hydrogeological Conceptual Model

In the context of groundwater investigation, utilization, and management within a river basin, it is vital to consider surface runoff, groundwater recharge, potential evapotranspiration, and the types and amounts of precipitation. Although the water balance equation may seem simple at the scales of catchments and sub-basins, it is fundamentally important for understanding groundwater yield (Negewo & Sarma, 2021). According to (UNESCO, 1974),(Szwed, 2015),(Nata et al., 2010),(David Keith Todd, 2005), ,(W.Mays, 2011),(Garg, 1978),(Seiler & Gat, 2007),(Jayarajan et al., 2022). And, according to Gidafie et al.(2019), Melo et al.(2015), and the conceptual model of the study area(Figure-10), the water balance formula for UBRB can be regarded as:

$$P - AET - Q - R = 0 \text{ ----------Eq- 3}$$

Where: -

- P = Rainfall,
- AET = Actual evapotranspiration,
- R = Recharge, and
- Q = surface runoff from the basin.

Assumption: As the calculations are conducted annually, the assumption is made that there is no change in groundwater storage. The assumption is made that surface and subsurface water are not exchanged with neighbouring basins, provided there are no intentional or artificial diversions from other basins

Baseflow Evaluation

Variable-Slope hydrograph separation: -Baseflow for the UBRB area (3,557.9 km²) was estimated using the Variable-Slope hydrograph separation method applied to the downstream gauging station that drains 5,518 km². Monthly mean baseflow values were derived from observed streamflow records, yielding a mean annual baseflow discharge from the gauged catchment.

To estimate baseflow for the ungauged study area, the gauged baseflow was first scaled by the catchment area ratio (k = 3,557.9 / 5,518 = 0.6448). And a precipitation adjustment factor was then applied to account for the lower mean annual rainfall of the study area (1,039.83 mm) relative to the gauged basin (1,165 mm): Adj = $P_{\_UBRB}$/ P_{gauge} = 0.8925

The adjusted baseflow was computed as:

$Q_{\_UBRB}$, adj = $Q_{gauge} \times k \times$ Adj, and

$D_{\_UBRB} = D_{gauge} \times$ Adj

Where:

• $Q_{\_UBRB}$, adj – Adjusted mean baseflow discharge (m^3/s)

• $D_{\_UBRB}$– Adjusted baseflow depth (mm/yr)

• Q_{gauge} – Mean baseflow at gauged catchment (m^3/s)

• D_{gauge} – Baseflow depth at gauged catchment (mm/yr)

• k – Area ratio ($A_{\_UBRB}$/ A_{gauge})

• Adj – Precipitation ratio (P_{UBRB}/ P_{gauge})

Baseflow depth often refers to equivalent water depth per unit catchment area. Calculated as:

$$h_b = \frac{Q_b \times t}{A}$$

Where h_b = baseflow depth Q_b = baseflow discharge (m^3/s), t = time (s), A = catchment area (m^2). When compared to rainfall depth, this gives recharge efficiency or runoff coefficients. This approach scales the gauged baseflow by both catchment size and rainfall input, providing a realistic estimate of mean annual baseflow for the ungauged study area.

Geological Map Preparation

The geological map is prepared using field and from Geological Map of Dilla Map Sheet NB37-6;2012, Hosaina Map Sheet NB37-2;2012 and Akaki-Beseka Map Sheet NC37-14;2009,] with 1:250,000 scale. The local lithology of the area is described primely from lithological well logging data and field work. The geomorphologic landform of the area is prepared using topographic map, and DEM using ArcMap.

Evaluating the hydrogeological controls on groundwater potential and delineate hydrogeological framework

Preparing and integration of thematic layers of hydrogeological controls to delineate the hydrogeological framework characteristics of groundwater potential in the UBRB is inevitable. Thematic layer controls namely Rainfall, AET, Geomorphology, Lithology, Slope, Natural Vegetation Difference Index (NVDI), lineament, Drainage, Land use Land cover (LULC), and Soil layers maps are used.

Natural Vegetation Difference Index (NVDI):-This remote sensing data can be accessed at this link: https://custom-scripts.sentinel-hub.com/sentinel-2/ndvi/.

NDVI is defined as:

- For Sentinel-2, the index looks like this:

$$NDVI := Index(B8, B4) = \frac{B8 - B4}{B8 - 84}$$

Where**: -**
B8 (NIR – Near-Infrared): 842 nm (10m or 20m resolution, depending on processing)
B4 (Red): 665 nm (10m resolution)

Lineament density: - A lineament density map shows the concentration of linear geological features (like faults, fractures, and joints) per unit area. The process involves three main phases:

1. Extract Lineaments: Derive linear features from the DEM.
2. Create Lineament Feature Class: Convert the extracted raster lines into a vector format (polylines).
3. Calculate Density: Compute the density of these polylines across the study area.

This method involves first generating multiple hillshades from a DEM with different illumination angles to enhance the visibility of linear features. These hillshades are then used as a base for manually digitizing and creating a polyline feature class of lineaments. The lengths of these polylines are calculated, and the Line Density tool is finally used to create a raster map where each cell's value represents the total length of lineaments per unit area, visually summarizing the concentration of geological structures.

Drainage density: - In ArcGIS 10.5, a Digital Elevation Model (DEM) is processed to create hydrological layers by filling sinks, determining flow direction, and calculating flow accumulation. A stream network is extracted by applying a threshold to the flow accumulation layer and converting it to polyline format. The total length of the stream is measured with the "Calculate Geometry" tool. Concurrently, the watershed area is delineated using the Watershed tool and its area calculated. Drainage density is computed by dividing the total stream length by the watershed area, expressed in kilometres per square kilometre (km/km²), reflecting the degree of landscape dissection useful for hydrological analysis.

Table 4. Thematic layers dictate the hydrogeological framework of UBRB

No	Parameter	Role in Groundwater Potential	Data Sources
1	Rainfall	High rainfall → Increased recharge	Ethiopian Meteorological Institute (EMI)
2	AET	High AET → Decrease recharge	Estimated from Eo & crop coefficient
3	Slope	Gentle slopes and flatter terrain→ Higher groundwater	Derived from DEM
4	Lithology	Fractured rocks → Higher storage	GSI, USGS
5	Geomorphology	Elevated landscape → Higher recharge	Derived from DEM
6	NDVI	High NDVI → Likely groundwater-fed vegetation	Sentinel-2
7	lineaments	Higher → Higher groundwater percolation	Derived from DEM
8	LULC	Forests/wetlands → Higher recharge	
9	Drainage Density	Higher density → lower groundwater Percolation	Derived from DEM
10	Soil Type	Sandy/porous soils → Better percolation	FAO Soil Maps, NBSS

Hydrostratigraphic sequences: -Vertical Electrical Sounding (VES) is an effective geophysical technique used to identify subsurface layers and understand hydrostratigraphic sequences. In this method, electrical resistivity measurements are taken at multiple locations to characterize variations of subsurface materials. Each measured resistivity curve is interpreted to reveal distinct modelled layers that correspond to different lithologies, such as aquifers and aquitards. Key parameters, including layer thickness, resistivity, and depth, are utilized to classify the subsurface into hydrostratigraphic units, distinguishing depth of productive groundwater zones (characterized by low resistivity and permeable layers) from less permeable layers (marked by high resistivity and poor permeability). Using software such as RockWorks-17, ArcMap, and Surfer-16, 3D lithological modelling can be performed, allowing for the determination of the thickness and spatial variability of modelled layers. Modelled layers profiles can define the hydrostratigraphic units of the UBRB.

Analytic Hierarchy Process (AHP)

The Analytical Hierarchy Process (AHP), introduced by (Saaty, 1980), is a widely applied multi-criteria decision-making method. It is useful to identify the topographic features that control the hydrogeological setup for groundwater potential mapping and natural resource evaluation, as it integrates expert judgment with quantitative analysis. The Steps in AHP:

- Problem Structuring: - Define the overall goal and organize criteria (layers tha control the hydrogeological setup of the study area) into a hierarchical structure.
- Pairwise Comparison: - Compare each pair of criteria/layer using Saaty's 1–9 scale.
- Weight Derivation: - Normalize the comparison matrix, and calculate the principal eigenvector to determine the relative weight of each criterion.
- Consistency Check: - To ensure reliable judgments, the Consistency Index (CI) and Consistency Ratio (CR) are computed:

$$CI = \frac{\lambda_{max} - n}{n - 1}$$

$$CR = \frac{CI}{RI}$$

where λ_{max} is the maximum eigenvalue, n is the number of criteria, and RI is the Random Index. A CR ≤ 0.1 indicates acceptable consistency.

- Weighted Overlay – The final weights are applied to thematic layers (e.g., geology, slope, rainfall, land use, lineament density) to produce the groundwater potential or suitability map.

Table 5. Saaty's 1–9 Scale for Pairwise Comparisons

Scale	Interpretation
1	Equal importance
3	Moderate importance
5	Strong importance
7	Very strong importance
9	Extreme importance
2,4,6,8	Intermediate values

When exploring groundwater resources in the UBRB, factors such as geomorphology, rainfall, and soil maps are analyzed, with weights assigned using the AHP method in ArcGIS 10.5 software.

Pumping test analysis for aquifer parameters calculation: - AquiferTest-2016 software and an Excel spreadsheet with the necessary equations is used to evaluate hydraulic charactestics such as K, and T. Because secondary and primary data are readily available, the quantitative method is a valuable technique in hydrogeological studies as it allows for improved data analysis

and interpretation of groundwater resource controlling aquifer parameters. All Wells are single-well. Thus, an appropriate calculation method can be chosen.

Single-well analysis with wells effect: - Financial constraints limit the establishment of observation wells for conventional pumping tests. Most drawdown measurements were conducted in our country and UBRB using a single pumping well. Factors affecting drawdown include aquifer characteristics, well storage, skin effects, and losses. The storage coefficient may not accurately reflect aquifer conditions from a single well analysis, so methods that account for well storage, like the Papadopulos-Cooper method, are recommended. Theis's recovery method is used for analysing recovery test data from various aquifers. To assess well yield challenges (partial penetration, wellbore storage, and well-design), productive casing design and pumping test data are employed in the UBRB aquifers.

Aquifer type classification:- Based on the common types of time–drawdown curves (UNESCO, 2004) has indicated the following aquafer type charactestics: A and A′ confined aquifer; B and B′, unconfined aquifer; C and C′, leaky (or semiconfined) aquifer; D and D′, effect of partial penetration; E and E′, effect of well-bore storage (large-diameter well); F and F′, effect of recharge boundary; G and G′, effects of an impervious boundary.

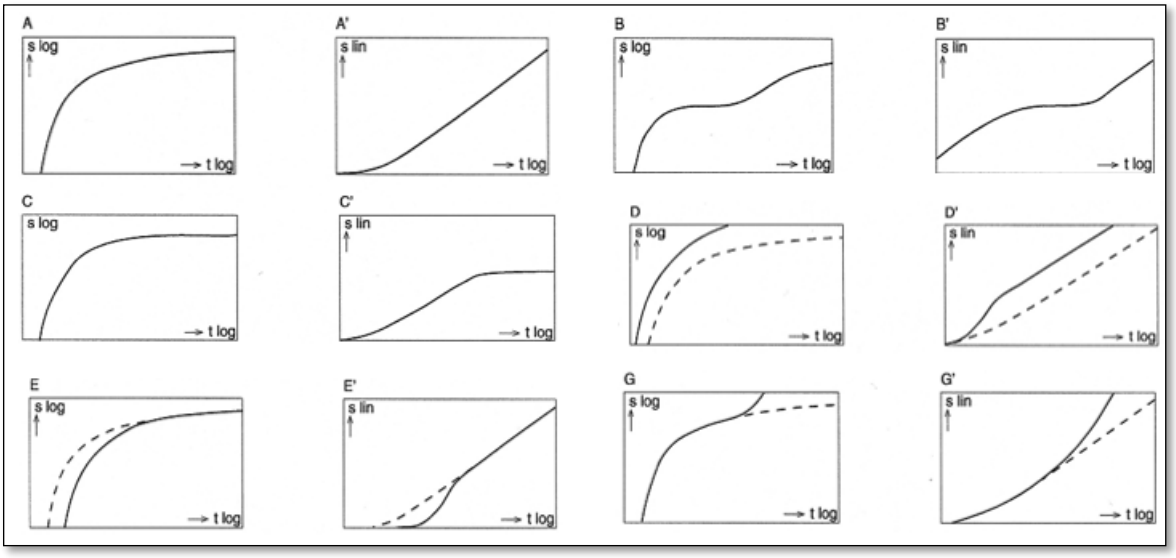

Figure 14. Types of Log-log and semi log curves of drawdown versus time.

Estimation of Hydraulic Conductivity (K): Hydraulic conductivity (K) represents the ease with which groundwater moves through pore spaces or fractures within the aquifer. It was

estimated using transmissivity (T) and aquifer thickness (b) based on the relationship: K = T / b, Where, T is Transmissivity and b is saturated thickness

Calculation of Transmissivity (T): Transmissivity (T) quantifies the ability of the aquifer to transmit water through its entire saturated thickness and was computed as: T = K × b. And this parameter was calculated for each well and added as an attribute field in the GIS database. The resulting transmissivity dataset was used to delineate areas of varying aquifer productivity and groundwater potential.

Spatial Interpolation and Map Preparation: The calculated T and K values were spatially interpolated using the Kriging method in ArcGIS to generate continuous surfaces across the study area. The interpolation grid was clipped to the watershed boundary. Resulting maps of K and T were classified into discrete categories based on reference values (Table 4.5) to represent groundwater potential zones.

Classification of Transmissivity (T) Ranges

The transmissivity map was classified according to globally recognized hydrogeological ranges (Freeze & A.Cherry, 1979; Heath, 1987; Kruseman & Ridder, 2000; C.W.Fetter, 2001; Todd & Mays, 2005; Driscoll, 2007)

Table 6. The transmissivity map was classification

Class	**Transmissivity (m^2/day)**	**Groundwater Potential**	**Hydrogeologic Interpretation**
Very Low	< 1	Poor	Impermeable or compact rock; negligible yield
Low	1 – 10	Moderate–Poor	Slightly weathered/fractured zones; limited local recharge
Moderate	10 – 100	Moderate	Weathered/fractured aquifers; suitable for domestic supply
High	100 – 500	Good	Productive aquifers; adequate for community water supply
Very High	> 500	Excellent	Highly permeable alluvial or karstic aquifers; high yield potential

Electrical Resistivity Method (Schlumberger Array)

Electrical Resistivity method is a geophysical technique used to analyse subsurface materials by measuring their resistance to electrical current. The Schlumberger array, commonly used in groundwater investigations, provides good depth penetration and resolution with minimal electrode movement. In this configuration, current electrodes (A and B) inject current into the

ground, while potential electrodes (M and N) measure the resulting voltage difference. The apparent resistivity (ρa) is then calculated from these measurements.

$$\rho_a = K \times \frac{\Delta V}{I}$$

Where K is the geometric factor:

$$K = \pi \left(\frac{(AB/2)^2 - (MN/2)^2}{MN} \right)$$

Data Presentation

- Plot apparent resistivity (ρa) versus AB/2 (log-log scale) to produce the VES curve.
- Perform curve matching or computer-based inversion to estimate true resistivity and thickness of subsurface layers.

Interpretation

Apparent resistivity measurements were collected at various electrode spacings to generate Vertical Electrical Sounding (VES) curves for study. The data were analyzed using IPI2Win software to model the subsurface as layered resistivity structures, which allowed us to estimate layer thicknesses and true resistivity. The interpreted models were combined with well lithological log data to identify aquifers, aquitards, and groundwater zones, resulting in a solid framework for mapping subsurface hydrogeological conditions.

Well-yield challenges: Partial penetration happens in an aquifer with thickness b when a well has a screen or open interval L length. The well is considered partially penetrating if the dimensionless screen length L/b is less than 1 (Driscoll, 2007). A well's partial penetration into an aquifer results in additional head losses, which are included in the aquifer losses (Dufresne, 2011).

Well Losses (C) : The Hantush-Bierschenk Well Loss Solution utilizes variable-rate step drawdown test data to determine linear and non-linear well loss coefficients (B and C), which aid in estimating the actual drawdown in a pumping well. Unlike the (Theis, 1935) method, which gives theoretical drawdown, this approach accounts for additional drawdown from well losses, often caused by turbulent flow near the well(Kruseman & Ridder, 2000). The effectiveness of development can be appraised from the results of a step-drawdown test. The value of **C** of a properly developed and designed well is generally less than 5**sec^2/ft^5** (Walton, 1962)·

Table 7.Range of Well Loss Coefficient (C) Values with the Well Conditions

C (sec^2/ft^5)	C (day^2/m^5)	Wall Condition
< 5	< 0.0000002293	Properly developed and designed well
5 to 10	0.0000002293 to 0.0000004586	Mild deterioration
> 10	> 0.0000004586	Clogging is severe
> 40	> 0.0000018344	Difficult to restore well to original capacity

Source: After Walton (1962).

Partial penetration ratio (L/b) is defined as the ratio of the well screen length (L) to the total aquifer thickness (b). It represents the degree to which a well hydraulically connects to the aquifer.

Table 8. International and Theoretical References

Source	Recommended or Observed Range	Remark
Walton (1970), Selected Analytical Methods for Well and Aquifer Evaluation	L/b → 0.7–1.0 for high efficiency	Partial penetration <1.0 causes additional head loss; efficiency improves as L/b increases.
Driscoll (1986), Groundwater and Wells	0.5–0.8 typical for production wells	Practical balance between yield and construction cost.
U.S. EPA (2002), Groundwater Monitoring Well Design and Installation	≤0.3 for monitoring wells, ≥0.5 for production wells	Screen length depends on well purpose.
Kazmann (1972), Modern Hydrology and Engineering	>0.3 recommended	Avoid L/b <0.3 to prevent excessive drawdown.
Ethiopian MoWR (2004), Water Well Design & Construction Manual	≈0.5–1.0 for production wells	Screen length should correspond to the water-bearing zone thickness.

Table 9. Consolidated Partial Penetration Design Ranges

Penetration Category	L/b Range	Design Context	Hydraulic Implication
Low (minimal)	0.2 – 0.33	Thin aquifers, monitoring wells	High drawdown, low efficiency
Moderate (typical)	0.4 – 0.7	Production wells	Balanced yield vs cost
High (near-full)	0.8 – 1.0	High-capacity wells	Optimal yield, minimal head loss

Recommended practical design range for water-supply wells: L/b = 0.4 – 0.8 (optimum balance).

For high-capacity municipal wells, L/b ≥ 0.8 is ideal.

Wellbore Storage Coefficient (Cw)

To check for well storage effects in early drawdown data, plot drawdown vs. time on a log-log graph—if the early trend is linear with a constant slope, storage effects are likely present.(Kruseman & Ridder, 2000).

Table 10.Thresholds of Wellbore Storage Coefficient (Cw)

Cw Range	Interpretation	Implications for Groundwater Potential / Yield
Cw < 0.1 (very low)	Negligible wellbore storage	Aquifer response dominates almost immediately. Test results are reliable for transmissivity/yield estimation. Indicates good well–aquifer connection.
0.1 ≤ Cw ≤ 0.3 (low–moderate)	Small but noticeable wellbore effect at early times	Aquifer parameters can still be estimated with minor correction. Indicates efficient well design and good aquifer potential.
0.3 < Cw ≤ 0.6 (moderate)	Wellbore storage influences early drawdown significantly	Aquifer response appears later in the test. Interpretation must focus on late-time data. Wells may still perform well but require careful test analysis.
0.6 < Cw ≤ 0.9 (high)	Strong wellbore influence	Early aquifer signal masked; transmissivity may be underestimated. Yield estimates uncertain unless long-duration tests are conducted. May indicate oversized casing, inadequate development, or partial aquifer penetration.
Cw ≥ 0.9 (very high)	Wellbore storage dominated system	Aquifer signal appears only at very late time (if at all). Pumping-test results unreliable for aquifer parameter estimation. Such wells face yield challenges and often require rehabilitation, redesign, or re-testing.

Relationship with Partial Penetration and Wellbore Storage

The Agarwal skin factor is used to correct the pressure transient data for the effects of partial penetration and wellbore storage. **AquiferTest** has implemented the Agarwal wellbore storage and skin solution for water wells using the following assumptions: Single pumping well, confined aquifer, and Observations only in the pumping well

Well Efficiency Assessment Method and Classification

The efficiency of a pumping well represents the ratio of aquifer loss (theoretical drawdown) to total (measured) drawdown in the well (Kruseman & de Ridder, 2000). It expresses how effectively a well converts aquifer potential into discharge with minimal energy loss due to head resistance around the well. According to Heath (1983), well efficiency can be defined as the ratio of drawdown (s_a) in the aquifer at the radius of the pumping well to the total drawdown (s_t)

measured inside the well. In general, a well efficiency of 70% or more is considered acceptable, while 65% is regarded as the minimum threshold for a properly developed and constructed well. Efficiencies below 65% typically indicate design flaws, poor development, or partial clogging of the well screen (Kresic, 2007).

Well efficiency (V) can be expressed mathematically as: $V = \frac{s_a}{s_t} \times 100$. Or equivalently, in terms of loss coefficients (Alam, 2007; Driscoll, 1986): $V = \frac{BQ}{BQ+CQ^2} \times 100$.

where:

- V= well efficiency (%),
- B= aquifer loss coefficient (m^3/s per m), representing laminar head losses,
- C= well loss coefficient (m^5/s^2 per m), representing turbulent head losses, and
- s_a = aquifer (formation) drawdown component (m), and
- s_t = total drawdown observed in the well (m).
- Q= discharge rate (m^3/s).

Both aquifer and well losses contribute to the overall drawdown in a pumping well. The linear head loss associated with laminar flow through the aquifer matrix is termed *aquifer loss*, while the non-linear head loss caused by turbulence near the well screen and gravel pack represents *well loss* (Kruseman & de Ridder, 2000).

To evaluate well efficiency in the study area, step-drawdown pumping test data were analyzed using the Jacob equation: $s = BQ + CQ^2$.

The total drawdown (s_t) was obtained as the difference between static and dynamic water levels measured at successive pumping rates. The *aquifer loss component* (BQ) was derived from the linear portion of the drawdown–discharge relationship, while the *well loss component* (CQ^2) was inferred from the non-linear term. These coefficients were then used to compute well efficiency for each test well. The resulting efficiencies were used to assess hydraulic performance and identify wells experiencing excessive head losses due to construction, design, or hydrogeological constraints. Based on literature standards(Driscoll, 2007;Todd & Mays, 2005; Kruseman & Ridder, 2000) the wells were classified into performance categories as shown inTable 11. Well efficiencies classification and performance categories (Table 11Table 11).

Table 11. Well efficiencies classification and performance categories

Efficiency Range (%)	**Classification**	**Performance Interpretation**
< 40	Poor Efficiency	High well losses; poor construction or clogging.
40 – 60	Fair Efficiency	Moderate losses; acceptable but suboptimal performance.
60 – 80	Good Efficiency	Efficient wells with minor losses.
> 80	Excellent Efficiency	Highly efficient wells; optimal design and aquifer conditions.

The classified efficiency values were further analyzed spatially using a GIS environment to examine the distribution of well performance across the study area. This spatial analysis helped identify relationships between well efficiency and key hydrogeological parameters such as transmissivity, lithology, aquifer type, and well depth, thereby aiding in diagnosing yield discrepancies and guiding future well design and development strategies.

Geoelectrical survey field data acquisition and analysis

Vertical Electrical Sounding (VES) is a resistivity method effective in various geological settings. Using a Schlumberger array with current electrode spacings (AB/2) of 500–700 m and Potential electrodes (MN) of 1–90 m, field data are collected and analyzed with IPI2win software. The software iteratively adjusts the resistivity model to minimize root mean square (RMS) error between observed and synthetic data. Combining resistivity surveys with pumping tests improves aquifer parameter estimation. Empirical relationships between geoelectrical and aquifer properties allow for broader assessment across the study area(Hasan et al., 2020).

Estimation of hydraulic parameters

An empirical correlation equation will be developed using electrical resistivity and aquifer parameters to estimate hydraulic conductivity (K) and transmissivity (T) across the UBRB. Based on Darcy's law and Ohm's law, two key parameters—longitudinal unit conductance (Sc) and transverse unit resistance (Tr)—are derived. Sc is the layer thickness divided by resistivity, while Tr is the product of thickness and resistivity. Known as Dar Zarrouk Parameters (DZP), introduced by Maillet (1947), these form the basis for the correlation. DZP are calculated from interpreted aquifer resistivities and thicknesses(Khalilidermani et al., 2021),(Hasan et al., 2020), and (Soupios et al., 2007).

$$a = K\rho_a \; ; \; T = aS_c$$

$$b = \frac{K}{\rho_a} \; ; \; T = bT_r$$

Where: -

- Sc = longitudinal conductance (Sc= h/ρ_a)
- Tr =transverse resistance (Tr=ρ_a ∗h)
- ρ_a =electrical resistivity of saturated thickness
- h =thickness of the aquifer
- a & b are constant proportionality.

4.1.1 The approach of the study

The flow chart in illustrates the sequential methodological framework adopted in this study, encompassing data collection, hydroclimatic and recharge analysis, thematic layer preparation, multi-criteria evaluation (AHP–MCE) for groundwater potential mapping, aquifer parameter–resistivity correlation, well efficiency assessment, and final integration for interpretation and mapping of hydrogeological conditions in the UBRB

.

The flow chart shows the method for exploring groundwater resources and well drilling problems in the UBRB

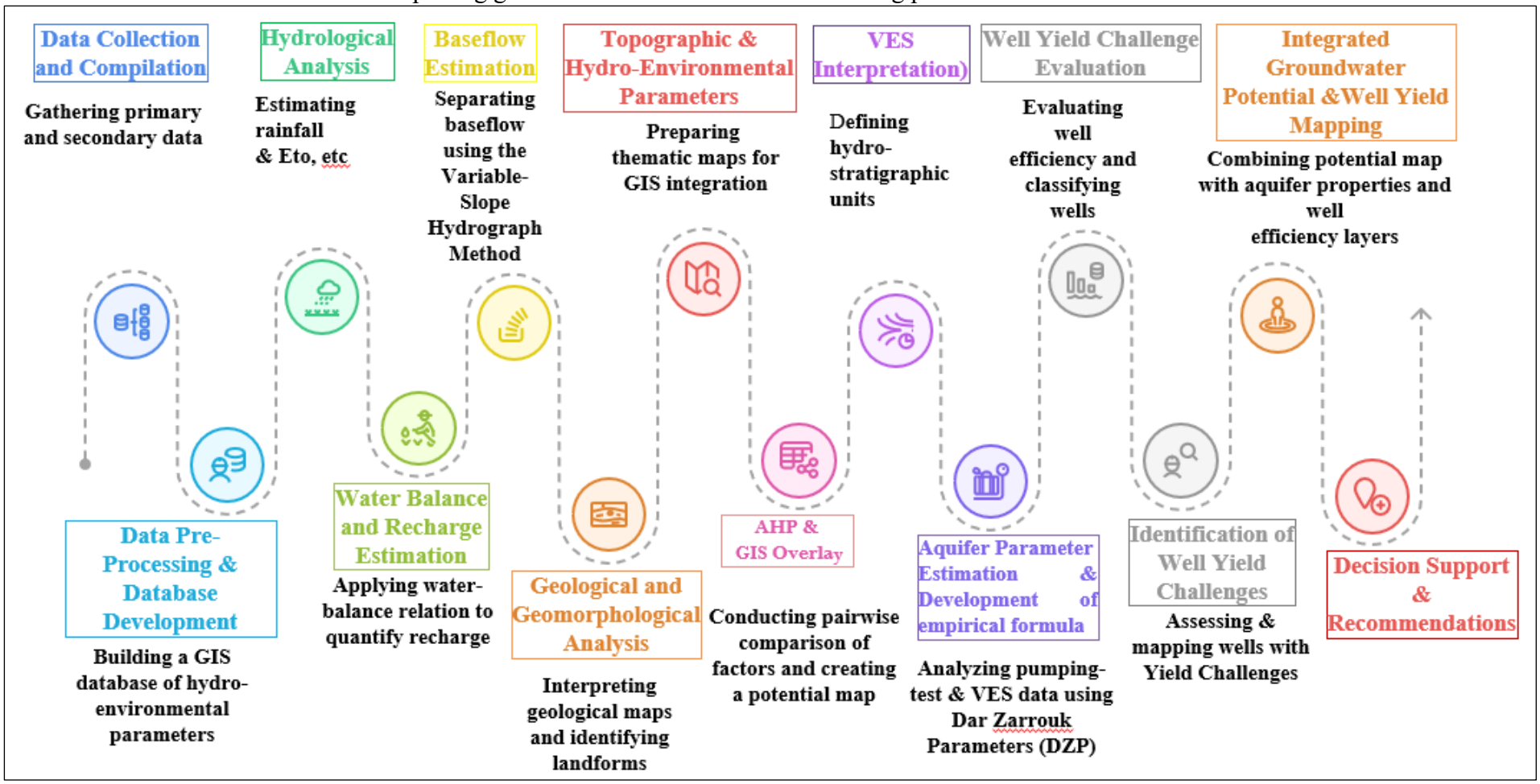

Figure 15. Flowchart of the research methodology

4.2 Material

To accomplish the stated objectives, various types of equipment and software ware used.

Table 12. Material and Software

No	Software types	Application
1	Portable resistivity meter IRIS instrument /SYSCAL Junior Switch 72 Model	To conduct the VES Survey
2	Deep-Meter	To measure SWL
3	Hand GPS: Garmin -GPSMAP64s model	To obtain the geographical location
4	ArcMap 10.5	To make geological and hydrogeological maps and for interpolation of point measurement
5	AquiferTest-2016	To analyse aquifer parameters
6	Surfer-16	To make overlay maps and cross-section
7	Strater-5 and Rockwork-17	To prepare lithological section, Strip-log, and 3D-lithological Model
8	IPI2win Geoelectrical software	To produce a geoelectric layer model
9	MS-Excel_2019	Point data, Graph, chart presentation, calculation
10	MS-Word_2019	Report Writing
11	MS-PowerPoint_2019	Thesis presentation

5 RESULTS AND DISCUSSIONS

5.1 Hydrometeorology

The hydrometeorological analysis for Hydrogeological Investigation examines the interaction between meteorological (weather) and hydrological (water) processes to assess groundwater resources. This analysis includes evaluating temperature, precipitation, Potential evapotranspiration (PET), actual evapotranspiration (AET), and other climatic factors to understand their impacts on groundwater recharge, aquifer dynamics, and water balance.

5.1.1 Temperature

The study area experiences a mean annual temperature of 19.25ºC. A discernible trend reveals that temperatures tend to be higher in the lower-elevation plains as opposed to the mountainous regions. Air temperature exhibits seasonal variation, with the monthly average fluctuating between 12.97 and 26.70ºC. The highest temperatures, approximately 28.85ºC, occur in November or April, while the lowest average temperature is noted in July. Temperature data were obtained from grid data collected by the National Meteorology Institute between 1983 and 2019. These records were merged with satellite data and station records to ensure the completeness of the dataset.

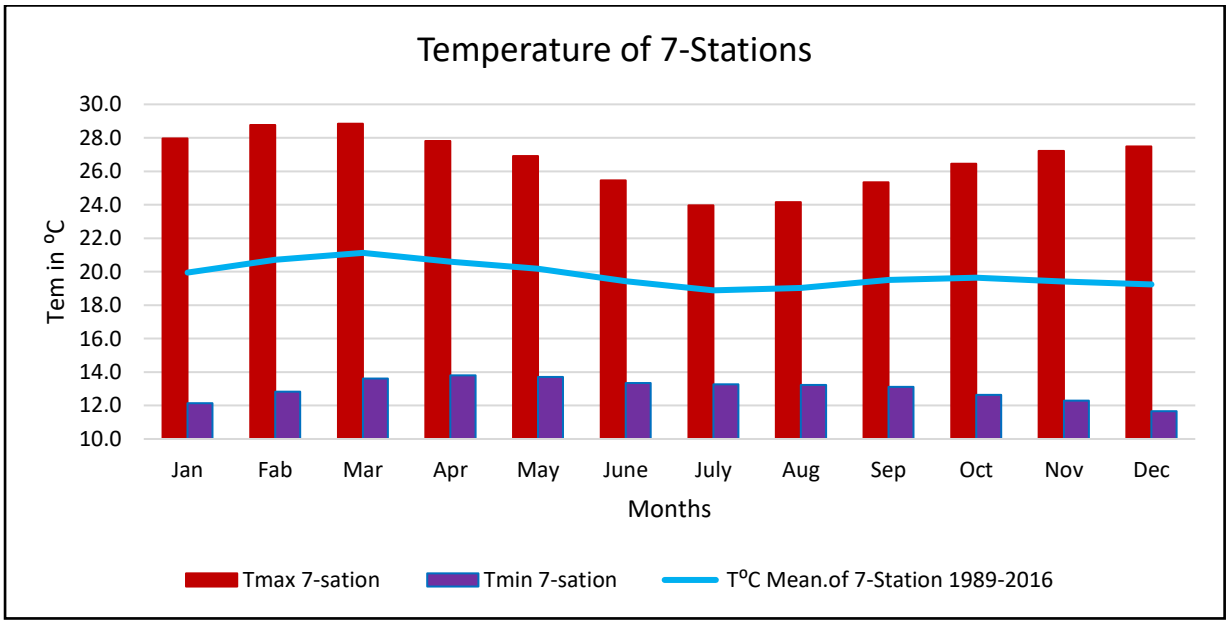

Figure 16. Mean monthly temperature graph.

5.1.2 Rainfall

The precipitation map was created using 12-station grid data from the National Meteorology Institute for the years 1983 to 2019. These data were combined with data from in situ stations and satellites to create a gridded precipitation time series without missing data. The maximum and minimum monthly rainfalls are 168.10mm and 13.41mm. The mean monthly rainfall is 83.92mm. The maximum and minimum annual rainfalls are 2004.11mm and 716.24mm.

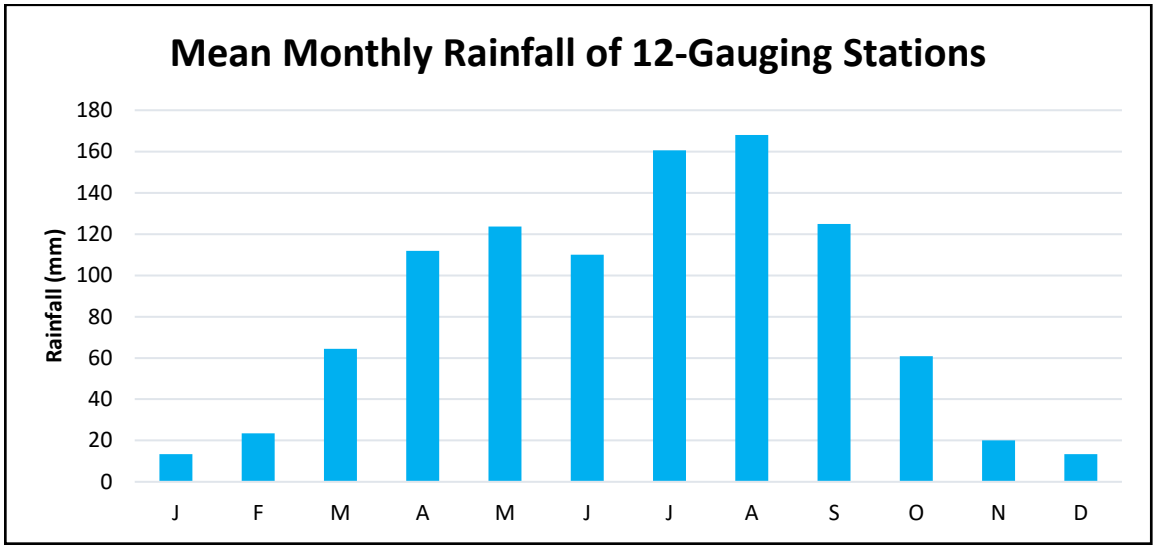

Figure 17. Mean monthly rainfall of the study area

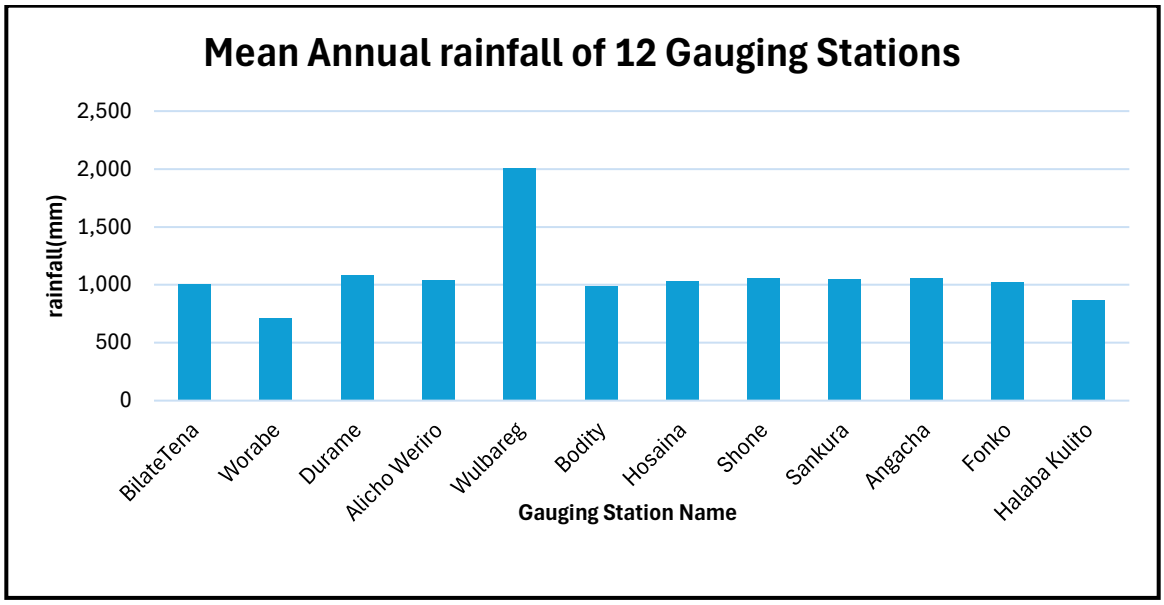

Figure 18. Mean annual rainfall of the study area

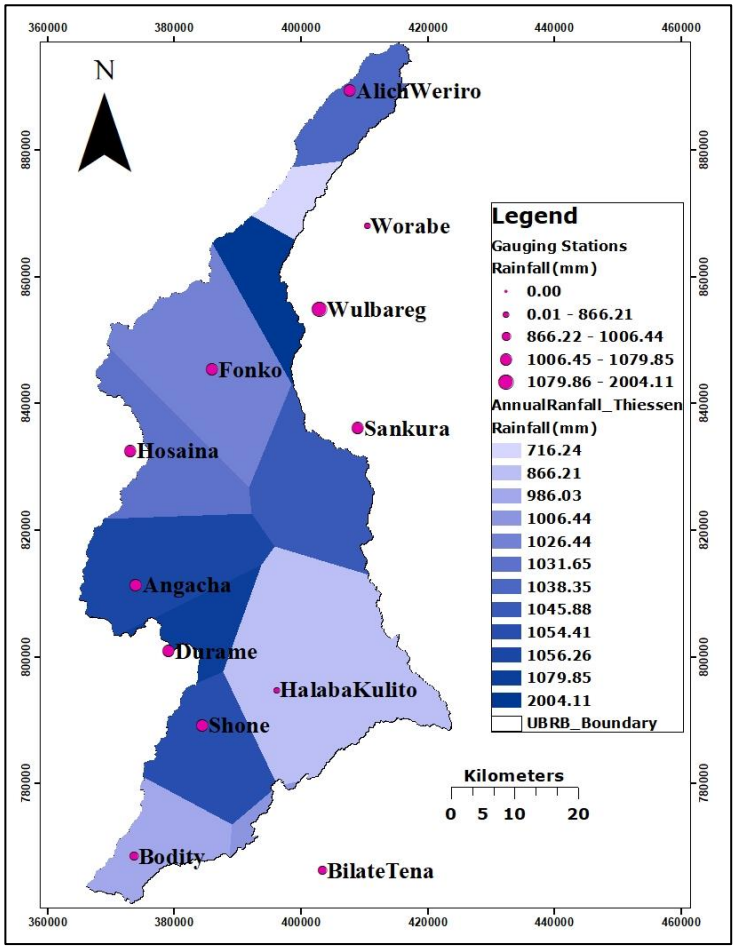

Figure 19. Mean annual rainfall maps over the UBRB, Thiessen

Table 13. Annual mean precipitation depth over the area under study

X(m)	Y(m)	Rainfall (mm)	Gauging Station Name	Area (Km^2)	Weighted Area	Weighted Rainfall (mm)
403433	766257	1006.44	BilateTena	27.34	0.008	8.19
410452	868043	716.24	Worabe	78.48	0.023	16.74
379133	800873	1079.85	Durame	135.43	0.040	43.55
407776	889287	1038.35	Alicho Weriro	166.88	0.050	51.60
402950	854852	2004.11	Wulbareg	168.70	0.050	100.69
373646	768571	986.03	Bodity	202.43	0.060	59.44
373122	832506	1031.65	Hosaina	277.62	0.083	85.29
384500	789206	1054.41	Shone	285.30	0.085	89.59
408938	836075	1045.88	Sankura	344.58	0.103	107.33
373959	811325	1056.26	Angacha	381.50	0.114	120.00
385999	845364	1026.44	Fonko	518.20	0.154	158.40
396212	794787	866.21	Halaba Kulito	771.46	0.230	199.01
				3357.90	1	**1039.83**

5.2 Reference Evapotranspiration

The Reference Evapotranspiration (ETo) interpolation map for the Upper Bilate River Basin (UBRB) shows ETo values ranging from 584 mm/year to 817 mm/year, increasing from the southern lowlands (Wolaita Sodo and Bilate Tena) to the northern highlands (Endibir and Worabe). This trend contradicts the typical elevation–ETo relationship, indicating the impact of microclimates, solar radiation, and meteorological data distribution.

In the south, areas like Bilate Tena and Wolaita Sodo have moderate ETo values and high rainfall (around 1000 mm/year), resulting in higher soil moisture. The central region, including Hossana, reflects transitional ETo values, while the northern highlands show higher ETo, likely due to increased solar exposure and drier air. From a groundwater perspective, lower ETo and higher rainfall in the southern and central regions enhance recharge potential due to less evaporative loss. In contrast, the northern zones, with higher ETo and lower rainfall, have reduced recharge capacity. Thus, groundwater potential in the UBRB increases toward the southern lowlands, correlating with lower evapotranspiration and higher effective rainfall

Table 14. Annual mean ETo and Rainfall data for 1st Class stations around the UBRB.

X	Y	ETo Annual (mm)	Rainfall (mm)	Sataion Name
403433	766257	571.07	1006.44	BilateTena
381733	897640	551.30	1024.676	Endibir
443285	779854	540.09	799.15	Hawassa
373121.7	832506.1	652.54	1031.65	Hossana
363937.4	694316.3	647.97	784.38	MirabAbaya
410452	868043	839.89	716.24	Worabe
359657.4	752860.7	733.61	1014.44	WolaitaSodo

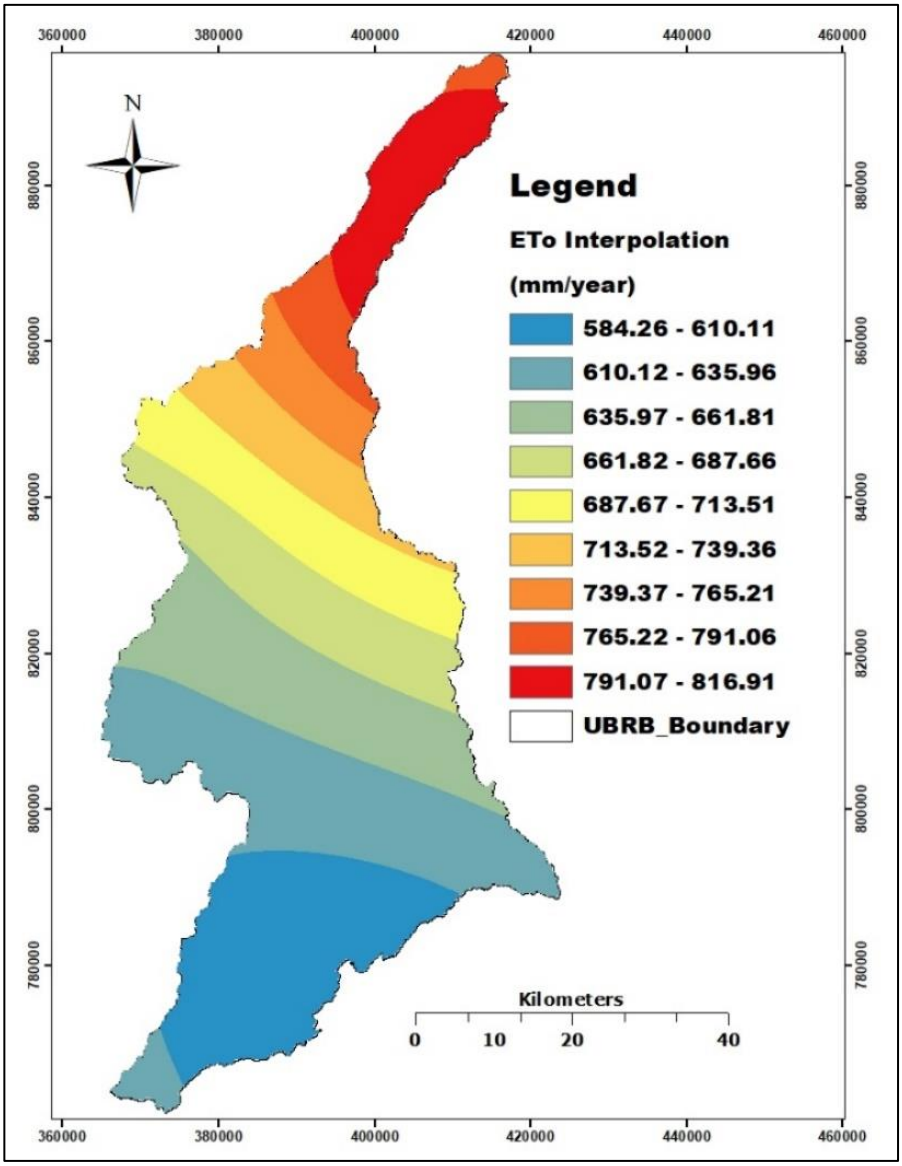

Figure 20. Spatial interpolation of annual ETo across the UBRB.

5.3 Estimation of actual evapotranspiration using the soil water balance method

That is, the actual amount of evapotranspiration that occurs: if $P < PET, then, AET = P - \Delta ST, and\ if\ P > PET\ then\ AET = PET.$

The water balance analysis, based on a root zone capacity of 214.09 mm, shows that annual precipitation (902.66 mm) exceeded potential evapotranspiration (648.07 mm), giving a net positive balance of 254.6 mm. Actual evapotranspiration (495.26 mm) accounted for about 76% of PET, with water deficits (152.81 mm) concentrated in the dry months (January–March and November–December). In contrast, the wet season (April–September) generated a significant surplus (254.20 mm), suggesting contributions to recharge and runoff. Soil moisture remained close to field capacity throughout the year, indicating limited storage depletion.

Table 15. Mean annual Water balance for UBRB

Para meters	**MAWC= 214.09mm**	Avarage root zone soil water capacity of Clay, loam=0.8125m											
	Jan	**Feb**	**Mar**	**Apr**	**May**	**June**	**July**	**Aug**	**Sep**	**Oct**	**Nov**	**Dec**	**Total**
P (mm)	12.55	19.46	55.31	95.94	112.96	100.61	152.72	155.08	104.76	57.92	22.42	12.92	902.66
PET (mm)	54.69	54.82	60.40	56.66	54.83	53.42	51.88	51.96	49.45	53.99	52.77	53.19	648.07
P-PET (mm)	-42.14	-35.36	-5.09	39.28	58.13	47.19	100.84	103.12	55.31	3.93	-30.35	-40.27	254.60
Accu.Pot. WL	-112.75	-148.11									-30.35	-70.62	-72.50
SM	213.86	213.80	214.09	214.09	214.09	214.09	214.09	214.09	214.09	214.09	214.09	214.06	
ΔSM= (SMi-SMi-1)	0.20	-0.06	0.29	0.00	0.00	0.00	0.00	0.00	0.00	0.00	0.00	-0.03	
AET (mm)	12.75	19.39	55.61	56.66	54.83	53.42	51.88	51.96	49.45	53.99	22.42	12.89	495.26
D = (PET-AET)	41.94	35.43	4.79	0.00	0.00	0.00	0.00	0.00	0.00	0.00	30.35	40.30	152.81
S = P - AET-ΔST	-42.33	-35.30	-5.38	39.28	58.13	47.19	100.84	103.12	55.31	3.93	-30.35	-40.23	254.20

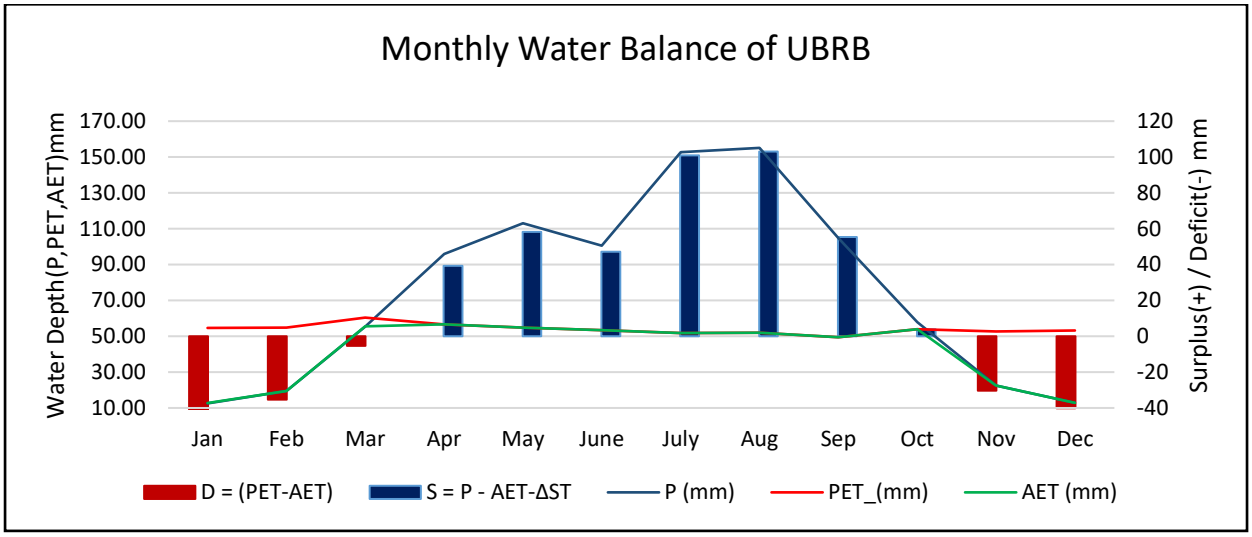

Figure 21 Monthly water balance of UBRB.

- From January–March and November–December, PET exceeds precipitation, creating significant water deficits(D).
- From April–September, rainfall far surpasses PET, leading to large surpluses(S) that can recharge soil and groundwater.
- AET closely follows PET in wet months, while it is limited by precipitation in dry months.

5.3.1 Maximum Available Water Capacity (MAWC)

Based on (Thornwhite & Matter, 1957) land use, soil texture types, and root depth are considered in determining Available Water Capacity (AWC) values using a Water Holding Capacity (WHC) table. Based on the values in the WHC table, a typical standard AWC value of 250 mm/m is assumed for each land use in UBRB. The maximum available water capacity of the UBRB is estimated to be 214.09 mm based on the data shown in the table below.

Table 16. Available water capacity estimated

LULC	Area	% Area	AWC[2] (mm/m)	Rooting Depth(m)	MAWC (mm)	Wt. MAWC (mm)
1. Built Area	677.48	20.27	250	0.25	62.5	12.67
2.Bare Ground	9.91	0.30	250	0.4	100	0.30
3. Crops Rangeland	2598.09	77.74	250	1	250	194.34
4. Trees	56.67	1.70	250	1.6	400	6.78
	3342.15	**100.00**				**214.09**

Turc Method:- The mean annual actual evapotranspiration of the study area is estimated using the Turc empirical formula(Gudulas et al., 2013):

Where: -

- AET =is the mean annual actual evapotranspiration (mm),
- P = is mean annual rainfall, =1039.83mm
- T = is mean annual temperature = 19.25℃
- L = is a thermal indicator, defined by the following equation:

$$L=300+25T+0.005*T^3 = \mathbf{1137.92}$$

Hence, actual evapotranspiration (AET) = **789.4mm.**

Crop Coefficient (Kc) Method: -The principle: to estimated AET is by adjusting Reference Evapotranspiration (ET_0) with a crop-specific coefficient: AET = Kc * ET_0. = 516.16mm

Table 17.Crop Coefficient (Kc) values for UBRB LULC

Class Code	LULC Class	Kc_ Representative
1	Built Area	0.28
2	Bare Ground	0.2
3	Crops	0.95
4	Trees	1.05
5	Water	1.1

The Actual Evapotranspiration calculated using the Soil Water Balance (495.26mm), Turc method estimated 789.4mm and using Crop Coefficient (Kc) from reference evapotranspiration (516.16mm). These values of AET difference arises from their fundamentally different principles, data requirements, and inherent assumptions.

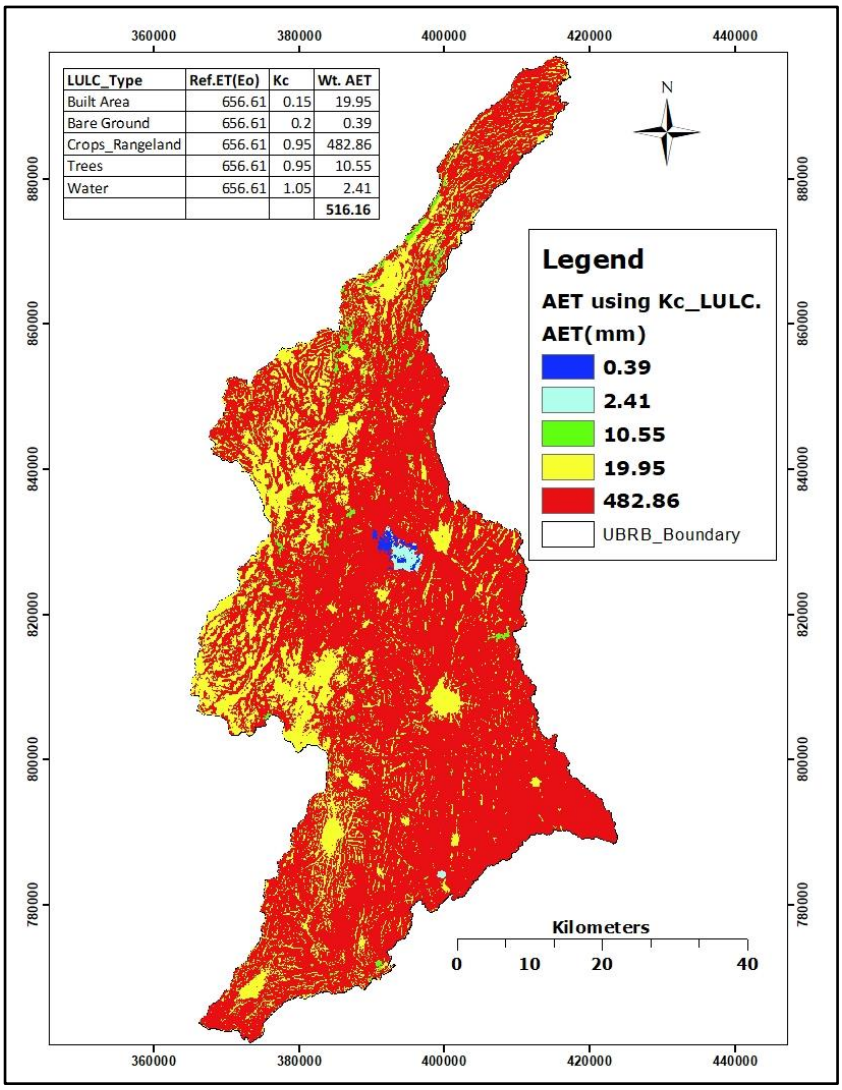

Figure 22. Actual evapotranspiration maps of the study area.

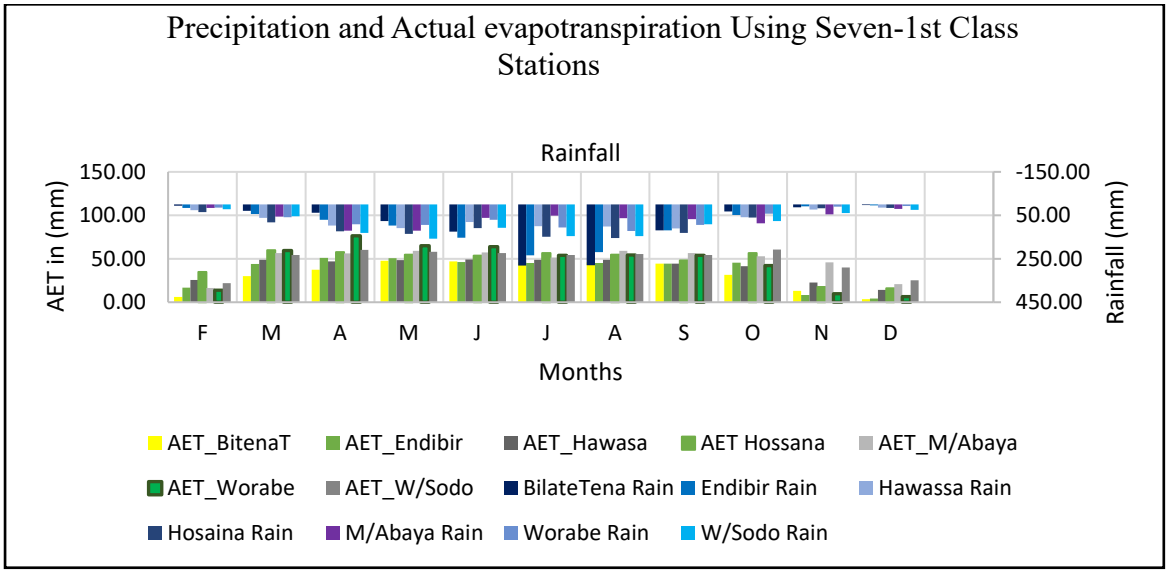

Figure 23. Graph of mean monthly Rainfall & Actual evapotranspiration.

Table 18.Summary of AET estimation methods

Method	Estimated ET (mm)	Type of ET Estimated	Key Consideration for Recharge Studies
Soil Water Balance	503.16	Actual ET (ET_a)	**Most Important.** Directly accounts for soil moisture change (ΔS) and allows for solving deep drainage (D), which is recharge.
Kc - ET_o	516.16	Potential Crop ET (ET_c)	Useful but secondary. Does not account for soil water stress, so may overestimate ET and underestimate recharge.
Turc	789.4	Climatic Potential ET	Least applicable. A gross overestimate for this case; ignores local conditions, making it unusable for accurate recharge calculation.

In hydrological and agricultural research, the crop coefficient method (Kc-ETo) estimates actual evapotranspiration (AET) by multiplying the reference evapotranspiration (ETo), calculated using the FAO Penman-Monteith equation, by a crop coefficient (Kc). AET = Kc × ETo

Table 19. Hydrologic soil group descriptions

Soil group	Description	Runoff characteristics
A	Loamy-sand, Sandy-loam, loam or silty-loam	When thoroughly wet, a low runoff Potential and facilitates the unrestricted flow of water through the soil
B	Loam sand or sandy loam	The soil exhibits a modest to small runoff Potential when fully saturated, and water movement within the soil is not hindered
C	Loam, silty-loam, sandy-clay-loam, clay-loam, and silty-clay-loam	Such soil exhibits a moderately high runoff Potential when fully wet with somewhat limited water movement
D	Clay	When soil is fully wet, the soil exhibits a high Potential for runoff, and water flow within the soil is either limited or very limited

Table 20. CN for land cover classes and HSG of the study area

LULC Type	Hydrologic soil group and curve number		
	B	C	D
1. Built Area	82	88	90
2. Bare Ground	80	85	90
3. Crops Rangeland	73	82	87
4. Trees	66	74	79
5. Water	100	100	100

(Mishra, Surendra Kumar, Singh, 2003)&(USDA, 2004) (Mutua & Klik, 2007)

For cases where the differences in the CN are greater than 5, weighting the Q rather than the CN is preferable. For the data above, the following shows the Q for each subarea(McCuen, 1998). Antecedent Moisture Condition (AMC) defines the amount of water in the soil at a certain point in time. This number represents the effect of infiltration on the discharge volume and velocity. Furthermore, the antecedent moisture condition II (AMC-II) is assumed to be relevant in this situation(P.Singh, 1994).

5.4 Hydrological analysis

Hydrology is essential for understanding water systems, with baseflow analysis and groundwater investigation as key methodologies. Baseflow analysis bridges surface water and groundwater research, improving our understanding of their interactions in the hydrological cycle. This approach highlights the significance of studying both surface and subsurface flows, enhancing water resource management and ecosystem health.

5.4.1 Groundwater recharge and discharge estimation

Groundwater discharge can be estimated using baseflow, river flow, and safe yield estimation from pumping test data.

5.5 Baseflow estimation

Baseflow indicates that a stream continuously obtains water from groundwater, which is a proxy to groundwater discharge, essential to maintaining flow in rivers (Miller et al., 2016).

Variable-slope method :- The variable-slope method is a graphical, recession-based hydrograph separation approach that allows different depletion rates (slopes) for different times of the year or different hydrologic conditions, making it more realistic than fixed-slope methods but also more subjective as seen in Table 21,and Figure 24 . The conversion of mean monthly discharge data yielded total runoff and baseflow depths for the gauged catchment and the UBRB after areal and precipitation correction. The annual total runoff depth at the gauged basin was estimated at 93.46 mm, while the total baseflow depth amounted to 65.96 mm. After applying precipitation correction, the adjusted baseflow depth for the UBRB was 58.89 mm, corresponding to approximately 63% of total runoff, indicating a dominant groundwater contribution to streamflow. Seasonal variation showed peak baseflow between June and October, coinciding

with the main rainy period, reflecting delayed groundwater response and subsurface storage contribution to stream discharge.

Table 21. Estimation of runoff and base flow using at Bilate Tena Station.

Month	Runoff_ gauge (m^3/s)	Runoff_ gauge (mm)	Baseflow. _gauge (m^3/s)	Baseflow_ gauge (mm)	Baseflow_ UBRB (areal) (mm)	Baseflow_ UBRB (precip-corr) (mm)
Jan	5.69	2.762	5.686	2.760	2.760	2.463
Feb	5.92	2.595	5.92	2.595	2.595	2.315
Mar	8.12	3.942	8.12	3.942	3.942	3.515
Apr	11.34	5.327	10.50	4.932	4.932	4.397
May	14.09	6.839	13.00	6.310	6.310	5.631
Jun	15.33	7.201	15.33	7.201	7.201	6.422
Jul	22.15	10.752	15.00	7.282	7.282	6.497
Aug	32.04	15.553	14.85	7.208	7.208	6.429
Sep	32.72	15.370	14.50	6.811	6.811	6.081
Oct	27.12	13.163	14.35	6.965	6.965	6.212
Nov	14.27	6.703	14.267	6.701	6.701	5.980
Dec	6.71	3.257	6.71	3.257	3.257	2.906
Total	-	93.46	-	65.96	65.96	58.89

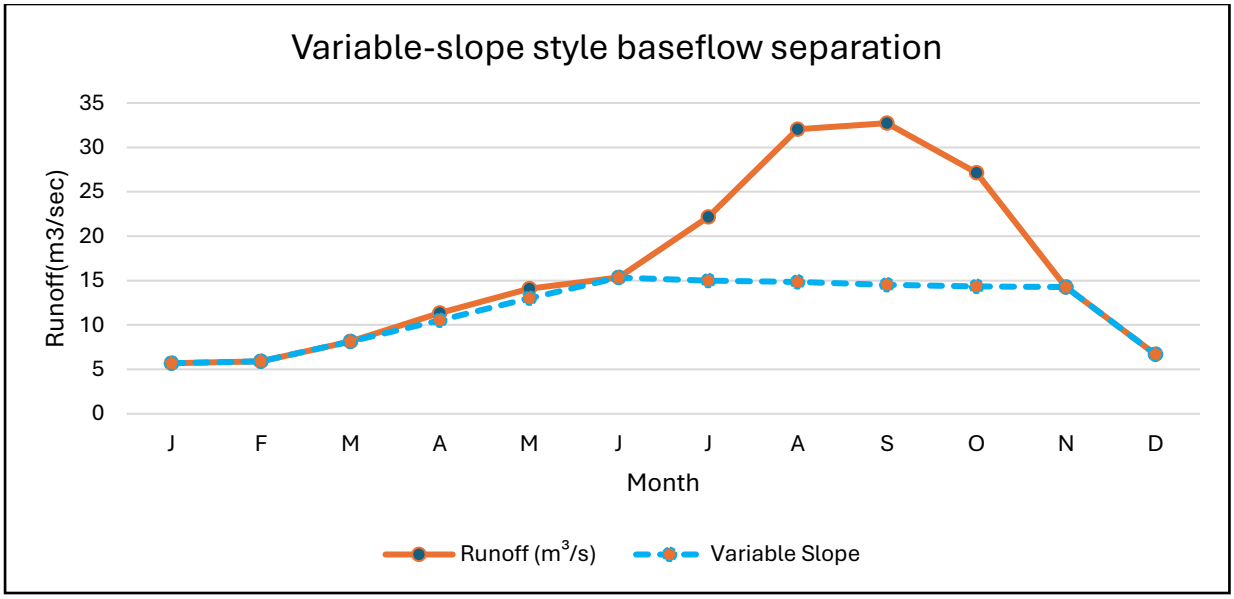

Figure 24. Graphical estimation of annual baseflow depth from Bilate River hydrograph.

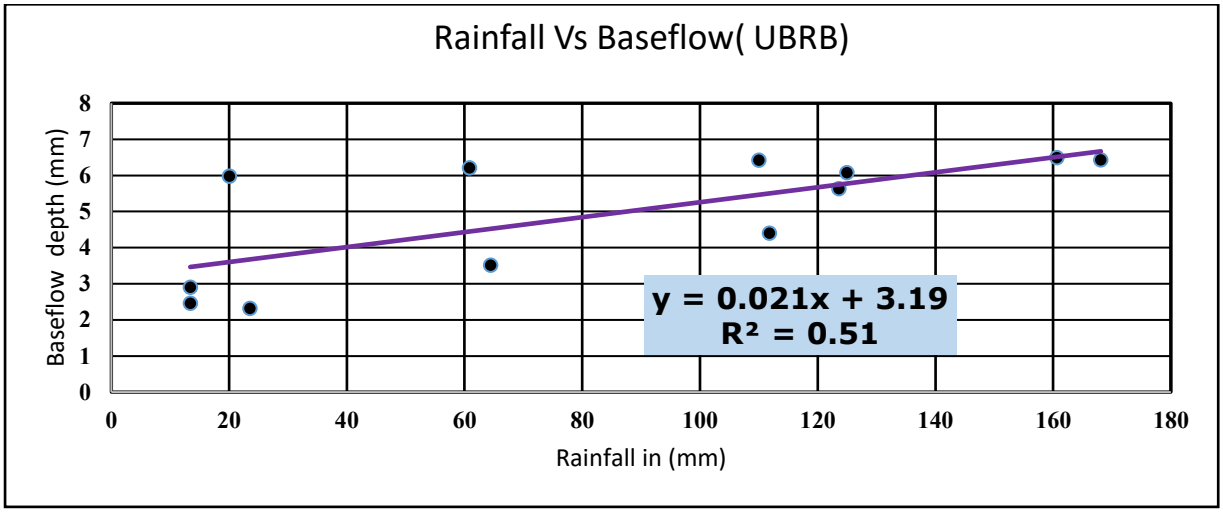

Figure 25. Rainfall and Baseflow Relationship

The regression analysis confirms a strong positive correlation (Multiple R = 0.710) between rainfall and baseflow, indicating that baseflow increases with rainfall. The coefficient of determination ($R^2 = 0.505$) shows that rainfall accounts for approximately 50.5% of the observed variation in baseflow. This establishes rainfall as a primary, but not exclusive, driver of baseflow in the catchment. The remaining variance (49.5%) is attributable to other factors not included in this model, such as antecedent soil moisture, evapotranspiration, and watershed characteristics. This signifies that a comprehensive predictive model would require the integration of these additional hydrological variables.

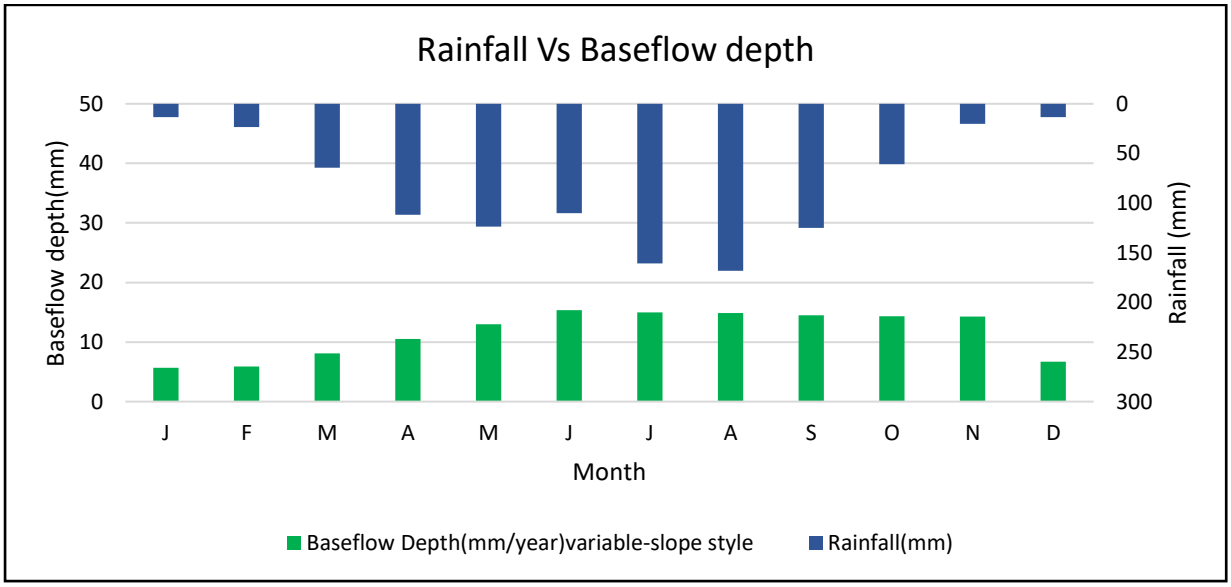

Figure 26. Rainfall and runoff relationship.

5.5.1 Groundwater recharge estimation

The groundwater recharge for the Upper Bilate River Basin (UBRB) was evaluated within a long-term water balance framework expressed as: $P - AET - Q - R = 0$ or $R = P - AET - Q$ where P is precipitation (mm), AET is actual evapotranspiration (mm), Q is total runoff (surface and subsurface discharge) (mm), and R represents groundwater recharge (mm). The mean annual precipitation and actual evapotranspiration (Crop Coefficient Method) were obtained from regional climatological analyses, while total runoff was derived from the gauged discharge data of the downstream catchment.

In this study, the baseflow component (Qb) of the total runoff was estimated using hydrograph separation techniques and interpreted as groundwater discharge that sustains streamflow during dry periods. Under quasi-steady-state hydrologic conditions—where long-term groundwater storage variations are negligible—the baseflow is assumed to approximate the groundwater recharge ($R \approx Qb$). Accordingly, the precipitation- and area-corrected annual baseflow depth of 58.9 mm yr^{-1} for the UBRB was adopted as the representative mean annual groundwater recharge. This value indicates that approximately 6% of the annual rainfall (1039.83 mm) percolates to recharge the aquifer system, consistent with semi-humid volcanic terrains characterized by moderate infiltration capacity and significant groundwater–surface water interactions.

5.5.2 Hydrological conceptual model

Although the water balance equation may seem simple at the scales of catchments and sub-basins, it is fundamentally important for understanding groundwater yield (Negewo & Sarma, 2021). And, according to Gidafie et al.(2019), Melo et al.(2015), and the hydrological conceptual model of the study area indicated in Figure 27.

Assumption:

As the calculations are conducted annually, the assumption is made that there is no change in groundwater storage. The assumption is made that surface and subsurface water are not exchanged with neighbouring basins, provided there are no intentional or artificial diversions from other basins.

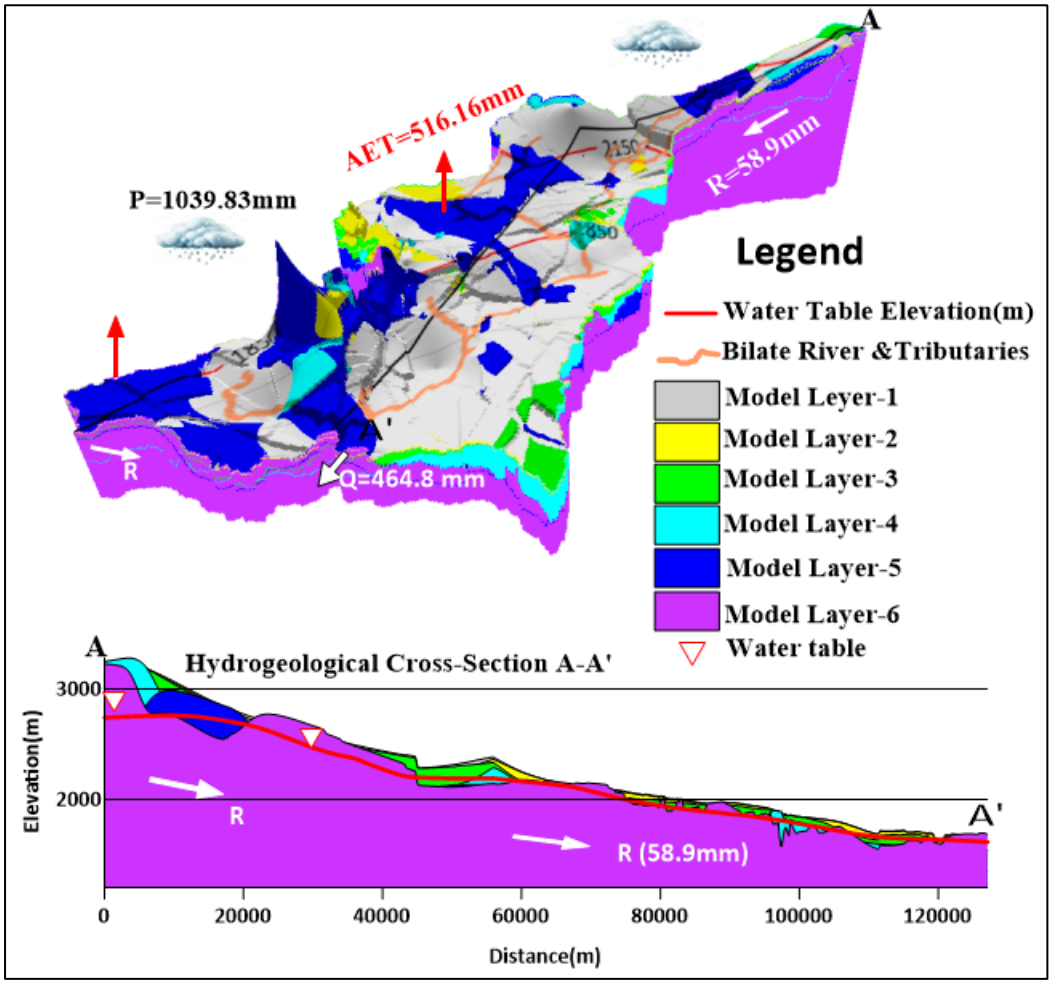

Figure 27. Schematic hydrological conceptual model of the UBRB

The annual water balance for the UBRB is expressed under the steady-state assumption as follows: P - AET - Q - R = 0. Here, (P) represents precipitation, which is 1,039.8 mm per year; (AET) stands for actual evapotranspiration at 516.2 mm per year; (Q) denotes streamflow at 464.8 mm per year; and (R) indicates recharge at 58.9 mm per year. This equation confirms the internal consistency of the soil-water balance. The precipitation-corrected baseflow-derived recharge of 58.9 mm per year corresponds to approximately 209.6 million cubic meters per year (or about 6.65 cubic meters per second) for the study area, which covers 3,557.9 square kilometers. This recharge represents roughly 5.7% of the annual rainfall. Although the total volumetric recharge is hydrologically significant, the recharge fraction is relatively modest. Therefore, groundwater development should be approached conservatively, considering seasonality and storage dynamics. To refine sustainable yield estimates, it is advisable to cross-check groundwater-level trends, utilize independent AET estimates, and explicitly account for pumping activities.

5.6 Hydrogeology

According to the Hydrogeological and Hydrochemical Maps of Hosaina NB 37-2, (2013) and Verner, (2025)the hydrogeological map shows aquifers and aquicludes defined based on the character of the groundwater flow (pores, fissures), the yield of springs and the hydraulic characteristics of Wells (Figure 28). The following aquifers and aquicludes were defined:

- Extensive and moderately productive or locally developed and highly productive porous aquifers. The aquifers consist of Quaternary lacustrine sediments (Ql).
- Extensive and moderately productive fissured aquifers. The aquifers consist of basalts of rift floor, ignimbrite, rhyolite and trachyte of highlands and escarpment.
- Extensive and moderately or locally developed and highly productive mixed porous and fissured aquifers. The aquifers consist of volcanic, sedimentary and pyroclastic rocks of the Central volcanic complexes, pumiceous pyroclastics of Dino formation.

Surface and sub-surface charactestics are important governing hydrogeological frameworks of the UBRB area. Any groundwater investigation study requires knowledge of the nature of the aquifer system and groundwater conditions relay on quality remote sensing geospatial data, well, and pumping test data (Kovalevsky et al., 2004).

5.6.1 Hydrogeological controls characteristics

Satellite data has proven to be very useful for surface study, especially in detecting surface features and characteristics such as lineaments and geology. Hydrogeological investigations of groundwater potential are shaped by topographic features like topography, landforms, drainage, soil, vegetation, and surface water. Key indicators include soil type, land use/cover, drainage, lineaments, Slope, and NDVI, all of which impact infiltration and drainage. In the UBRB, tectonic and volcanic geomorphology strongly influence groundwater recharge. Understanding geomorphology is crucial for interpreting hydrogeological conditions and surface–subsurface interactions.

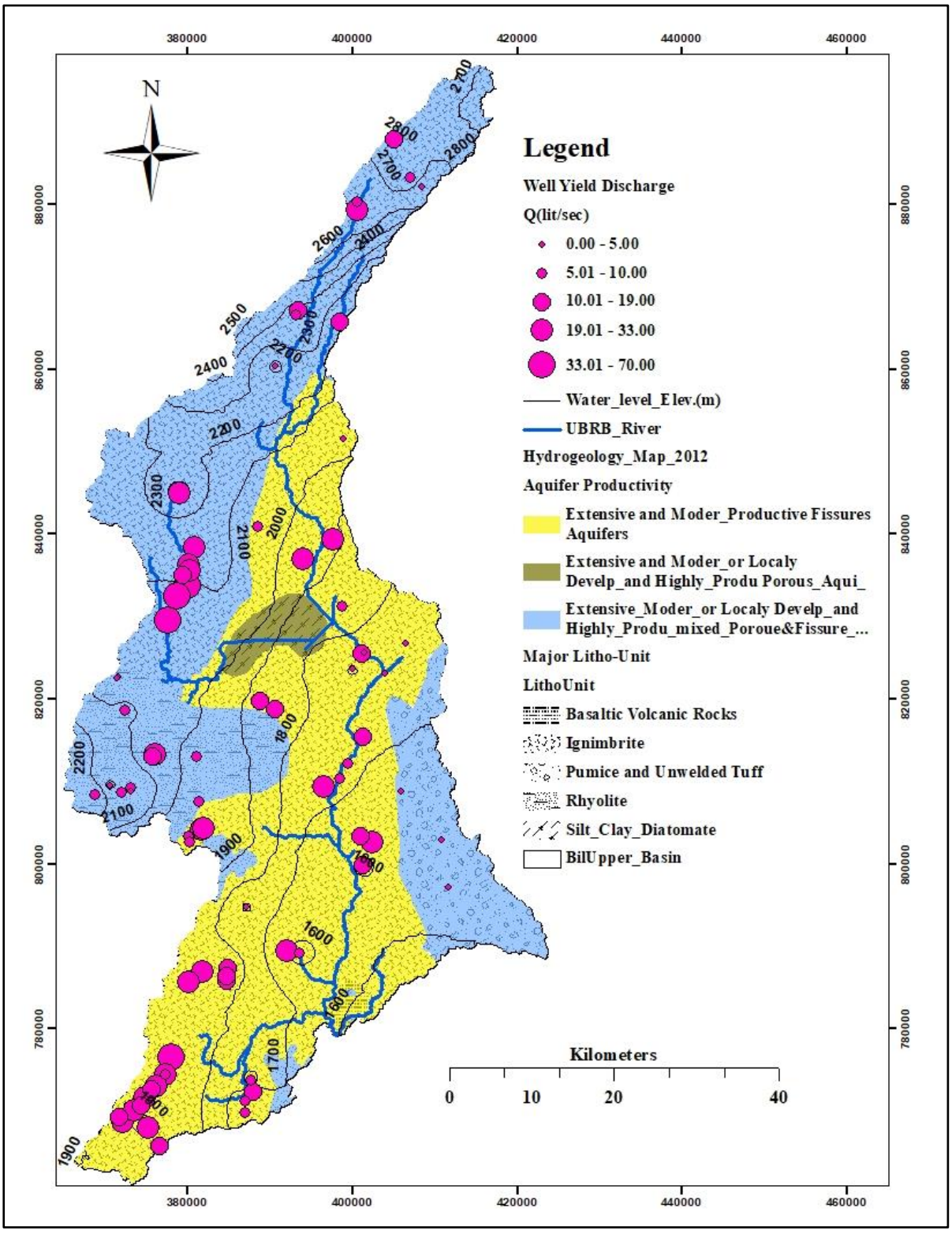

Figure 28.Hydrogeology map of the Upper Bilate River Basin

NDVI range for groundwater potential occurrence

Studies (Abdullahi et al., 2019;Sener et al., 2005; Nag & Kundu, 2018;Jha et al., 2007) show that areas with moderate to high NDVI values tend to have better groundwater Potential, as vegetation indicates sufficient moisture. Based on peer-reviewed studies (Abdullahi et al., 2019) ,(Sener et al., 2005),(Nag & Kundu, 2018),(Jha et al., 2007) the following NDVI ranges correlate with groundwater Potential. From a groundwater perspective, the NDVI classification of UBRB reveals a distinct hydrological gradient: the highest NDVI values (0.71-0.93) delineate vibrant riparian corridors indicative of shallow groundwater discharge and phreatic access; the moderate class (0.31-0.7) suggests mixed soil moisture and periodic groundwater use; the low class (0.11-0.3) represents recharge-dominated areas reliant on precipitation; and the lowest values (-1 to 0.1) primarily mark the active river channels and barren surfaces, directly mapping the groundwater system's effluent drainage network.

Table 22. NDVI ranks and interpretation to groundwater potential

NDVI Range	Interpretation	Likely Groundwater Potential
-1.0 to 0.1	Bare soil, water bodies, or urban areas	Low
0.1 to 0.3	Sparse vegetation (low moisture)	Moderate
0.31 to 0.7	Moderate to dense vegetation (high moisture)	High groundwater Potential
0.7 to 0.93	Very dense vegetation (forests, wetlands)	Very high (but may depend on other factors)

Slope: - Groundwater can be recharged by water infiltration into flat or slightly sloping areas. Conversely, water runs off steep slopes and does not seep deep into the ground. Areas with the lowest gradient favour minimum runoff and high percolation is ranked highest. Conversely, areas with the steepest slopes are ranked lowest because they have low percolation and high runoff(Roy et al., 2020).

Table 23. Rate and rank of slope

Class	Rank	Area (Km^2)	Percentage%
Flat	5	1686.50	50.22
Gentle	4	1003.89	29.90
Medium	3	451.62	13.45
Steep	2	170.31	5.07
Very Steep	1	45.60	1.36

Lineament density: - Weathered zones shaped by tectonic and volcanic activity influence groundwater flow. Understanding this movement involves analyzing lineaments—linear features that reflect subsurface structures. Groundwater moves through these fractures, especially where porosity and secondary permeability are present. High lineament density suggests greater groundwater Potential and better circulation(Gopinathan et al., 2020).

Drainage density: - In the study area, groundwater movement is influenced by slope, vegetation, soil absorption, and geology. A key factor is drainage density—the spacing between streams. High drainage density leads to more runoff and less infiltration, making it less suitable for groundwater development. Low drainage density indicates better groundwater Potential due to higher rock permeability (Magesh et al., 2012; Meijerink et al., 2007; Pande et al., 2021; Shao et al., 2019; Guduru & Jilo, 2022). The area has five drainage density classes, from extremely low (<1) to very high (>5), with low-density areas ranked higher. The central and southern parts have lower drainage densities, while the north and west are higher. The study area characterized by primarily dendritic, with minor local influences of radial drainage in elevated parts.

Land use land cover (LULC):- Man-made and natural features on Earth are described through land use and land cover (LULC), which influence key hydrological processes like evapotranspiration, infiltration, and runoff(Roy et al., 2020). In the UBRB, five LULC types are identified: water bodies (0.35%), built-up areas (20.26%), trees (1.69%), cultivated and pasture land (77.41%), and undeveloped land (0.30%). Cultivated and pasture lands dominate, promoting infiltration and reducing runoff. In contrast, urban areas limit infiltration due to impervious surfaces. This highlights the importance of preserving agricultural and pasture lands for water retention, while built-up areas offer limited benefit. Sentinel-2 provides global remote sensing data for such assessments. LULC map at 10-meter resolution can be accessed using the link https://ieeexplore.ieee.org/document/9553499/authors(Karra et al., 2021).

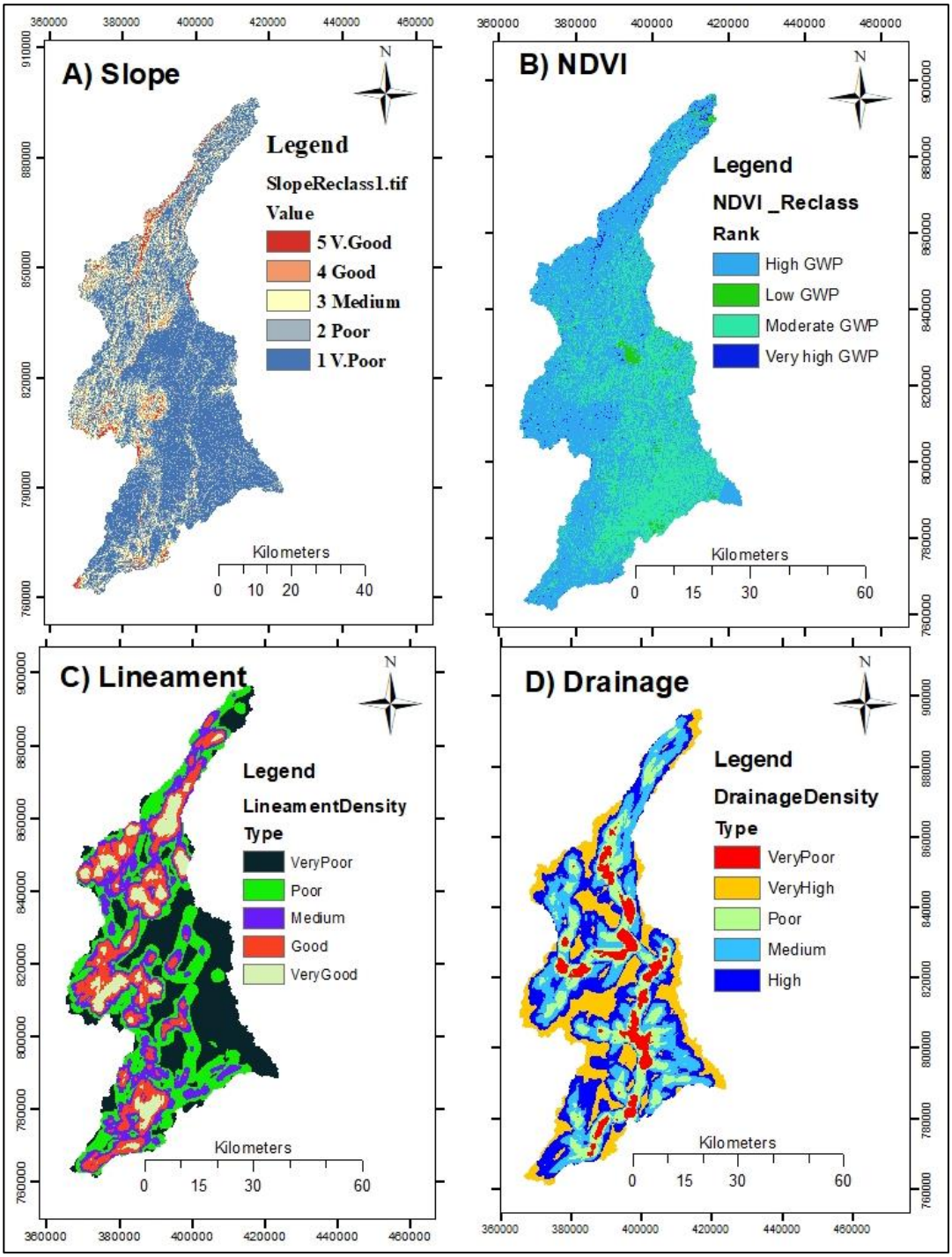

Figure 29.Map showing Slope(A), NDVI(B), Lineament (C) & Drainage (D).

Table 24. Rate and rank of LULC and Crop Coefficient (Kc)

Type	Rank	Kc Representative	Area Sq_Km	Percentage
1. Built Area	1	0.28	680.16	20.26
2. Bare Ground	3	0.2	9.91	0.30
3. Crops	4	0.95	2599.30	77.41
4. Trees	3	1.05	56.82	1.69
5. Water	5	1.1	11.72	0.35

Soil types: - Determining groundwater zones requires assessing soil properties like permeability, infiltration, and seepage, which affect how surface water enters aquifers. In the UBRB (Figure 30), clay, clay-loam, and loam dominate. While clayey soils have low infiltration and water retention, clay soils are prioritized for their high percolation capacity

Table 25. Soil type and areal coverage

Texture	**AreaSqKm**	**Percent**	**Soil Type**
clay	832.35	24.79	Andosols
clay loam	289.11	8.61	Anthrosols
loam	2236.44	66.60	Fluvisols
Total	**3357.9**	100.0	

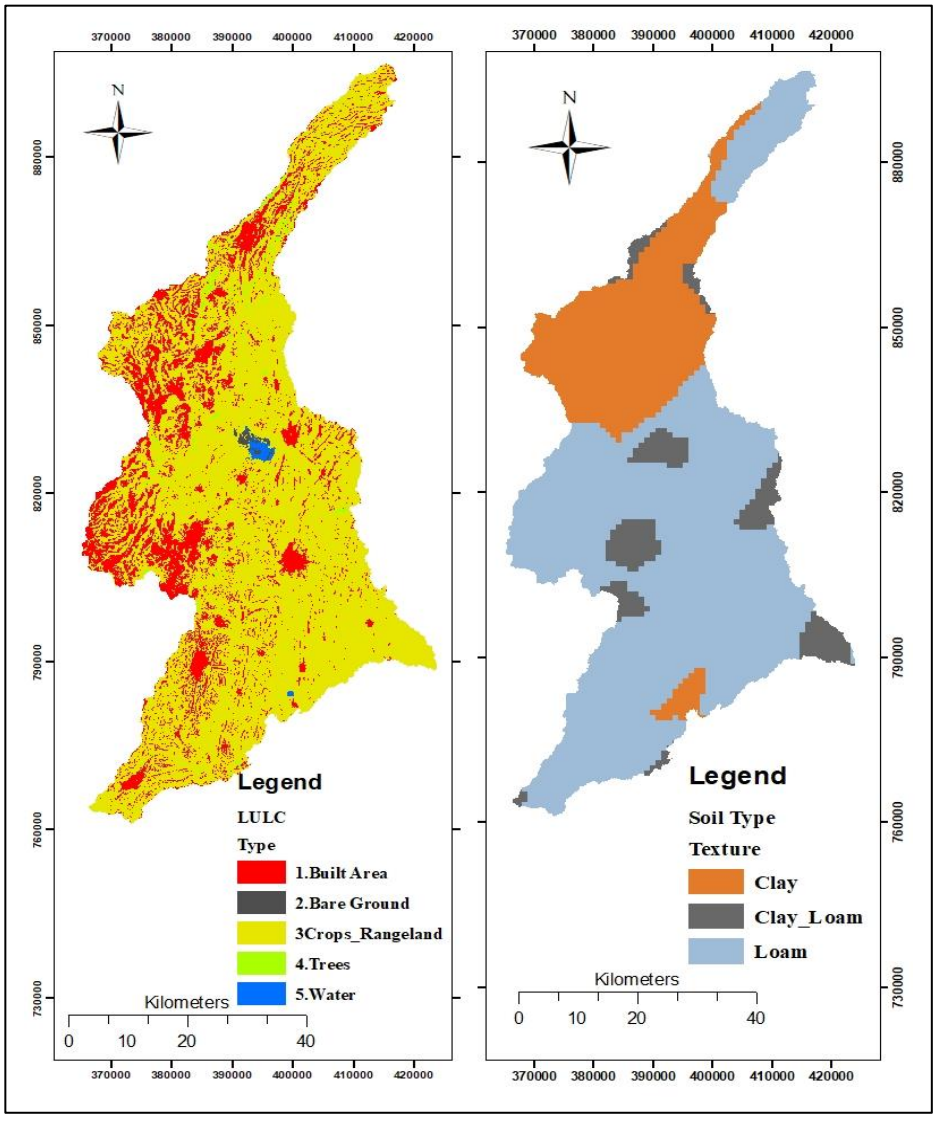

Figure 30. LULC (left) and Soil texture(right) thematic map of UBRB.

5.6.2 Aquifer parameter estimation

Pumping Tests: Theis Method (transient flow) or Thiem Equation (steady-state) to calculate transmissivity (T) and storativity (S). Cooper-Jacob Approximation simplifies drawdown analysis for confined aquifers. For a single well pumping from a confined aquifer, the two most important factors that cause a deviation from the Theis solution are wellbore storage and well-skin effects. These two factors cause additional drawdown in the wellbore that is not representative of the drawdown in the aquifer. Agarwal (1970) introduced the idea of log-log curve matching of dimensionless pressure versus dimensionless time to analyze pressure data at a well dominated by wellbore storage and skin effects. AquiferTest has implemented the Agarwal wellbore storage and skin solution for water wells using the following assumptions: single-pumping well, confined aquifer, and observations only in the pumping well.

Hydrostratigraphic analysis

Lithostratigraphic correlation: Integrate well logs data to delineate layers (aquifers, aquitards).
Lithological Logging: Well logs aid in identifying different stratigraphic layers.

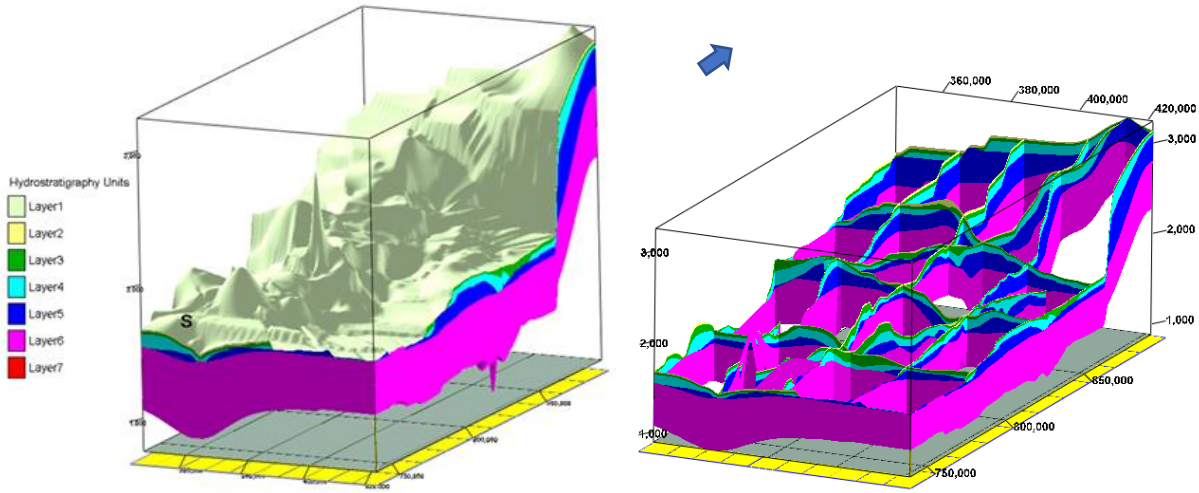

Figure 31.Hydrostratigraphic layers thickness model(left), and fence diagram(right).

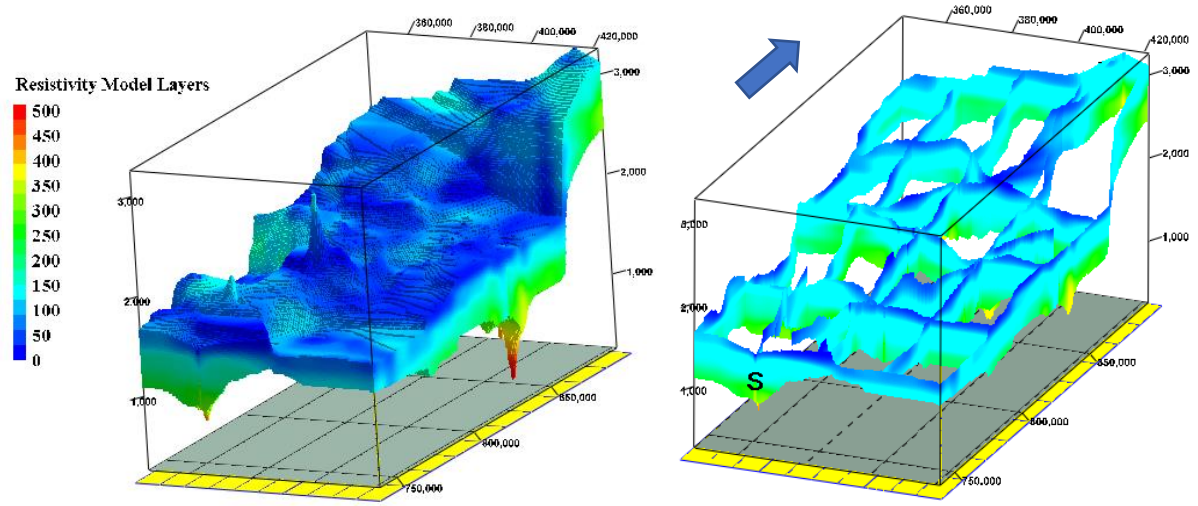

Figure 32.Model layer resistivity value(left), and fence diagram(right).

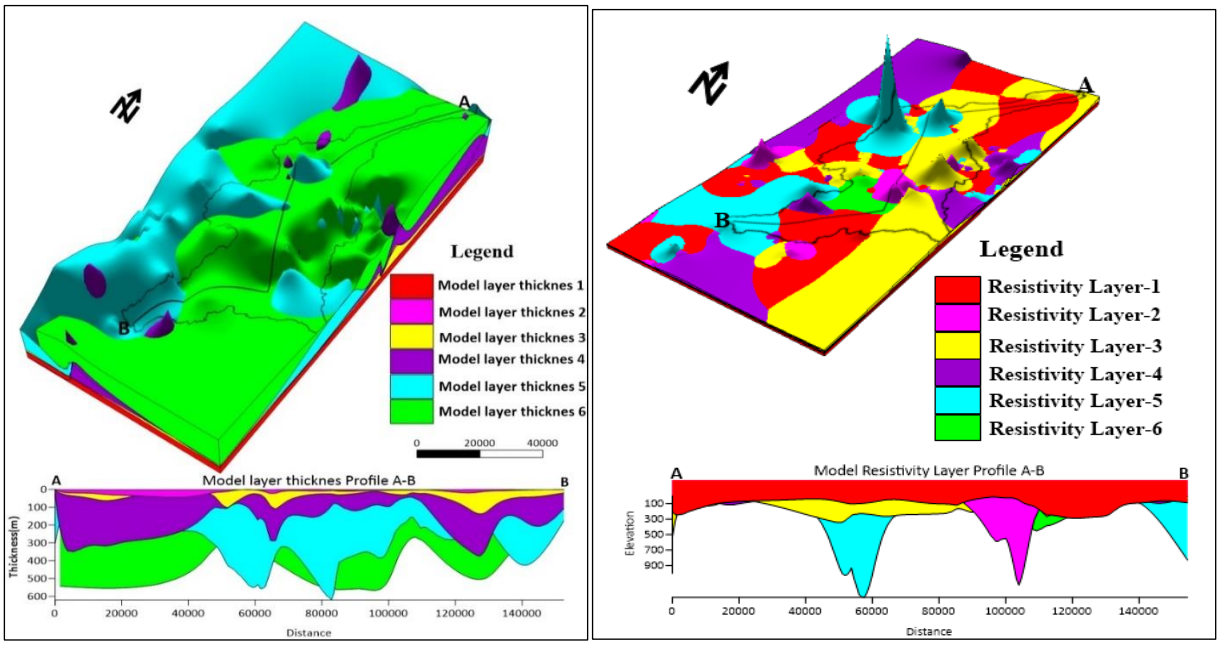

Figure 33. Model layer thickness (left) and model layer resistivity(right).

Table 26. Layer resistivity descriptive statistics

Layer Thickness	Mean	Minimum	Maximum	Confidence Level (95.0%)
Layer Thickness 1	1.71	0.39	30.30	0.28
Layer Thickness 2	9.48	0.02	144.00	2.25
Layer Thickness 3	54.06	0.83	790.00	13.37
Layer Thickness 4	144.25	2.15	913.00	23.94
Layer Thickness 5	292.40	9.73	906.00	31.00
Layer Thickness 6	452.29	36.40	832.00	36.29

The subsurface layering displays increasing thickness from shallow to deep layers. Layer 1 is the thinnest at an average of 1.71 meters, with significant variability (0.39 to 30.30 meters). Layer 2 has a moderate average of 9.48 meters and can reach up to 144 meters. Starting from Layer 3, thickness increases considerably, with a mean of 54.06 meters and a maximum of 790 meters. Layer 4 averages 144.25 meters, while Layer 5 averages 292.40 meters, ranging from 9.73 to 906 meters. Layer 6, the deepest, has the highest mean thickness at 452.29 meters, with less variability (36.40 to 832.00 meters). The 95% confidence intervals widen with depth, reflecting increased uncertainty in the deeper layers. Overall, the findings reveal a subsurface with thin, variable upper strata and progressively thicker, more heterogeneous deeper layers, illustrating complex geological processes.

Table 27. Layer thickness descriptive statistics

Layer Resistivity	Mean	Minimum	Maximum	Confidence Level (95.0%)
Layer Resistivity 1	120.58	3.41	626.00	14.13
Layer Resistivity 2	93.05	0.49	2882.00	36.55
Layer Resistivity 3	137.46	1.84	2564.00	35.50
Layer Resistivity 4	161.52	3.02	1972.00	37.62
Layer Resistivity 5	181.71	0.60	10237.00	115.59
Layer Resistivity 6	59.76	0.35	795.00	23.67

Table 28.Description of the main hydrostratigraphic units of UBRB

Units	Estimated Depth	Average Thickness	Avg Resistivity	Major Lithology	Hydraulic behavior /Aquifer type
Layer1	1.71	1.71	120	Clay/Top Soil	Aquitard
Layer2	11.19	9.48	93.05	Alluvial/lacustrin deposit	Unconfined Aquitard
Layer3	65.25	54.06	137.46	Moderately weathered trachy-basalt units	Leaky Aquifer
Layer4	209.50	144.25	161.52	Moderately weathred & fractured volcano sedimentary unit	Confined Aquifer
Layer5	501.90	292.4	181.71	Weatherd and fractured proclastic unit	Confined Aquifer
Layer6	954.19	452.29	59.76	Highly weatherd and fractured pyroclastic unit	Confined Aquifer

5.6.3 Hydrogeological framework and groundwater potential delineation

The UBRB is dominantly characterized by Pyroclastic Rocks (Ignimbrite and Tuff with minor Pitchstones/Obsidian), a central volcanic complex (Rhyolite and Trachyte) formation, and Volcanic and Volcano-Sedimentary Formations.

In the UBRB, Potential Groundwater Resource zones governed by surface and sub-surface charactestics of hydrogeological frameworks were identified by overlaying ten (10) relevant thematic layers associated with groundwater contribution. An indirect method, a weighted overlay analysis, was performed using ArcGIS, resulting in the creation of a GWPZ map (Figure 5). The Potential groundwater zones were rated as poor, medium, good, or very good based on their weights. According to the results, approximately 1.39% of the total area fell into the excellent category, 17.9% were classified as very high, 79.17% as high, and low areas constituted about 1.54% of the study area, as shown in Table 4. The map revealed significant groundwater potential in the very high, which comprised 79.17% of the study area.

Table 29.Pairwise comparison matrix and weights of groundwater controlling factor

Matrix		Rainfall	AET	TWI	Geomor-phology	Litholog y	NDVI	Lineame nt	LULC	Drainage	Soil	**Normalized principal Eigenvector**
		1	2	3	4	5	6	7	8	9	10	
Rainfall	1	1	1	1	3	5	5	5	5	7	7	22.15%
AET	2	1	1	1	3	3	5	5	5	7	7	20.46%
TWI	3	1	1	1	3	3	3	3	5	7	7	18.65%
Geomorph-ology	4	1/3	1/3	1/3	1	3	3	3	5	7	7	12.50%
Lithology	5	1/5	1/3	1/3	1/3	1	3	3	5	5	5	9.07%
NDVI	6	1/5	1/5	1/3	1/3	1/3	1	1	1	5	5	5.01%
Lineament	7	1/5	1/5	1/3	1/3	1/3	1	1	1	3	5	4.67%
LULC	8	1/5	1/5	1/5	1/5	1/5	1	1	1	3	3	3.83%
Drainage	9	1/7	1/7	1/7	1/7	1/5	1/5	1/3	1/3	1	1	1.85%
Soil	10	1/7	1/7	1/7	1/7	1/5	1/5	1/5	1/3	1	1	1.79%

Consistency Ratio (CR) =5%

Table 30.Thematic layers weight and sub layers ranking of UBRB

No	Layers	Waight	Subclass	Rank
1	Rainfall	**22**	Very Low	1
			Low	2
			Moderate	3
			High	4
			Very High	5
2	AET	20	Very Low	5
			Low	4
			Moderate	3
			High	2
			Very High	1
3	Geomorphology	13	Western Escarpment	1
			Pediment	2
			Rift Floor	3
			Bajada_maar	4
			Water _Swampy	5
4	Lithology	9	Mod._High_Welded_ Gnimbrite	1
			Ignimbtire_Basaltic Trachyte	2
			Unwelded_Pumice Taff_Silicics_Undifferentiated	3
			Volcano_Sedi.Rocks_ WaterlainPyroclastic	4
			Mod.High_Welded_Gnimbrite	5
5	Slope	19	Very Low	5
			Low	4
			Moderate	3
			High	2
			Very High	1

No	Layers	Waight	Subclass	Rank
6	**NDVI**	5	Low GWP	1
			Moderate GWP	2
			High GWP	3
			Very High GWP	4
7	**Lineament**	5	VeryPoor	1
			Poor	2
			Medium	3
			Good	4
			VeryGood	5
8	LULC	4	Built Area	1
			Bare Ground	2
			Crops Rangeland	3
			Trees	4
			Water	5
9	Drainage	2	VeryHigh GWP	1
			High GWP	2
			Medium GWP	3
			Poor GWP	4
			VeryPoor GWP	5
10	Soil	1	Clay	1
			Clay Loam	2
			Loam	3

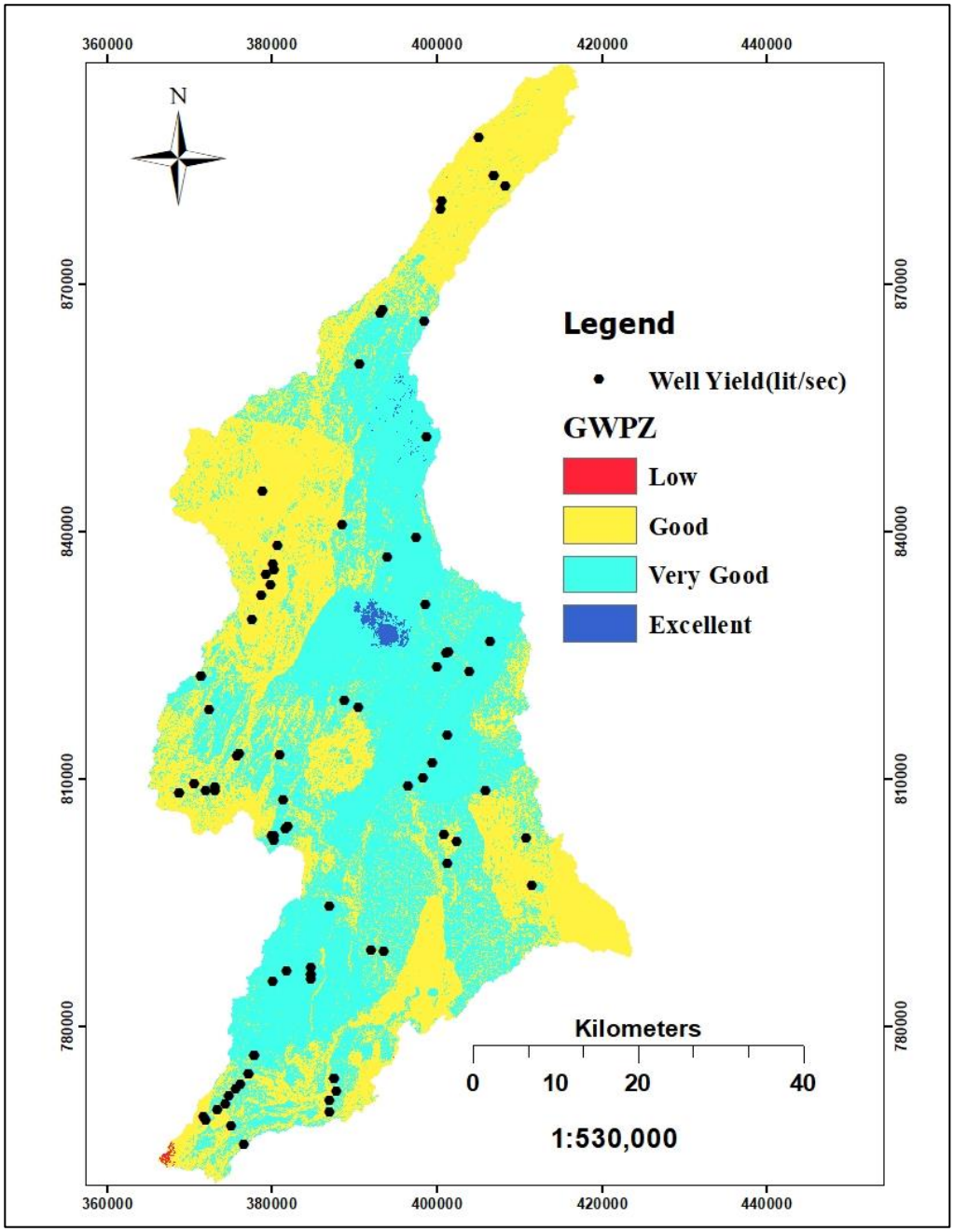

Figure 34. Groundwater Potential zone

Table 31. Groundwater potential zone map (GWPZ) statistics.

Value	Class	Area Sq. km.	Areal Percentage (%)
1	Low	1.95	1.54
2	High	1552.73	79.17
3	Very High	1783.65	17.9
4	Excellent	16.61	1.39

5.6.4 Validation of groundwater potential map using well yield data

The UBRB has a total area of 3,354.9 km². To validate the results of groundwater potential controlling characteristics, a total of 85 Wells were used.

Table 32. Distribution of Wells by Potential Classes

Groundwater Potential Class	Area (km²)	% of Area	Wells	% of Wells
Low	1.95	0.06%	0	0.0%
High	1552.7	46.3%	22	25.9%
Very High	1783.7	53.2%	63	74.1%
Excellent	16.6	0.5%	0	0.0%

Validation Findings

• Strong Agreement: 74% of Wells fall within the Very High Potential zone (covering ~53% of the area), showing reliable prediction of productive zones.

• Moderate Agreement: 25.9% of Wells occur in the High Potential zone (covering 46% of the area), indicating acceptable consistency.

• Low & Excellent Zones: No Wells fall in these classes. The Low zone prediction is consistent (non-productive), while the Excellent zone requires more field data or re-evaluation.

Success Rate Curve (SRC) Analysis

- At 46% cumulative area, the map predicts 25.9% of Wells.
- At 99.5% cumulative area, the map predicts 100% of Wells.
- AUC (Area Under Curve): ~0.78, indicating good predictive accuracy (better than random, close to reliable).

5.7 Aquifer parameter estimation

Aquifer parameters play a crucial role in assessing potential groundwater zones and drilling challenges, particularly in the context of groundwater exploration and well drilling. Understanding these parameters helps in designing and executing drilling operations more efficiently and economically. Here are some key aquifer parameters and their significance in assessing drilling challenges:

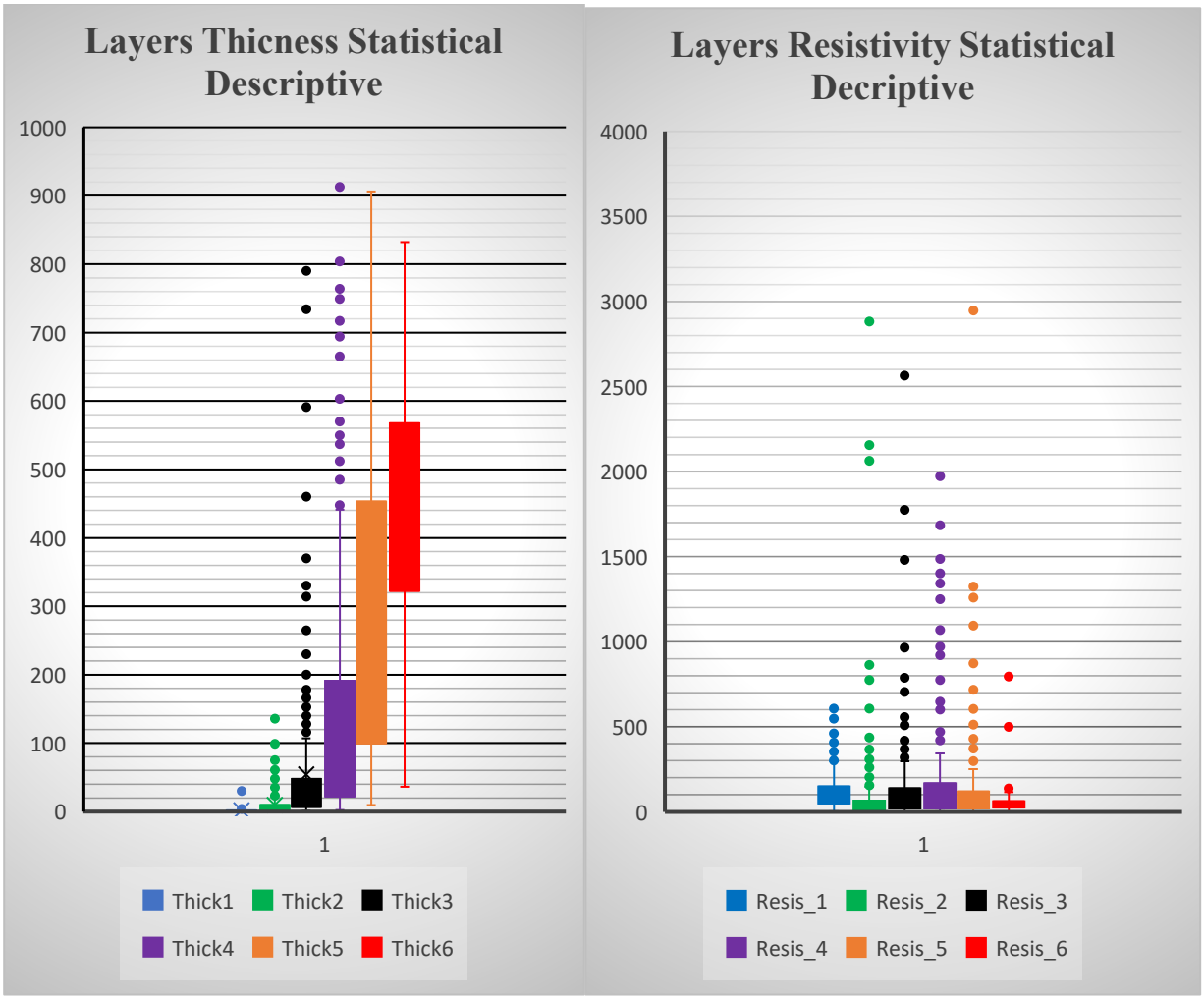

Figure 35. Box and whisker plot showing layer thickness (left) and layer resistivity(right)

Table 33. Statistical description os aquifer layer thickness and layer resistivity

Thick1		*Thick4*	
Mean	1.71	Mean	144.25
St.Dev.	2.23	St.Dev.	185.45

Thick2		*Thick5*	
Mean	9.48	Mean	292.40
St.Dev.	17.71	St.Dev.	213.70

Thick3		*Thick6*	
Mean	54.06	Mean	452.29
St.Dev.	105.36	St.Dev.	159.88

Resis_1		*Resis_4*	
Mean	120.58	Mean	161.52
St.Dev.	111.34	St.Dev.	291.42

Resis_2		*Resis_5*	
Mean	93.05	Mean	181.71
St.Dev.	288.03	St.Dev.	796.91

Resis_3		*Resis_6*	
Mean	137.46	Mean	59.76
St.Dev.	279.74	St.Dev.	104.29

5.7.1 Time -drawdown curve characteristics

A Time-drawdown pumping test conducted in the top and foot of the western rift escarpment, and in a pediment morphology (recharging zones), indicates that these areas are actively receiving recharge from precipitation and streams, revealing distinct characteristics compared to tests in the floor of the rift areas. In a recharging zone, drawdown occurs more slowly because water is being replenished into the aquifer during the pumping period. The drawdown curve shows a "flattening" or "recovery trend" while pumping is still ongoing. This is known as the recharge boundary effect—a sign that the cone of depression has reached a zone where replenishment occurs, like a stream or recharge mound.

A Time-drawdown pumping test conducted in a rift floor of the UBRB **(**discharge zone) is an area where groundwater naturally flows out of the aquifer, such as to springs, rivers, wetlands, or drains has its distinct characteristics (caving and circulation loss that enhance groundwater movement)) compared to tests in recharge zones.

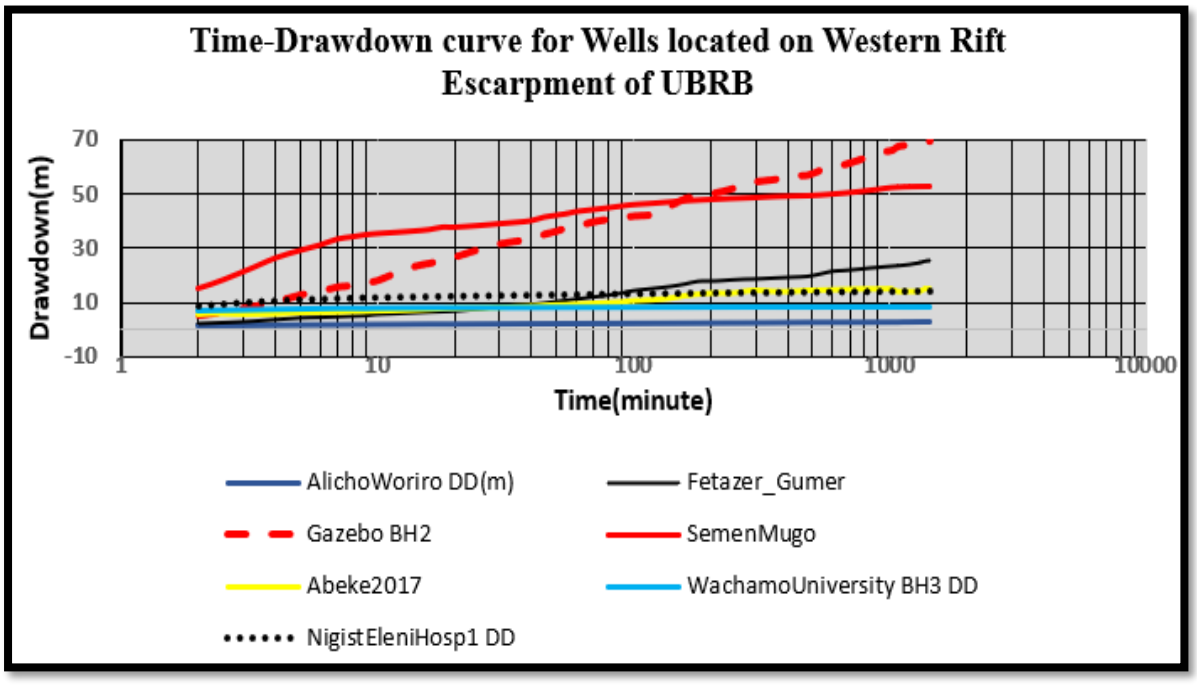

Figure 36. Time -drawdown curve for wells located on Western Rift Escarpment of UBRB

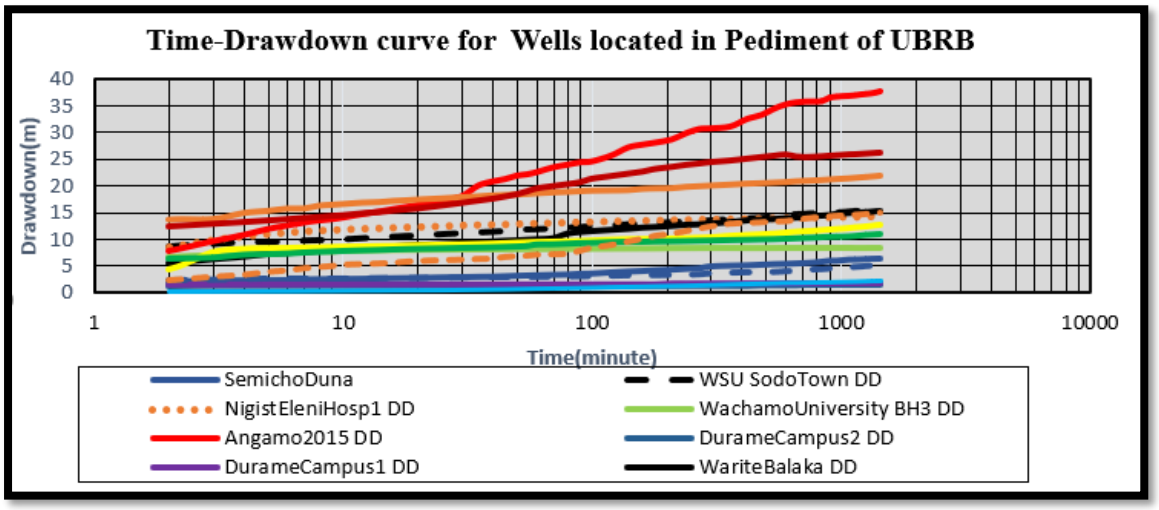

Figure 37.Time -drawdown curve for wells located in Pediment of UBRB.

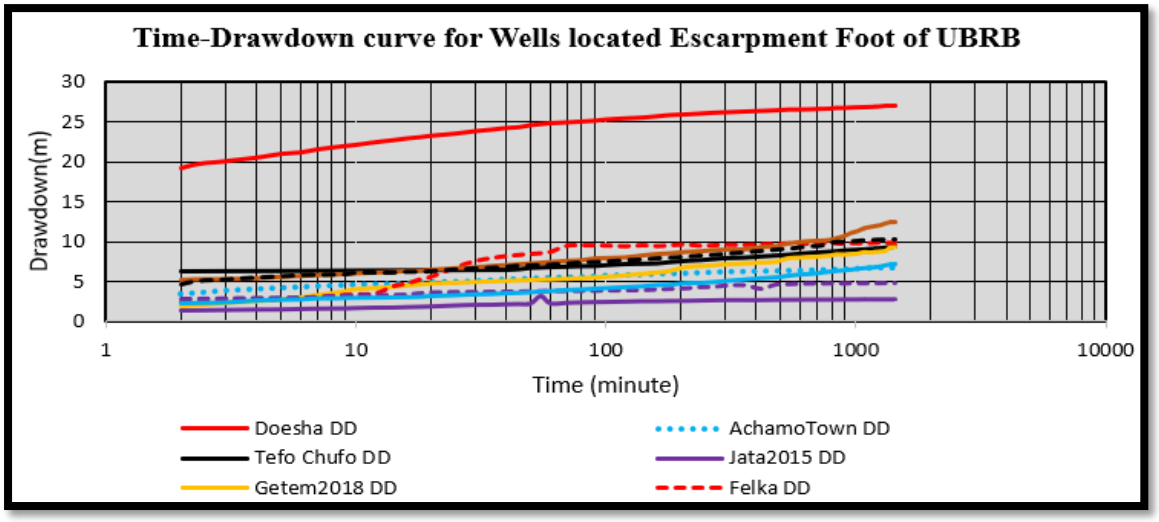

Figure 38.Time -drawdown curve for wells located on Escarpment Foot of UBRB.

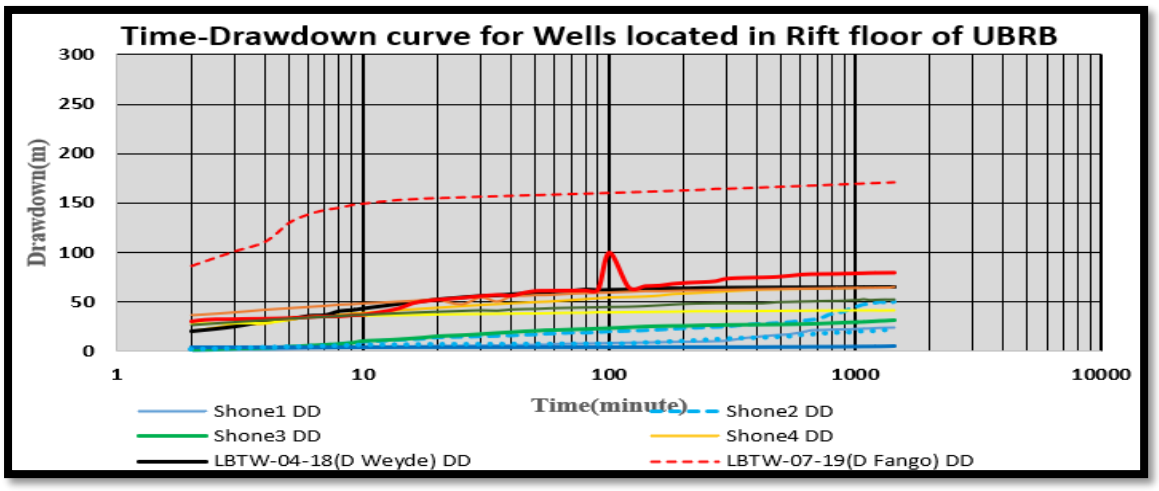

Figure 39.Time -drawdown curve for wells located in Rift Floor of UBRB

5.7.2 Transmissivity characteristics

Transmissivity (T) represents the capacity of an aquifer to transmit groundwater through its saturated thickness and is a fundamental parameter for assessing groundwater potential and well productivity. The computed transmissivity values for the study area range from 0.05 to 841.10 m²/day, with a mean value of approximately 117.6 m²/day, a median of 42.4 m²/day, and a standard deviation of about 175 m²/day. This wide variation indicates a heterogeneous aquifer system, reflecting differences in lithology, degree of fracturing, and weathering across the area. Out of the total wells analyzed, approximately 10% exhibit very low transmissivity, 26% low, 30% moderate, 18% high, and 4% very high. The predominance of moderate transmissivity (50–200 m²/day) signifies that the aquifers are generally moderately productive,

The interpolated and reclassified transmissivity values of the aquifer system range from 44.68 to 112.6 m²/day, indicating variable groundwater flow potential across the study area. Spatial reclassification delineates five transmissivity zones:

- Moderately Low (44.68–59.76 m²/day): 15.96% coverage, mainly in the southwestern and central areas, indicating low aquifer permeability and restricted groundwater movement. Moderate (59.77–74.84 m²/day): 28.58% coverage, widely spread in southern and central zones, representing fair groundwater transmission and moderate well yields. Moderately High (74.85–89.93 m²/day): 30.88% coverage, dominating central and northern regions with good aquifer potential and high transmissivity. High (89.94–105.0 m²/day): 19.27% coverage, primarily in the central-eastern sector, indicating enhanced groundwater movement and suitability for high-yield wells. Very High (105.1–112.6 m²/day): 5.31% coverage, localized in the northeast, representing the most productive aquifer sections, likely due to highly fractured formations.

Overall, moderate to moderately high transmissivity zones dominate, indicating that the area generally possesses good groundwater potential, though localized variability reflects lithologic and structural heterogeneity.

Table 34. Reclassified Transmissivity (m^2/day)

Value	Class	Range in (m^2/day)	Area (Km^2)	Areal %	Description
1	Moderately Low	44.68–59.76	536.29	15.96	Low permeability and restricted flow
2	Moderate	59.77–74.84	959.28	28.58	Fair transmissivity and moderate well yield
3	Moderately High	74.85–89.93	1036.60	30.88	Good transmissivity and enhanced flow
4	High	89.94–105.0	646.77	19.27	High groundwater movement and favorable yield
5	Very High	105.1–112.6	177.97	5.31	Highly productive zones, fractured/permeable strata

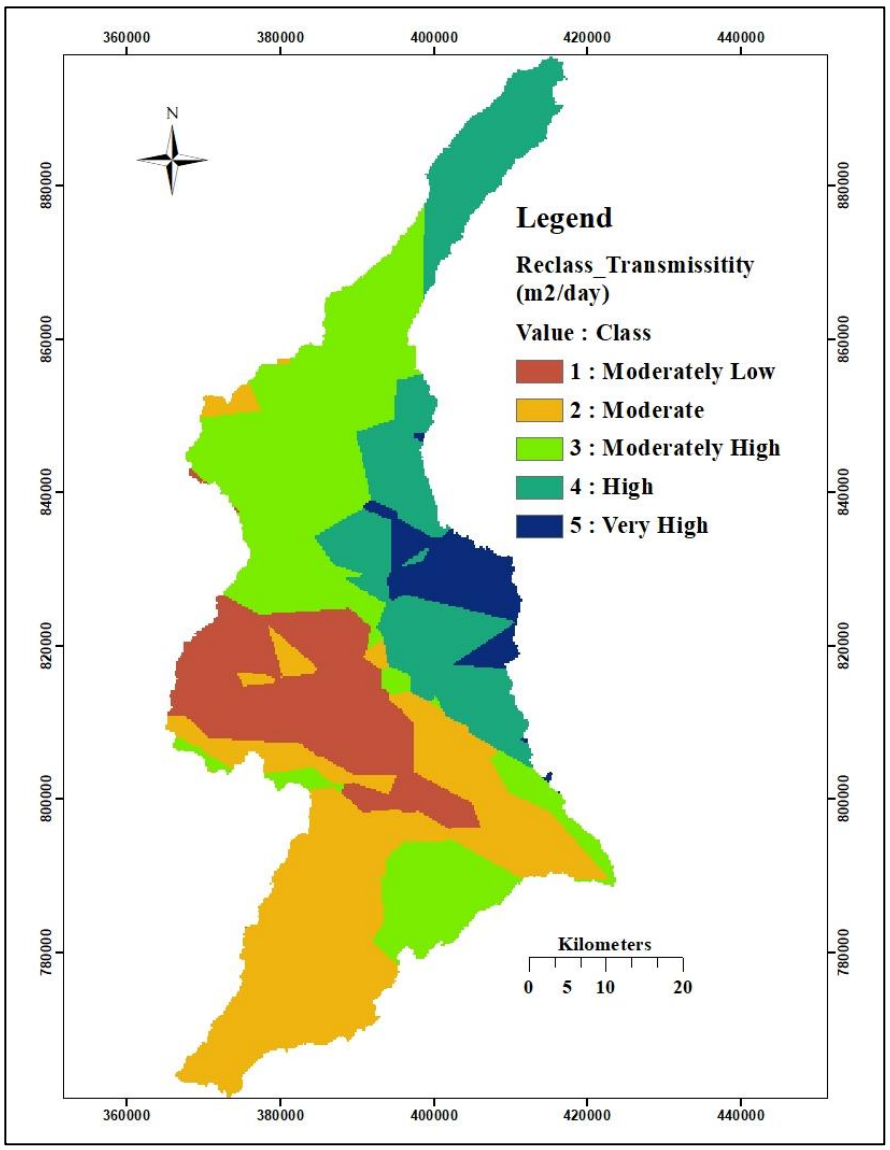

Figure 40. Hydraulic conductivity (K) and Transmissivity(T) of the UBRB.

5.8 Development of analytical equation for aquifer parameters and resistivity.

To evaluate the predictive capacity of geophysical parameters for groundwater potential, empirical correlations were established between aquifer parameters from pumping tests and resistivity variables derived from Vertical Electrical Sounding (VES) data. The analysis focused on transmissivity (T), hydraulic conductivity (K), transverse resistance (Tr), longitudinal conductance (Sc), and apparent resistivity (ρ_a). Pearson's correlation revealed a strong positive relationship between transmissivity and transverse resistance ($r = 0.83$, $p = 1.32\times10^{-13}$), indicating that zones with higher Tr values correspond to higher transmissivity. A linear regression model developed for transmissivity prediction, $T = 0.41Tr - 5.1$ ($R^2 = 0.69$), shows that about 69% of the transmissivity variation is explained by Tr. This demonstrates that transverse resistance serves as a reliable geophysical predictor of aquifer hydraulic properties in the fractured volcanic and alluvial settings of the study area.

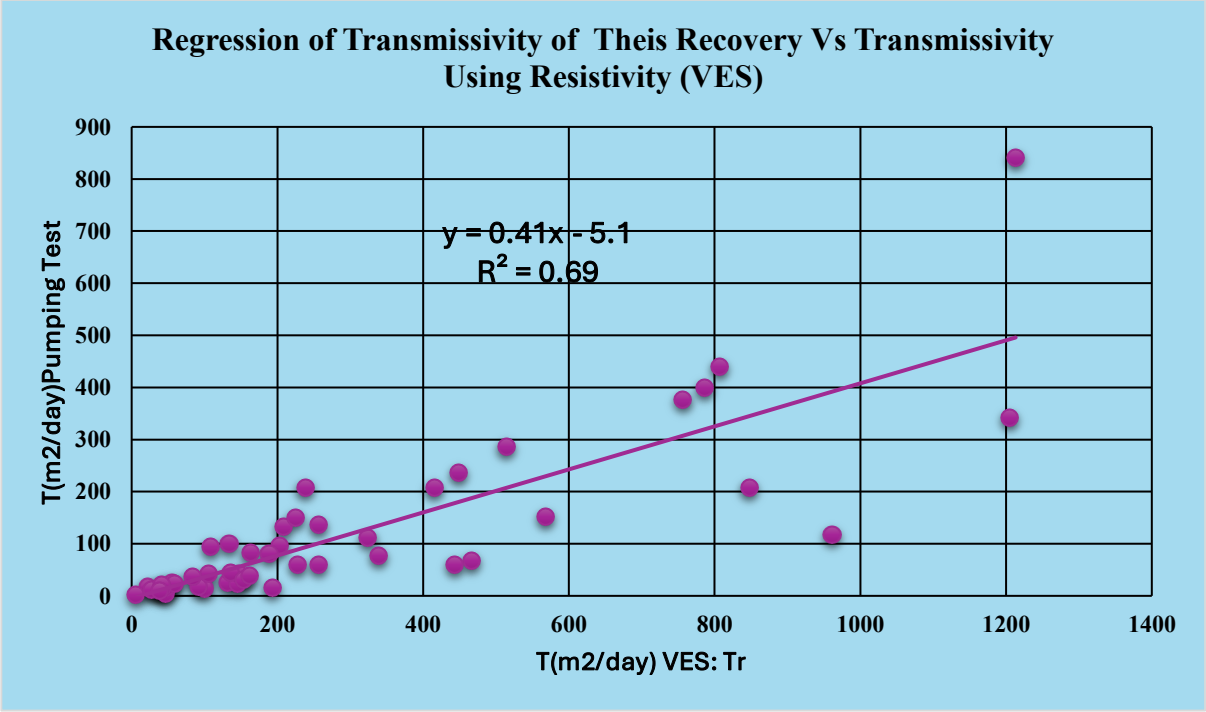

Figure 41. Regression of Transmissivity and Transverse resistance

$R^2 = 0.692$, meaning 69.2% of the variability in y is explained by the model.

Significance F =1.32E-13, Strong evidence that the model is significant (Significance F< 0.01).

5.8.1 Model verification and interpretation

The regression model shows a strong relationship (R = 0.832) between actual and predicted values. It explains approximately 69% of the variability in the dependent variable, which is quite good for many real-world scenarios. The small drop in Adjusted R^2 (to 0.685) confirms the model's robustness with minimal overfitting. Significance F=0.000000000000132, (Significance F< 0.01), an extremely small value. This means there is very strong statistical evidence that your model explains significant variance in the dependent variable.

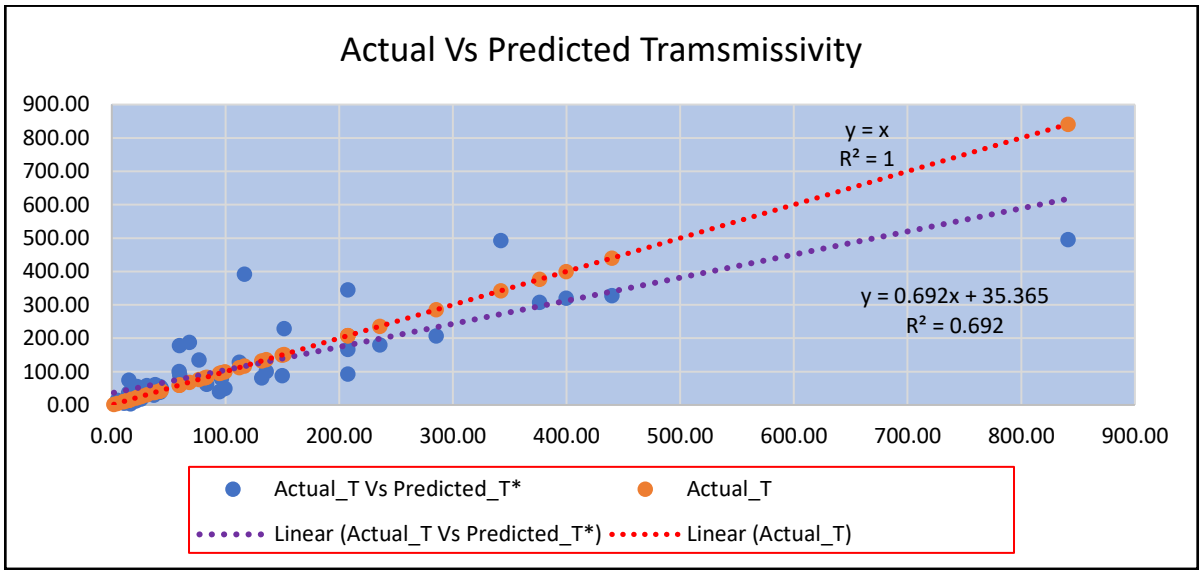

Figure 42. Actual and predicted transmissivity graph

5.9 Well yield challenges

5.9.1 Partial penetration

An analysis of approximately 220 Wells indicates significant variability in the Partial Penetration ratio (L/b), which assesses the ratio of the length of the screened interval to the total aquifer thickness. The ratios range from 0.13 to 0.96, with a mean of 0.56 and a median of 0.55. This statistical distribution suggests that the majority of wells are designed for moderate penetration, with screening that typically covers about half of the aquifer. Such a design reflects a hydraulically balanced approach aimed at optimizing sustainable yield and recharge while effectively managing costs and drawdown. Notably, the Coefficient of Variation of 30.4% and a standard deviation of 0.17 highlight a considerable spatial variability in well design throughout the area, likely attributable to differences in aquifer geometry and construction design.

Wells characterized by low penetration (L/b < 0.33) are often indicative of thin or limited aquifers, resulting in reduced hydraulic efficiency. In contrast, wells with high penetration (L/b > 0.8) are generally situated in robust, productive zones with significant groundwater potential. In summary, while the predominant design approach among wells accommodates moderate production levels, the observed variability underscores the potential for localized optimization strategies to enhance hydraulic efficiency and bolster water supply reliability.

Table 35. Classification of Wells by Penetration Range and Implications

Penetration Category	**L/b Range**	**No. of Bh**	**%**	**Hydraulic Implication**	**Groundwater Potential and Yield Characteristics**
Low (Minimal)	0.20 – 0.33	~33	15%	High drawdown, low efficiency	The penetrated aquifer has limited saturated thickness and constrains well yield.
Moderate (Typical)	0.40 – 0.70	~120	55%	Balanced yield vs. construction cost.	Represents the most functional and sustainable wells. Moderate penetration ensures adequate inflow area, stable drawdown, and reasonable efficiency. .
High (Near-Full)	0.80 – 1.00	~67	30%	Optimal yield, minimal head loss	Indicates wells fully intersecting the main water-bearing zones, leading to maximum yield and minimal head loss.

Low Penetration Wells (L/b ≤ 0.33):- Often underperform due to restricted inflow area and greater head losses. Require rehabilitation, deepening, or screen extension to enhance discharge capacity. In thin or fractured aquifers, even small increases in penetration can significantly improve yield.

Moderate Penetration Wells (0.4 ≤ L/b ≤ 0.7):-Typically provide reliable and sustainable yields under moderate pumping rates. However, heterogeneous aquifer conditions may cause uneven inflow along the screen, necessitating periodic maintenance.

High Penetration Wells (L/b ≥ 0.8):-Provide maximum potential yield with minimum drawdown and high efficiency. Main challenge lies in higher drilling and casing cost. In multi-layered aquifers, full penetration might risk hydraulic mixing between different quality zones.

Table 36. Summary Interpretation

Category	**Range (L/b)**	**Groundwater Potential**	**Typical Well Yield**	**Main Challenge**
Low	0.20–0.33	Low	Low	Excessive drawdown
Moderate	0.40–0.70	Moderate to High	Moderate to High	Heterogeneous inflow, partial efficiency loss
High	0.80–1.00	High	High	Increased drilling cost, risk of inter-layer mixing

The prevailing moderate penetration indicates technically sound well design practice across much of the UBRB. However, improving low-penetration wells (15%) could significantly enhance groundwater development efficiency. Areas where high L/b wells coincide with strong aquifer continuity represent priority zones for sustainable groundwater exploitation and future development planning.

5.9.2 Wellbore storage coefficients

The Wellbore Storage Coefficient (Cw) values obtained from 63 Wells (excluding any negative or invalid entries) show considerable variability across the study area. The Cw values range from a minimum of 0.0000001 to a maximum of 0.99, with a total range of 0.99. This indicates a wide variety of wellbore storage behaviors among the wells tested. The mean value of 0.41 and the median of 0.50 suggest that, on average, most wells exhibit a moderate to high influence of wellbore storage. This means that early drawdown behavior is significantly affected by well storage until the aquifer response becomes dominant. The relatively high standard deviation of 0.42 further confirms substantial dispersion within the dataset, indicating spatial variability in well design, aquifer characteristics, and well development efficiency.

The wide range and high standard deviation show strong spatial variability in wellbore storage behavior, reflecting differences in well construction, aquifer confinement, and development efficiency across sites.

Table 37. Classification Summary

Cw Range	Interpretation	No. of Wells	%	Groundwater Potential Implication
Cw < 0.1 (very low)	Negligible wellbore storage	17	27%	Strong aquifer–well connection and reliable transmissivity estimates; good potential zones.
0.1 ≤ Cw ≤ 0.3 (low–moderate)	Small but noticeable storage	5	8%	Efficient well design and favorable yield prospects with minimal corrections needed.
0.3 < Cw ≤ 0.6 (moderate)	Significant early-time influence	6	10%	Moderate wellbore effects, semi-confined aquifers; good potential with long-term testing.
0.6 < Cw ≤ 0.9 (high)	Strong wellbore influence	4	6%	Early drawdown dominated by casing storage; transmissivity underestimated, yield uncertain.
Cw ≥ 0.9 (very high)	Wellbore storage dominated	31	49%	Dominant wellbore control, poor test reliability, potential yield inconsistency; needs redevelopment.

Hydrogeological Interpretation: -Nearly half of the wells (≈49%) exhibit very high Cw (≥0.9), indicating wellbore storage dominance and delayed aquifer response. About 27% of wells fall into the very low Cw category (<0.1), implying rapid aquifer response, minimal wellbore interference, and good connectivity. Moderate storage wells (0.1–0.6) represent around 18% and show balanced performance typical of confined or semi-confined systems. High to very high storage wells (>0.6) demonstrate substantial wellbore effects that obscure aquifer responses, requiring longer test durations.

Implications for Groundwater Potential Mapping: Spatially, the dominance of high Cw values suggests localized well inefficiencies rather than uniformly poor aquifer conditions. Hydraulically, low Cw (<0.1) zones correspond to areas of strong aquifer permeability and recharge potential, aligning with favorable groundwater targets. Operationally, wells with Cw ≥ 0.9 require rehabilitation (air-lift surging, acid treatment) to reduce wellbore effects and improve yield consistency.

In summary the overall mean Cw of 0.41 reflects a moderate to high influence of wellbore storage in the study area, with nearly half of the wells dominated by casing effects. This emphasizes that well design, well development, and maintenance strongly affect yield assessment. Wells with Cw < 0.1 represent reliable, high-potential zones for groundwater abstraction, while those with Cw ≥ 0.9 indicate inefficient wells needing technical intervention.

5.9.3 Well loss coefficient

In the UBRB Basin, the well loss coefficient (C), expressed in day²/m⁵, indicates the magnitude of head loss caused by turbulent flow and clogging within a well during pumping. Higher C-values reflect greater hydraulic inefficiency, typically associated with clogging, corrosion, or partial collapse of the well screen or gravel pack. Based on the given classification thresholds, the dataset was analyzed to assess the condition and restoration potential of each well.

Table 38. Statistical Summary of C (Well Loss Coefficient) Values

Statistic	**Value (day²/m⁵)**
Number of wells analyzed	25
Minimum	4.00×10^{-7}
Maximum	5.00×10^{-5}
Mean	1.40×10^{-5}
Standard deviation	1.56×10^{-5}
Median	8.00×10^{-6}

The well loss coefficients vary considerably, showing that the wells experience different levels of hydraulic resistance due to clogging and development quality. The analysis of 25 wells shows that the well loss coefficient (C) ranges from 4.0×10^{-7} to 5.0×10^{-5} day²/m⁵, with a mean of 1.40×10^{-5} day²/m⁵. This broad range highlights varying degrees of well deterioration and clogging across the study area.

Severe Clogging and Low Efficiency: Approximately 72% of the wells (e.g., WSU Sodo City, BodityBH wells, Shone wells, and Halaba_Alemtena490) fall under the "Difficult to restore well to original capacity" class. These wells show advanced clogging and screen corrosion, indicating prolonged operational stress or poor maintenance. Redevelopment may yield limited improvement.

Moderate Clogging: Wells such as LBTW-01-19, LBTW-08-18, DurameCampus1, and SiraroBadawacho Abuka SRBH fall under the "Clogging is severe" category, suggesting partial efficiency loss that could potentially be improved through redevelopment.

Mild Deterioration: Only WSodo2010WG-5 shows mild deterioration, reflecting partial obstruction or sediment accumulation. Preventive cleaning and proper maintenance can restore full efficiency.

Properly Developed Wells: None of the wells fall under the "Properly developed and designed well" category, indicating a general decline in performance across the network.

In summary, the majority of wells exhibit significant hydraulic inefficiency, primarily attributable to screen clogging and structural degradation. This is quantitatively confirmed by a mean well loss coefficient (C) of 1.40×10^{-5} day²/m⁵, a value which substantially exceeds the established threshold for properly developed wells. To mitigate permanent damage, wells demonstrating a C-value of $\leq 1 \times 10^{-6}$ day²/m⁵ should be prioritized for routine rehabilitation, including methods such as surging or air-lift cleaning. Conversely, wells with extreme C-values ($> 1.8 \times 10^{-6}$ day²/m⁵) are often beyond cost-effective restoration and are likely candidates for replacement.

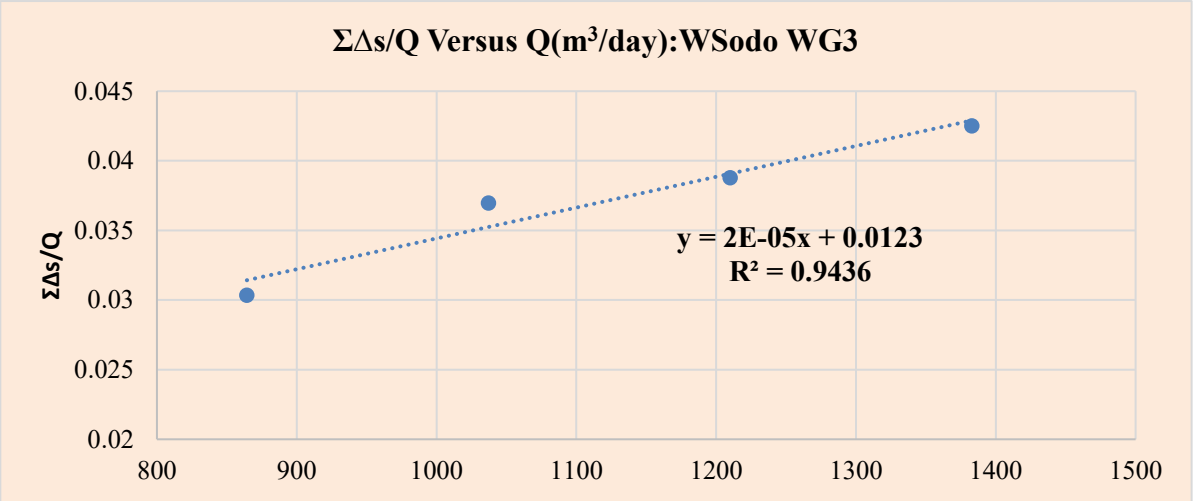

Figure 43. Aquifer coefficient (B) and well loss coefficient (C) equation

Table 39.Statistical descriptions of aquifer parameter (T) and well-yield challenges.

Descriptive Statistics	**T (m2/day))**	**Well loss C_(day²/m⁵)**	**Partial Penetration Ratio(L/b)**	**Wellbore Storage Coeff.**	**Lp(%)**
Mean	110.32	1.40E-05	0.555	0.465	**67.36**
Standard Error	21.24	3.11E-06	0.011	0.057	**5.918**
Median	59.41	8.00E-06	0.555	0.372	**74**
Mode	#N/A	2.00E-05	0.500	0.990	**100**
Standard Deviation	151.68	1.56E-05	0.157	0.452	**30.75**
Sample Variance	23005.94	2.42E-10	0.025	0.204	**945.72**
Minimum	0.05	4.00E-07	0.133	0.0000001	**11.22**
Maximum	841.10	5.00E-05	0.963	0.990	**100**
Count	51	25	1951	62	**27**

5.9.4 Well efficiency

The well efficiency of the study area was computed from step-drawdown pumping test data using the Jacob (1947) method, as described in Section (Well Efficiency Assessment Method and Classification). The analysis quantified the ratio of aquifer loss to total drawdown, thereby indicating the hydraulic performance and construction quality of individual wells. The calculated efficiency values ranged from 11.22% to 100%, with a mean efficiency of approximately 70.3%, a median of 74.0%, and a standard deviation of 27.2%. This broad variability reflects differences in aquifer characteristics, well design, and development quality across the study area.

According to the classification criteria adapted from Driscoll (1986), Todd & Mays (2005), and Kruseman & de Ridder (2000), well efficiencies were grouped into four performance categories: poor (<40%), fair (40–60%), good (60–80%), and excellent (>80%). Spatial analysis of the classified results revealed that approximately 18% of the wells exhibited poor efficiency, 22% fell within the fair range, 30% demonstrated good performance, and 30% showed excellent efficiency.

Wells with efficiency values below 40% indicate excessive head losses due to construction or development deficiencies, possibly resulting from partial clogging of the well screen, inadequate well development, or improper gravel packing.

Moderate efficiencies (40–60%) reflect acceptable but suboptimal well performance, often associated with transitional flow conditions or partially penetrating wells. Efficiencies between 60% and 80% represent well-developed and hydraulically efficient wells with minimal turbulence and effective hydraulic connection to the aquifer. The highest efficiencies (>80%) correspond to optimally designed wells tapping highly permeable zones, typically associated with coarse alluvial or fractured volcanic aquifers.

The spatial distribution of well efficiency (**Error! Reference source not found.**) demonstrates c lear correspondence with hydrogeological conditions. Wells drilled in zones of high transmissivity and coarse-grained alluvial deposits generally exhibit good to excellent efficiency, indicating minimal well losses and favorable aquifer hydraulics. Conversely, low-efficiency wells are concentrated in low-permeability lithological units and areas with high drawdown response, suggesting partial clogging, fine-grained sediments, or well construction issues.

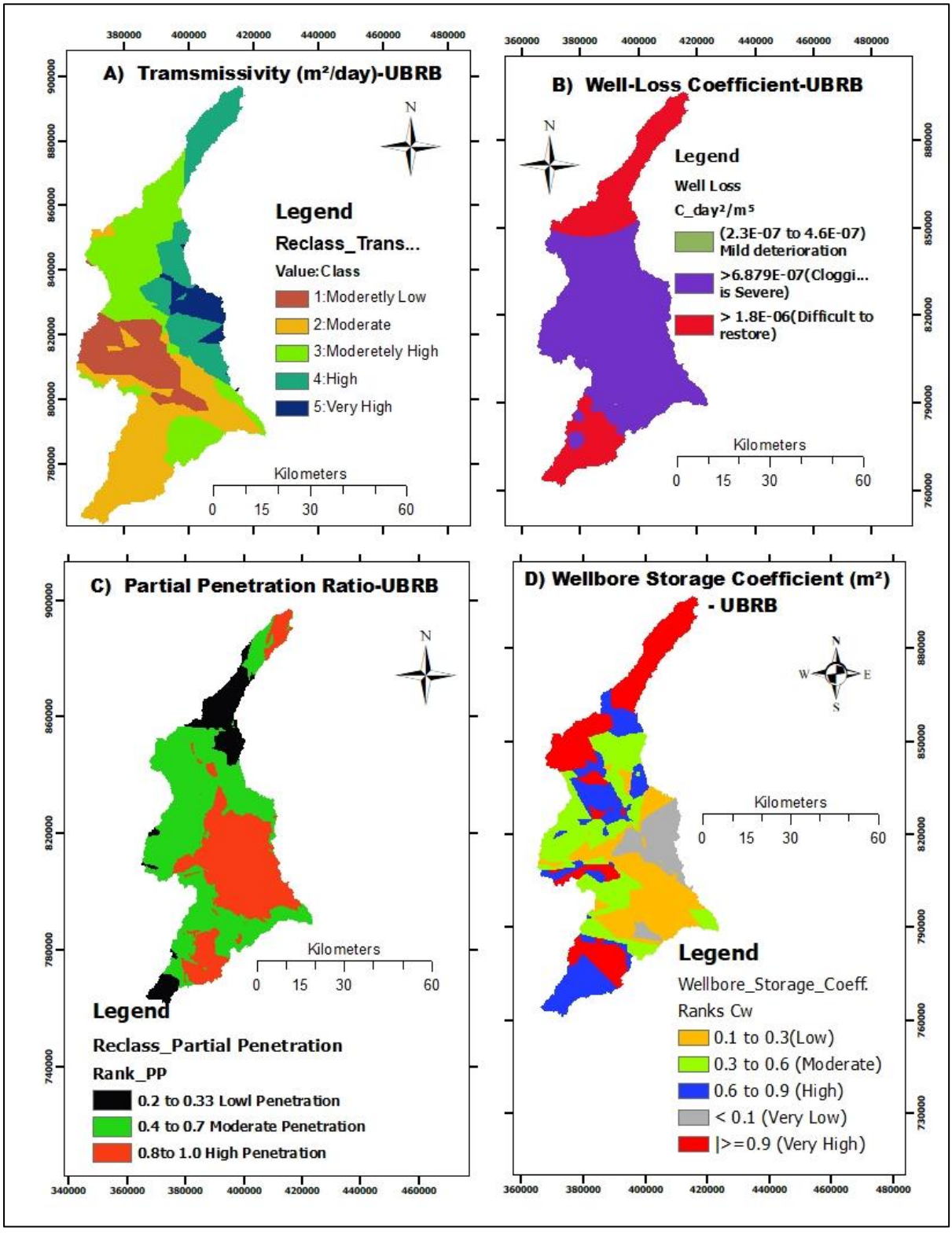

Figure 44. Well Yield challenges: map

Overall, the well efficiency results reflect the hydraulic variability and yield discrepancies of the study area. The analysis confirms that well performance is strongly influenced by both hydrogeological factors (transmissivity, lithology, and aquifer type) and engineering factors

(well design, screen length, and development quality). The integration of well efficiency classification with other aquifer parameters provides a reliable basis for identifying inefficient wells and guiding targeted rehabilitation or redevelopment programs to enhance groundwater utilization.

Table 40. Summary of Well Efficiency Results

Efficiency Range (%)	**Classification**	**Interpretation**	**Proportion of Wells (%)**
< 40	Poor Efficiency	High well losses; poor design or clogging	18
40.1 – 60	Fair Efficiency	Moderate losses; acceptable but suboptimal	22
60.1 – 80	Good Efficiency	Efficient wells with minor losses	30
> 80.1	Excellent Efficiency	Optimal design and aquifer connection	30

The results emphasize that well efficiency is a sensitive diagnostic indicator of both hydraulic and engineering conditions. High-efficiency wells correspond to well-developed aquifers with coarse materials and adequate design, while low-efficiency wells highlight localized performance constraints, possibly due to improper development, partial screen blockage, or fine-grained formations. The observed pattern substantiates that improving well efficiency through proper design, screen selection, and development procedures is crucial for maximizing groundwater yield and ensuring the sustainability of production wells within the study area.

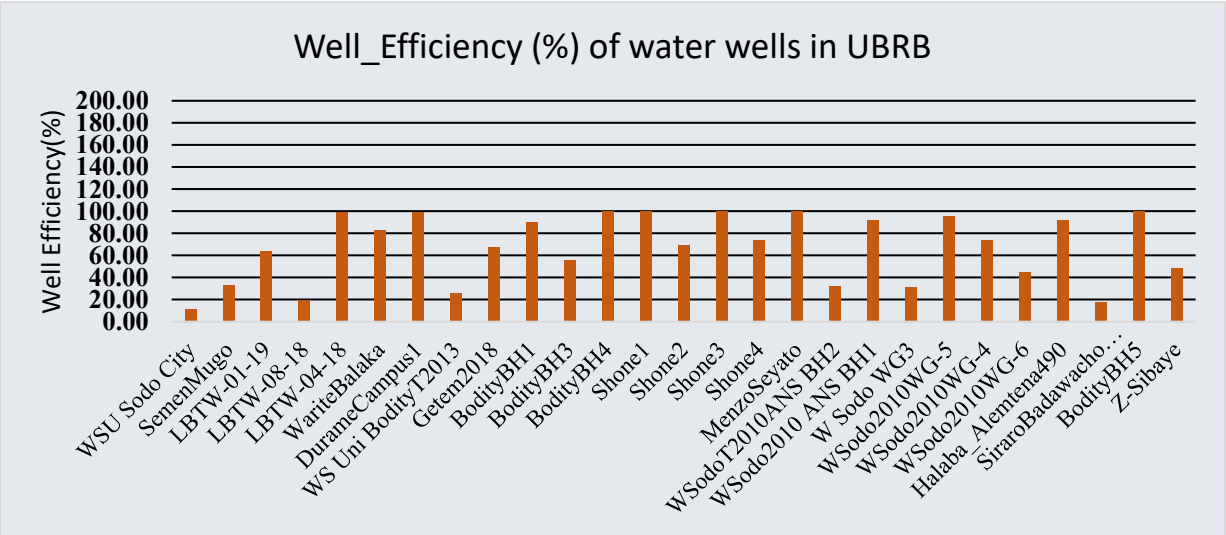

Figure 45. Graphical presentation of variable well-efficiency percentage of the Wells.

The transmissivity map (Figure 40) illustrates the spatial variability of the aquifer's ability to transmit water, categorized from Moderately Low to Very High. High transmissivity zones, indicated by shades from green to dark blue, are predominantly located in the central and northeastern regions, signifying favorable groundwater potential and higher sustainable yields. In contrast, the southwestern and western sectors exhibit moderately low to moderate transmissivity, reflecting constraints on aquifer productivity. The well efficiency map (Figure 46) presents the performance of wells under pumping conditions, classified from Poor to Excellent Efficiency. Regions demonstrating Excellent and Good Efficiency (colored blue to cyan) largely overlap with areas characterized by High and Very High Transmissivity. This correlation corroborates the assertion that aquifer properties significantly influence well performance, as these regions typically exhibit reduced drawdown and stable discharge rates. Conversely, zones labeled with Poor and Fair Efficiency (represented in red and yellow), particularly in the northernmost and southern sectors, align with Moderately Low transmissivity areas. This suggests potential hydraulic limitations, including low permeability, partial penetration, or inherent aquifer heterogeneity.

Implications for Groundwater Potential and Well Yield:

High Potential Zones: The central and northeastern sectors, characterized by both high transmissivity and well efficiency, indicate favorable conditions for further groundwater development.

Moderate Potential Zones: The central-southern regions with moderate transmissivity and good efficiency suggest moderate yields, making them suitable for domestic applications and small-scale irrigation.

Low Potential/Challenging Zones: The northern and southwestern margins, exhibiting low transmissivity and poor well efficiency, encounter challenges such as low discharge rates, rapid drawdown, and the risk of well failure.

The observed correlation between transmissivity and well efficiency shows that the hydraulic properties of the aquifer play a key role in determining groundwater potential and well yield. Typically, areas with higher transmissivity correspond to wells that operate more efficiently, indicating favorable conditions in the aquifer that support sustained groundwater extraction. However, in some regions where transmissivity is moderate but well efficiency remains low, this discrepancy may be attributed to non-hydrogeological factors. These factors could include

suboptimal well design, inadequate screen penetration, or clogging caused by poor maintenance. This pattern suggests that even though the aquifer has sufficient transmissive capacity, technical limitations at the well level can hinder performance. Therefore, to maximize groundwater productivity in these areas with moderate transmissivity, it is essential to improve well construction standards, ensure proper screen placement, and implement routine maintenance.

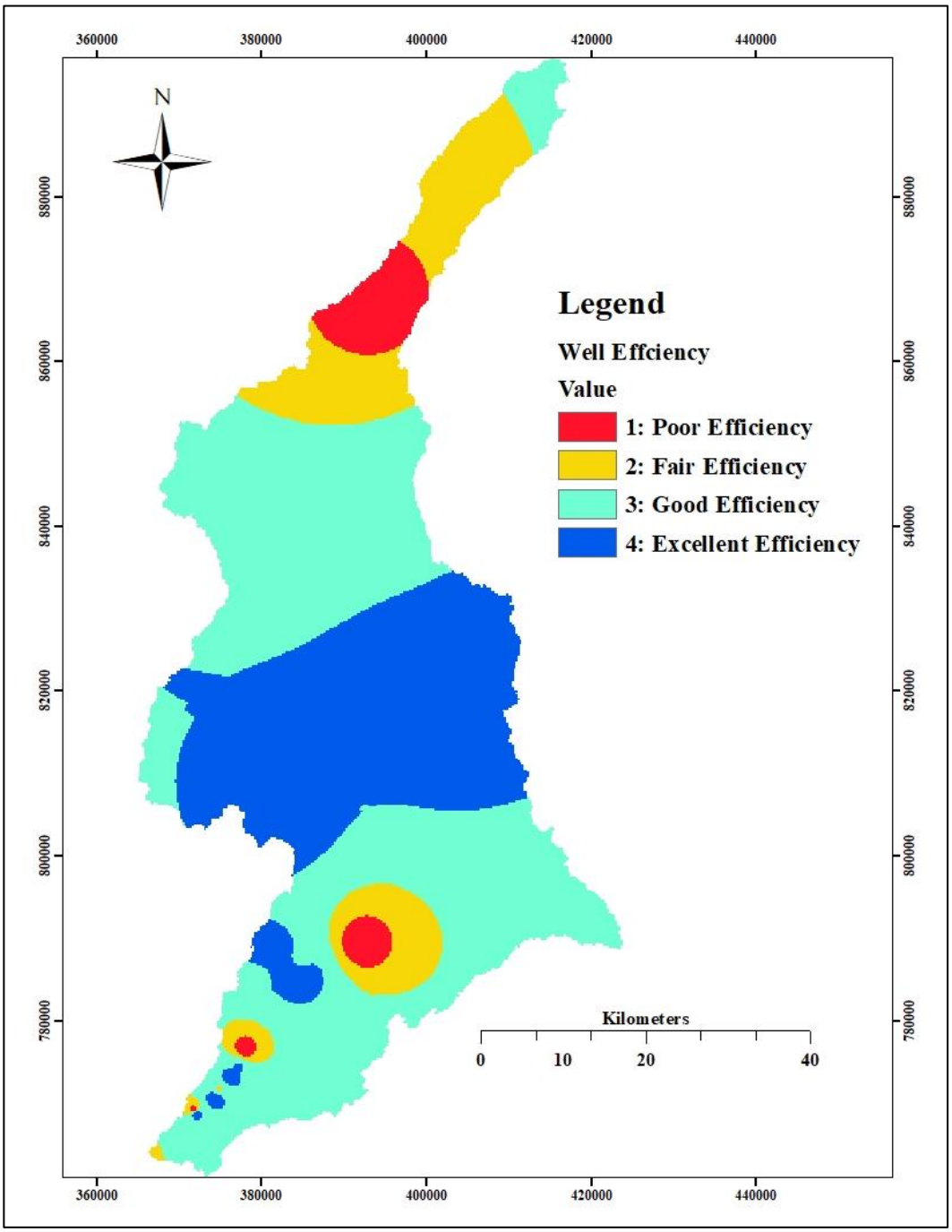

Figure 46. Distribution of well efficiency variability in the UBRB.

6 CONCLUSION AND RECOMMENDATION

6.1 Conclusion

This study concludes that the Upper Bilate River Basin is a semi-humid volcanic system with a positive water balance. A net surplus of 254.6 mm enables significant groundwater recharge, quantified at 58.9 mm/year (209.6 million m^3). This recharge, which sustains 63% of streamflow as baseflow, represents a modest 6% of annual rainfall. Consequently, while the groundwater resource is substantial, its development must be conservative, managed alongside the strong rainfall-baseflow linkage and seasonal variability to ensure sustainability.

The groundwater potential of the UBRB is mainly influenced by three lithological units: 1) Pyroclastic Rocks (Ignimbrite/Tuff) - the primary aquifer system; 2) Central Volcanic Complex (Rhyolite/Trachyte) - a localized aquifer with secondary permeability; and 3) Volcanic and Volcano-Sedimentary Formations - important aquitards that define the basin's hydrostratigraphic boundaries.

A hydrogeological and groundwater potential zone (GWPZ) map was delineated using a weighted overlay analysis of ten thematic layers, categorizing the area into four groups: excellent (1.39%), very good (17.9%), good (79.17%), and low (1.54%). The majority, 79.17%, shows good groundwater potential, emphasizing its importance for water resource management. The potential map shows high predictive accuracy, with 74% of Wells in the very good potential zone covering ~53% of the area, and 26% in the good potential zone covering 46% of the area. No Wells are found in the Low class, confirming its non-productive status, while the lack of data in the Excellent zone indicates a need for re-evaluation.

The analysis of groundwater potential shows significant heterogeneity in aquifer characteristics, impacting well performance and sustainability. Transmissivity (T) values range from 1.85 to 439,776 m^2/day, with a mean of 10,844.78 m^2/day and a high standard deviation. This variability highlights the diverse productivity across the area, with some wells in highly transmissive zones and others facing yield challenges. This variability indicates the presence of diverse aquifer materials, ranging from poorly permeable zones to highly conductive fractured or coarse granular strata. Such differences emphasize the necessity for meticulous siting and well design to optimize groundwater abstraction.

The groundwater potential of the study area is highly favorable in the deeper horizons. The most promising aquifer is Layer 6 (highly weathered and fractured pyroclastic unit) with a thickness of 452.29 m and resistivity of 59.76 Ωm, offering excellent storage and transmissivity due to extensive fracturing. This is followed by Layer 5 (weathered and fractured pyroclastic unit) with 292.4 m thickness and 181.71 Ωm resistivity, and Layer 4 (moderately weathered & fractured volcano-sedimentary unit) with 144.25 m thickness and 161.52 Ωm resistivity, both forming reliable confined aquifers. Layer 3 (moderately weathered trachy-basalt, 54.06 m thick, 137.46 Ωm) provides moderate potential as a leaky aquifer, but with limited sustainable yield. In contrast, the shallow Layer 2 (alluvial/lacustrine deposits, 9.48 m thick, 93.05 Ωm) and Layer 1 (clay/topsoil, 1.71 m thick, 120 Ωm) act mainly as aquitards with poor to negligible groundwater potential. Overall, Layers 6, 5, and 4 are the best targets for sustainable groundwater development, while the upper layers serve primarily as protective covers.

The study indicates that geophysical parameters from VES can reliably predict groundwater potential. A significant positive correlation between transmissivity and transverse resistance was found ($r = 0.83$, $p = 1.32\times10^{-13}$), indicating that higher transverse resistance values align with aquifers having greater water-transmitting capacity. This supports the use of transverse resistance as a proxy for transmissivity and endorses the integration of geophysical methods with pumping test data for groundwater assessment.

Analysis of approximately 220 Wells reveals the Partial Penetration ratio (L/b) varies significantly from 0.13 to 0.96. With a mean of 0.56, the data indicate that well designs typically screen about half of the total aquifer thickness, reflecting a moderate penetration approach.
Wellbore storage analysis revealed two dominant responses: approximately 49% of wells showed very high storage ($Cw \geq 0.9$), indicating significant wellbore effects that delay aquifer response, while 27% exhibited very low storage ($Cw < 0.1$), suggesting rapid aquifer response and good formation connectivity. The remaining wells demonstrated moderate storage, characteristic of confined conditions.
Analysis of 25 wells reveals significant hydraulic deterioration, with well loss coefficients (C) ranging from 4.0×10^{-7} to 5.0×10^{-5} day^2/m^5. A majority (72%) exhibit severe clogging and are classified as difficult to restore, while none meet the criteria for a properly developed well. This

indicates widespread well performance decline across the network, primarily due to clogging and poor development.

Well efficiency across the study area ranged from 11.22% to 100%, with a mean of 70.3% and high variability (standard deviation: 27.2%). Based on established criteria, wells were classified as: Poor (<40%, 18%), Fair (40-60%, 22%), Good (60-80%, 30%), and Excellent (>80%, 30%). This distribution reflects significant differences in aquifer properties and well construction quality. The high proportion of non-excellent wells (40% rated Fair or Poor) indicates widespread issues such as well screen clogging or inadequate development, underscoring a need for improved design and construction practices.

The correlation between transmissivity and well efficiency reveals that well efficiency is governed by aquifer transmissivity, with efficient wells concentrated in high-transmissivity zones. Conversely, the observed low efficiency in moderately transmissive areas is predominantly a consequence of technical factors—such as flawed well design, partial penetration, or elevated wellbore storage—rather than the inherent aquifer properties. Therefore, refining well construction techniques is essential to unlock the full groundwater potential of these zones.

6.2 Recommendation

The findings of this study provide valuable insight into the hydrogeological dynamics and groundwater development potential of the Upper Bilate River Basin (UBRB). In light of the results, the following recommendations are proposed to enhance groundwater resource management, optimize well performance, and ensure long-term sustainability.

1. Groundwater abstraction in the Upper Bilate River Basin (UBRB) should remain conservative. Recharge constitutes only 6% of annual rainfall (58.9 mm/year), sustaining 63% of streamflow as baseflow. Development plans must therefore align abstraction with recharge rates and seasonal rainfall variability to maintain long-term sustainability.
2. Future drilling should focus on the deep pyroclastic and fractured volcanic units (Layers 6, 5, and 4), which exhibit high transmissivity and storage potential. The shallow clayey and alluvial layers (Layers 1 and 2) should be treated as protective covers rather than main aquifers. Proper targeting of deeper productive horizons will enhance well yields and resource reliability.

3. A strong positive correlation (r = 0.83) between transmissivity and transverse resistance confirms the reliability of VES data for aquifer prediction. Future exploration should integrate geophysical interpretations, pumping test results, and lithological logs to improve accuracy, reduce drilling uncertainty, and refine groundwater potential mapping.
4. The mean partial penetration ratio (L/b = 0.56) and widespread clogging highlight the need for improved design and development. Wells should:
    - Extend screens across the most transmissive zones;
    - Apply proper gravel packing and screen slot sizing;
    - Undergo thorough development (surging, airlifting, and backwashing). These measures will improve efficiency, reduce well loss, and ensure sustainable performance.
5. About 72% of wells show severe clogging, and none qualify as fully developed. A regular rehabilitation and maintenance program is needed, including:
    - Scheduled redevelopment and cleaning;
    - Routine performance monitoring; and
    - Record-keeping of efficiency trends.
    - Such actions will restore and maintain well productivity across the basin.
6. Establish a basin-wide groundwater monitoring network to record water levels, abstraction rates, and water quality. A centralized hydrogeological database should support adaptive management, enabling early detection of depletion or contamination and informed decision-making.
7. No Wells currently exist in the “Excellent” potential zone. Targeted exploratory drilling and testing are recommended to validate and refine the Groundwater Potential Zone (GWPZ) map, improving its reliability for future resource planning and well siting.
8. Capacity building for local water bureaus, drilling contractors, and research institutions is essential. Training should focus on hydrogeophysical interpretation, well development, groundwater monitoring, and sustainable abstraction management to strengthen local expertise and governance.

7 REFERENCES

Abbott, M. B., & Refsgaard, J. C. (Eds.). (1996). *Distributed Hydrological Modelling* (Vol. 22). Springer Netherlands. https://doi.org/10.1007/978-94-009-0257-2

Abdullahi, D. R., Oladosu, O. O., Samson, S. A., Abegunde, L. O., Balogun, T. A., & Mzuyanda, C. (2019). Geospatial Analysis of Groundwater Potential Zones in Keffi, Nassarawa State, Nigeria. *Journal of Geography, Environment and Earth Science International*, *September*, 1–16. https://doi.org/10.9734/jgeesi/2019/v23i130161

Abebe, G. H. (1999). Case studies on well drilling problems. *Integrated Development for Water Supply and Sanitation: Proceedings of the 25th WEDC Conference*, 172–176.

Akinfemiwa Akanbi, O. (2023). Estimation of aquifer productivity and groundwater recharge from single - well pumping test. *Global Journal of Geological Sciences*, *21*(1), 19–30. https://doi.org/10.4314/gjgs.v21i1.2

Alam, S. M. (2007). *Step-drawdown tests Determining well performance and hydraulic parameters*. *October 2014*, 37–41. https://doi.org/10.1080/07900629108722521

Ali, M. H., Hasanuzzaman, M., Biswas, P., Islam, M. A., & Karim, N. N. (2022). Estimating Hydraulic Conductivity , Transmissibility and Specific Yield of Aquifer in Barind Area , Bangladesh Using Pumping Test. *European Journal of Environment and Earth Sciences Www.Ej-Geo.Org*, *3*(4), 90–96.

Allen, R. G., Pereira, L. S., Raes, D., & Smith, M. (1998). *FAO Irrigation and Drainage Paper Crop Evapotranspiration*. *November 2017*.

Avci, C. B., Ciftci, E., & Sahin, A. U. (2010). Identification of aquifer and well parameters from step-drawdown tests. *Hydrogeology Journal*, *18*(7), 1591–1601. https://doi.org/10.1007/s10040-010-0620-2

Ayenew, T., Demlie, M., & Wohnlich, S. (2008). Hydrogeological framework and occurrence of groundwater in the Ethiopian aquifers. *Journal of African Earth Sciences*, *52*, 97–113. https://doi.org/10.1016/j.jafrearsci.2008.06.006

Berhanu, B., And, Y. S., & Melesse, A. M. (2014). SurfaceWater and Groundwater Resources of Ethiopia: Potentials and Challenges ofWater Resources Development. *Nile River Basin: Ecohydrological Challenges, Climate Change and Hydropolitics*, *June 2018*, 1–718. https://doi.org/10.1007/978-3-319-02720-3

Bhuiyan, C. (2020). Application of different aquifer parameters for groundwater potential evaluation—implications for resources development. *Arabian Journal of Geosciences*, *13*(15). https://doi.org/10.1007/s12517-020-05678-z

Bitsiet, D., & Dessie, N. (2018). *Groundwater Recharge Estimation Using WetSpass Modeling in Upper Bilate*. *11*(1), 37–51.

Boonstra, J. (1992). *Aquifer tests with partially penetrating wells : theory and practice*. *137*, 165–179.

Borges, V. M., Fan, F. M., Reginato, P. A. R., & Athayde, G. B. (2017). *Groundwater recharge estimating in the Serra Geral aquifer system outcrop area - Paraná State , Brazil Estimativa de recarga das águas subterrâneas no sistema aquífero Serra Geral no Estado do Paraná , Brasil*. 338–346.

C.W.Fetter. (2001). *Applied Hydrogeology 1 Fetter.pdf*.

Chandra, S., Ahmed, S., Ram, A., & Dewandel, B. (2009). *Estimation of hard rock aquifers hydraulic conductivity from geoelectrical measurements : A theoretical development with field application*. *December*. https://doi.org/10.1016/j.jhydrol.2008.05.023

Clark, L. (1977). The analysis and planning of step drawdown tests. *Quarterly Journal of Engineering Geology and Hydrogeology 1977, v.10;*, p125-143. https://doi.org/10.1144/GSL.QJEG.1977.010.02.03

CSA, 2007. (2007). *Federal Republic of Ethiopia Central Statistical Agency. 2007. Statistical Tables for the 2007 population and Housing Census of Ethiopia. CSA, May 2007. Addis Ababa. May*, 2007.

David Keith Todd, L. W. M. (2005). *Groundwater_Hydrology.pdf*.

Dingman, S. L. (2015). *PHYSICAL HYDROLOGY* (Third Edit).

Driscoll, F. G. (2007). Groundwater and Well. In *Groundwater and Well* (p. 231). Johnson Screen.

Dufresne, D. P. (2011). *Developing Reginal Groundwater Flow Models with Effective Use of Step-Drawdown Test Results* (Issue February).

Eckhardt, K. (2008). A comparison of baseflow indices, which were calculated with seven different baseflow separation methods. *Journal of Hydrology*, *352*(1–2), 168–173. https://doi.org/10.1016/j.jhydrol.2008.01.005

Elango, S. P. R. K. B. L. (2015). Geological and geomorphological controls on groundwater occurrence in a hard rock region. *Applied Water Science*. https://doi.org/10.1007/s13201-

015-0327-6

Freeze, R. A., & A.Cherry, J. (1979). *Groundwater*.

Garg, S. K. (1978). *Irrigation engineering and hydraulic structures / Santosh Kumar Garg*.

Genjebo, M. G., Kemal, A., & Nannawo, A. S. (2023). Assessment of surface water resource and allocation optimization for diverse demands in Ethiopia's upper Bilate Watershed. *Heliyon*, *9*(10), e20298. https://doi.org/10.1016/j.heliyon.2023.e20298

Gidafie, D., T Tafesse, N., & Hagos, M. (2019). *Estimation of groundwater recharge using water balance model : A case study Estimation of Groundwater Recharge Using Water Balance Model : A Case Study in the Gerado Basin , North Central Ethiopia*. *May*.

Gopinathan, P., Nandini, C. V, Parthiban, S., Sathish, S., Singh, A. K., & Singh, P. K. (2020). A geo-spatial approach to perceive the groundwater regime of hard rock terrain- a case study from Morappur area, Dharmapuri district, South India. *Groundwater for Sustainable Development*, 100316. https://doi.org/10.1016/j.gsd.2019.100316

Graham, M. T., Ball, D. F., Ó Dochartaigh, B. É., & MacDonald, A. M. (2009). Using transmissivity, specific capacity and borehole yield data to assess the productivity of Scottish aquifers. *Quarterly Journal of Engineering Geology and Hydrogeology*, *42*(2), 227–235. https://doi.org/10.1144/1470-9236/08-045

Hosaena mapsheet, (2012).

Gudulas, K., Voudouris, K., Soulios, G., & Dimopoulos, G. (2013). Comparison of different methods to estimate actual evapotranspiration and hydrologic balance. *Desalination and Water Treatment*, *51*(13–15), 2945–2954. https://doi.org/10.1080/19443994.2012.748443

Guduru, J. U., & Jilo, N. B. (2022). Groundwater potential zone assessment using integrated analytical hierarchy process-geospatial driven in a GIS environment in Gobele watershed, Wabe Shebele river basin, Ethiopia. *Journal of Hydrology: Regional Studies*, *44*(March), 101218. https://doi.org/10.1016/j.ejrh.2022.101218

Ha, D., Zheng, G., Zhou, H., Zeng, C., & Zhang, H. (2019). Estimation of hydraulic parameters from pumping tests in a multiaquifer system. *Underground Space (China)*, *5*(3), 210–222. https://doi.org/10.1016/j.undsp.2019.03.006

Hailu, A. A. F. A. K. T. G. & G. (2015). Spatial analysis of groundwater potential using remote sensing and GIS-based multi-criteria evaluation in Raya Valley , northern Ethiopia. *Hydrogeology*, 195–206. https://doi.org/10.1007/s10040-014-1198-x

Haji, M., Wang, D., Li, L., Qin, D., & Guo, Y. (2018). *Geochemical Evolution of Fluoride and*

Implication for F − Enrichment in Groundwater : Example from the Bilate River Basin of Southern Main Ethiopian Rift. 1–20. https://doi.org/10.3390/w10121799

Hasan, M., Shang, Y., Jin, W., & Akhter, G. (2020). *Estimation of hydraulic parameters in a hard rock aquifer using integrated surface geoelectrical method and pumping test data in southeast Guangdong, China*.

Hirata, R., & Foster, S. (2020). The guarani aquifer system – from regional reserves to local use. *Quarterly Journal of Engineering Geology and Hydrogeology*, *54*(1). https://doi.org/10.1144/qjegh2020-091

Hossain Khan, M. F., Monir, M. U., Ahmed, M. T., Hasan, M. Y., Islam, M. N., Hasan, M. M., & Akter, R. (2022). Hydrostratigraphic Evaluation using Lithological and Step-drawdown Test: A Case Study on the Aquifer of Ukhia, Cox's Bazar, Bangladesh. *The Dhaka University Journal of Earth and Environmental Sciences*, *June*, 53–62. https://doi.org/10.3329/dujees.v10i3.59071

Israil, M., Al-hadithi, M., & Singhal, D. C. (2006). Application of a resistivity survey and geographical information system (GIS) analysis for hydrogeological zoning of a piedmont area, Himalayan foothill region, India. *Hydrogeology Journal*, *14*(5), 753–759. https://doi.org/10.1007/s10040-005-0483-0

Ivezic, V., Bekic, D., & Ranko, Z. (2017). *A Review of Procedures for Water Balance Modelling*. *February*.

Jayarajan, P., Kumar, S., Schneider, M., & Elango, L. (2022). *The State of the Art Estimation of Groundwater Recharge and Water Balance with a Special Emphasis on India : A Critical Review*.

Jha, M. K., Chowdhury, A., Chowdary, V. M., & Peiffer, S. (2007). Groundwater management and development by integrated remote sensing and geographic information systems: Prospects and constraints. *Water Resources Management*, *21*(2), 427–467. https://doi.org/10.1007/s11269-006-9024-4

JICA, Kokusai Kogyo Co., L. (2012). *The study on groundwater resources assessment in the rift valley lakes basin in the federal democratic republic of ethiopia final report* (Issue March).

Karami, G. H., & Younger, P. L. (2016). *Analysing step-drawdown tests in heterogeneous aquifers*.

Karra, K., Kontgis, C., Statman-Weil, Z., Mazzariello, J. C., M. Mathis, & Brumby, S. P. (2021). *Global land use/land cover with Sentinel-2 and deep learning. IGARSS 2021-2021 IEEE*

International Geoscience and Remote Sensing Symposium. IEEE, 2021.

Kebede, S. (2013). *Groundwater In Ethiopia features,numbers and opportunities*.

Khalilidermani, M., Knez, D., & Zamani, M. A. M. (2021). Empirical correlations between the hydraulic properties obtained from the geoelectrical methods and water well data of arak aquifer. *Energies*, *14*(17). https://doi.org/10.3390/en14175415

Kovalevsky, V. S., Kruseman, G. P., & Rushton, K. R. (2004). *Groundwater Studies- An international guide for Hydrogeological Investigation*.

Kresic, N. (2007). *HYDROGEOLOGY and GROUNDWATER MODELING* (2nd ed.).

Kruseman, G. P., & Ridder, N. A. d. (2000). *Analysis and Evaluation of Pumping Test Data*.

Kumar, A., Chaurey, R., & Singh, R. M. (2021). *Recharging of groundwater by the geophysical method based on resistivity meter , a case study of Naya Raipur Chhattisgarh*. *3*(2), 69–77.

LANG., L. E. R. & S. M. (1961). *A Simple Method for Determining Specific Yield from Pumping Tests*.

Li, B., Zhang, X., Xu, C.-Y., Zhang, H., & Song, J.-X. (2015). *Water balance between surface water and groundwater in the withdrawal process : a case study of the Osceola watershed Bing-dong_USA*. 943–953. https://doi.org/10.2166/nh.2015.137

Li, Z., Tang, R., Wan, Z., Bi, Y., Zhou, C., Tang, B., Yan, G., & Zhang, X. (2009). *A Review of Current Methodologies for Regional Evapotranspiration Estimation from Remotely Sensed Data*. 3801–3853. https://doi.org/10.3390/s90503801

Liu, W., Park, S., Bailey, R. T., Navarro, E. M., Andersen, H. E., Thodsen, H., Nielsen, A., Jeppesen, E., Jensen, J. S., Jensen, J. B., & Trolle, D. (2020). Quantifying the streamflow response to groundwater abstractions for irrigation or drinking water at catchment scale using SWAT and SWAT – MODFLOW. *Environmental Sciences Europe*. https://doi.org/10.1186/s12302-020-00395-6

Magesh, N. S., Chandrasekar, N., & Soundranayagam, J. P. (2012). Delineation of groundwater potential zones in Theni district, Tamil Nadu, using remote sensing, GIS and MIF techniques. *Geoscience Frontiers*, *3*(2), 189–196. https://doi.org/10.1016/j.gsf.2011.10.007

Makombe, G., Namara, R., Hagos, F., Awulachew, S. B., Ayana, M., & Bossio, D. (2011). A comparative analysis of the technical efficiency of rain-fed and smallholder irrigation in Ethiopia. In *IWMI Working Papers* (Vol. 143). https://doi.org/10.5337/2011.202

McCuen, R. H. (1998). *HYDROLOGIC ANALYSIS AND DESIGN* (2nd ed.).

Meijerink, A., Bannert, D., Batelaan, O., Lubczynki, M. W., & Pointet, T. (2007). Remote

Sensing Applications to Groundwater. *IHP-VI, Series on Groundwater No.16*, *6667*(16), 304. http://scholar.google.com/scholar?hl=en&btnG=Search&q=intitle:REMOTE+SENSING+APPLICATIONS+to+GROUNDWATER#5

Melo, D. C. D., Wendland, E., & Guanabara, R. C. (2015). Estimate of Groundwater Recharge Based on water Balance in the unsaturated soil Zone. *Revista Brasileira de Ciencia Do Solo*, *39*(5), 1335–1343. https://doi.org/10.1590/01000683rbcs20140740

Miller, M. P., Buto., S. G., D.D.Susong., & C.A.Rumsey. (2016). The importance of base flow in sustaining surface water flow in the Upper Colorado River Basin Matthew. *Water Resour. Res., 52, 3547–3562,* 3547–3562. https://doi.org/10.1002/2015WR017963.Received

Mishra, Surendra Kumar, Singh, V. P. (2003). SCS-CN METHOD. In *Soil Conservation Service Curve Number (SCS-CN) Methodology Volume 42 || SCS-CN Method*.

Molin, P., & Corti, G. (2015). Topography, river network and recent fault activity at the margins of the Central Main Ethiopian Rift (East Africa). *Tectonophysics*, *664*, 67–82. https://doi.org/10.1016/j.tecto.2015.08.045

Moss, R., & Company. (1990). *Handbook of Ground Water Development.*

Mutua, B. M., & Klik, A. (2007). Predicting daily streamflow in ungauged rural catchments : the case of Masinga catchment ,. *IAHS Pres*, *February*. https://doi.org/10.1623/hysj.52.2.292

Nag, S. K., & Kundu, A. (2018). Application of remote sensing, GIS and MCA techniques for delineating groundwater prospect zones in Kashipur block, Purulia district, West Bengal. *Applied Water Science*, *8*(1), 1–13. https://doi.org/10.1007/s13201-018-0679-9

Nata, T., Shishay, T., & Mekides, T. (2010). *The Water Balance of May Nugus Catchment , Tigray , Northern Ethiopia*. *03*(05), 609–625.

Negewo, T. F., & Sarma, A. K. (2021). *Estimation of Water Yield under Baseline and Future Climate Change Scenarios in Genale Watershed , Genale Dawa River Basin , Ethiopia , Using SWAT Model*. *26*(3), 1–13. https://doi.org/10.1061/(ASCE)HE.1943-5584.0002047

Osuagwu, B. C. (2024). *Geoelectric Assessment Of Groundwater Potentials In A Complex Basement Terrain Around Modomo Ile-Ife , Southwestern Nigeria*. *12*(3), 23–33. https://doi.org/10.9790/0990-1203012333

P.Singh, V. (1994). *Elementary Hydrology*.

Poernomo, I., Suripin., & Kodoatie J, R. . (2020). Annual Baseflow Estimation by Combining Hydrological Models and Graphic Hydrograph Methods. *International Journal of*

Innovative Technology and Exploring Engineering, *9*(7), 426–434. https://doi.org/10.35940/ijitee.g5129.059720

Rehman, A., Islam, F., Tariq, A., Ul Islam, I., Brian J, D., Bibi, T., Ahmad, W., Ali Waseem, L., Karuppannan, S., & Al-Ahmadi, S. (2024). Groundwater potential zone mapping using GIS and Remote Sensing based models for sustainable groundwater management. *Geocarto International*, *39*(1). https://doi.org/10.1080/10106049.2024.2306275

Richter, B., & D. Ho, M. (2022). *Sustainable groundwater management for agriculture*. https://files.worldwildlife.org/wwfcmsprod/files/Publication/file/9bzpayei7i_Sustainable_Groundwater_Management_for_Agriculture_ONLINE2.2.pdf?_ga=2.16662198.109877390.1694203555-2138850230.1692287051%0Ahttps://www.worldwildlife.org/publications/sustainabl

Roy, S., Hazra, S., Chanda, A., & Das, S. (2020). Assessment of groundwater potential zones using multi - criteria decision - making technique : a micro - level case study from red and lateritic zone (RLZ) of West Bengal , India. *Sustainable Water Resources Management*, 1–14. https://doi.org/10.1007/s40899-020-00373-z

Saaty, T. L. (1980). *Analytic hierarchy process:Planning, Priority Setting, Resource Allocation*.

Savoca, M. E., Senay, G. B., Maupin, M. A., Kenny, J. F., & Perry, C. A. (2013). Actual Evapotranspiration Modeling Using the Operational Simplified Surface Energy Balance (SSEBop) Approach. *U.S Geologica Survey Scientific Investigations Report 2013–5126*, *January*, 16 p. http://pubs.usgs.gov/sir/2013/5126

Seiler, K.-P., & Gat, J. R. (2007). GROUNDWATER RECHARGE FROM RUN-OFF, INFILTRATION AND PERCOLATION. In *Hydrology and Water Resources of Africa* (Issue map C). https://doi.org/10.1007/0-306-48065-4

Sener, E., Davraz, A., & Ozcelik, M. (2005). An integration of GIS and remote sensing in groundwater investigations: A case study in Burdur, Turkey. *Hydrogeology Journal*, *13*(5–6), 826–834. https://doi.org/10.1007/s10040-004-0378-5

Shang, Y., Yang, C., Jin, W., Chen, Y., Hasan, M., Wang, Y., Li, K., Lin, D., & Zhou, M. (2021). *applied sciences Application of Integrated Geophysical Methods for Site Suitability of Research Infrastructures (RIs) in China*. 1–16.

Sindalovskiy, L. N. (2017). *Aquifer Test Solutions*.

Singh, P., Hasnat, M., Rao, N. M., & Singh, P. (2020). *Fuzzy- Analytical Hierarchy Process based GIS Modelling for Groundwater Prospective Zones in Prayagraj, India*.

Sintayehu Legesse, G. (2009). *INTEGRATED HYDROGEOLOGICAL INVESTIGATION OF UPPER BILATE RIVER CATCHMENT: SOUTH WESTERN ESCARPMENT OF MAIN ETHIOPIAN RIFT*.

Soupios, P. M., Kouli, M., Vallianatos, F., Vafidis, A., & Stavroulakis, G. (2007). Estimation of aquifer hydraulic parameters from surficial geophysical methods: A case study of Keritis Basin in Chania (Crete - Greece). *Journal of Hydrology*, *338*(1–2), 122–131. https://doi.org/10.1016/j.jhydrol.2007.02.028

Szwed, M. B. (2015). *The Elements of Water Balance in the Changing Climate in Poland*. *2015*.

Tesfaye Tessema, G. (2010). *Ground Water Potential Evaluation Based on Integrated GIS and Remote Sensing Techniques , in Bilate River Catchment : South Rift Valley of Ethiopia*. 85–120.

Theis, C. V. (1935). The relation between the lowering of the Piezometric surface and the rate and duration of discharge of a well using ground-water storage. *Eos, Transactions American Geophysical Union*, *16*(2), 519–524. https://doi.org/10.1029/TR016i002p00519

Thornthwaite, C. W., & Mather, J. R. (1955). *THE WATER BALANCE*.

Thornwhite, & Matter. (1957). Instructions Tables Computing Potential Evapotranspiration Water Balance. *Publication in Climatology*, *10*(3), 185–311.

Todd, D. K., & Mays, L. W. (2005). *Groundwater Hydrology*.

Ullah, F., Su, L., Ullah, H., & Asghar, A. (2020). *Estimation of hydraulic parameters of an unconfined aquifer by using geoelectrical and pumping test data : a case study of the Mandi Bahauddin District , Pakistan*.

UNESCO. (1974). *Methods for water balance computation; An international guide for research and practice*.

UNESCO. (2004). *Groundwater Studies: An international guide for Hydrogeological investigations* (V. S. Kovalevsky, G. P. Kruseman, & K. R. Rushton (Eds.)).

United Nations. (2022). *Water Development Report 2022: Groundwater: Making the Invisible Visible*.

USDA. (2004). Hydrologic Soil-Cover Complexes. In *Part 630 Hydrology National Engineering Handbook*.

Vainu, M., & Terasmaa, J. (2016). The consequences of increased groundwater abstraction for groundwater dependent closed-basin lakes in glacial terrain. *Environmental Earth Sciences*, *October 2017*. https://doi.org/10.1007/s12665-015-4967-5

Valigi, D., Cambi, C., Checcucci, R., & Di Matteo, L. (2021). Transmissivity estimates by specific capacity data of some fractured italian carbonate aquifers. *Water (Switzerland)*, *13*(10). https://doi.org/10.3390/w13101374

Verner, K. (2025). *A Synopsis of the Regional Geology and Hydrogeology of Ethiopia*.

W.Mays, L. (2011). Water Resource Engineering. In *Analytical Biochemistry* (2nd ed., Vol. 11, Issue 1). http://link.springer.com/10.1007/978-3-319-59379-1%0Ahttp://dx.doi.org/10.1016/B978-0-12-420070-8.00002-7%0Ahttp://dx.doi.org/10.1016/j.ab.2015.03.024%0Ahttps://doi.org/10.1080/07352689.2018.1441103%0Ahttp://www.chile.bmw-motorrad.cl/sync/showroom/lam/es/

Walton, W. C. (1962). *Selected Analytical Methods for Well and Aquifer Evaluation*.

Willmann, M., Ramírez, J. C., Sanchez-Vila, X., & Vázquez-Suñé, E. (2007). *On the Meaning of the Transmissivity Values Obtained from Recovery Tests On the meaning of the transmissivity values obtained from recovery tests*. *July*. https://doi.org/10.1007/s10040-006-0147-8

Yehualaw, E., Haile, T., & Nigusse, W. (2023). Groundwater Potential Mapping Using Geophysical Techniques: a Case Study in Hosanna Area, Western Margin of The Central Main Ethiopian Rift, Ethiopia. *Journal of Economic Research & Reviews*, *3*(3), 192–195. https://doi.org/10.33140/jerr.03.03.05

Zech, A., Arnold, S., Schneider, C., & Attinger, S. (2015). Estimating parameters of aquifer heterogeneity using pumping tests - implications for field applications. *Advances in Water Resources*, *83*, 137–147. https://doi.org/10.1016/j.advwatres.2015.05.021

Zegeye, H. (2018). *Climate change in Ethiopia : impacts , mitigation and adaptation*. *5*, 18–35.

Zotarelli, L., Dukes, M. D., Romero, C. C., Migliaccio, K. W., & Kelly, T. (2018). *Step by Step Calculation of the Penman-Monteith Evapotranspiration (FAO-56 Method) 1*. 1–10.

8 ANNEXES

Annex-1 Well and pumping test data

Annex-2 Aquifer parameters evaluation for 65 Wells using AquiferTest-10 software.

Annex-3. Aquifer loss, Well loss well-efficiency

Annex-4. Pumping test and resistivity data for empirical relationship

Annex-5. Electrical resistivity (VES) data layer resistivity and thickness)

Annex-2. Well and pumping test data

Bore	Easting	Northing	Elevation	Total Depth	Q	SWL	DWL	TDD	PP	Top Aqui.	Bottom Aqui.	Screen Length (L)	MRWL	L/b	Aquifer Thick Ness(b)
A_Woriro_ Edo2	414732	884875	3061	220	0	219	220	1		26	220	0	0.00		194.00
A_Woriro_ Kichen	406948	883233	2879	175	9	96.1	99.2	3.1	145	79	169	52.74	96.55	0.59	90.00
Abeke1997	394728	875018	2841	150	0	149.0	150	1		15	150	0	0.00	0.00	135.00
Abeke2017	400495	879244	2747	185	21	51.0	66.05	15.05		91.4	179.15	52.65	51.60	0.60	87.75
AbelaFaracho	370458	736178	1383	205	9	96.5	116.08	19.58	152	75.3	198.15	64.4	98.40	0.52	122.85
AbotaUlto	377944	776542	1906	502.9	60	49.42	76.23	26.81	202	50	195.8	140.4	50.64	0.96	145.80
A-Dawe	376630	765762	1886	256	18	65.39	84.92	19.53	150	41.4	244.4	81.2	65.81	0.40	203.00
Adeb	498006	892978	3130	104	20	9.9	33.7	23.8	99	44	98	36	14.00	0.67	54.00
AdeDamot	442797	777230	1840	135	4	80.05	94.16	14.11	133	88.36	133	22.64	83.85	0.51	44.64
Agata	388454	872670	2852	171	5	91.0	175	84		89.8	165.2	46		0.61	75.40
Alella	368326	833816	2153	209	11	81.36	88.01	6.65	184	83.6	203.3	62.7	82.77	0.52	119.70
Alichowuriro	406948	883233	2879	175	9	96.1	99.2	3.1	145	79	169	52.74	96.55	0.59	90.00
AmbichoGode	378914	844927	2370	141	30	36.48	54.29	17.81	79	69	135	48	40.45	0.73	66.00
Amecho Watto	371398	822513	2184	210.0	4.0	112.39	113.55	1.16	132	158.87	197.06	29.3		0.77	38.19
AmechoWato2	371477	822577	2186	202.0	4.8	110.9	120.42	9.52	166	119.2	191.2	30	111.45	0.42	72.00
Ana Tigo	380733.6	838350.2	2169	226	32	2	19.82	17.82	100	50.5	220.15	87.75	6.15	0.52	169.65
AnberichGimba	398846	851572	2114	151	4.0	98.75	108.37	9.62	141	109.24	148	23.81	100.30	0.61	38.76
Angamo2015	398521	865613	2321	153.0	18.33	75.3	113	37.66	138	24	141	48	80.15	0.41	117.00
AnkaDuguna	377217	774360	1897	130	10	69.3	79.85	10.55	105	77.35	118.3	35.1	69.80	0.86	40.95
ArchumaGola	430117	856734	1828	150	18.0	64.28	65.23	0.95	120	87	138	30	64.30	0.59	51.00
Areka AR2006	355275	781031	1796	168	3	41.98	119.27	77.29		78	156	30	46.67	0.38	78.00
Areka ARC2007	355143	780262	1787	151	4.77	60	94.96	34.96	142	60	139	30	66.02	0.38	79.00
AruseWoyde	387915	772279	1720	501	12.2	98	183.55	85.55	245	215.13	482.54	121.01	106.40	0.45	267.41
Asora	401280	799802	1724	280	15	130.2	138.15	7.95	160	130	250	74	130.90	0.62	120.00
Aziga1	373120	809120	2360	266	8	150.2	177.4	27.2	230	122	254	78	153.71	0.59	132.00
Aziga2	373120	808707	2351	312	4	187.8	221.2	33.4	265	162	306	96	191.02	0.67	144.00
Aziga3	372005	808652	2370	274	8	166.6	205.59	38.99	240	142	268	72	177.10	0.57	126.00

Bore	Easting	Northing	Elevation	Total Depth	Q	SWL	DWL	TDD	PP	Top Aqui.	Bottom Aqui.	Screen Length (L)	MRWL	L/b	Aquifer Thick Ness(b)
Aziga4	375781	812891	2134	314	14	73.5	196.1	122.6	273	134	296.4	110.2	93.18	0.68	162.40
Aziga6	376046	813225	2113	290	22	74	85.85	11.85	230	66	264	102	85.85	0.52	198.00
Bakafa	372435	818556	2184	209	7	76.25	89.11	12.86	145	88.25	197.5	67.25	79.23	0.62	109.25
Banteweson1	387077	794708	1947	252	0	251	252	1		69	222	0	0.00		153.00
Banteweson2	364308	697038	1256	241	6.4	134.5	151.17	16.67	211	196	238	36	134.77	0.86	42.00
Bilalo	390586	860382	2290	250	1.6	101.0	183.33	82.3	184	63.3	226.8	64.9	104.95	0.40	163.50
Bilate Sp.Force BH1	396314	744983	1260	250	10	26.5	125.77	99.27	175	70.2	222.3	70.2	36.10	0.46	152.10
Bilate Sp.Force BH2	396095	744542	1247	243	26	25	58	33	142	67.5	237.15	70.2	25.35	0.41	169.65
Bitena3	376278	756602	1765	272	3.28	189.32	191.52	2.2	240	180	270	66	-	0.73	90.00
Bodity BH1_ 2006	373443	770018	1956	122	20	15.75	80.21	64.46	108	50	116	42	25.06	0.64	66.00
Bodity BH2_ 2006	375147	768002	1947	110	22	30.46	38.04	7.58	84	44	104	42	31.98	0.70	60.00
BodityBH1	376149	773034	1932	290	20	38.64	125.93	87.29	180	63.84	284.18	87.3	56.83	0.40	220.34
BodityBH2	375620	772544	1923	297.2	19	50.53	100.59	50.06	190	66.3	291.42	80.9	57.98	0.36	225.12
BodityBH3	374814	771631	1932	294	27	60.5	138.32	77.82	174	77.8	282.36	88.16	61.76	0.43	204.56
BodityBH4	374344	770651	1940	300	17	50.7	140.67	89.97	195	85.8	288.8	98.4	63.06	0.48	203.00
BodityBH5	372069	768686	1932	250	28	26.23	99.11	72.88	190	63.76	174.34	58.2	33.97	0.53	110.58
Bonesh2009	401160	825370	1938	250.0	14	85.9	86.8	0.9	162	164	244.28	57.28	156.00	0.71	80.28
BoneshaHadiya	398671	831195	1940	126	8.5	66.66	74.2	7.54	120	83	125	30	67.76	0.71	42.00
Boricha3_2006	409237	767220	1647	352	11.5	136	159.9	23.9	324	148	346	108	138.00	0.55	198.00
Bubisa	414533	820061	2010	383	5.8	280.9	288.65	7.75	330	278.84	380	62.92	281.20	0.62	101.16
Chambulla	396543	809304	1786	187	25	60.4	70.71	10.31	117	70	160	56.1	64.55	0.62	90.00
D Kare	340820	766544	1293	225	17	2.54	37.14	34.6	160	39.4	219.2	69.6	2.98	0.39	179.80
DagneDaba	395240	742296	1216	250.0	21	18.4	45.2	26.8	167	93.84	244.28	99.45	18.70	0.66	150.44
DangaraSalata 2004	360056	775363	1814	182	4.4	69.1	112.3	43.2	154	84	180	30	76.40	0.31	96.00
DebenchoBH	399435	812076	1765	160	8	53	58.22	5.22	130	100	154	46	53.10	0.85	54.00
DegaBirbir	346528	699185	2600	110	7.33	15.3	23.98	8.68	85	47	107	36	15.83	0.60	60.00

Bore	Easting	Northing	Elevation	Total Depth	Q	SWL	DWL	TDD	PP	Top Aqui.	Bottom Aqui.	Screen Length (L)	MRWL	L/b	Aquifer Thick Ness(b)
Demboya	381019	812998	2088	262	5.35	164	206.65	42.65	228	152.65	236.65	48.65	166.70	0.58	84.00
DileDate	413220	869496	2063	238	15.0	143.45	146.2	2.75	175	146	232	66	143.54	0.77	86.00
Doesha	397556	839336	1912	274	21	6.95	33.97	27.02	119	64	268	102	8.78	0.50	204.00
Dola-04	360056	774274	1835	134	5.94	39.3	68.5	29.2	108	72	126	36	41.34	0.67	54.00
Dola2004	360056	774274	1836	134	5.94	39.3	68.5	29.2	108	72	126	36	41.30	0.67	54.00
Dongoro Bonkoya	393564	789143	1692	345	10	120.04	129.4	9.36	87.47	122	300	120	120.45	0.67	178.00
DoyoGena2004	363483	813176	2305	146	18	38	48.2	10.2	110	78	138	54	39.35	0.90	60.00
DugunaBoloso	387636	773697	1702	151	5.6	92.6	98.1	5.5	137	103	145	30	93.40	0.71	42.00
DugunaBolso 2013	386969	771172	1771	182	6.6	127.87	134.99	7.12	171	138	180	36	128.86	0.86	42.00
DugunaSore 2006	387001	769755	1788	202	6	128	130.08	2.08	180	134.2	192.2	40.6	132.87	0.70	58.00
Durame	377491	799312	2016	150	4.3	65	144	79	145	70	145	15	68.71	0.20	75.00
Durame Campus1	381943	804326	2055	340	20.0	148.38	150.29	1.91	179	154	334	102	148.48	0.57	180.00
Durame Campus2	381676	804073	2059	250	22.0	134.9	136.5	1.6	154	154	244	72	134.88	0.80	90.00
Enjama Gutancho	410248	867461	2107	186	5.2	122.3	123.87	1.53	164	81	177	60	122.51	0.63	96.00
Fango Gelchecha	356370	734693	1629	244	6	18.05	166.35	148.3	220	87.25	241	88.1	65.40	0.57	153.75
Fetazer	405066	887876	2885	126.85	12	76.0	102.7	26.75	104	74.2	121	35.1	73.10	0.75	46.80
F-Koysha	400413.6	770548.2	1747	300	0	299	299.5	0	-	205	207	0	0.00		2.00
Garame Ambercho	381344	807520	2115	272	6.5	188.5	198.5	10	255	129	268.2	69.6	190.00	0.50	139.20
Gazebo_BH2	400559	880230	2753	148	8	48.3	119.7	71.44	132	79	142.25	40.25	57.50	0.64	63.25
Gedesha	366752	864478	2142	200	0	199	200	1		45	184	0	0.00		139.00
GerbaJilo	380058	803224	2088	283	6.5	126.33	157.26	30.93	264	138	277.2	69.6	141.53	0.50	139.20
Gerbeber Health	431648	879627	1837	170	20	26.3	45.6	19.34	124	65.6	164.2	69.6	26.92	0.71	98.60

Bore	Easting	Northing	Elevation	Total Depth	Q	SWL	DWL	TDD	PP	Top Aqui.	Bottom Aqui.	Screen Length (L)	MRWL	L/b	Aquifer Thick Ness(b)
Geshara4	377000	798004	1966	163	7.5	71.02	97.22	26.2	138	108.85	161.5	46.8	78.55	0.89	52.65
Getem2018	411425	839312	1836	288.0	17	130.0	139.35	9.35	164	110.37	282.27	74.5	131.91	0.43	171.90
Getem Gurbiye	405313	840739	1940	246	4.4	124.9	133.52	8.6	174	12	234	48	126.25	0.22	222.00
Goffesa	417218	810556.2	1840	328	4	242.7	260	17.3	288	100	325	30	-	0.13	225.00
Gombora 2004	352235	836144	1944	70	24	0	7.7	7.7	25	31	67	30	0.00	0.83	36.00
GorigisSefer	369648	830996	2135	300	11	85.9	127.65	41.75	204.8	109.26	288.4	86.7	88.40	0.48	179.14
Gulibana2	376832	797596	1966	210	7	77	96.3	19.3	162	99	207	54	80.80	0.50	108.00
GurumuKoisha	361172	770263	1938	150	6	48.12	74.5	26.38		102.8	144.8	24	53.85	0.57	42.00
HadayeGibe	359874	850706	2013	96	24.4	24.66	41.1	16.44	78	36	90	24	27.80	0.44	54.00
Halaba_ Alemtena 490	401245	815396	1793	490.00	14	75.1	87.92	12.85	170	203.35	478.3	105.3	75.98	0.38	274.95
Hangeda	358471	821488	2137	193	12.5	11.3	85.97	74.67	132	103	187	54	27.31	0.64	84.00
HanjaGotmana	390571	818746	1948	220	14	77.65	87.06	9.41	178	86.6	150.4	43.6	78.28	0.68	63.80
HantameBH	398425	810279	1762	148	8	45.5	49.46	3.96	124	70	142	66	45.87	0.92	72.00
Hantazo	414556	821098	2036	430	5.5	317.65	325.95	8.3	380	286	424.24	69.12	319.10	0.50	138.24
Hawela Nure	439737	766442	1881	187	21	107.85	115.06	7.21	170	111.15	181.35	52.65	109.00	0.75	70.20
Hayse	377606	829469	2070	300	60	21.1	72.57	51.47	132	36	294	90	36.28	0.35	258.00
HomaGera	393984	836965	1985	127.3	26.0	33.75	34.25	0.5	84	37.25	109.25	42	33.79	0.58	72.00
Hossana2	369827	836590	2199	167	11	70.5	111.5	41	130	75	161	30	78.38	0.35	86.00
Hulbareg Fugo2006	407225	862981	2081	130	6.4	65.55	83.9	18.35	105	74	122	30	65.91	0.63	48.00
ilalaGelila	456837	885218	1771	180	6.5	0	9.12	9.12	0	106	178	30	0.88	0.42	72.00
Jata2015	406497	826739	1885	216.0	4.3	128.6	131.36	2.78	156	120	210	42	129.00	0.47	90.00
Jembero_ 1995EC	393891	886059	2770	175	5.95	93.0	107.05	14.1	172.53	112	169	32	94.23	0.56	57.00
Jenboro	395287	886845	2772	190	2.56	153.8	169.3	15.5	174	130.5	188	34.5	154.15	0.60	57.50
Kedida Gamela2001	387636	773697	2016	260	6.75	159.6	164.57	4.97	235	215	254	36	159.53	0.92	39.00
Kedida	374351	799980	2023	247	6.5	131.1	133.55	2.45	200	107.8	241.2	75.8	133.00	0.57	133.40

Bore	Easting	Northing	Elevation	Total Depth	Q	SWL	DWL	TDD	PP	Top Aqui.	Bottom Aqui.	Screen Length (L)	MRWL	L/b	Aquifer Thick Ness(b)
Gamela2006															
Kekich_WGKW2	360858	813183	2274	400	65	15.3	38.2	22.9	113	78.8	386.2	116	17.10	0.38	307.40
Konicha	417940	815083	1838	358	1.91	163.85	258.2	94.35	324	220	352	90	176.53	0.68	132.00
Kulubi	418084	828669	1811	350	21.2	93.25	101.35	8.1	173	164.11	343.46	92.52	94.44	0.52	179.35
LaloGerbe	384724	786331	1915	235.0	14.0	85.9	86.8	0.9	162	127	229	66	85.90	0.65	102.00
LaloGorbe	384724	786331	1915	235	14	85.9	86.8	0.9	162	127	229	66	85.90	0.65	102.00
Lay Lenda	405907	808709	1821	270	4	201.4	236.2	34.8	244	201.4	260	48	207.55	0.82	58.60
Lay.Gimbichu	400008	823627	1838	157.8	0	157	157.8	0.8	-	75	81	0	0.00		6.00
LBSTW-02-18	417027	740776	1782	596.0	10	192	241.98	49.98	250	156.13	576.1	180.55	192.30	0.43	419.97
LBSTW-03-18	423106	742745	1640	500.0	50.15	29.6	198.78	169.18	250	149	482.45	134.55	46.66	0.40	333.45
LBTW-01-19	375649	732105	1313	500.0	64.85	59.6	109.4	49.8	160	121.82	483.44	145.27	65.30	0.40	361.62
LBTW-04-18	385027	758346	1488	480.0	18	122.98	188.33	65.35	240	153.29	467.35	149.49	127.33	0.48	314.06
LBTW-05-19	388403	732486	1202	500.0	52.03	23.9	89.41	65.51	140	127.48	488.67	157.19	24.26	0.44	361.19
LBTW-06-19	414515	773789	1781	500.0	18	207.4	229.34	21.94	280	174.3	483.04	116.13	211.31	0.38	308.74
LBTW-07-19	397739	750795	1320	532.0	34.9	1.63	175.92	174.29	189	311.41	502.95	93.02	11.60	0.49	191.54
LBTW-08-18	377944	776542	1907	500.0	58.1	49.74	76.67	26.93	202	189.95	470.75	139.8	54.91	0.50	280.80
Lissana Seina	380225	835486	2153	193.25	25	35	45.03	10.03	120	61.25	187.25	72	36.54	0.57	126.00
Loka Abaya	364308	697038	1256	141	6.5	0	9.12	9.12	100	72	138	42	0.88	0.64	66.00
LukeFeka	440733	876079	1995	320	12.0	2.45	5.79	3.34	85	236	314	60	2.70	0.77	78.00
Mareko	446123	888941	1820	600	51.0	20.82	34.69	13.87	80	161.25	570.75	169.65	22.96	0.41	409.50
Megera	428375	736871	1789	249	18	35.4	77.3	41.9	180	141	243	78	41.27	0.76	102.00
MehalMugo	393126	866552	2407	218	10	34.3	80.05	45.8	133	78.8	206.8	52.2	37.02	0.41	128.00
Mekana3	380285	802617	2089	236	5.833	159.9	194.15	34.25	210	165.8	230.15	52.65	165.50	0.82	64.35
MenzoSeyato	413226	839300	1809	130.0	27	41.3	50.32	9.07	90	61.24	124.27	34.38	42.16	0.55	63.03
MerabMugo	382202	866687	3049	275	0	274	275	1	-	142	190	0	0.00		48.00
MisrakAnlemo 2008	380146	836224	2157	170	25	24.57	39	14.43	164	38	164	72	26.65	0.57	126.00
MMS_TW02	443675	909350	1905	411.46	60	24.1	53.1	28.97	84.55	99.1	405.52	135.55	25.80	0.44	306.42
MMS_TW03	446946	889884	1855	591	73.7	17.5	21.54	4.08	67.6	104.69	579.02	143.01	17.97	0.30	474.33
MMS_TW04	421268	876639	2065	500	15.5	175.5	187.1	11.61	212	131.82	480.89	166.95	177.02	0.48	349.07
MMS_TW05	434900	871870	1859	502	50.6	54.7	71.1	16.45	84	105.13	472.2	172.25	55.16	0.47	367.07

Bore	Easting	Northing	Elevation	Total Depth	Q	SWL	DWL	TDD	PP	Top Aqui.	Bottom Aqui.	Screen Length (L)	MRWL	L/b	Aquifer Thick Ness(b)
MMS_TW06	443675	909350	1905	255.59	200	0.1	0.2	0.1							0.00
MMS-TW01	426868	899213	2147	600	17	62.5	87.22	24.72	137	93.67	444.8	144.78	71.00	0.41	351.13
MorochoYirba	433977	762572	1876	250	13.84	102.26	145.06	42.8	198	46	238	78	110.06	0.41	192.00
NigistEleni Hosp1	371223	835707	2222	316	24.0	104.44	118.64	14.2	190	88	280	120	105.75	0.63	192.00
Regidina	403961	823093	1834	180	5	110.75	126.25	15.5	169	115	169	36	111.80	0.67	54.00
Satame5	370571	809494	2381	322	0	321	322	1	-	192	312	0	0.00		120.00
SemenMugo	393404	867064	2430	184	12.22	28.2	80.83	52.68	129	91.2	178.2	58	37.28	0.67	87.00
Senbete Sinkile	411609	797112	1890	400	4.4	282	295	13	340	217.1	394.1	118	-	0.67	177.00
Serara	368736	808334	2470	280	7.6	163.75	167.65	3.9	200	123	279	48	164.13	0.31	156.00
Shanto	372373	776546	1934	189	7.5	69.8	81.14	11.34	120	98	182	48	70.04	0.57	84.00
Sheketa	400923	803325	1758	284	15	136.1	140.55	4.45	160	136	270	74	135.63	0.55	134.00
Shelemat	408353	882012	2901	252	0.0	251	252	1		64	126	0	0.00		62.00
Shemsa Gimbichu	401469	825539	1869	220	4.5	121.52	127.38	5.86	150	178	214	30	122.10	0.83	36.00
Shinshicho BH1	360604	795680	1703	284	11.77	77.76	143.61	65.85	235	74.29	265.52	96.77	77.76	0.51	191.23
Shinshicho BH2	363646	796818	1806	330.06	18.5	81.2	102.85	21.65	144	110.17	318.68	110.13	82.12	0.53	208.51
Shinshicho BH3	360806	796317	1720	312.5	45	0	2.01	2.01	65	93.42	301.01	115.18	0.00	0.55	207.59
Shochora Fesho	361883	744893	1873	182	11	102.8	110.66	7.86	145	103.25	178.2	51.79	104.65	0.69	74.95
SholaKode	354544	756220	1894	150	5	78.5	105.35	26.85	126	102	144	27	87.15	0.64	42.00
Shone1	384739	785811	1916	350	16.7	132.8	158.3	25.5	186	130.55	341.15	122.86	135.80	0.58	210.60
Shone2	384827	787239	1930	257.4	15	102	154.15	52.15	210	35.16	245.7	105.3	104.80	0.50	210.54
Shone2006	403093	779404	1608	215	7.85	71	73.1	2.1	186	99	203.4	63.8	71.11	0.61	104.40
Shone3	381768	786819	1898	351	28	57.37	96.13	38.76	180	105.4	339.3	111.15	57.50	0.48	233.90
Shone4	380144	785558	1,880	350	25	22.18	90.05	67.87	163	75.05	344.15	111.15	22.80	0.41	269.10
Sil_Wor_BH2	413128	867522	2005	350.0	28	57.1	82.13	25.03	180	40.6	285.8	139.2	58.75	0.57	245.20
Sil_Wor_BH3	416439	863336	1956	338.0	28	78.1	93.23	15.13	154	140.8	326.4	98	80.65	0.53	185.60

Bore	Easting	Northing	Elevation	Total Depth	Q	SWL	DWL	TDD	PP	Top Aqui.	Bottom Aqui.	Screen Length (L)	MRWL	L/b	Aquifer Thick Ness(b)
Sil_Wor_BH4	408857	869283	2127	344.0	33	73.4	86.7	13.3	159	143.4	332	105.8	76.82	0.56	188.60
Sil_Wor_BH5	414525	865143	1954	350.0	33	38.1	68.55	30.45	186	99.6	302.6	98.6	41.00	0.49	203.00
Sil_Wor_BH6	408859	869384	2134	177.0	23.2	72.9	76.13	3.28	150	51	171	60	73.00	0.50	120.00
Sil_Wor_BH7	410498	872023	2164	197.0	28	46.3	48.76	2.46	123	88	190	60	46.41	0.59	102.00
Sil_Wor_BH8	408815	864631	2097	165.0	7	94.0	116.56	22.56	136	48	162	48	95.15	0.42	114.00
Sil_Wor_BH9	409067	865035	2105	183.0	7	98.0	130.66	32.69	166	96	180	42	99.44	0.50	84.00
Sil_Wor_Guest	412192	870730	2117	250.0	22	93.8	104.82	11.04	169	135	234.2	63.8	92.22	0.64	99.20
Silase_1995EC	386999	877426	2764	160	5	107.5	149.2	41.7	154.5	12	154	32	112.00	0.23	142.00
Simbita480m	415950	834753	1790	480.00	36.7	53.8	72.04	18.29	122	104.4	439.25	147.59	57.13	0.44	334.85
Sirara2004	368736	808334	2470	280	7.6	163.75	167.65	3.9	200	123	279	48	164.13	0.31	156.00
Siraro Badawacho Abuka SRBH	392030	789350	1732	410	21	126	136.82	10.82	210	114.2	392.6	139.2	126.29	0.50	278.40
Sodo-Gurage	446158	899288	1849	513	40	20.94	35.68	14.74	135	111	501	156	21.65	0.40	390.00
Somicho	349126	812583	2585	180	37	9.79	16.33	6.54	85	58.2	174.2	75.4	11.06	0.65	116.00
Tachi.Ambicho	379334	834957	2185	220	13.0	75.4	116	40.6	177	112	214	60	81.50	0.59	102.00
Tefo Chufo	413306	813861	1923	320	4	230	239.38	9.38	268	213.4	306.2	58.2	230.76	0.63	92.80
TekleHaymanot	411856	901024	3195	300	0	299.0	300	1		41	290	0	0.00		249.00
Ushegola	388852	819666	1977	237.15	14	74.2	119.87	45.67	132	52.8	231.2	83.28	75.50	0.47	178.40
W_Sodo AgriColle	363609	755752	1868	180	5.3	13.5	89.8	76.3	168	138	174	30	14.10	0.83	36.00
W_SodoT 2003	362263	759694	2057	250	6.4	127	137.81	10.81	222	112	244	60	128.58	0.45	132.00
WachoUniv1	378737	832414	2097	179	60.0	21.5	26.5	5	110	30.98	101.66	64.79	21.88	0.92	70.68
WachoUniv3	379930	833668	2136	172	70.0	63.8	72.28	8.48	120	70	160	60	64.14	0.67	90.00
Wada	349138	812474	2586	194	7	44.3	104.63	60.33	170	86	188	66	52.60	0.65	102.00
Wagebeta1	361947	812591	2265	372	61	5.67	22.05	16.38	120	30.38	360.4	121.6	7.79	0.37	330.02
Wagebeta2	361414	812117	2258	360	57	0	11.8	11.8	70	53.1	354.2	104.26	11.80	0.35	301.10
Wagebeta3	361886	811789	2262	400	62.5	12.42	37.75	25.33	112	52.5	388.4	115.84	13.89	0.34	335.90
Wagebeta4	361780	811288	2271	400	60	13.67	17.19	3.52	107	46.72	388.4	133.3	14.18	0.39	341.68
WariteBalaka	377217	774360	1897	400	33	47.54	65.77	18.23	164	92.9	388.4	127.6	49.36	0.43	295.50

Bore	Easting	Northing	Elevation	Total Depth	Q	SWL	DWL	TDD	PP	Top Aqui.	Bottom Aqui.	Screen Length (L)	MRWL	L/b	Aquifer Thick Ness(b)
WarshaShanka	433920	869585	1841	135	24.4	36.38	38.77	2.39	100	57	132	36	36.49	0.48	75.00
WashaWayra	448644	879236	1854	252	9.0	164.3	176.38	12.08	216	132	246	60	165.20	0.53	114.00
W-Busha	351923	746148	1559	139.2	10	40	58.65	18.65		72.4	139.2	26.2	46.52	0.39	66.80
Webo BolosoSore	354246	776963	1807	150	2.5	44	68.54	24.54	122	84	144	42	47.65	0.70	60.00
Weta1	380240	803217	2078	217	8.5	81.16	109.28	28.12	144	91	211	72	86.30	0.60	120.00
Wetatte2	415951	828627	1874	256.8	4	151	179	28	255	210	252	30	152.15	0.71	42.00
Wogilla BH	388517	840914	2235	420	6	198	215	17	280	204	414	120	199.75	0.57	210.00
Wolaita T WS Utility2002	362895	757971	2039	205	7.2	102.2	105.08	2.88	150	130	201	30	102.32	0.42	71.00
Wonjela	370232	825456	2153	167.4	4.88	87.88	103.84	15.96	157	99.67	164.4	29.16	91.23	0.45	64.73
Worab AgriColle	405843	870387	2311	201	9.0	164	176.38	12.38	219	117	195	60	165.20	0.77	78.00
WS Town1	364216	757722	1964	169	7.5	93.6	96.27	2.67	150	49	163	32	94.14	0.28	114.00
WS Town2	362895	757971	2039	205	7.2	102.2	105.08	2.88	150	130	202	30	102.32	0.42	72.00
WS Uni BodityT 2013	371736	769200	1933	293	12	60.2	89.75	29.55	215	95.95	276.37	52.8	62.40	0.29	180.42
WS Uni GununoT 2012	350750	764434	2026	310	16.5	17.5	42.2	24.7	195	83.2	269.26	87.3	17.50	0.47	186.06
WS Uni SodoCity 2013	361096	760253	1947	340	20.6	23.98	40.36	16.38	145.5	66.46	328.36	87.3	24.12	0.33	261.90
W-SodoT Gerara	359460	756647	1867	176	5	47	61	14	162	134	170	30	49.20	0.83	36.00
WSUniversity1	361868	755320	1877	136.8	2.6	50.9	114.14	63.24	121	64	124	36	58.60	0.60	60.00
WSUniversity2	361575	754559	1855	136	7.6	33.1	48.96	15.86	115	55	121	42	39.27	0.64	66.00
Wulbareg	397182	883625	2858	286	0	285.0	286	1		24	156	0	0.00		132.00
Yen BH1 BishanJilba	440516	910053	1963	248	3.5	23.7	93.1	69.4	218	38	242	96	27.05	0.47	204.00
Yirgalem-IAIP BH1	424951	742850	1628	360	22	1.5	132.4	130.9	140	60	355	120	2.05	0.41	295.00

Bore	Easting	Northing	Elevation	Total Depth	Q	SWL	DWL	TDD	PP	Top Aqui.	Bottom Aqui.	Screen Length (L)	MRWL	L/b	Aquifer Thick Ness(b)
Yirgalem-IAIP BH2	428668	744596	1745	222	13.75	72.8	103.43	30.63	186	74	216	74.75	77.84	0.53	142.00
Yirgalem-IAIP BH4	428668	744596	1745	184	17	66.63	69.03	2.4	168	31.9	178.15	76.05	67.98	0.52	146.25
Yirgalem-IAIP BH8	428205	745329	1748	247	6	72.4	197.4	125	212	112	241	87	97.05	0.67	129.00
Z-Sibaye	369191	771341	1950	195	16	50.26	65.2	14.94	150	37.72	189.17	52.44	53.35	0.35	151.45

Annex-2 Aquifer parameters evaluation for 65 Wells using AquiferTest-10 software.

Well Name	GPS Location			Wellbore Storage and Skin Effects (Agarwal 1980)				Papadopulos-Cooper			Theis Recovery			
	X	Y	Z	Transmissivity,T(m2/sec)	Hydraulic Conductivity, K(m/sec)	Wellbore Storage Coeff.	Skin factor	Transmissivity, T (m2/sec)	Hydraulic Conductivity, K(m/sec)	Wellbore Storage Coeff.	T(m2/sec)	K(m/sec)	Aquifer Thichness(m)	Q (lit/sec)
AlichoWoriro_Kichen	406948	883233	2879	0.00278	0.0000309	0.99	0.0508	0.0028	0.0000311	0.0336	0.00374	0.0000415	90	9
Fetezer	405061	887875	2892	0.000168	0.00000358	0.407	-2.39	0.000409	0.0000874	0.99	0.000181	0.00000387	46.9	12
GazeboBH2	400559	880230	2753	0.0509	0.000805	0.97	-4.2	0.181	0.00286	0.99	0.0000599	0.000000946	63.25	8
WachamoUniv3	379930	833668	2136	0.045	0.0005	0.0000001	20	0.0178	0.000198	0.0000001	0.0158	0.000175	90	70
Hadiya E_NigistBH1	371223	835707	2222	0.00255	0.0000277	0.0000673	-0.0101	0.00255	0.0000277	0.0000687	1.14	0.0124	92	24
Hadiay Somicho	349126	812583	2585	0.00366	0.0000316	0.467	-2.06	0.00665	0.0000573	0.5	5.09	0.0438	116	37
AmbichoGode	378914	844927	2161	0.000748	0.0000113	0.696	-2.15	0.00167	0.0000253	0.99	0.0014	0.0000212	66	30
Hadiya Kekicho	360858	813183	2274	0.00459	0.000149	0.0222	-0.0273	0.00459	0.0000149	0.0235	0.00479	0.0000156	307.4	65
Aziga 6-Angacha	376046	813225	2113	0.00012	0.000000606	0.217	-2.92	0.00311	0.0000157	0.99	0.000195	0.000000986	198	22
Hayse	377606	829469	2070	0.000726	0.00000282	0.78	-1.3	0.00106	0.0000411	0.99	0.00116	0.00000449	258	60
Ana Tigo	380733.6	838350.2	2169	0.00104	0.00000615	0.213	-2.05	0.00163	0.000000959	0.99	0.00135	0.00000794	169.65	32
WSU Sodo City	361096	760253	1947	0.00148	0.00000566	0.99	1.96	0.0015	0.00000574	0.0165	0.00158	0.00000604	261.9	20.6
SemenMugo	393404	867064	2430	0.00026	0.00000299	0.00192	-0.0144	0.00026	0.00000299	0.00198	0.000176	0.00000202	87	12
MisrakAnlemo	380146	836224	2157	1.26	0.01	0.5	-5	3.8	0.0302	0.5	1.26	0.01	126	25
Gorigis Sefer	369648	830996	2135	0.263	0.00147	0.466	-1.45	0.331	0.00185	0.5	0.000185	0.00000103	179.14	10
LBTW-01-19	375649	732105	1313	0.00189	0.00000522	0.000341	0.664	0.00174	0.00000481	0.000341	0.00249	0.00000689	361.62	64.85
LBTW-08-18	377944	776542	1907	0.00211	0.00000753	0.99	1.08	0.00214	0.00000762	0.1	0.00249	0.00000887	280.8	58.1
LBTW-04-18	385027	758346	1488	0.000492	0.00000157	0.000000393	0.000247	0.000492	0.00000157	0.000000401	0.000198	0.000000629	314.06	18
LBTW-07-19	397739	750795	1320	0.000565	0.00000295	0.000000239	4.8	0.000414	0.00000216	0.0000001	0.000309	0.00000161	191.54	34.9
LBTW-05-19 Sidama-LokaAbaya	388403	732486	1202	0.0016	0.00000442	0.00000461	1.42	0.0016	0.00000442	0.000000267	0.00114	0.00000315	361.19	52.03

Well Name	GPS Location			Wellbore Storage and Skin Effects (Agarwal 1980)				Papadopulos-Cooper			Theis Recovery			
	X	Y	Z	Transmissivity,T(m2/sec)	Hydraulic Conductivity, K(m/sec)	Wellbore Storage Coeff.	Skin factor	Transmissivity, T (m2/sec)	Hydraulic Conductivity, K(m/sec)	Wellbore Storage Coeff.	T(m2/sec)	K(m/sec)	Aquifer Thichness(m)	Q (lit/sec)
LBTW-06-19(Sidama_Boricha)	414515	773789	1781	0.00259	0.00000839	0.0000001	2	0.000957	0.0000031	0.0000001	0.0012	0.00000387	308.74	18
Gelima Well	377509	800788	2065	0.0000578	0.000000321	0.000102	-0.0189	0.0000578	0.000000321	0.000106	0.0000214	0.000000119	179.8	3.8
Abeke2017	400495	879244	2747	0.000861	0.00000981	0.954	-0.735	0.108	0.0000124	0.99	0.000821	0.00000935	87.75	21
WariteBalaka	377217	774360	1897	0.00189	0.00000639	0.44	-0.00187	0.00189	0.00000639	0.442	0.00283	0.00000958	295.5	33
DurameCampus2	381676	804073	2059	0.0747	0.00083	0.0000001	20	0.0296	0.000329	0.0000001	0.0292	0.000325	90	22
DurameCampus1	381943	804326	2055	0.0230	0.000128	0.00000339	1	0.02304	0.000128	0.000000454	0.02304	0.000128	180	20
Angamo2015	398521	865613	2321	0.000284	0.00000242	0.44	-1.14	0.000369	0.00000315	0.99	0.00308	0.00000263	117	18.33
Jata2015	406497	826739	1885	0.00143	0.0000159	0.794	0.768	0.00145	0.00000161	0.156	0.000714	0.00000793	90	4.3
Tefo Chufo	413306	813861	1923	0.000641	0.0000069	0.99	4	0.000663	0.000000715	0.000195	0.000269	0.0000029	92.8	4
Doesha	397556	839336	1912	0.00166	0.00000815	0.00000136	1.84	0.00159	0.00000778	0.0000001	0.000509	0.0000025	204	21
WS Uni BodityT2013	371736	769200	1933	0.000719	0.00000399	0.0000036	0.000189	0.000719	0.00000398	0.00000363	0.000521	0.00000289	180.42	12
Getem2018	411425	839384	1836	0.00124	0.00000724	0.75	-0.996	0.00164	0.00000953	0.99	0.0041	0.0000239	171.9	17
BodityBH1	376149	773034	1932	0.151	0.000685	0.839	-3.4	0.325	0.00148	0.99	0.131	0.000593	220.34	20
BodityBH2	375620	772544	1923	0.000352	0.00000156	0.0677	-0.00323	0.000352	0.00000156	0.0722	0.000282	0.00000125	225.12	19
BodityBH3	374814	771631	1932	0.000226	0.00000111	0.822	-0.674	0.000277	0.00000136	0.99	0.000186	0.000000909	204.56	27
BodityBH4	374344	770651	1940	0.0000832	0.00000041	0.927	-1.39	0.000153	0.000000755	0.99	0.000162	0.000000799	203	17
Weyira(HBH-1)	402443	802506	1742	0.0012	0.0000265	0.000331	0.00492	0.00812	0.0000265	0.000331	0.001	0.00000327	306	22.5
Kulubi	418084	828669	1811	0.00176	0.0000098	0.911	-1.33	0.00256	0.0000143	0.99	0.00249	0.0000139	179.35	21.2
Simbita BH407	417212	835995	1902	0.00226	0.00000638	0.00000542	0.0123	0.00226	0.00000638	0.00000542	0.00163	0.00000461	354	68
Aroge Arada SodoBH	364308	757939	1975	0.00466	0.0000299	0.99	0.482	0.00466	0.0000299	0.375	0.0101	0.0000647	156	22
Bakafa	372435	818556	2184	0.000402	0.00000368	0.987	-0.203	0.000429	0.00000393	0.99	0.00037	0.00000339	109.25	7
Hobicha	367814	747884	1725	0.000107	0.00000204	0.617	-2	0.000273	0.00000519	0.99	0.000203	0.00000385	52.65	7

Well Name	GPS Location			Wellbore Storage and Skin Effects (Agarwal 1980)				Papadopulos-Cooper			Theis Recovery			
	X	Y	Z	Transmissivity,T(m2/sec)	Hydraulic Conductivity, K(m/sec)	Wellbore Storage Coeff.	Skin factor	Transmissivity, T (m2/sec)	Hydraulic Conductivity, K(m/sec)	Wellbore Storage Coeff.	T(m2/sec)	K(m/sec)	Aquifer Thichness(m)	Q (lit/sec)
Shone1	384739	785811	1916	0.000161	0.000000764	0.402	-2.93	0.000604	0.00000287	0.99	0.000508	0.00000241	210.6	16.7
Shone2	384827	787239	1930	0.0000893	0.000000424	0.755	-1.99	0.587	0.00278	0.99	0.00013	0.000000618	210.6	15
Shone3	381768	786819	1898	0.000447	0.00000191	0.977	-0.885	0.000597	0.00000255	0.99	0.000445	0.0000019	233.9	28
Shone4	380144	785558	1,880	0.000404	0.0000015	0.00639	-0.0585	0.000404	0.0000015	0.00718	0.000254	0.000000944	269.1	25
MenzoSeyato	413226	839300	1809	0.00332	0.0000527	0.037	-0.0478	0.00332	0.0000527	0.0407	0.00321	0.0000509	63	27
WSodoT2010 ANS BH2	361503	751012	1831	0.000654	0.0000126	0.99	0.781	0.000668	0.0000128	0.172	0.000712	0.0000137	52.04	18
WSodo2010 ANS BH1	361657	751538	1833	0.000949	0.0000158	0.83	-0.933	0.0012	0.0000201	0.99	0.00182	0.0000303	60	19
W Sodo WG3	358840	755708	1848	0.00012	0.00000109	0.0465	-0.602	0.000128	0.00000118	0.99	0.000123	0.00000113	109.35	14
Chambulla	396543	809304	1786	0.00226	0.0000402	0.343	-0.0344	0.00226	0.0000402	0.368	0.00447	0.0000797	56.1	25
Wagebeta1	361947	812591	2265	0.00405	0.0000123	0.99	0.206	0.00405	0.0000123	0.645	0.00529	0.000016	330.02	61
Wagebeta2	361414	812117	2258	0.00678	0.0000225	0.266	1.88	0.00678	0.0000225	0.00623	0.00452	0.000015	301.1	57
Wagebeta3	361886	811789	2262	0.00678	0.0000202	0.00000108	1.42	0.00678	0.0000202	0.0000001	0.00341	0.0000102	335.9	62.5
Wagebeta4	361780	811288	2271	0.00383	0.0000112	0.722	-4.89	0.0265	0.0000777	0.99	0.0111	0.0000326	341.68	60
WSodo2010 WG-5	358750	755513	1848	0.000761	0.00000698	0.99	0.95	0.000768	0.00000705	0.135	0.000718	0.00000659	108.94	16
WSodo2010 WG-4	358847	756053	1849	0.000338	0.00000346	0.99	0.665	0.000342	0.0000035	0.233	0.000457	0.00000467	97.77	17
WSodo2010 WG-6	358448	755232	1834	0.000583	0.0000062	0.317	-1.61	0.0008	0.00000851	0.99	0.000921	0.0000098	94	16
Halaba_Alemtena490	401245	815396	1793	0.000961	0.00000349	0.99	0.181	0.000953	0.00000346	0.731	0.000981	0.00000357	274.95	14
SiraroBadawacho Abuka	392030	789350	1732	0.0016	0.00000575	0.861	-1.49	0.00238	0.00000854	0.99	0.0018	0.00000646	278.4	21
Senbete Sinkile well	411609	797112	1890	0.000643	0.00000363	0.0000001	0.0506	0.000643	0.00000363	0.0000001	No Data	No Data	177	4.4
Z-Sibaye	369191	771341	1950	0.000519	0.00000343	0.859	-1.48	0.000897	0.0000592	0.99	0.000136	0.000000901	151.45	16
ArusiWoyide	387915	772279	1720	0.000157	0.000000589	0.00277	-0.00904	0.000157	0.000000589	0.00282	0.000157	0.000000589	267.41	12.2

Annex-3. Aquifer loss, Well loss well-efficiency

x	y	z	B	C	Lp	Skin factor	Aquifer Thichness	Q	Well ID
361096	760253	1947	0.0007	0.000008	4.91	1.96	261.9	20.6	WSU Sodo City
393404	867064	2430	0.0203	0.00004	32.86	-0.0144	87	12	SemenMugo
375649	732105	1313	0.0059	0.0000005	68.08	0.664	361.62	64.85	LBTW-01-19
377944	776542	1907	0.0009	0.0000007	19.87	1.08	280.8	58.1	LBTW-08-18
385027	758346	1488	0.0436	-0.0000009	103.32	0.000247	314.06	18	LBTW-04-18
414515	773789	1781	0.0268	-0.000001	106.16	2	308.74	18	LBTW-06-19(Sidama_Boricha)
377217	774360	1897	0.0072	0.000004	38.69	-0.00187	295.5	33	WariteBalaka
381943	804326	2055	0.0006	0.0000009	27.83	1	180	20	DurameCampus1
371736	769200	1933	0.014	0.00005	21.26	0.000189	180.42	12	WS Uni BodityT2013
411425	839384	1836	0.0031	0.000001	67.84	-0.996	171.9	17	Getem2018
376149	773034	1932	0.0626	0.00005	38.64	-3.4	220.34	20	BodityBH1
374814	771631	1932	0.0331	0.00002	48.91	-0.674	204.56	27	BodityBH3
374344	770651	1940	0.0039	0.00003	8.13	-1.39	203	17	BodityBH4
384739	785811	1916	0.0623	0.00008	33.36	-2.93	210.6	16.7	Shone1
384827	787239	1930	0.0099	0.00001	36.42	-1.99	210.6	15	Shone2
381768	786819	1898	0.0385	0.00002	42.61	-0.885	233.9	28	Shone3
380144	785558	1880	0.008	0.00001	23.58	-0.0585	269.1	25	Shone4
413226	839300	1809	0.0102	-0.000003	176.10	-0.0478	63	27	MenzoSeyato
361503	751012	1831	0.0475	0.00006	33.73	0.781	52.04	18	WSodoT2010ANS BH2
361657	751538	1833	0.0013	0.000004	16.52	-0.933	60	19	WSodo2010 ANS BH1
358840	755708	1848	0.0123	0.00002	30.78	-0.602	109.35	14	W Sodo WG3
358750	755513	1848	0.011	0.0000004	95.21	0.95	108.94	16	WSodo2010WG-5
358847	756053	1849	0.0133	0.000003	74.02	0.665	97.77	17	WSodo2010WG-4
358448	755232	1834	0.0034	0.000003	45.04	-1.61	94	16	WSodo2010WG-6
401245	815396	1793	0.0005	0.0000001	82.82	0.181	274.95	14	Halaba_Alemtena490
392030	789350	1732	0.0004	0.000001	16.17	-1.49	278.4	21	SiraroBadawacho Abuka SRBH
372069	768686	1932	0.0268	0.00002	34.07				BodityBH5

369191	771341	1950	0.0088	0.00001	63.27	-1.48	151.45	16	Z-Sibaye

Annex-4. Pumping test and resistivity data

Well Name	**X**	**Y**	**Z**	**Thickness Resistivity**	**K(m/sec) Theis Recovery**	**T(m2/sec) Theis Recovery**	**Wellbore Storage Coeff.(Agarwal 1980)**	**ρ_a Resistivity**	**a = K*ρ_a**	**b=K/ρ_a**	**Sc** (Long. Cond) =h/ρ_a	**Tr** (Trans Resis) =ρ_ah	**T= a*Sc**	**T= b*Tr**
AlichoWoriro_Kichen	406948	883233	2879	598.35	4.15E-05	3.74E-03	9.90E-01	1.34E+02	5.56E-03	3.10E-07	4.47E+00	8.01E+04	2.48E-02	2.48E-02
Fetezer	405061	887875	2892	598.35	3.87E-06	1.82E-04	4.07E-01	1.34E+02	5.18E-04	2.89E-08	4.47E+00	8.01E+04	2.32E-03	2.32E-03
GazeboBH2	400559	880230	2753	598.35	9.46E-07	5.98E-05	9.70E-01	1.34E+02	1.27E-04	7.07E-09	4.47E+00	8.01E+04	5.66E-04	5.66E-04
WachamoUniv 3	379930	833668	2136	490.3	1.75E-04	1.58E-02	1.00E-07	1.34E+02	2.34E-02	1.31E-06	3.66E+00	6.56E+04	8.58E-02	8.58E-02
Hadiya E_ NigistBH1	371223	835707	2222	478.5	1.24E-02	1.14E+00	6.73E-05	3.51E+02	4.35E+00	3.53E-05	1.36E+00	1.68E+05	5.93	5.93E+00
Hadiay Somicho	349126	812583	2585	418.25	4.38E-02	5.08E+00	4.67E-01	1.24E+02	5.43E+00	3.53E-04	3.37E+00	5.18E+04	1.83E+01	1.83E+01
AmbichoGode	378914	844927	2161	544.32	2.12E-05	1.40E-03	6.96E-01	2.14E+02	4.53E-03	9.93E-08	2.55E+00	1.16E+05	1.15E-02	1.15E-02
Hadiya Kekicho	360858	813183	2274	605.25	1.56E-05	4.80E-03	2.22E-02	1.24E+02	1.93E-03	1.26E-07	4.88E+00	7.50E+04	9.44E-03	9.44E-03
Aziga 6-Angacha	376046	813225	2113	544.32	9.86E-07	1.95E-04	2.17E-01	1.34E+02	1.32E-04	7.37E-09	4.07E+00	7.29E+04	5.37E-04	5.37E-04
Hayse	377606	829469	2070	544.32	4.49E-06	1.16E-03	7.80E-01	2.93E+02	1.32E-03	1.53E-08	1.86E+00	1.60E+05	2.44E-03	2.44E-03
Ana Tigo	380733.6	838350.2	2169	490.3	7.94E-06	1.35E-03	2.13E-01	3.73E+02	2.96E-03	2.13E-08	1.31E+00	1.83E+05	3.89E-03	3.89E-03
WSU Sodo City	361096	760253	1947	415.15	6.04E-06	1.58E-03	9.90E-01	1.69E+02	1.02E-03	3.57E-08	2.45E+00	7.03E+04	2.51E-03	2.51E-03
SemenMugo	393404	867064	2430	598.35	2.02E-06	1.76E-04	1.92E-03	1.34E+02	2.70E-04	1.51E-08	4.47E+00	8.01E+04	1.21E-03	1.21E-03
MisrakAnlemo	380146	836224	2157	490.3	1.00E-02	1.26E+00	5.00E-01	3.73E+02	3.73E+00	2.68E-05	1.31E+00	1.83E+05	4.90E+00	4.90E+00
Gorigis Sefer	369648	830996	2135	541.85	1.03E-06	1.85E-04	4.66E-01	3.06E+02	3.15E-04	3.37E-09	1.77E+00	1.66E+05	5.58E-04	5.58E-04

LBTW-01-19	375649	732105	1313	415.15	6.89E-06	2.49E-03	3.41E-04	1.69E+02	1.17E-03	4.07E-08	2.45E+00	7.03E+04	2.86E-03	2.86E-03
LBTW-08-18	377944	776542	1907	562.33	8.87E-06	2.49E-03	9.90E-01	5.42E+01	4.81E-04	1.64E-07	1.04E+01	3.05E+04	4.99E-03	4.99E-03
LBTW-04-18	385027	758346	1488	415.15	6.29E-07	1.98E-04	3.93E-07	1.24E+02	7.80E-05	5.07E-09	3.35E+00	5.15E+04	2.61E-04	2.61E-04
LBTW-07-19	397739	750795	1320	415.15	1.61E-06	3.08E-04	2.39E-07	1.24E+02	2.00E-04	1.30E-08	3.35E+00	5.15E+04	6.68E-04	6.68E-04
LBTW-05-19 Sidama-LokaAbaya	388403	732486	1202	415.15	3.15E-06	1.14E-03	4.61E-06	1.69E+02	5.33E-04	1.86E-08	2.45E+00	7.03E+04	1.31E-03	1.31E-03
LBTW-06-19(Sidama_Boricha)	414515	773789	1781	415.15	3.87E-06	1.19E-03	1.00E-07	7.85E+01	3.04E-04	4.93E-08	5.29E+00	3.26E+04	1.61E-03	1.61E-03
Gelima Well	377509	800788	2065	605.25	1.19E-07	2.14E-05	1.02E-04	7.85E+01	9.34E-06	1.52E-09	7.71E+00	4.75E+04	7.20E-05	7.20E-05
Abeke2017	400495	879244	2747	598.35	9.35E-06	8.20E-04	9.54E-01	1.34E+02	1.25E-03	6.98E-08	4.47E+00	8.01E+04	5.59E-03	5.59E-03
WariteBalaka	377217	774360	1897	562.33	9.58E-06	2.83E-03	4.40E-01	5.42E+01	5.19E-04	1.77E-07	1.04E+01	3.05E+04	5.39E-03	5.39E-03
DurameCampus2	381676	804073	2059	562.33	3.25E-04	2.93E-02	1.00E-07	5.42E+01	1.76E-02	6.00E-06	1.04E+01	3.05E+04	1.83E-01	1.83E-01
DurameCampus1	381943	804326	2055	562.33	2.30E-02	4.14E+00	3.39E-06	5.42E+01	1.25E+00	4.25E-04	1.04E+01	3.05E+04	1.29E+01	1.29E+01
Angamo2015	398521	865613	2321	598.35	2.63E-06	3.08E-04	4.40E-01	1.34E+02	3.52E-04	1.96E-08	4.47E+00	8.01E+04	1.57E-03	1.57E-03
Jata2015	406497	826739	1885	670.39	7.93E-06	7.14E-04	7.94E-01	2.93E+02	2.33E-03	2.70E-08	2.29E+00	1.97E+05	5.32E-03	5.32E-03
Tefo Chufo	413306	813861	1923	605.25	2.90E-06	2.69E-04	9.90E-01	2.15E+02	6.23E-04	1.35E-08	2.82E+00	1.30E+05	1.76E-03	1.76E-03
Doesha	397556	839336	1912	706.41	2.50E-06	5.10E-04	1.36E-06	2.93E+02	7.33E-04	8.52E-09	2.41E+00	2.07E+05	1.77E-03	1.77E-03
WS Uni BodityT2013	371736	769200	1933	562.33	2.89E-06	5.21E-04	3.60E-06	5.42E+01	1.57E-04	5.33E-08	1.04E+01	3.05E+04	1.63E-03	1.63E-03
Getem2018	411425	839384	1836	605.25	2.39E-05	4.11E-03	7.50E-01	1.24E+02	2.96E-03	1.93E-07	4.88E+00	7.50E+04	1.45E-02	1.45E-02
BodityBH1	376149	773034	1932	562.33	5.93E-04	1.31E-01	8.39E-01	5.42E+01	3.21E-02	1.09E-05	1.04E+01	3.05E+04	3.33E-01	3.33E-01

BodityBH2	375620	772544	1923	562.33	1.25E-06	2.81E-04	6.77E-02	5.42E+01	6.77E-05	2.31E-08	1.04E+01	3.05E+04	7.03E-04	7.03E-04
BodityBH3	374814	771631	1932	562.33	9.09E-07	1.86E-04	8.22E-01	5.42E+01	4.92E-05	1.68E-08	1.04E+01	3.05E+04	5.11E-04	5.11E-04
BodityBH4	374344	770651	1940	562.33	7.99E-07	1.62E-04	9.27E-01	5.42E+01	4.33E-05	1.47E-08	1.04E+01	3.05E+04	4.49E-04	4.49E-04
Weyira(HBH-1)	402443	802506	1742	598.35	3.27E-06	1.00E-03	3.31E-04	4.53E+02	1.48E-03	7.22E-09	1.32E+00	2.71E+05	1.96E-03	1.96E-03
Kulubi	418084	828669	1811	731.95	1.39E-05	2.49E-03	9.11E-01	1.24E+02	1.72E-03	1.12E-07	5.91E+00	9.07E+04	1.02E-02	1.02E-02
Simbita BH407	417212	835995	1902	668.6	4.61E-06	1.63E-03	5.42E-06	1.24E+02	5.71E-04	3.72E-08	5.39E+00	8.29E+04	3.08E-03	3.08E-03
Aroge Arada SodoBH	364308	757939	1975	225	6.47E-05	1.01E-02	9.90E-01	2.15E+02	1.39E-02	3.01E-07	1.05E+00	4.83E+04	1.46E-02	1.46E-02
Bakafa	372435	818556	2184	544.32	3.39E-06	3.70E-04	9.87E-01	5.42E+01	1.84E-04	6.26E-08	1.00E+01	2.95E+04	1.85E-03	1.85E-03
Hobicha	367814	747884	1725	288.45	3.85E-06	2.03E-04	6.17E-01	1.69E+02	6.52E-04	2.27E-08	1.70E+00	4.88E+04	1.11E-03	1.11E-03
Shone1	384739	785811	1916	526.32	2.41E-06	5.08E-04	4.02E-01	2.93E+02	7.07E-04	8.22E-09	1.79E+00	1.54E+05	1.27E-03	1.27E-03
Shone2	384827	787239	1930	526.32	6.18E-07	1.30E-04	7.55E-01	5.42E+01	3.35E-05	1.14E-08	9.71E+00	2.85E+04	3.25E-04	3.25E-04
Shone3	381768	786819	1898	526.32	1.90E-06	4.44E-04	9.77E-01	2.93E+02	5.57E-04	6.48E-09	1.79E+00	1.54E+05	1.00E-03	1.00E-03
Shone4	380144	785558	1,880	526.32	9.44E-07	2.54E-04	6.39E-03	2.93E+02	2.77E-04	3.22E-09	1.79E+00	1.54E+05	4.97E-04	4.97E-04
MenzoSeyato	413226	839300	1809	605.25	5.09E-05	3.21E-03	3.70E-02	1.24E+02	6.31E-03	4.11E-07	4.88E+00	7.50E+04	3.08E-02	3.08E-02
WSodoT2010ANS BH2	361503	751012	1831	225	1.37E-05	7.13E-04	9.90E-01	1.69E+02	2.32E-03	8.09E-08	1.33E+00	3.81E+04	3.08E-03	3.08E-03
WSodo2010 ANS BH1	361657	751538	1833	225	3.03E-05	1.82E-03	8.30E-01	1.69E+02	5.13E-03	1.79E-07	1.33E+00	3.81E+04	6.82E-03	6.82E-03
W Sodo WG3	358840	755708	1848	415.15	1.13E-06	1.24E-04	4.65E-02	1.24E+02	1.40E-04	9.12E-09	3.35E+00	5.15E+04	4.69E-04	4.69E-04
Chambulla	396543	809304	1786	634.37	7.97E-05	4.47E-03	3.43E-01	2.14E+02	1.70E-02	3.73E-07	2.97E+00	1.36E+05	5.06E-02	5.06E-02
Wagebeta1	361947	812591	2265	605.25	1.60E-05	5.28E-03	9.90E-01	1.34E+02	2.14E-03	1.20E-07	4.52E+00	8.10E+04	9.68E-03	9.68E-03

Wagebeta2	361414	812117	2258	605.25	1.50E-05	4.52E-03	2.66E-01	1.34E+02	2.01E-03	1.12E-07	4.52E+00	8.10E+04	9.08E-03	9.08E-03
Wagebeta3	361886	811789	2262	605.25	1.02E-05	3.43E-03	1.08E-07	1.34E+02	1.37E-03	7.62E-08	4.52E+00	8.10E+04	6.17E-03	6.17E-03
Wagebeta4	361780	811288	2271	605.25	3.26E-05	1.11E-02	7.22E-01	1.34E+02	4.36E-03	2.44E-07	4.52E+00	8.10E+04	1.97E-02	1.97E-02
WSodo2010WG-5	358750	755513	1848	415.15	6.59E-06	7.18E-04	9.90E-01	1.24E+02	8.17E-04	5.32E-08	3.35E+00	5.15E+04	2.74E-03	2.74E-03
WSodo2010WG-4	358847	756053	1849	415.15	4.67E-06	4.57E-04	9.90E-01	1.24E+02	5.79E-04	3.77E-08	3.35E+00	5.15E+04	1.94E-03	1.94E-03
WSodo2010WG-6	358448	755232	1834	415.15	9.80E-06	9.21E-04	3.17E-01	1.24E+02	1.21E-03	7.91E-08	3.35E+00	5.15E+04	4.07E-03	4.07E-03
Halaba_Alemtena490	401245	815396	1793	634.37	3.57E-06	9.82E-04	9.90E-01	2.14E+02	7.63E-04	1.67E-08	2.97E+00	1.36E+05	2.26E-03	2.26E-03
SiraroBadawacho Abuka SRBH	392030	789350	1732	418.25	6.46E-06	1.80E-03	8.61E-01	5.42E+01	3.50E-04	1.19E-07	7.72E+00	2.27E+04	2.70E-03	2.70E-03
Senbete Sinkile well	411609	797112	1890	562.33	6.43E-04	1.14E-01	1.00E-07	2.14E+02	1.37E-01	3.01E-06	2.63E+00	1.20E+05	3.62E-01	3.62E-01
Z-Sibaye	369191	771341	1950		1.36E-04	9.01E-07	8.59E-01		0.00E+00	#DIV/0!	#DIV/0!	0.00E+00	#DIV/0!	#DIV/0!
ArusiWoyide	387915	772279	1720		1.57E-04	5.89E-07	2.77E-03		0.00E+00	#DIV/0!	#DIV/0!	0.00E+00	#DIV/0!	#DIV/0!

Annex-5. Electrical resistivity (VES) data layer resistivity and thickness.

X	Y	Z	Resis_ 1	Resis_ 2	Resis_ 3	Resis_ 4	Resis_ 5	Resis_ 6	Thick 1	Thick 2	Thick 3	Thick 4	Thick 5	Thick 6	VES Name
355200	746356	1715	120	1.01	10	71.5	35.3		0.75	0.324	18.7	195	305		Sodo Zuriya VP-1
355159	745844	1750	230	0.799	16.7	67.7	67.9		0.756	0.298	23.4	61.6	371		Sodo Zuriya VP-2
356057	746749	1769	155	31.4	23.9	142	10.6		2.69	50.5	27.1	266	281		Sodo Zuriya VP-3
388296	777380	1683	156	17.7	14.9	79.9	102	21.2	1.6	2.3	15.1	95.8	65.3	570	DF_AW-VP1
388510	777920	1658	406	20.5	51.5	19.2			1.05	13.9	230	367			DF_AW-VP2
388099	776571	1680	135	14.8	130	11	23.3		1.97	22.2	131	249	314		DF_AW-VP3
401684	781803	1623	607	79.3	556	19.1	8.7		0.75	0.867	3.44	192	389		SB-VP1
403123	779413	1614	179	17.6	326	17.5	76.3	28.8	2.45	9.86	8.91	15.1	105	428	SB-VP2
402049	779973	1599	411	48.6	10.5	22.3			3.43	144	154	297			SB-VP3
420739	826548	1789	54	7.86	71.8	173	159	34.7	0.752	0.32	14.3	52.2	82.8	547	UC-VP1
421345	826596	1814	67.1	4.8	965	55.1	215	35.7	0.75	0.555	1.24	55.5	66.4	524	UC-VP2
420952	826037	1821	49.4	5.47	167	27.3	314		0.75	0.4622	156	371	62.9		UC-VP3
402443	802506	1742	136	26	1775	9.51	140		1.3	10.8	31.6	98.6	494		WT-VP1
401615	800813	1737	353	16.6	412	240	2.54		0.887	10.7	100	14.7	520		WT-VP2
400936	803350	1745	163	15.9	77.9	343	15.7		0.938	1.15	40.6	115	371		WT-VP3
379998	785359	1878	22.2	4.78	19	1684			0.756	7.86	330	189			SHV 1
379849	786538	1880	5.72	9.44	18.5	103			0.799	45.8	166	537			SHV 2
380067	787942	2896	16.9	5.79	28.5	8.96	48.5		2.83	3.31	3.38	72.8	421		SHV 3
376754	790400	1904	34.4	11.8	6.77	17.7	1259		1.41	5.76	1.59	244	255		SHV 4
377082	790864	1908	8.69	16.4	26	22.7			1.35	29.6	149	252			SHV 5
377768	790997	1908	6.52	21.1	8.15	44.7			0.784	0.748	30.4	512			SHV 6
384481	783932	1900	110	11.5	18.1	107			0.943	10.6	98.9	485			SHV 7
384618	784731	1906	36.9	8.91	25.1	1250			0.75	30.3	161	190			SHV 8
384866	786994	1925	27	8.56	5.61	21.3			1.96	14.7	5.78	298			SHV 9
383316	767460	1832	196	48.6	160	249	79.4		1.37	5.27	43.7	198	381		BDV1
383181	767033	1810	58.3	129	41.7	102			1.68	4.05	25.5	539			BDV2
381956	766901	1826	51	82.8	11.4	138			0.751	3.86	9.66	580			BDV3
381485	766795	1839	27.4	87.8	81.9	275			3.54	5.63	72.9	418			BDV4
381061	814161	2055	40.8	13.3	39.3	46.4			1.57	29.5	116	307			DBV1
381129	814977	2047	101	2.9	18.4	58			0.966	0.804	57.5	441			DBV2
382086	815485	2062	147	16.1	15.5	41.3			1.44	8.03	21	448			DBV3

X	Y	Z	Resis_ 1	Resis_ 2	Resis_ 3	Resis_ 4	Resis_ 5	Resis_ 6	Thick 1	Thick 2	Thick 3	Thick 4	Thick 5	Thick 6	VES Name
381444	815848	2020	9.91	66.9	16.8	55.4			4.49	35	18.7	521			DBV4
379765	816843	2009	177	15.6	134	37.7			1.1	31	46.7	548			DBV5
390207	819086	1949	126	13.1	87	4.26	47.9		1.2	10.3	23.2	32.2	537		DBV6
389139	818463	1979	13	60.7	5.52	59.3	18.4		6.49	9.7	34.8	57.6	391		DBV7
389030	819071	1961	34.2	4.89	139	4.56	28		0.764	5.47	26	49.3	668		DBV8
353789	764107	1965	189	67.3	124	54.9			2.03	4.84	26.8	764			GUNV1
352729	764856	1991	147	105	60.2	28.1			2.79	10.9	72.6	550			GUNV2
351431	764293	2010	163	68.7	37.2	35.4			1.95	75	184	263			GUNV3
350572	796928	1548	79.2	114	25.4	115	873		0.948	2.64	11.5	176	392		HV1
353620	796321	1613	464	2882	20.6	240	71.5		1.13	1.08	1.98	27.1	559		HV2
355071	796754	1657	106	124	27.9	75.1	468		0.85	3.7	78.2	226	187		HV3
355453	797231	1673	102	482	562	90.5	63.9		1.27	19.3	16.8	65.9	229		HV4
355737	796242	1695	461	188	58	50.7	64.5		3.46	11.4	123	65.1	397		HV5
356113	796662	1691	125	204	52.9	195	54		3.18	2.08	38.8	23.8	285		HV6
359232	794685	1686	101	38.5	13.3	52.7	33.3		1.19	2.82	18.5	113	474		HV7
359710	794959	1690	70.4	12	109	39.4	30.1		2.21	23.3	35.2	72.8	733		HV8
353488	834844	1952	50.1	133	24.1	136	41.3		0.75	1.29	11.5	18	600		HBV1
401050	880650	2756	86	18.5	35.5	140	7.98		1.68	27	68.6	240	126		A SBH1
400434	881119	2757	46.5	12.2	199	13.8	61.5		0.76	9.44	9.77	13.7	550		A SBH2
400985	881799	2761	44.1	6.98	368	4.54	251	28.2	0.75	1.3	7.29	19.1	98.9	534	A SBH3
357920	785185	1710	51.6	36.4	18.9	188	28.9		0.75	10.2	9.47	24.7	624		A SBH-1
357290	783469	1712	125	18.8	60.7	53.3			1.9	12.7	200	301			A SBH-2
356543	785926	1704	62	111	38.5	164	60	35.2	0.874	3.56	9.55	11	73.9	332	A SBH-3
355556	786625	1681	120	44.8	174	39.2	57	22.6	1.62	3.78	14	114	89.1	324	A SBH-4
355144	787316	1683	194	75.7	296	32.5	35		4.27	7.25	11.8	28.1	660		A SBH-5
354036	789185	1713	118	58.8	23.7	115	30.7		1.2	7.82	36.3	128	445		A SBH-6
353932	788367	1683	86.5	7.03	98	11.5	65.6	32.3	0.75	0.276	2.34	4.92	111	36.4	A SBH-7
353535	790002	1681	164	68	8.22	73.8	72.1		0.82	6.6	4.6	198	373		A SBH-8
357165	785418	1722	302	94.1	28.9	184	80.3	23.8	0.75	4.47	5.06	30.4	151	558	A SBH-9
356412	781967	1720	57.6	18.2	8.23	252	19.3		1.82	8.7	15.1	64.7	410		A BH11(3)
356463	780725	1734	183	66.3	7.97	86.6	18.6		1.19	3.12	9.48	114	622		A BH10(4)
356413	783197	1719	80.5	210	15.7	24.7	120	25.9	0.776	0.847	5.68	24.7	168	523	A BH12(5)

X	Y	Z	Resis_ 1	Resis_ 2	Resis_ 3	Resis_ 4	Resis_ 5	Resis_ 6	Thick 1	Thick 2	Thick 3	Thick 4	Thick 5	Thick 6	VES Name
390564	848612	2020	21.7	4.52	370	19.7	123	15.6	0.764	3.1	4.59	98.2	120	523	F_SBH_1
387355	847566	2116	153	22.8	55.9	9.25	133	20.3	0.75	1.03	7.52	18.7	193	310	F_SBH_2
385911	847332	2157	95.7	13	131	28.1	2947		2.18	15.6	136	136	451		F_SBH_3
388578	849932	2093	24.6	14.2	5.76	31.6	72.8	12	1.73	2.73	7.8	50	330	358	F_SBH_4
390554	848048	2023	133	14.7	63.2	246	38.4		1.02	2.47	10.3	13.1	474		F_SBH_5
380909	838765	2183	19.3	2.79	286	5.67	121		2.78	2.91	2.68	30.6	711		F_SBH_6 (optional)
413144	839101	1816	72.3	22.4	23	515	67.1		1.07	8.65	0.827	15.1	291		MS VES-1
410616	839497	1857	87.5	9.91	31	617	21.8		0.75	4.04	7.38	17.7	720		MS VES-2
415512	839203	1811	29.5	3.31	20.5	255	3.44	1.95	0.75	1.06	44.1	66.5	95.6	155	MSVES-5
416688	840551	1849	45.5	1.39	42.1	65.9	318	9.22	0.75	0.312	14.3	20.7	63.5	503	JS VES-3
413919	841041	1824	39.5	4.51	45.2	471	2.19	29.6	0.75	1.08	30.4	45	60.2	265	JS VES-4
414590	835435	1799	38	6.47	14.5	6.77	9.69		2.67	0.745	21.1	49.7	359		WS VES-18
416181	837573	1797	38.3	8.55	29.7	240	4.39	0.8113	0.938	11.2	54	78.1	114	388	WS VES-6
408307	840764	1912	113	2.77	27.1	57	16.8	48.7	0.75	0.362	2.06	24.9	27.1	289	G VES-7
407459	841967	1910	173	3.03	55.1	473	6.78	70	0.75	0.291	11	17.6	25.5	529	GG VES-8
405972	840640	1937	247	3.11	105	53.7	122	45.4	0.75	0.351	15.4	24.7	21	640	GG VES-10
406736	837805	1906	149	2.7	394	24.7	47.6	33.1	0.75	0.942	6.93	57.3	319	410	GZ VES-11
407632	837715	1887	18.3	11.5	291	36.6	23.3		0.809	9.65	29.2	180	530		GZ VES-35
409657	842904	1862	71.2	16.6	207	35.8	70.1	1.7	0.75	2.95	78	135	268	728	JL VES-9
401821	841853	2004	141	3.8	169	3.02	32.2		0.75	0.94	7.79	9.99	496		D VES-12
409971	837486	1875	115	3.9	39.8	648	19.3	74.5	0.75	0.412	8.79	8.42	99.7	193	ZD VES-13
402837	837190	1966	83.3	2.48	1778	6.25	53.3	47.2	0.75	0.676	1.13	14.5	125	394	IG VES-21
408307	835523	1876	178	28.3	52.5	162	69.2	49.6	1.01	4.8	9.76	21.7	178	488	AG VES-14
408424	836153	1877	45.5	11.9	25.6	92.2	11.1	0.353	0.797	4.23	4.66	203	102	472	AG VES-15
407601	830833	1880	64.4	6.01	237	14.4	40.2		0.786	3.76	42.4	45.4	635		TK VES-26
407817	829004	1878	93.9	9.96	286	49.5	17		0.75	4.58	36.8	244	396		TK VES-24
406634	830061	1875	59.4	7.06	509	67.8	32	46.1	0.75	3.93	22.8	103	132	495	TK VES-25
403611	831683	1928	34.9	1.63	345	11.2	513	29.9	0.75	0.768	7.28	33.6	39.8	579	G VES-27
403568	822891	1822	225	160	444	52.9	30.6		0.968	4.69	73	171	500		R VES-34
403296	825289	1874	110	2155	27.6	69.7	48.6		4.93	7.62	14.5	72.9	536		RK VES-32
406536	826738	1876	211	29.4	388	18.8	72		0.75	20.8	46.6	127	293		J VES-22

X	Y	Z	Resis_ 1	Resis_ 2	Resis_ 3	Resis_ 4	Resis_ 5	Resis_ 6	Thick 1	Thick 2	Thick 3	Thick 4	Thick 5	Thick 6	VES Name
405882	824926	1868	197	13.6	10.9	142	120	23.8	0.855	1.39	4.35	44.8	135	508	J VES-30
403801	827562	1903	56.6	2.44	20.2	419	39.2		0.75	0.933	5.8	7.24	906		KG VES-28
407405	828071	1874	57.8	29.8	34.9	600	54.4	37.6	1.47	7.18	13.9	9.93	220	237	KB VES-23
409843	834622	1866	40	12.8	290	145	36.5	32.8	0.937	4.15	3.68	50.4	252	349	MG VES-16
410980	836231	1852	128	3.39	33.9	506	59.2	9.2	0.755	1.26	9.56	10.3	296	654	MG VES-17
412484	831628	1871	28.5	10.4	50.3	12.3	28.3	53.9	1.77	3.62	36.7	25.8	209	473	Weteta VES-19
408434	826619	1895	77.5	10.7	22.8	5.1	67.9	33.2	0.75	4.17	31.2	26	128	293	BK VES-29
401162	828380	1936	87.9	6.79	118	5.94	53.8	56	0.75	0.888	3.89	11.7	86.7	566	B VES-31
401179	826398	1907	223	21	62	20.7	108	81.6	0.811	2.73	4.5	22.2	13.6	832	BA VES-33
390002	762357	1455	309	2.71	107	119			1.21	0.907	70.9	278			Dam VES-1
390043	762370	1457	156	5.88	179	3.53			0.754	0.71	34.5	175			Dam VES-2
389964	762484	1468	27.5	774	31.7				2.27	3.73	205				Dam VES-7
389907	762299	1455	71	606	56.7	8.05	108		0.756	0.369	10	6.93	131		Dam VES-3
389875	762261	1459	105	13.1	99.5				1.9	11	178				Dam VES-4
389746	762387	1467	51.4	20.5	456	5.18			1.89	6.53	31.3	153			Dam VES-5
379350	853301	2565	96.4	31.9	551	182			5.49	136	13.5	391			L VES1
379426	852655	2560	129	5.53	56.8	301			2.56	1.1	181	448			L VES2
379725	851980	2546	106	17.8	435	9.49	605	80.5	1.6	15.6	27.6	59.8	198	346	L VES3
379188	851776	2556	135	17.8	68.8	6.93	172	59.7	1.7	4.52	8.55	21.7	180	263	L VES4
356564	827846	2025	50.3	10.7	42.1	-	-	-	3	1.23	460	-	-	-	Jaj VES1
357116	827893	2030	50	309	28.6	143	6.82	63.2	0.75	0.668	8.24	11.8	11.1	464	Jaj VES2
357621	827699	2027	70	45.1	20.3	187	11.4	-	0.75	6.83	82.8	112	429	-	Jaj VES3
357053	827438	2035	67.9	30.4	112	17.2	72.2	-	2.19	7.11	12.2	29.8	610	-	Jaj VES4
357029	826694	2045	55	11.3	56.1	-	-	-	1.81	6.65	602	-	-	-	Jaj VES5
374384	814299	2151	52.5	14.3	57.8	13.2	109		3.8	11.4	25.5	49.6	568		Ang VES 1
375848	814573	2119	76.66	56.7	13.8	5.05	51.6		1.1	0.725	29.8	19.3	568		Ang VES 2
377036	815691	2027	72.6	15.6	382	21.4	66.2		1.5	2.41	3.59	36.9	696		Ang VES 3
374017	845004	2354	147	43.6	263	81.7	36.2	116	0.773	0.987	2.37	21.4	77.7	397	Mor V1
373352	845223	2353	71	628	26.5	304	22.4	-	3.38	7.62	36.7	8.26	288	-	Mor V2
373916	843930	2335	96.9	135	597	45	66.3	-	0.75	8.82	4.71	53.8	432	-	Mor V3
372633	846289	2400	95.3	58.2	46.7	14.1	167	-	3.01	11.8	4.68	24.1	351	-	Mish V4
362294	812707	2270	11.1	0.851	11.8	12.5	23.9		0.75	0.242	13.8	23.3	536		Doyg V1

X	Y	Z	Resis_ 1	Resis_ 2	Resis_ 3	Resis_ 4	Resis_ 5	Resis_ 6	Thick 1	Thick 2	Thick 3	Thick 4	Thick 5	Thick 6	VES Name
361868	811789	2268	7.21	12.5	8.18	7.5	20.2		0.889	5.02	5.44	12.1	704		Doyg V2
362226	811050	2269	116	0.486	8.49	23.6	20.2		0.799	0.191	37.3	119	540		Doyg V3
401978	813894	1799	52.8	10.7	82.7	190	5.22	48	0.879	6.84	9.73	19.7	28.9	574	AT VES2
402998	819401	1836	42.3	6.28	2564	11.8	127		0.959	4.2	7.18	112	745		LB VES 5
400563	812830	1781	168	280	7.24	59.8	7.39	76.6	6.11	9.58	4.82	129	137	455	Mo VES3
401850	812424	1794	126	9.87	25.1	120	13.2	33	0.75	4.62	3.76	28.9	88	242	To VES4
402359	814366	1812	16.8	56.6	240	21	19.3		5.49	6.01	33.3	210	292		Ze VES1
417531	834069	1801	52.7	5.4	50.9	1972			1.43	16.3	591	913			**Si VES7 Selected BH**
417039	835227	1775	36.2	9.94	82.4	71.1			1.12	15.7	10.9	749			**SI VES6 Simbita at existing BH**
417633	813038	1839	125	4.46	15.3	1486	182	71.1	0.75	0.523	11.6	17.8	251	321	HI-BH1
417733	812633	1838	168	8.65	85.1	512	64.3		0.75	1.15	26	68.8	413		HI-VES1
417517	813483	1842	202	13.9	174	108	885	78.9	0.75	1.54	2.42	23.3	53.9	604	HI-VES2
411565	812495	1904	73.9	8.12	78.6	74.3	34.1		0.948	1.62	7.69	199	42.4		HI-BH2
411593	813021	1902	358	11.6	249	131	55.3		0.768	1.16	35.6	187	378		HI-VES3
411587	811978	1899	238	11	31.4	1401	118	52.2	0.839	1.06	1.74	2.58	166	477	HI-VES4
389245	802559	1839	51.4	8.7	14.7	17.2	47.9	7.52	1.03	5.61	17.7	58.2	141	526	SHC-BH1
388664	802578	1832	37.7	33	13.2	92.9	15.2		0.391	0.639	12.4	5.16	607		SHC-VES
390137	802146	1827	64	8.31	17.8	66.5	5.52		1.42	5.09	41	184	257		HG-BH2
390530	801222	1822	57.7	7.97	13.1	50.9	12.3		0.78	6.07	116	169	458		HG-VES
366291	746756	1725	428	134	51.7	10.7	47.7		0.75	3.68	130	84.3	328		HDV-1
366257	746630	1735	306	13.9	119	474	7.19		2.93	0.801	78.5	28.5	167		HDV-2
366016	746702	1735	372	24.2	145	85	1323		0.75	0.237	4.85	76.2	44.1		HDV-3
366163	747100	1743	118	25.7	508	10.5	39.8		0.75	0.243	1.47	2.15	55		HDV-4
366344	746946	1730	407	12.3	52.4	162			1.88	1.36	12.3	110			HDV-5
366452	747141	1736	626	158	17.3	87.8	128		1.78	2.39	4.58	39.6	172		HDV-6
366680	746650	1724	548	95.7	263				2.97	48	105				HDV-7
366562	746418	1740	252	108	46.3	185	75		3.35	6.89	7.99	36.2	29.4		HDV-8
366632	746532	1721	132	353	79.8	1343			4.03	0.984	56.1	30.4			HDV-9
366730	746827	1730	221	172	21	298	92.8		2.27	5.49	3.52	8.33	166		HDV-10
413212	889790	3177	307	14.9	18.9	88.6	32.4	1.76	0.775	2.36	4.84	6.73	167	544	INFV1

X	Y	Z	Resis_ 1	Resis_ 2	Resis_ 3	Resis_ 4	Resis_ 5	Resis_ 6	Thick 1	Thick 2	Thick 3	Thick 4	Thick 5	Thick 6	VES Name
414136	891987	3254	158	10.5	788	7.39	53		0.785	1.62	5.9	5.62	657		INFV2
413567	888628	3167	197	87.2	89.3	42.1			2.43	33.2	48.8	612			INFV3
382811	806582	2053	103	15.7	704	18.4	214	63.3	1.2	10.4	4.84	27.2	89.2	390	Dur VES #1
383037	806344	2032	48.4	18	154	14.2	451	23.2	1.38	6.15	12.5	27.1	80.3	292	Dur VES #2
383076	806033	2026	231	147	51.2	299	17.6		0.788	17.8	94	108	414		Dur VES #3
383028	805718	2017	188	9.61	1481	9.2	109	107	1.12	1.38	2.43	19.2	15.6	287	Dur VES #4
383291	805898	1996	95.7	16.6	417	7.4	224	28.8	1.88	2.38	5.54	19.9	61.6	710	Dur VES #5
383790	805815	2014	55.1	436	27.5	451	36.5		5.34	5.29	36.2	90.6	507		Dur VES #6
384048	805723	1988	72.2	10.1	320	12.1	94.9		1.17	3.19	8.59	20.3	388		Dur VES #7
381229	803499	2072	47.4	14.5	6.85	32	76.1		0.75	3.68	20.3	113	310		Dur VES #7'
381791	803973	2059	177	18.3	75.3				1.08	55.1	265				Dur VES #8
382754	804970	2055	100	4.6	29.2	20.3	112		0.752	0.211	30.9	77.7	405		Dur VES #9
383029	805089	2030	65.2	27	242	39.9	202		2.23	1.69	2.81	52.5	441		Dur VES #10
383287	805356	2016	292	31.1	25.8	1068	26.5		1.65	1.94	44.8	51	455		Dur VES #11
383486	805308	2000	70.2	247	11.3	161	15.6	795	1.84	1.31	2.41	14.1	46.6	569	Dur VES #12
383926	805261	1987	125	13.9	248	31.4			0.893	19.4	35.9	490			Dur VES #13
374495	798333	1981	115	33.1	7.85	19.8	5.77	55.5	1.18	3.27	6.36	16.6	37.3	685	Dur VES #14
374404	797945	1969	260	12.6	72.3				1.1	99	734				Dur VES #15
374356	797546	1963	69.3	1.87	19.6	7.98	7.97	79.5	0.754	0.309	13.1	17.4	39.7	662	Dur VES #16
375983	797165	1966	97.2	41.7	18.2	4.48	57.7		0.75	2.54	14.8	20.1	633		Dur VES #17
375919	796660	1957	144	8.16	102				1.23	60.9	790				Dur VES #18
373602	798970	1990	64.3	67	112	25.1	5.9	46.6	1.38	2.23	3.41	22.4	36.4	434	Dur VES #19
373370	798741	1978	91.1	35.7	3.31	34.6	4.21	43.1	2.24	3.86	4.57	9.6	28.5	563	Dur VES #20
373217	798494	1980	141	33.3	10.4	68.7			1.93	7.04	88.5	665			Dur VES #21
373198	798081	1972	61.6	24.3	5.2	12.1	5.17	61.2	0.75	3.27	9.55	23.7	19.8	384	Dur VES #22
373285	797653	1966	297	8.53	9.87	49.5			1.94	10.7	66	671			Dur VES #23
373328	797355	1957	140	22	1.84	12.3	4.62	53.9	1.62	3.26	1.76	28.8	26.8	546	Dur VES #24
377531	799280	2016	45.9	21.4	600	90			1.1	40.5	23.4	435			Dur VES #25
377171	799050	2010	192	13.5	25.8	684	36.6		1.72	3.57	34.9	70.6	556		Dur VES #26
376944	798709	1995	56.4	15.5	29.4	921	4.82		4.39	14.7	35.4	60.4	472		Dur VES #27
376941	798320	1992	84.9	12.5	36.9	128			2.49	8.99	56.2	570			Dur VES #28
376907	797809	1965	108	17	7.06	192			1.21	7.92	60.9	408			Dur VES #29

X	Y	Z	Resis_ 1	Resis_ 2	Resis_ 3	Resis_ 4	Resis_ 5	Resis_ 6	Thick 1	Thick 2	Thick 3	Thick 4	Thick 5	Thick 6	VES Name
380502	781931	1873	19	5.21	13.1	15.6	37.9		0.75	9.34	52.9	4.57	335		Lam VES #1
380376	782203	1867	9.64	2.32	7.94	5.09	23.7		0.777	0.612	13.6	4.54	767		Lam VES #2 (BH)
380302	782486	1873	21.2	8.22	29.8	63.6	14.2		3.39	26.8	128	69.4	272		Lam VES #3
375818	779382	1930	62.5	4.45	9.8	6.65	38.8		0.763	4.95	30.7	16.9	603		HK VES #1
376002	779607	1927	61.1	7.89	9.8	55.3	15.5		1.1	4.73	77.7	227	172		HK VES #2 (BH)
376221	779946	1925	36	5.27	3.07	8.62	34.4	25.2	0.75	1.93	0.93	59.9	151	239	HK VES #3
370273	888966	2005	211	296	82.7	213			30.3	51.8	314	364			GCHV1
369609	887311	2031	126	42.8	48	775			3.93	0.386	370	235			GCHV2
370268	887017	2041	108	9.46	73.4	80.1			2.69	15.6	107	430			GCHV3
370713	890379	1996	475	171	55.3	34.8			0.831	12	67.1	281			GCHV4
369932	890227	2015	95.2	58.9	11.5	307	54.9		0.75	4.02	27.4	58.3	543		GCHV5
369346	890644	2001	571	163	43.9	1259			3.08	9.66	320	396			GCHV6
371294	887048	2058	322	99.5	31.4	64.8			1.17	18.7	12.8	717			GCHV7
369981	834526	2187	184	30	7.17	20.1	174	14.7	0.781	1.87	4.43	92.3	137	480	Ho VES1
371306	835716	2220	17.5	269	8.57	293	10237	62.7	3.83	2.47	40.6	7.67	67.7	304	Ho VES2
382397	804920	2040	153	5.53	63.6	263	7.5	137	0.75	0.179	7.07	18.3	28.6	708	DU VES1
381989	804496	2060	21.2	6.05	175	18.1	97.9	-	6.4	3.39	7.42	62.1	421		DU VES2
381688	804090	2062	93.7	1.73	19.2	128	5.5	108	0.757	0.164	13.1	11.4	30.4	635	DU VES3
375379	839743	2299	83.4	6.19	63.3	65.5	-	-	4.36	1.41	74.2	694	-	-	HO VES3
375418	839298	2292	162	47.8	116	52.1	429	-	1.59	6.45	25.7	160	213	-	HO VES4
379546	834930	2161	48.1	11.5	81.9	75.3	-	-	0.801	43.7	153	523	-	-	MC VES1
379833	833460	2143	35.9	9.63	27.9	124	-	-	1.14	9.49	107	197		-	MC VES2
379343	833255	2153	116	24.6	6.82	14.8	717	-	0.75	3.24	4.64	104	131	-	MC VES3
368250	760552	2142	97.3	18	54.9	7.63	1095	45.2	1.02	0.534	10.3	11.9	56.8	45	Wolma VES1
368114	760384	1244	106	44.6	20.5	971	3.06		0.75	5.39	41.8	61.8	334		Wolma VES2
366698	759873	2159	242	2.07	157	49.6	195		0.756	0.024	5.99	69.4	235		Wolma VES3
400549	813502	1712	122	31.4	347	70.8	29		0.789	3.84	30.1	140	576		HK_VP1
400563	812830	1718	23.5	37	155	20.9	0.604		1.97	31.3	140	12.8	409		HK_VP2
399644	812020	1720	19.4	53.9	143	26.3			4.98	52	67	603			HK_VP3
398831	810818	1698	58.8	184	147	39	221	18.3	0.984	2.46	6.4	84.4	125	298	HK_VP4
398261	809673	1734	6.11	774	27.3	30.1	124	13.9	0.752	1.09	9.14	89.3	60.9	565	HK_VP5
397738	808287	1760	10.4	863	227	18.8	298		0.75	1.2	1.74	32.2	444		HK_VP6

X	Y	Z	Resis_1	Resis_2	Resis_3	Resis_4	Resis_5	Resis_6	Thick 1	Thick 2	Thick 3	Thick 4	Thick 5	Thick 6	VES Name
397985	807092	1756	78.9	297	116	40.8	116		0.833	13.6	2.2	32.4	615		HK_VP7
398631	804406	1744	13.4	127	124	56.8	24.3		1.63	4.23	23	249	469		HK_VP8
398766	803756	1776	76.2	367	230	58	90.1	48.4	1.78	3.95	8.27	7.32	95.1	612	HK_VP9
398768	803204	1755	32.5	2063	213	39	84.1	173	2.48	2.99	2.47	3.54	114	349	HK_VP10
417511	829940	1806	124	16	18.6	232	25.3	34.6	0.77	6.41	6.03	63.1	138	303	WD VES1
417613	829458	1809	99.8	26.1	20.9	144	180	32.8	0.75	0.834	6.56	40.9	69.8	605	WD VES2
417929	822911	1810	54.8	17.2	40.7	168	14.3	65.2	0.751	4.04	24.9	70.8	113	328	WD VES3
418084	818669	1811	58	4.47	22.4	138	126	19.4	0.75	0.34	8.04	56.3	102	583	WD VES4
418141	828461	1807	75.5	7.42	51.8	277	167	26.2	1.64	1.08	15.7	11.5	65.1	625	WD VES5
417039	835227	1775	37.4	9.95	9.74	86.6	78		1.06	15.3	1.28	22	472		WD VES6
347958	797317	1590	115	32.7	12.5	62.1	153		1.35	4.38	16.4	164	297		Bob VES1
397417	797167	1589	75.4	261	14.7	21	55.4	500	3.07	3.69	7.91	51.7	100	262	Bob VES2
346900	798118	1543	21	156	25.8	470	297		0.867	0.744	37.8	64.3	247		Tu VES3
348903	797839	1600	19.7	77.8	17.3	197	79.1		0.802	2.86	64.2	67.6	314		Tu VES4
347775	757879	1607	211	376	114	49.1	371		1.59	2.47	46.2	38.3	704		Bob ves5
347325	797647	1594	187	39.2	35.9	225	175		6.88	15.6	86.9	160	404		Albo ves6
364816	738820	1500	3.41	141	3.35	25.9	83.9	47.9	1.06	1.46	1.97	16.1	9.73	582	Humbo V1
365396	740471	1538	92.1	42.6	41.3	127			3.2	8.06	28.4	804			Humbo V2
364298	739761	1556	18.1	5.2	61.7	216	53.4		0.789	1.1	35.7	28	451		Humbo V3
365135	739219	1520	26.2	66.8	9.92	298	5.09		6.36	25.5	36.8	66.2	471		Humbo V4
363104	740709	1623	39.4	136	9.65	55.7	11.7	31	2	3.29	2.67	66.4	114	561	Humbo V5

Pumping Test data (Constant rate) Time-Drawdown curve for Wells Located on Western Rift Escarpment of UBRB

Time since pumping starting(min)	AlichoWoriro DD(m)	Fetazer_ Gumer	Gazebo BH2	Semen Mugo	Abeke 2017	Wachamo University BH3 DD	NigistEleni Hosp1 DD
0	0	0	0	0	0	0	0
1	1.16	0.75	2.6	8.23	0.85	5.79	6.91
2	1.27	1.85	5.1	15.05	5.26	6.83	8.61
3	1.33	2.55	7.7	21.17	5.3	7.15	9.9
4	1.46	3.35	10.08	26.2	5.45	7.41	10.54
5	1.55	4.04	12.69	29.03	5.95	7.58	10.97
6	1.6	4.24	13.99	31.07	6.05	7.72	11.26
7	1.63	4.48	15.64	33.25	6.15	7.84	11.48
8	1.7	4.7	16.04	34.08	6.35	7.88	11.6
9	1.72	4.88	17.14	34.83	6.43	7.82	11.71
10	1.77	5.35	18	35.26	6.57	7.94	11.79
12	1.81	5.68	21.02	35.75	6.75	8	11.95
14	1.88	6	23.26	36.23	6.95	8.05	12.03
16	1.93	6.25	24.37	36.74	7.2	8.08	12.13
18	1.93	6.4	25.44	37.65	7.44	8.09	12.21
20	1.94	6.59	26.64	37.63	7.57	8.1	12.27
25	2	7.4	29.54	38.24	7.71	8.13	12.41
30	2.04	8.18	31.54	38.9	7.95	8.15	12.56
35	2.08	8.64	32.54	39.43	8.2	8.18	12.63
40	2.12	9.07	33.54	40.01	8.35	8.19	12.69
45	2.14	9.6	35.14	41.35	8.7	8.21	12.74
50	2.16	10.2	36.24	42.01	8.9	8.23	12.82
55	2.2	10.66	37.54	42.59	9	8.23	12.87
60	2.2	11.12	38.14	43.38	9.2	8.24	12.92
70	2.23	11.93	39.74	44.13	9.45	8.26	13.01
80	2.26	12.61	40.64	44.78	9.7	8.27	13.08
90	2.29	13.38	41.24	45.42	9.95	8.29	13.14
100	2.32	14.32	41.84	45.94	10.45	8.3	13.18
120	2.36	15.17	42.54	46.45	10.85	8.32	13.3
140	2.39	15.92	45.74	46.94	11.45	8.33	13.35
160	2.42	16.86	48.44	47.35	12.4	8.34	13.41
180	2.44	17.9	49.09	47.63	12.95	8.35	13.45
210	2.5	18.01	50.44	47.93	13.45	8.39	13.55
240	2.53	18.4	51.81	48.21	13.27	8.4	13.57
270	2.55	18.67	53.39	48.39	13.98	8.41	13.62
300	2.58	18.78	54.54	48.56	14.45	8.42	13.63
360	2.65	19.16	55.44	48.94	14.02	8.42	13.69
420	2.72	19.46	56.69	49.13	14.03	8.41	13.76
480	2.78	19.75	56.99	49.25	14.45	8.41	13.8
540	2.81	20.68	58.89	49.51	14.55	8.42	13.85
600	2.82	21.7	59.94	49.83	14.65	8.43	13.9
660	2.83	21.95	60.81	50.15	14.75	8.43	13.94

Time since pumping starting(min)	AlichoWoriro DD(m)	Fetazer_ Gumer	Gazebo BH2	Semen Mugo	Abeke 2017	Wachamo University BH3 DD	NigistEleni Hosp1 DD
720	2.84	22.25	61.84	50.5	14.85	8.43	13.99
780	2.85	22.57	62.99	50.84	14.95	8.43	14.02
840	2.86	22.91	64.04	51.22	14.96	8.43	14.04
900	2.87	23.15	64.76	51.55	14.97	8.44	14.05
960	2.88	23.4	65.71	51.95	14.98	8.44	14.07
1020	2.89	23.6	66.14	52.24	14.99	8.44	14.1
1080	2.9	23.78	67.64	52.39	14	8.44	14.11
1140	2.99	24	67.99	52.51	14	8.42	14.12
1200	3	24.25	68.33	52.57	14	8.42	14.15
1260	3.04	24.6	68.48	52.61	14	8.42	14.15
1320	3.07	24.91	68.77	52.64	14	8.43	14.18
1380	3.09	25.55	69.14	52.66	15	8.43	14.19
1440	3.1	25.75	69.64	52.68	15	8.43	14.2

Time-Drawdown curve for Wells Located in Pediment of UBRB

Time since pumping starting (min)	Semi cho Duna	Wa gebeta 1 DD	Wa Gebeta 2 DD	Wa Gebeta 3 DD	Wa Gebeta 4 DD	Warite Balaka DD	Angamo 2015 DD	Durame Campus2 DD	Durame Campus 1 DD	WSU Sodo Town DD	Aroge Arada Sodo BH DD	LBTW-08-18(D Pulasa) DD	Z-Sibaye DD
0	0	0	0	0	0	0	0	0	0	0	0	0	0.94
1	1.97	2.32	6.01	12.46	0.15	4.36	5.51	1.54	1.24	7.16	2.27	11.66	1.79
2	2.15	4.35	6.35	13.8	0.18	5.64	7.97	1.57	1.54	8.59	2.5	12.36	2.43
3	2.35	7.57	6.55	13.9	0.2	6.38	9.76	1.58	1.58	9.04	2.6	12.84	3.05
4	2.39	8.2	7.05	15.05	0.22	6.87	10.93	1.58	1.6	9.36	2.7	13.17	3.42
5	2.42	8.32	7.19	15.45	0.24	7.36	12.04	1.58	1.6	9.43	2.8	13.46	3.95
6	2.45	8.36	7.31	15.88	0.25	7.58	12.71	1.58	1.6	9.55	2.8	13.71	4.23
7	2.56	8.45	7.5	15.89	0.27	7.74	13.25	1.58	1.61	9.7	2.8	13.96	4.63
8	2.61	8.48	7.61	16.42	0.29	7.94	13.64	1.58	1.61	9.78	2.8	14.13	4.84
9	2.64	8.54	7.7	16.59	0.3	8.08	13.87	1.58	1.61	9.87	2.8	14.31	5.05
10	2.66	8.6	7.79	16.74	0.32	8.24	14.18	1.58	1.61	9.93	2.8	14.45	5.29
12	2.69	8.66	7.9	17	0.35	8.47	14.83	1.58	1.61	10.15	2.85	14.8	5.42
14	2.76	8.72	7.98	17.1	0.36	8.64	15.29	1.58	1.61	10.31	2.87	15.03	5.53
16	2.81	8.75	8.08	17.33	0.39	8.78	15.76	1.58	1.62	10.45	2.89	15.32	5.65
18	2.84	8.82	8.15	17.45	0.4	8.91	16.14	1.58	1.62	10.57	2.9	15.52	5.85
20	2.85	8.88	8.2	17.58	0.41	9.02	16.53	1.58	1.62	10.64	2.92	15.7	5.97
25	2.96	8.97	8.28	17.8	0.44	9.21	17.34	1.58	1.62	10.92	2.96	16.26	6.14
30	3.01	9.05	8.36	18.03	0.49	9.39	18.11	1.58	1.62	11.1	3	16.75	6.23
35	3.07	9.12	8.42	18.18	0.52	9.57	20.11	1.58	1.62	11.25	3.05	17.18	6.35
40	3.1	9.19	8.48	18.36	0.56	9.71	20.89	1.58	1.62	11.38	3.06	17.53	6.43
45	3.18	9.27	8.55	18.45	0.59	9.83	21.34	1.58	1.62	11.51	3.06	17.95	6.75
50	3.26	9.36	8.62	18.55	0.64	9.91	21.97	1.58	1.62	11.64	3.07	18.36	6.86
55	3.32	9.42	8.71	18.64	0.68	10.03	22.22	1.58	1.62	11.83	3.08	18.9	6.97
60	3.37	9.48	9	18.76	0.72	10.11	22.61	1.58	1.62	11.87	3.1	19.44	7.15
70	3.45	9.54	9.05	18.93	0.77	10.31	23.51	1.58	1.62	12.02	3.13	19.89	7.23
80	3.5	9.61	9.16	19.04	0.82	11.19	24.01	1.58	1.62	12.2	3.16	20.24	7.33
90	3.64	9.67	9.27	19.17	0.87	11.47	24.46	1.58	1.62	12.28	3.19	20.61	7.89
100	3.69	9.76	9.32	19.26	0.92	11.64	24.61	1.58	1.62	12.42	3.23	21.26	8.43
120	3.91	9.92	9.44	19.31	1.02	11.88	25.72	1.58	1.62	12.61	3.3	21.77	8.95
140	4.07	10	9.5	19.36	1.07	12.07	27.21	1.58	1.62	12.8	3.36	22.21	9.59
160	4.18	10.04	9.52	19.6	1.12	12.3	27.74	1.58	1.62	12.92	3.4	22.59	10.09
180	4.32	10.09	9.58	19.68	1.18	12.41	28.11	1.58	1.62	13.05	3.4	23.09	10.64
210	4.44	10.14	9.62	19.73	1.24	12.62	28.71	1.58	1.82	13.2	3.44	23.47	11.03

Time since pumping starting (min)	Semi cho Duna	Wa gebeta 1 DD	Wa Gebeta 2 DD	Wa Gebeta 3 DD	Wa Gebeta 4 DD	Warite Balaka DD	Angamo 2015 DD	Durame Campus2 DD	Durame Campus 1 DD	WSU Sodo Town DD	Aroge Arada Sodo BH DD	LBTW-08-18(D Pulasa) DD	Z-Sibaye DD
240	4.6	10.21	9.66	19.98	1.3	12.82	29.89	1.58	1.82	13.36	3.47	23.86	11.54
270	4.71	10.28	9.71	20.1	1.36	12.9	30.64	1.58	1.84	13.41	3.55	24.11	11.97
300	5.06	10.36	9.75	20.21	1.42	13.07	30.76	1.58	1.84	13.55	3.72	24.36	12.39
360	5.2	10.64	9.84	20.4	1.54	13.33	31.1	1.58	1.85	13.78	3.85	24.66	12.89
420	5.26	10.79	9.9	20.58	1.62	13.64	32.5	1.58	1.86	13.96	3.92	25	13.04
480	5.38	10.92	9.96	20.67	1.68	13.76	33.24	1.59	1.86	14.06	3.92	25.31	13.15
540	5.49	11.05	10	20.77	1.75	13.9	34.42	1.59	1.87	14.33	3.98	25.55	13.3
600	5.54	11.24	10.08	20.86	1.82	14.05	35.21	1.59	1.88	14.52	4.1	25.78	13.35
660	5.62	11.38	10.16	21.02	1.83	14.16	35.59	1.59	1.89	14.73	4.2	25.41	13.63
720	5.7	11.49	10.24	21.1	1.86	14.28	35.74	1.6	1.89	14.8	4.32	25.3	13.84
780	5.78	11.59	10.29	21.18	1.9	14.46	35.76	1.6	1.89	14.91	4.44	25.36	14.03
840	5.95	11.71	10.38	21.26	1.92	14.53	35.82	1.6	1.89	14.98	4.5	25.44	14.14
900	6.12	11.82	10.44	21.35	1.95	14.64	36.46	1.6	1.9	15.05	4.6	25.55	14.25
960	6.13	11.91	10.46	21.44	1.99	14.88	36.66	1.6	1.9	15.09	4.69	25.63	14.33
1020	6.24	11.99	10.48	21.51	2.01	14.95	36.76	1.6	1.9	15.12	4.72	25.72	14.42
1080	6.35	12.09	10.52	21.58	2.04	15.01	36.81	1.6	1.9	15.22	4.82	25.8	14.48
1140	6.36	12.21	10.6	21.67	2.06	15.08	36.91	1.6	1.9	15.34	4.89	25.83	14.55
1200	6.39	12.3	10.7	21.76	2.1	15.14	37.06	1.6	1.9	15.37	4.95	25.89	14.6
1260	6.44	12.39	10.79	21.83	2.13	15.18	37.16	1.6	1.9	15.46	5.05	25.95	14.68
1320	6.49	12.5	10.85	21.91	2.18	15.25	37.26	1.6	1.91	15.5	5.1	26.01	14.79
1380	6.52	12.61	10.9	21.98	2.19	15.34	37.41	1.6	1.91	15.59	5.2	26.07	14.86
1440	6.54	12.69	10.96	22.07	2.22	15.39	37.66	1.6	1.91	15.61	5.26	26.12	14.94

Time-Drawdown curve for Wells Located on Escarpment foot of UBRB

Time since pumping starting (min)	Achamo Town DD	Doesha DD	Jata2015 DD	Getem 2018 DD	Tefo Chufo DD	Felka DD	Cham bulla DD	Halaba_ Alemtena 490 DD	Kulubi DD	Weyira (HBH-1) DD
0	0	0	0	0	0	0.00	0	0	0	0
1	3.05	15.3	1.25	1.7	6.3	2.10	1	4.34	2.13	2.76
2	3.4	19.25	1.3	2	6.33	2.40	4.7	5.24	2.36	2.77
3	3.81	20.1	1.37	2.4	6.35	2.48	5.3	5.34	2.46	2.83
4	4	20.55	1.42	2.6	6.36	2.60	5.55	5.47	2.7	2.88
5	4.15	21.02	1.44	2.85	6.37	2.75	5.7	5.64	2.8	2.91
6	4.26	21.2	1.5	3.1	6.38	2.87	5.85	5.74	2.83	2.94
7	4.36	21.58	1.54	3.35	6.39	3.02	5.9	5.84	2.96	3
8	4.43	21.8	1.56	3.6	6.4	3.15	5.93	5.89	2.96	3.11
9	4.5	22	1.57	3.85	6.41	3.26	5.96	5.98	3	3.16
10	4.56	22.15	1.62	4.12	6.42	3.35	6.15	6.07	3.03	3.2
12	4.62	22.48	1.68	4.27	6.43	3.45	6.16	6.17	3.05	3.23
14	4.67	22.72	1.69	4.41	6.44	4.35	6.17	6.24	3.08	3.25
16	4.73	22.95	1.75	4.55	6.45	4.72	6.28	6.38	3.11	3.32
18	4.8	23.1	1.79	4.69	6.46	5.22	6.28	6.4	3.15	3.46
20	4.88	23.28	1.84	4.82	6.47	5.57	6.35	6.51	3.25	3.56
25	4.94	23.55	1.97	4.91	6.48	6.77	6.55	6.72	3.35	3.62
30	5	23.85	2.05	5.01	6.49	7.55	6.7	6.84	3.45	3.63
35	5.12	24.05	2.06	5.09	6.5	7.94	6.77	7	3.5	3.65
40	5.22	24.25	2.13	5.14	6.5	8.19	6.89	7.11	3.6	3.67
45	5.27	24.35	2.16	5.2	6.58	8.34	7.05	7.22	3.65	3.69
50	5.33	24.6	2.22	5.24	6.75	8.45	7.08	7.3	3.72	3.71
55	5.39	24.73	3.23	5.28	6.8	8.55	7.12	7.41	3.8	3.73
60	5.42	24.85	2.24	5.31	6.85	8.72	7.16	7.5	3.85	3.74
70	5.47	24.95	2.32	5.39	6.9	9.50	7.3	7.64	4	3.74
80	5.52	25.05	2.38	5.47	6.96	9.55	7.42	7.72	4.05	3.76
90	5.61	25.15	2.42	5.56	6.98	9.55	7.48	7.94	4.15	3.78

Time since pumping starting (min)	Achamo Town DD	Doesha DD	Jata2015 DD	Getem 2018 DD	Tefo Chufo DD	Felka DD	Cham bulla DD	Halaba_ Alemtena 490 DD	Kulubi DD	Weyira (HBH-1) DD
100	5.7	25.3	2.44	5.65	7.08	9.53	7.55	7.99	4.23	3.81
120	5.76	25.45	2.49	5.83	7.22	9.43	7.7	8.08	4.35	3.83
140	5.8	25.55	2.54	6.01	7.26	9.57	7.81	8.32	4.45	3.86
160	5.88	25.7	2.54	6.19	7.3	9.45	7.95	8.49	4.6	3.94
180	5.93	25.85	2.57	6.37	7.45	9.55	8.03	8.58	4.65	4
210	5.97	25.95	2.59	6.87	7.62	9.66	8.15	8.77	4.85	4.08
240	6.05	26.05	2.63	6.98	7.71	9.50	8.3	8.84	4.86	4.23
270	6.1	26.15	2.66	7.09	7.83	9.56	8.38	8.99	4.97	4.26
300	6.15	26.2	2.69	7.2	7.95	9.63	8.5	9.04	5.1	4.41
360	6.19	26.3	2.69	7.31	8.02	9.60	8.7	9.09	5.28	4.46
420	6.23	26.38	2.69	7.42	8.16	9.70	8.87	9.37	5.45	4.01
480	6.27	26.45	2.72	7.53	8.27	9.75	9.03	9.48	5.55	4.56
540	6.3	26.55	2.73	7.97	8.38	9.81	9.15	9.83	5.75	4.59
600	6.33	26.55	2.74	8.04	8.5	9.80	9.3	10.01	5.91	4.65
660	6.36	26.58	2.75	8.11	8.6	9.73	9.46	10.12	5.98	4.67
720	6.39	26.62	2.75	8.18	8.67	9.91	9.5	10.17	6.1	4.67
780	6.42	26.65	2.75	8.25	8.74	9.90	9.8	10.24	6.25	4.69
840	6.46	26.75	2.75	8.45	8.8	9.78	10	10.49	6.35	4.69
900	6.5	26.75	2.77	8.39	8.9	9.75	10.01	10.74	6.42	4.69
960	6.53	26.8	2.77	8.46	8.95	9.82	10.06	11.14	6.5	4.7
1020	6.57	26.83	2.77	8.53	8.98	9.81	10.12	11.37	6.61	4.7
1080	6.6	26.85	2.78	8.73	9.03	9.79	10.2	11.72	6.69	4.7
1140	6.62	26.87	2.78	8.67	9.1	9.83	10.22	11.87	6.75	4.71
1200	6.65	26.9	2.78	8.74	9.14	9.88	10.25	12.01	6.8	4.71
1260	6.66	26.95	2.78	8.81	9.19	9.88	10.28	12.12	6.9	4.72
1320	6.66	27.02	2.78	8.88	9.25	9.88	10.3	12.35	7.05	4.72
1380	6.66	27.02	2.78	9.33	9.33	9.88	10.31	12.5	7.15	4.73
1440	6.66	27.02	2.78	9.35	9.38	9.88	10.31	12.5	7.2	4.74

Time-Drawdown curve for Wells Located in Rift floor of UBRB

Time since pumping starting (min)	**Shone 1 DD**	**Shone 2 DD**	**Shone 3 DD**	**Shone 4 DD**	**LBTW-04-18(D Weyde) DD**	**LBTW-07-19(D Fango) DD**	**LBTW-05-19(Loka Abaya) DD**	**LBTW-06-19 (Borich) DD**	**Siraro Badawacho Abuka SRBH DD**	**Aruse Woyde DD**	**Hobicha DD**	**LBTW-01-19 (Humbo) DD**
0	0	0	0	0	0	0	0	0	0	0	0.00	0
1	0.4	0.8	0.78	10.82	13.6	58.38	33.1	23.82	3.75	13.65	0.70	20.65
2	1	1.4	1.85	20.07	19.97	85.84	36.9	27.7	3.8	30.35	2.30	26.78
3	2.2	2.6	2.93	26.7	24.89	100.71	39.8	28.27	3.8	32.65	3.30	29.85
4	2.4	3	3.8	27.92	30.45	110.57	42.32	28.7	3.85	33.15	4.15	31.9
5	2.8	4.2	4.86	33.8	32.51	129.77	43.87	31.9	3.9	33.65	4.70	33.38
6	3.4	5.25	6.01	35	35.92	138.17	45.13	35.18	3.9	34.65	5.10	34.52
7	3.6	6.3	6.84	36.2	36.67	142.56	46.16	35.85	3.9	35.45	5.55	35.4
8	3.9	7.35	7.69	37.09	40.87	144.76	47.35	36.02	3.9	35.45	5.75	36.13
9	4	8.4	8.76	38.27	41.89	147.64	47.78	36.36	3.9	36.55	6.30	36.93
10	4.1	9.43	10.62	38.98	43.57	148.92	48.56	36.55	3.95	37.15	6.50	37.36
12	4.35	10.46	11.43	40.43	46.15	151.17	49.5	36.75	3.95	40.25	6.70	38.3
14	5	11.4	12.34	41.77	48.33	152.68	50.41	36.98	4	43.75	6.85	38.98
16	5.3	11.9	13.33	42.68	50.01	153.44	51.15	37.2	4	49.05	6.90	39.6
18	5.7	12.69	14.36	43.58	51.62	154.17	51.81	37.41	4	51.05	7.15	40.08
20	6	13.85	15.44	44.32	52.94	154.48	52.34	37.71	4	52.35	7.23	40.5
25	6.16	14.4	16.47	45.93	54.99	155.31	47.68	38.08	4	54.25	7.28	41.3
30	6.35	14.83	17.53	47.22	56.47	155.97	54.5	38.26	4	56.05	7.30	41.97

Time since pumping starting (min)	Shone 1 DD	Shone 2 DD	Shone 3 DD	Shone 4 DD	LBTW-04-18(D Weyde) DD	LBTW-07-19(D Fango) DD	LBTW-05-19(Loka Abaya) DD	LBTW-06-19 (Borich) DD	Siraro Badawacho Abuka SRBH DD	Aruse Woyde DD	Hobicha DD	LBTW-01-19 (Humbo) DD
35	6.55	15.3	18.71	48.07	57.12	156.43	50.4	38.46	4	57.21	7.35	41.57
40	6.8	15.75	19.53	48.92	58.3	156.86	55.73	38.64	4	56.45	7.41	42.83
45	6.95	16.4	20.35	49.62	59.07	157.27	56.11	38.81	4	59.45	7.43	43.2
50	7.16	16.8	20.84	50.2	59.85	157.55	56.74	38.77	4	61.25	7.45	43.38
55	7.35	17.5	21.51	50.56	60.35	157.81	56.78	38.99	4	61.45	7.50	43.85
60	8	17.8	21.66	51.08	61.02	158.09	57.2	39.27	4	61.55	7.56	44.23
70	8.3	18.565	22.22	52.17	61.7	158.63	58.13	39.51	4	61.65	7.65	44.6
80	8.5	18.565	22.65	53.24	63.27	159.05	58.64	39.58	4	61.75	7.70	44.88
90	8.7	19.1	23.14	54.11	62.61	159.44	59.01	40.12	4	62.75	7.75	45.13
100	9	19.9	23.56	54.92	62.91	159.77	59.33	39.99	4	100.05	7.79	45.38
120	9.3	20.4	24.43	55.42	63.23	160.4	60.05	40.23	4	64.7	7.83	45.65
140	9.5	21	25.23	55.92	63.75	160.95	60.69	40.37	4	66.15	8.90	46.3
160	9.8	21.7	25.59	56.9	64.27	161.45	60.69	40.58	4	66.7	9.25	47.12
180	10.1	22.45	25.81	58.36	64.39	161.87	60.95	40.7	4	68.45	10.00	47.86
210	10.3	23.3	25.99	59.17	64.4	162.49	61.34	41.07	4	69.65	10.60	48.68
240	10.46	23.85	26.47	59.92	64.86	163.02	61.45	41.24	4	70.25	11.40	48.99
270	10.8	24.35	26.65	60.61	64.96	163.91	61.86	41.13	4	71.15	12.00	49.2
300	11.4	24.8	26.83	61.27	65.1	164.05	62.05	41.21	4	73.75	12.83	49.2
360	14.2	26.8	27.02	62.34	65.22	164.67	62.38	41.3	4	74.65	13.40	49.2
420	15.8	27.6	27.17	63.2	65.29	165.32	62.6	41.46	4.05	75	13.80	49.2
480	17	28.4	27.26	63.35	65.37	165.85	62.8	41.58	4.15	75.55	14.40	50.36
540	17.85	29.3	27.43	63.57	65.43	166.35	63	41.68	4.2	76.65	15.00	50.62
600	19.6	30.4	27.64	63.75	65.48	166.77	63.1	41.73	4.24	77.85	16.30	50.92
660	21.8	31.6	27.86	63.89	65.52	167.19	63.28	41.8	4.36	78.35	16.95	51.15
720	22.05	33	28.19	64.14	65.54	167.52	63.41	41.93	4.38	78.45	17.70	51.42
780	22.4	36.8	28.53	64.33	65.58	167.91	63.51	41.81	4.4	78.55	18.27	51.57
840	22.7	38.46	28.84	64.45	65.62	168.18	63.61	41.9	4.45	78.65	18.70	51.57
900	22.8	40	29.15	64.65	65.65	168.49	63.78	41.96	4.5	78.85	18.70	51.79
960	22.9	43.6	29.42	64.84	65.66	168.81	63.89	42.1	4.6	78.95	19.15	52.24
1020	23.3	45.2	29.64	65.02	65.7	169.06	63.9	42.17	4.65	79.15	19.50	52.38
1080	23.5	47.2	29.88	65.2	65.75	169.3	63.95	42.11	4.75	79.3	20.30	53.32
1140	23.7	47.44	30.21	65.33	65.77	169.56	64	42.15	4.78	79.5	20.30	52.48
1200	24	48.55	30.53	65.49	65.8	169.71	64.02	42.11	4.84	79.6	20.30	52.67
1260	24.3	49.66	30.86	65.67	65.8	169.94	64.14	41.97	4.9	79.65	20.70	52.88
1320	24.4	49	31.02	65.76	65.81	170.1	64.17	42.06	5	79.7	21.20	53
1380	24.5	48.34	31.34	65.78	65.83	170.32	64.23	42.09	5.15	79.75	21.50	52.94
1440	24.6	49.85	31.61	65.81	65.86	170.52	64.83	42.18	5.35	79.8	21.80	53.05